SOME ASPECTS OF THE

ELECTROCHEMISTRY OF INDIUM

by

Robert Piercy

Supervisor: Dr. N.A. Hampson

Submitted in partial fulfilment of the requirements for the degree of Doctor of Philosophy of Loughborough University of Technology, April 1975.

The work described in this thesis has not been submitted, in full or in part, to this or any other institution for a higher degree.

ACKNOWLEDGEMENTS

I would like to express my gratitude to my supervisor, Dr. N.A. Hampson, for guiding me to this topic and for his continued help and encouragement throughout the duration of the work.

I would like to thank Professor R. F. Phillips, Head of the Chemistry Department, for providing the facilities to carry out this work and also the Science Research Council for the provision of a research grant.

I am grateful to the technical staff of the University for their valuable assistance and also to my fellow research students for their friendship and many hours of stimulating discussion.

Finally I wish to express my thanks to Mrs. Christine Sills for typing this thesis so carefully and to my wife for her understanding and at times necessary patience.

SUMMARY

The electrochemical behaviour of indium in some aqueous electrolytes has been examined using a variety of experimental techniques.

A study of cells of the type $In_{(s)} | InCl_{3(aq)}, HCl_{(aq)} | AgCl_{(s)} | Ag_{(s)}$ has shown that hydrolysis of $InCl_3$ occurs at certain pH's and consequently determinations of the parameters $E^{\ominus}$ and $(\partial E^{\ominus}/\partial T)_p$ are only possible under conditions where hydrolysis does not interfere with the electrode reaction In(III) + 3e = In. Complementary with these cell EMF measurements, differential capacitance studies have yielded useful information regarding conditions under which the In(III)/In exchange reaction can be studied without hindrance from adsorption or films.

The kinetics of the In(III)/In reaction have been investigated in acidic, aqueous media. In perchlorate electrolytes the anodic reaction occurs via a stepwise mechanism in which the $In \longrightarrow In(I) + e$ reaction is relatively fast. Subsequent reaction of In(I) to form the more stable In(III) species occurs either by an electrochemical step or chemically by reaction with available hydrogen ions in solution. In chloride electrolytes the mechanism of the anodic oxidation of indium is more complex.

The anodic behaviour of indium in alkaline electrolytes has also been investigated. Galvanostatic measurements show that the anodic reaction conforms to passivation due to the progressive growth of a solid film on the electrode surface: under some conditions a precursory solution reaction may be observed. The polarisation behaviour is influenced by semi-conductor properties of oxide formed in the passivating layer. An investigation of

the kinetics of active dissolution in alkaline electrolytes shows that a stepwise mechanism occurs, the anodic reaction order with respect to hydroxyl ions being three. Possible industrial applications of the indium electrode in alkali are discussed.

CONTENTS

		Page
CHAPTER 1.	INTRODUCTION	1
CHAPTER 2.	THEORETICAL PRINCIPLES	4
CHAPTER 3.	EXPERIMENTAL TECHNIQUES	23
CHAPTER 4.	THE ELECTROCHEMICAL BEHAVIOUR OF INDIUM - A LITERATURE REVIEW	30
CHAPTER 5.	A STUDY OF THE DIFFERENTIAL CAPACITANCE OF INDIUM IN SOME AQUEOUS ELECTROLYTES	45
CHAPTER 6.	STUDIES OF THE EQUILIBRIUM POTENTIAL OF THE INDIUM ELECTRODE IN AQUEOUS CHLORIDE ELECTROLYTES	62
CHAPTER 7.	THE INDIUM ELECTRODE IN PERCHLORATE ELECTROLYTES - A KINETIC STUDY	75
CHAPTER 8.	THE INDIUM ELECTRODE IN CHLORIDE ELECTROLYTES - A KINETIC STUDY	89
CHAPTER 9.	THE ANODIC BEHAVIOUR OF INDIUM IN ALKALINE ELECTROLYTES	102
CHAPTER 10.	FINAL DISCUSSION	116
	REFERENCES	131
APPENDIX 1.	ANALYSES OF ELECTROLYTE SOLUTIONS AND PREPARATION OF ACTIVATED CHARCOAL	139
APPENDIX 2.	THE KINETICS OF MULTISTEP ELECTRON TRANSFER PROCESSES.	141

LIST OF SYMBOLS

A	electrode area
A,B	constants in Debye-Huckel equation
$\underset{a}{a}$	ion size parameter
C	total differential capacitance
C_{comp}	differential capacitance of compact double layer
C_{diff}	differential capacitance of diffuse double layer
C_{dl}, C_L	double layer capacitance
C_{xs}, R_{xs}	measured series capacitance and resistance
C_p, R_p	equivalent parallel circuit capacitance and resistance
C_O^s, C_R^s	surface concentrations of O and R
C_O^b, C_R^b	bulk concentrations of O and R
D_O, D_R	diffusion coefficients of O and R
E	electrode potential on a suitable reference scale
$E^{\ominus}$	standard electrode potential
E_r	reversible electrode potential (potential at $i \simeq 0$)
E_R	rational potential
E_z	potential of zero charge
F	Faraday constant
i	current density
i_o	exchange current density
i_a, i_c	partial anodic and cathodic current densities
i_L	limiting current density
i_∞	current density at infinite electrode rotation speed
I	ionic strength ($\frac{1}{2} \sum m_i z_i^2$)
j	$(-1)^{\frac{1}{2}}$

k_c, k_a	potential dependent rate constants for cathodic and anodic reactions
K_{sp}	solubility product
K_w	ionic product for water
k^o	apparent standard rate constant
k_{sh}	standard heterogeneous rate constant
n,z	number of electrons involved in electrode reaction
q	charge on electrode, flux of diffusing species
R	gas constant
R_D, θ	charge transfer resistance
R_{sol}	electrolyte ohmic resistance
T	temperature
t	time
t_p	passivation time
V	reaction velocity of chemical reaction
W	Warburg impedance
x	distance from electrode
Z	total cell impedance
Z'	real part of total impedance
Z''	imaginary part of total impedance
α	cathodic charge transfer coefficient
α_a, α_k	anodic and cathodic transfer coefficients governing the overall potential dependence of the rate of reaction, when the reaction is considered in terms of a stepwise electron transfer process.
$\beta_{a,m}, \beta_{k,m}$	anodic and cathodic symmetry coefficients of the rate determining electron transfer step
$\gamma_{\pm}$	mean ionic activity coefficient
δ	diffusion boundary layer thickness

δ_o	hydrodynamic boundary layer thickness
ΔH_s	hydration energy of a given ion
η_D	charge transfer overpotential
θ'	apparent charge transfer resistance (value of θ when $E \neq E^{\ominus}$)
ν	kinematic viscosity
σ	Warburg coefficient as defined by equation (2.46)
ϕ_M	potential difference between metal and solution
ϕ_s	potential on solution side of double layer
ϕ_2	potential at plane of closest approach
ω	angular velocity, angular frequency
$\longrightarrow$	direction of a given reaction

CHAPTER 1

INTRODUCTION

A knowledge of the processes occuring at solid metal electrodes is of considerable importance in the understanding of electrochemical applications such as corrosion, electrodeposition and electrochemical energy conversion. Progress in the study of electrode processes at solid metal electrodes has been greatly facilitated in recent years by the development of new experimental methods and improvement of existing techniques. Metals of which uni- and divalent ions are the most stable solution species have received much more attention electrochemically than metals such as indium for which the most stable ion in solution is three-valent. This thesis is concerned with indium.

Indium is a metal of interest technologically as it has attractive possibilities as an anode material for alkaline primary batteries[1], it is also a metal of great academic interest as it affords the possibility for studying multistep electron transfer reactions. Thus, for example, Pchel'nikov and Losev[2] and Visco[3] have suggested that during the anodic dissolution of indium a series of successive, one electron, unit steps occur, viz

$$In(0) \longrightarrow In(I) + e$$

$$In(I) \longrightarrow In(II) + e$$

$$In(II) \longrightarrow In(III) + e$$

It should, however, be noted that some controversy still exists concerning the existence of oxidation states of indium intermediate between zero and three. There is overwhelming evidence for the existence of In(I) species under certain experimental conditions (see chapter 4), but only Hepler et. al.[4] report the detection of In(II). In a similar set of experiments Biedermann and Wallin[5] found no evidence for In(II) species.

It is evident from a survey of the relevant literature (chapter 4) that most electrochemical investigations of indium have been restricted to studies of indium amalgams. The main reasons for studying amalgam systems may be summarised as follows: mercury and liquid amalgam electrodes provide structureless, smooth surfaces of readily determinable area. The surface area of a solid metal differs from its superficial area in that a multiplicity of crystal planes, steps, dislocations and so forth may contribute to the superficial area. Whilst an amalgam electrode is homogeneous, at a solid metal each exposed crystal plane is potentially a different surface. It is believed that incorporation of atoms into a metal lattice (or vice versa) can only take place at a limited number of sites (kink sites); an amalgam is able to incorporate an atom at any point since all points are equivalent. A further reason for the many indium amalgam studies is that indium amalgams up to 70 mol percent can be prepared[6], consequently the amalgam electrode can be studied over a wide range of concentrations.

In the present studies the electrochemical behaviour of solid indium in a number of aqueous electrolyte solutions has been investigated, with a view to providing data pertaining to the mechanistic aspects of the anodic reactions in these electrolyte

solutions. Equilibrium potential and differential capacitance measurements were employed in order to isolate suitable conditions under which the kinetics of the In(III)/In(O) exchange reaction could be investigated. Rotating disc and faradaic impedance techniques were selected as a means of investigating the In(III)/In(O) exchange reaction. The rotating disc electrode is a particularly useful tool for investigating electrochemical reactions in that it enables the true kinetic currents, corresponding to the charge transfer process under investigation, to be easily and relatively accurately obtained in the absence of concentration polarisation effects. These measurements are particularly desirable since the majority of investigations of the kinetic behaviour of the indium electrode in aqueous electrolyte solutions have been based on steady state polarisation techniques. Under these experimental conditions diffusion of electroactive species in solution is often the rate controlling process. The faradaic impedance technique is of great value as it yields information concerning the kinetic parameters of the electrode reaction; also, the concentration and diffusion coefficients of the reacting species, the double layer capacity of the electrode/electrolyte interphase, the ohmic resistance of the electrolyte solution and the charge transfer resistance of the electrode/electrolyte system under investigation, may be obtained.

CHAPTER 2

THEORETICAL PRINCIPLES

2.1. The Electrode-Electrolyte Interphase

The structure of the electrode-electrolyte interphase is of basic importance in determining the course of electrode reactions, since electrochemical reactions take place within this interphasial region. An interphase may be considered as the region between two phases in which the properties have not yet reached those of the bulk of either phase.

At a metal/solution interphase there exists an electrical double layer. An electrical double layer consists of two layers of electrical charge of opposite sign and equal magnitude separated by a distance of the order of Angstrom units. As a consequence of this charge separation there exists a potential gradient or potential difference across the interphasial region. The force per unit charge experienced at any point in an electric field is equal to the potential gradient at that point. In view of the small distance of charge separation at the electrical double layer the potential gradient will be large. Clearly the magnitude of this potential gradient will influence the rate of transfer of charge from one phase to the other at the electrode/electrolyte interphase. It is apparent that the distribution of charge (i.e. the distance between the charged particles) is a major factor influencing the interphasial electric field strength and hence the speed of electron transfer between the two phases.

The simplest model of the distribution of ions at the interphase was proposed by Helmoltz[7] who regarded the interphase as consisting

of two layers of equal and opposite charge, one layer situated on the electrode and the other on the solution side of the interphase, approximating to a parallel plate condenser. The following assumptions are inherent in this and other models of the double layer:

(a) the separated charges at the interphase are in electrostatic equilibrium.

(b) there is no transfer of charge in either direction across the interphase with changes in electrode potential.

(c) with changes in electrode potential the charge in solution near to the metal interphase changes.

The above assumptions imply that the electrical double layer is purely capacitive and has no resistive components in parallel with it. In practice metal-solution interphases only approximate to this ideal condition. The mercury/solution interphase approaches this ideal situation because of the high hydrogen overvoltage and relatively poor affinity for oxygen of the mercury electrode in a number of solutions over a wide potential range. Such electrodes (which closely obey the above conditions (a)-(c)) are termed "ideally polarisable".

Gouy[8] and Chapman[9] have extended the Helmoltz concept of the double layer structure to the extent of assuming a diffuse (rather than compact) layer which would be effected by the thermal motion of ions. Chapman's mathematical theory[9] was based on the assumption that the ions were point charges which could approach the electrode within any distance. A physically more realistic model is that of Stern[10] who proposed that ions have finite sizes and approach the electrode only to within a certain critical distance. Stern also postulated that in some cases ions may be specifically adsorbed (i.e. undergo adsorption due to other than purely electrostatic

interactions). Thus based on the ideas of Stern[10] the double layer can be divided into two regions; a compact layer comprised between the electrode and the plane of closest approach and the diffuse double layer extending from the plane of closest approach to the bulk of solution. The difference of potential between the metal and solution can therefore be divided into two parts[10]:

$$\phi_M = (\phi_M - \phi_2) + \phi_2 \qquad (2.1)$$

where ϕ_M is the potential difference between the metal and solution (ϕ_s , the potential on the solution side of the double layer, is zero by convention) and ϕ_2 is the potential at the plane of closest approach. From (2.1) we obtain

$$\frac{\partial \phi_M}{\partial q} = \frac{\partial (\phi_M - \phi_2)}{\partial q} + \frac{\partial \phi_2}{\partial q} \qquad (2.2)$$

which may be written as

$$\frac{1}{C} = \frac{1}{C_{comp}} + \frac{1}{C_{diff}} \qquad (2.3)$$

where C is the double layer differential capacitance and C_{comp} and C_{diff} are the differential capacities corresponding to the compact and diffuse double layers respectively. It is evident that the double layer can be regarded as two capacitors in series. Grahame[11] modified Stern's[10] model of the double layer by considering two distinct planes of closest approach, whereas a common plane was postulated by Stern. Grahame considered the compact layer as consisting of the inner plane of closest approach (inner Helmoltz plane) within which anions can approach the electrode; this plane is located at a closer distance

to the electrode than the distance within which solvated cations approach the electrode (outer Helmoltz plane).

A more recent theory (1963) of the distribution of ions and solvated dipoles in the double layer has been advanced by Devanathan, Bockris and Müller[12], in which adsorbed solvated cations are regarded as remaining outside a layer of strongly orientated solvent dipoles. Specifically adsorbed anions are regarded as being able to penetrate the inner solvent layer. Figure 2-1 shows a schematic representation of the solvent adsorption model of the electrode-electrolyte interphase according to Devanathan et. al[12] Water molecules are regarded as being adsorbed with their negative ends pointing either towards or away from the metal surface, depending on the electrode charge or potential.

Equation (2.3) shows that when $C_{comp} \gg C_{diff}$, $C \sim C_{diff}$, and when $C_{diff} \gg C_{comp}$, $C \sim C_{comp}$. The value of the smaller capacity contribution thus mainly determines the overall value of the double layer differential capacitance. Grahame[11] has shown, using the Gouy-Chapman theory, that C_{diff} is related to potential and concentration of an aqueous, symmetrical, electrolyte (C^s) at 25°C by

$$C_{diff} = 228.5\,|z|\,(C^s)^{\frac{1}{2}} \cosh\,(19.46|z|\,\Phi_2) \qquad (2.4)$$

It is apparent from equation (2.4) that as the electrolyte concentration is lowered C_{diff} is reduced and consequently the overall double layer capacitance is determined by C_{diff}. The observed capacity-potential curve for an ideally polarisable electrode in a symmetrical electrolyte which exhibits little specific adsorption (e.g. mercury in NaF solutions), shows a pronounced minimum which becomes less pronounced and ultimately disappears

Fig·2-1 Possible structure of a metal–electrolyte interphase (Bockris et al., 1963)

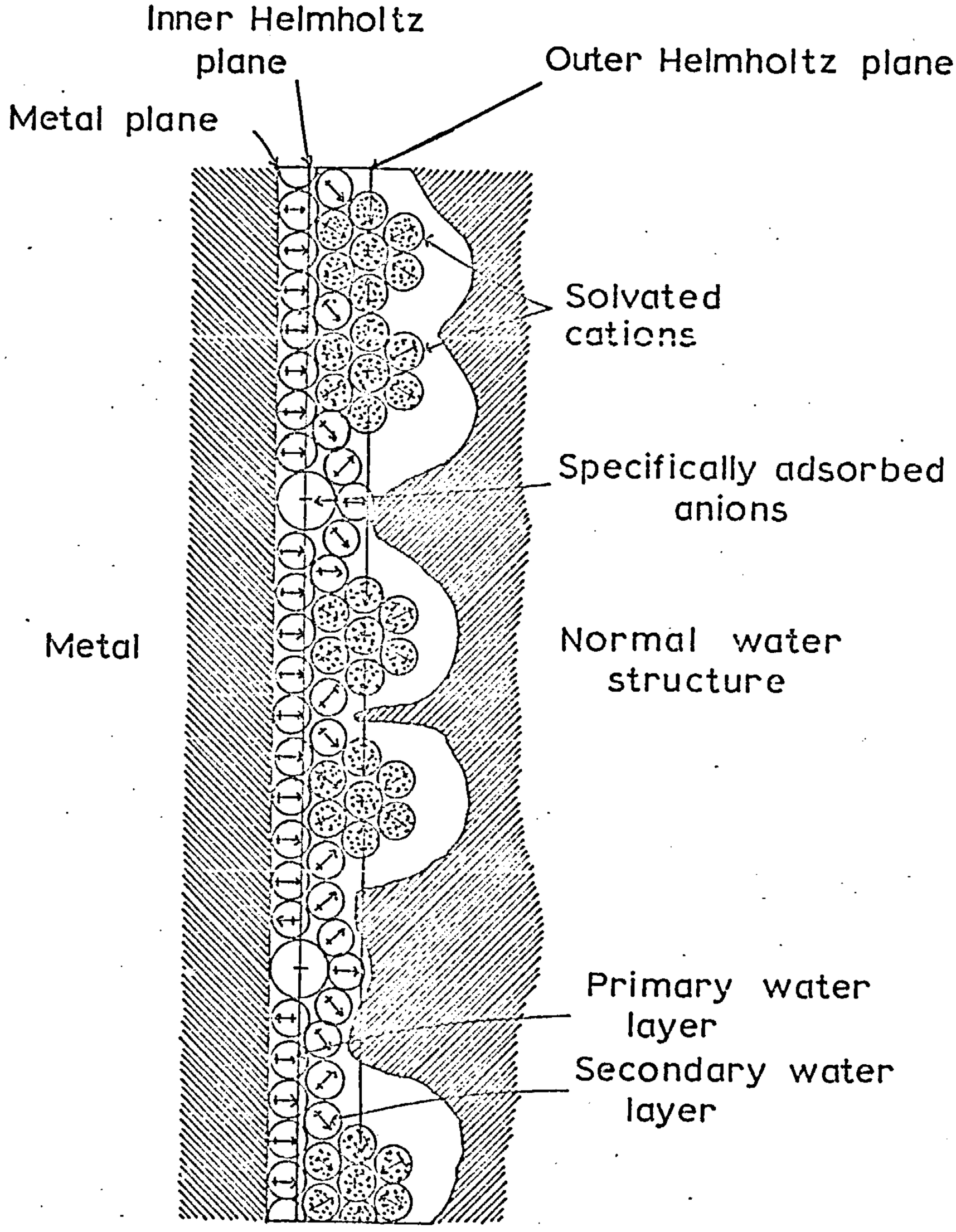

with increasing concentration. This minimum corresponds to a predominant influence of the diffuse double layer capacitance and the dependence of C_{diff} on ϕ_2 as calculated from equation (2.4) corresponds to this shape of curve. The minimum of the capacitance-potential curve occurs at the potential of zero charge (p.z.c.) for a z-z electrolyte. Grahame[13] has modified the theory for unsymmetrical electrolytes.

The C_{comp} term of equation (2.3) is not accessible for experimental determination. However, Grahame[11] calculated C_{comp} from experimental values of C and from C_{diff} values calculated from the Gouy-Chapman theory. The C_{comp} values were computed for concentrated electrolyte solutions since C_{diff} is then much higher than C_{comp} (equation 2.4) . Grahame's work[11] shows that C_{comp} depends solely on the charge on the electrode and not on the electrolyte concentration, for the case of an electrolyte exhibiting little specific adsorption.

Many attempts have been made to improve the above model of the electrical double layer and the comprehensive review of Payne[14](1973) gives details of recent progress in this field.

Frumkin[15,16] has discussed the influence of the p.z.c. (or E_z) on the electrochemical behaviour of metals. The charge on the electrode plays an important role in determining which species are adsorbed at the electrode. The magnitude of the charge is determined by the quantity $(E-E_z)$ which is referred to as a rational potential, E_R. At positive E_R's adsorption of negative ions is favoured and at negative E_R's adsorption of positive ions is favoured. When E_R tends to E_z adsorption of neutral molecules competes favourably with ionic adsorption.

In conclusion, a study of the differential capacitance together with a knowledge of the p.z.c., is of fundamental importance in establishing conditions under which the exchange reaction at an electrode-electrolyte interphase may be studied in the absence of adsorption and film formation at the electrode surface.

2.2. The Charge Transfer Process

Electrode processes are heterogeneous chemical reactions occurring at the interphase of a metal and an electrolyte, accompanied by the transfer of electric charge through this interphasial region. Since charge transfer always involves electrons, the electrode process is the transfer of electrons from one substance to another. The electrode process is therefore a redox type reaction and may be represented by the overall equation

$$O + ze \underset{k_a}{\overset{k_c}{\rightleftharpoons}} R \qquad (2.5)$$

The overall current (per unit electrode area) flowing in (2.5), at a given potential, can be expressed as the difference between the forward and reverse rates

$$i = zF(k_c C_O^s - k_a C_R^s) \qquad (2.6)$$

In (2.6) C_O^s and C_R^s are the surface concentrations of O and R, whilst k_c and k_a are potential dependent rate constants given by

$$k_c = k_c^o \exp\left(\frac{-\alpha zFE}{RT}\right) \qquad (2.7)$$

$$k_a = k_a^o \exp\left(\frac{(1-\alpha)zFE}{RT}\right) \qquad (2.8)$$

where α is the charge transfer coefficient, E the potential of the electrode on a suitable reference electrode scale and k_c^o and k_a^o are the values of k_c and k_a at the reference potential.

Putting (2.7) into (2.6) we obtain

$$i = zF\left[k_c^o C_O^s \exp\left(\frac{-\alpha zFE}{RT}\right) - k_a^o C_R^s \exp\left(\frac{(1-\alpha)zFE}{RT}\right)\right] \qquad (2.9)$$

when $i = 0$, i.e. at the reversible potential (E_r)

$$i_c = i_a = i_o \qquad (2.10)$$

i_o is defined as the exchange current density and it follows from (2.10) that

$$i_o = zFk_c^o C_O^s \exp\left(\frac{-\alpha zFE_r}{RT}\right) = zFk_a^o C_R^s \exp\left(\frac{(1-\alpha)zFE_r}{RT}\right) \qquad (2.11)$$

By solving (2.11) for $zFk_c^o C_O^s$ and $zFk_a^o C_R^s$ and substituting into (2.9) we obtain

$$i = i_o\left[\exp\left(\frac{-\alpha zF(E-E_r)}{RT}\right) - \exp\left(\frac{(1-\alpha)zF(E-E_r)}{RT}\right)\right] \qquad (2.12)$$

where $(E-E_r)$ is defined as the charge transfer overpotential[17] (η_D). Equation (2.12) describes the current density-overpotential relationship for an electrode/electrolyte system in the presence of excess supporting electrolyte and was first derived by Erdey-Gruz and Volmer[18]. Marcus[19] has shown that the charge transfer coefficient is a function of several terms which are dependent on potential, however, if the effects due to the double layer are small and the potential is not far removed from the equilibrium potential ($\pm$250 mV)

then α becomes independent of potential.

For low overpotentials ($|\eta_D| \ll \frac{RT}{\alpha zF}$ or $|\eta_D| \ll \frac{RT}{(1-\alpha)zF}$) the overpotential-current curve is linear. Differentiation of the Erdey-Gruz and Volmer equation (2.12) putting $\eta_D = 0$ gives

$$-\left(\frac{di}{d\eta_D}\right)_{\eta_{D\to 0}} = \frac{zF}{RT} \cdot i_o \qquad (2.13)$$

Since the current-overpotential characteristic is of the form of Ohm's law the reciprocal of the left hand side of (2.13), according to Vetter[20,21], is defined as the charge transfer resistance, R_D (or Θ), thus:

$$\Theta = R_D = \frac{RT}{zF} \cdot \frac{1}{i_o} \qquad (2.14)$$

At high overpotentials we have $|\eta_D| \gg \frac{RT}{\alpha zF}$ or $|\eta_D| \gg \frac{RT}{(1-\alpha)zF}$ and one of the exponentials in equation (2.12) can be dropped. At high cathodic overpotentials we obtain

$$\eta_D = \frac{RT}{\alpha zF} \log i_o - \frac{RT}{\alpha zF} \log i \qquad (2.15)$$

and at high anodic overpotential

$$\eta_D = \frac{RT}{(1-\alpha)zF} \log i_o + \frac{RT}{(1-\alpha)zF} \log i \qquad (2.16)$$

(2.15) and (2.16) are the well known Tafel relationships[22].

The exchange current density can therefore be obtained from the charge transfer resistance at low overpotentials and from high overpotential measurements by extrapolation of η_D vs log i plots

to the equilibrium potential. The concept of exchange current was introduced by Butler[23] in 1936 and its dependence on reactant concentration is given by[24]

$$i_o = zFk^o(C_O)^{(1-\alpha)}(C_R)^{\alpha} \qquad (2.17)$$

where k^o is the apparent standard rate constant first introduced by Randles[25].

The theory of the charge transfer process as outlined above applies only to the simple electrode reaction for which the rate determining step can be identified with the overall reaction, i.e. for a process with $z > 1$ all the electrons are transferred simultaneously. Electrode reactions in which a number of electrons are transferred successively have been recently, comprehensively, reviewed by Losev[26] from both theoretical and experimental viewpoints. Losev[26] has considered processes with a single limiting step and processes with comparable rate constants for successive steps. The salient aspects of Losev's arguments are presented in Appendix 2.

2.3. Mass Transfer Processes

Equation (2.5) may be considered to be composed of the following individual parts:

$$O_{bulk} \longrightarrow O_{electrode} \qquad (2.18)$$

$$O_{electrode} + ze \longrightarrow R_{electrode} \qquad (2.19)$$

$$R_{electrode} \longrightarrow R_{bulk} \qquad (2.20)$$

The overall flow of electrons can be limited by either (2.18) or (2.19). If (2.18) has a slower rate than (2.19) the process is limited by mass transfer of O to the electrode. Such electrode reactions are termed mass transfer controlled. If, however, (2.19) has a slower rate than (2.18) the rate of electron transfer limits the process and the electrode reaction is said to be charge transfer controlled. It should be noted that in some instances neither of the above processes are as slow as a chemical transformation involving the electroactive species, in which case the chemical transformation is the rate determining process.

Three modes of mass transfer are normally encountered: migration, convection and diffusion.

Mass transfer by migration is a result of the forces exerted on charged particles by an electric field. In the presence of a large excess of supporting electrolyte migration of electroactive material is minimised to an extent where it can be neglected.

Natural or free convection develops spontaneously in any solution, undergoing electrolysis, as a result of density differences which develop near the electrode, it may also arise from thermal or mechanical disturbances. Forced convection may be effected by stirring the solution, rotating the electrode (see section 2.4), bubbling gas near to the electrode and so forth.

Diffusion exists whenever concentration differences are established. Since a concentration gradient develops as soon as electrolysis is initiated, diffusion occurs to some extent in every practical electrode reaction. If we consider a plane electrode immersed in an electrolyte solution containing O which is reduced typically according to equation (2.5), then the number of moles of

O which diffuse past a given cross-section area (A cm^2) in a time dt, is proportional to the concentration gradient of diffusing species

$$\frac{dN}{Adt} = D_O \frac{\partial c_O}{\partial x} \qquad (2.21)$$

Equation (2.21) is Fick's first law, relating diffusion rates to concentration. The left hand side of (2.21) is called the flux (q) and is the number of moles diffusing per unit time through unit area. D_0 is the diffusion coefficient, defined as the number of molecules per second crossing unit area under unit concentration gradient. If one now considers the electrolysis over a period of time, it is evident that C_0 and hence $\frac{\partial c_0}{\partial x}$ must decrease with time since O is being consumed at the electrode. Fick's second law describes the variation of C_0 with time and may be summarised as

$$\frac{\partial c_O}{\partial t} = D_O \frac{\partial^2 c_O}{\partial x^2} \qquad (2.22)$$

The solution of (2.22) in terms of C_0 (x,t) is

$$C_O(x,t) = C_O^b \frac{2}{\pi^{\frac{1}{2}}} \int_0^{x/2 D^{\frac{1}{2}} t^{\frac{1}{2}}} e^{-y^2} dy \qquad (2.23)$$

The conditions for the solution of (2.22) are

at t = 0: $C_O^s = C_O^b$

at t > 0: $C_O^s = 0$

also, $C_O \longrightarrow C_O^b$ as $x \longrightarrow \infty$

The instantaneous current, i_t, is proportional to the flux at x = 0, thus

$$i_t = zFAq(0,t) = (zFAD \left(\frac{\partial c_0}{\partial x}\right)_{0,t} \qquad (2.24)$$

The value of $\left(\frac{\partial c_0}{\partial x}\right)_{0,t}$ is obtained by differentiating equation (2.23) and evaluating at x = 0. The final expression for the instantaneous current at a plane electrode under diffusion control becomes

$$i_t = \frac{zFAD_0^{\frac{1}{2}} C_0^b}{\pi^{\frac{1}{2}} t^{\frac{1}{2}}} \qquad (2.25)$$

Since the instantaneous current is purely diffusion controlled it is often denoted by i_d. The term i_t is preferable as it emphasises the transient nature of the instantaneous current.

2.4. The Rotating Disc Electrode (RDE)

The RDE gives rise to the phenomenon of forced convection. The fundamental problem in stirred solutions is that one is dealing with a fluid moving past a solid surface. At the surface of the solid the fluid flow velocity is zero. Some distance away from the solid surface, measured in the x direction normal to the electrode surface, the flow velocity has a value characteristic of the bulk of solution uneffected by the solid body. Between these extremes there exists a thin layer in which the main change in velocity gradient occurs. This layer is the hydrodynamic boundary layer (δ_o). If the moving fluid contains solute, the concentration of which varies throughout the solution, the effect of molecular or ionic diffusion must be considered. If a potential

is applied, the solute is transported to the electrode surface by diffusion as a result of the concentration gradient produced. Furthermore, solute species are carried along by the physically moving liquid. Thus forced convection consists of diffusion and convective transfer, one or the other of which may predominate in magnitude.

Hydrodynamic treatment[27] of the problem leads to the concept of a thin diffusion boundary layer close to the electrode surface. The largest change of concentration occurs in this layer. The hydrodynamic approach shows that the diffusion boundary layer thickness (δ) is related to the physical properties of the solution by[27]

$$\delta = 1.62 D^{\frac{1}{3}} \nu^{\frac{1}{6}} \omega^{-\frac{1}{2}} \qquad (2.26)$$

where ν is the kinematic viscosity of the electrolyte and ω the angular velocity of the electrode. In principle each electroactive species has its own value of δ . It should be noted that $\delta \ll \delta_o$

In the present work the RDE was used to investigate the anodic behaviour of indium in various electrolyte solutions. Consider the general reaction

$$R \underset{k_c}{\overset{k_a}{\rightleftharpoons}} O + ze \qquad (2.27)$$

The overall current (per unit electrode area) flowing in (2.27) at a given potential, may be written as

$$i = zF(k_a C_R^s - k_c C_O^s) \qquad (2.28)$$

In (2.28) the convention that an anodic current is positive is adopted. Harrison and Thirsk[28] have pointed out that when studying an anodic reaction it is often convenient to allow the net current to be positive. Using Nernst's[29] assumption that concentration varies linearly with distance within the diffusion layer, the current flow is given by

$$i = zF \frac{D_R}{\delta_R}(C_R^b - C_R^s) = zF \frac{D_O}{\delta_O}(C_O^s - C_O^b) \qquad (2.29)$$

The limiting current density occurs when $C_R^s = 0$, thus

$$i_{L,R} = zF \frac{D_R C_R^b}{\delta_R} \qquad (2.30)$$

Putting (2.30) into (2.29) we obtain

$$i = i_{L,R} - zF \frac{D_R C_R^s}{\delta_R} = zF \frac{D_O}{\delta_O} C_O^s - i_{L,O} \qquad (2.31)$$

solving (2.31) for C_R^s and C_O^s and substituting in (2.28) we obtain

$$i = k_a \frac{\delta_R}{D_R}(i_{L,R} - i) - k_c \frac{\delta_O}{D_O}(i + i_{L,O}) \qquad (2.32)$$

multiplying out (2.32) and rearranging gives

$$i(1 + k_a \frac{\delta_R}{D_R} - k_c \frac{\delta_O}{D_O}) = k_a \frac{\delta_R}{D_R} i_{L,R} - k_c \frac{\delta_O}{D_O} i_{L,O} \qquad (2.33)$$

substituting for the limiting currents we obtain

$$i(1 + k_a \frac{\delta_R}{D_R} - k_c \frac{\delta_O}{D_O}) = zF(k_a C_R^b - k_c C_O^b) \qquad (2.34)$$

The right hand side of (2.34) is defined as i_∞, thus

$$i(1 + k_a \frac{\delta_R}{D_R} - k_c \frac{\delta_O}{D_O}) = i_\infty \qquad (2.35)$$

cross multiplication of (2.35) and multiplying out the left hand side gives

$$\frac{1}{i_\infty} + \frac{1}{i_\infty}(k_a \frac{\delta_R}{D_R} - k_c \frac{\delta_O}{D_O}) = \frac{1}{i} \qquad (2.36)$$

Introducing the Levich equation (2.26) into (2.36) we obtain

$$\frac{1}{i_\infty} + \frac{K}{\omega^{\frac{1}{2}}} = \frac{1}{i} \qquad (2.37)$$

Equation (2.37) predicts that the measured anodic currents are a function of $\omega^{-\frac{1}{2}}$. Furthermore a plot of i^{-1} vs. $\omega^{-\frac{1}{2}}$ should be linear with an intercept i_∞^{-1} which gives a measure of the true kinetic current in the absence of diffusion effects.

In equation (2.37) K is given by the following expression

$$K = \frac{\frac{k_a(\delta_R/\omega^{\frac{1}{2}})}{D_R} + \frac{k_c(\delta_O/\omega^{\frac{1}{2}})}{D_O}}{i_\infty} \qquad (2.38)$$

substituting for i_∞ from (2.34) and dividing through by k_a we obtain

$$K = \frac{\frac{(\delta_R/\omega^{\frac{1}{2}})}{D_R} + \frac{k_c}{k_a}\frac{(\delta_O/\omega^{\frac{1}{2}})}{D_O}}{zF(C_R^b - \frac{k_c}{k_a} C_O^b)} \qquad (2.39)$$

The quotient $\frac{k_c}{k_a}$ follows from (2.7) and (2.8) as

$$\frac{k_c}{k_a} = \frac{k^o_c}{k^o_a} \exp \frac{zFE}{RT} \qquad (2.40)$$

which we may rewrite as

$$\frac{k_c}{k_a} = k' \exp \frac{zF(E-E_r)}{RT} \qquad (2.41)$$

putting (2.41) into (2.39) gives

$$K = \frac{\frac{(\delta_R/\omega^{\frac{1}{2}})}{D_R} + k' \frac{(\delta_O/\omega^{\frac{1}{2}})}{D_O} \exp \frac{zF(E-E_r)}{RT}}{zF(C^b_R - k' C^b_O \exp \frac{zF(E-E_r)}{RT})} \qquad (2.42)$$

When R is a solid $\frac{(\delta_R/\omega^{\frac{1}{2}})}{D_R} = 0$ and if $C^b_R \gg k' C^b_O \exp \frac{zF(E-E_r)}{RT}$ because C^b_O is very small, then (2.42) reduces to

$$K = \frac{k' \exp \frac{zF(E-E_r)}{RT}}{zFC^b_R} \cdot \frac{(\delta_O/\omega^{\frac{1}{2}})}{D_O} \qquad (2.43)$$

Equation (2.43) shows that for an anodic reaction, in a system where C^b_O is very small, the slopes of i^{-1} vs. $\omega^{-\frac{1}{2}}$ plots are potential dependent. Also a plot of $\log(\frac{\partial i^{-1}}{\partial \omega^{-\frac{1}{2}}})$ vs. $(E-E_r)$ will be linear, with a slope proportional to z.

2.5. Faradaic Impedance

The basis of this technique is to represent the various factors

contributing to the polarisation at an electrode as a model impedance network. Randles[30,31] proposed the equivalent circuit for the electrode impedance shown in figure 2-2a., where R_{sol} is the electrolyte ohmic resistance, C_L the double layer capacitance which varies with d.c. potential depending on the concentration and nature of the electrolyte. R_D (or Θ) is the charge transfer resistance and is related to the exchange current density by equation (2.12). The Warburg impedance[32](W) is the impedance to a.c. current due to the charged species diffusing to and from the electrode. Randles derived the following expression for Θ and W,

$$\Theta = \frac{RT}{z^2F^2k_{sh}} (C_O^s)^{\alpha} (C_R^s)^{1-\alpha} \qquad (2.44)$$

and

$$W = \sigma \omega^{-\frac{1}{2}} (1 - j) \qquad (2.45)$$

where σ is the Warburg coefficient, ω the angular frequency and $j = (-1)^{\frac{1}{2}}$. The Warburg coefficient can be expressed as

$$\sigma = \frac{RT}{z^2F^2 2^{\frac{1}{2}}} \left(\frac{1}{C_O^s D_O^{\frac{1}{2}}} + \frac{1}{C_R^s D_R^{\frac{1}{2}}} \right) \qquad (2.46)$$

In (2.44) and (2.46) if measurements are made at the equilibrium potential C_O^s and C_R^s can be replaced by C_O^b and C_R^b. At d.c. potentials away from the equilibrium potential σ and Θ can be expressed in terms of bulk concentrations of O and R, provided that (2.44) and (2.46) are suitably modified[33].

Fig·2-2a Equivalent circuit of electrode impedance

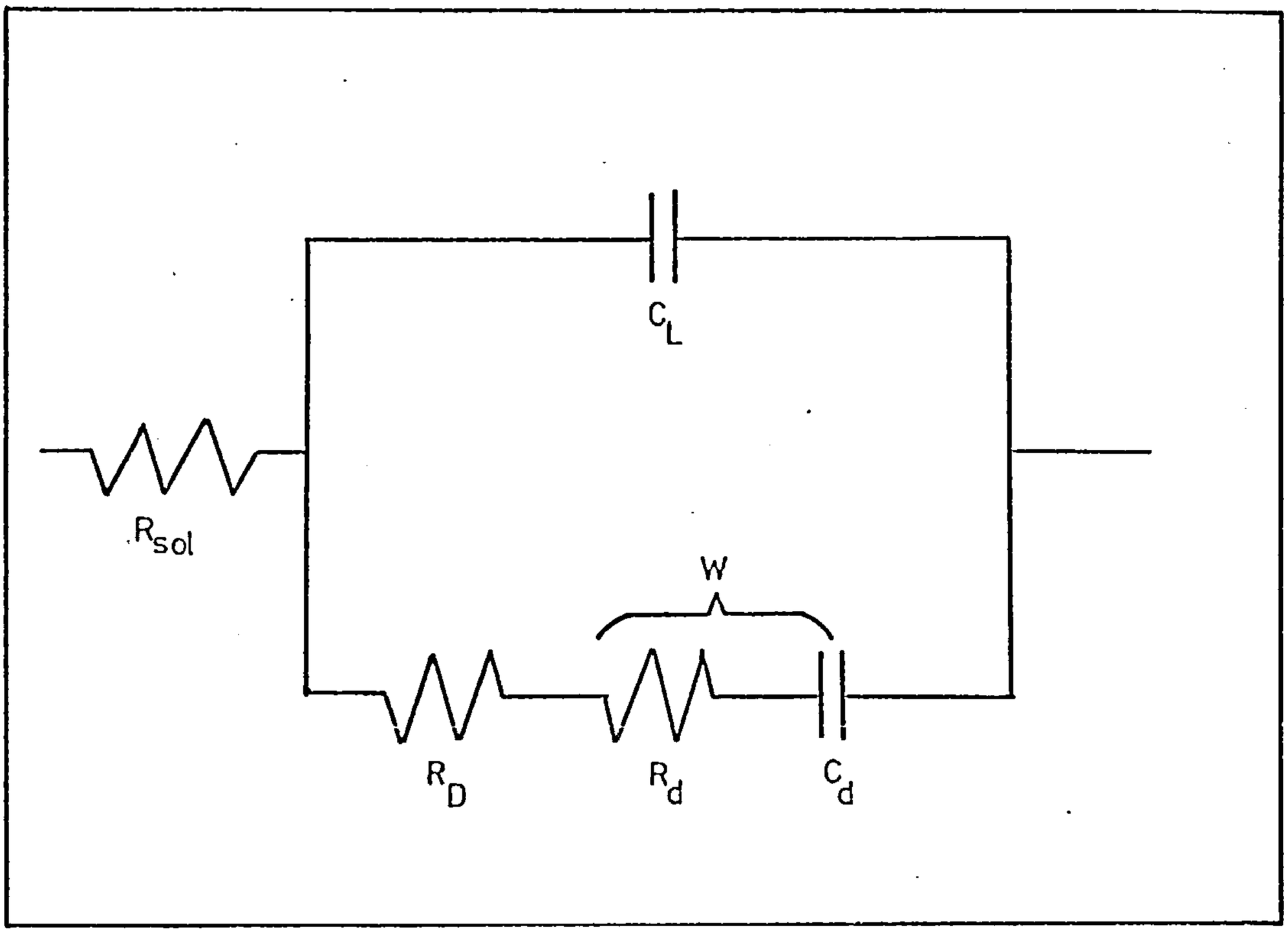

Fig·2-2b Z'-Z'' plot at low frequencies

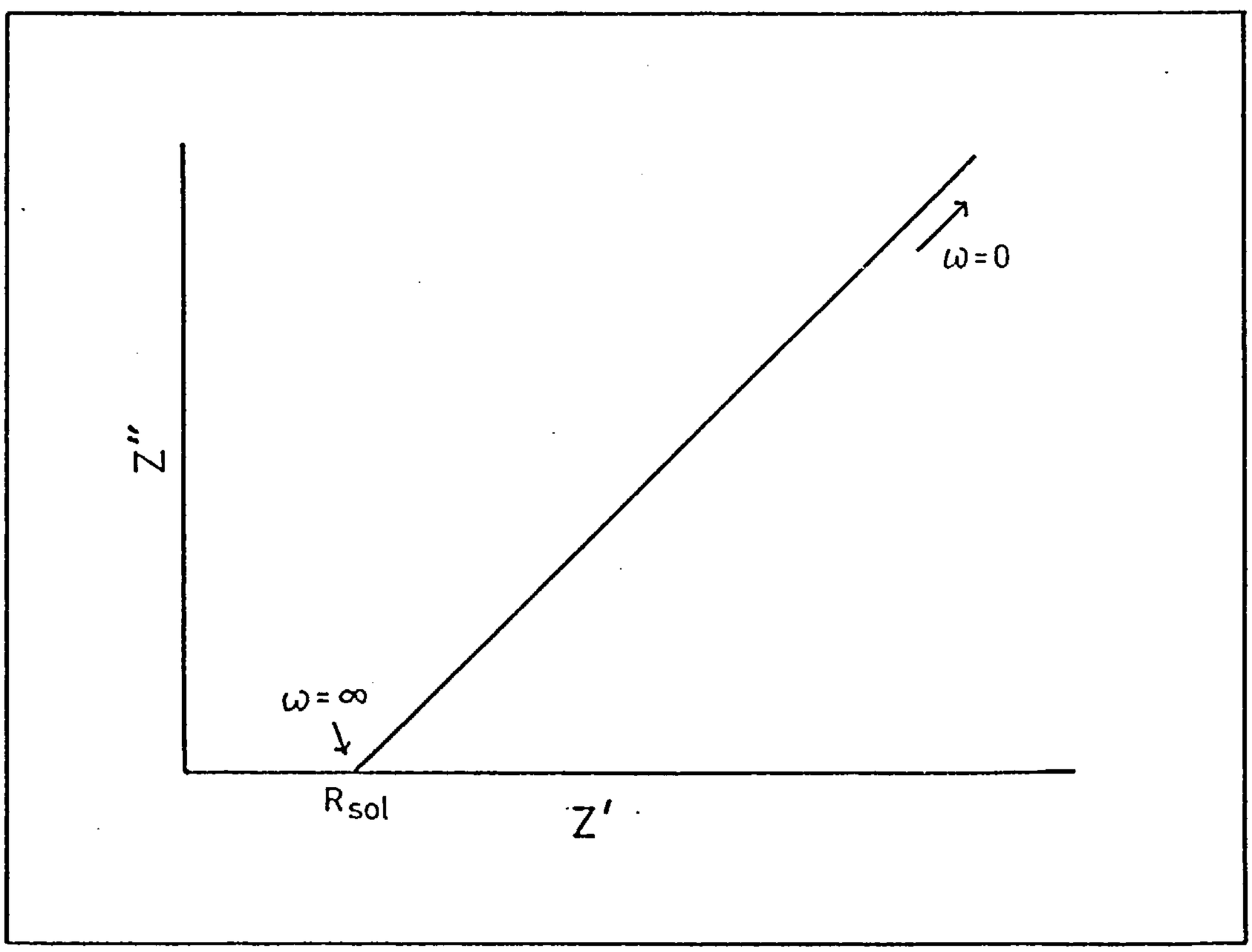

Various methods have been proposed for the determination of Θ and σ from impedance measurements. Vector methods were used by Randles[30] and Delahay et. al[34]. Gerischer[35] determined σ and Θ, however in this treatment[35] the imaginary part of the Warburg impedance was neglected. Vetter[36] corrected the cell impedance for the double layer capacitance and solution ohmic resistance. In the present studies the so called "complex plane" impedance technique devised by Sluyters[37] was used. This method entails plotting the real component (Z') and the imaginary component (Z'') of the cell impedance against each other as a function of some varied parameter (frequency, concentration or d.c. voltage). It is possible to calculate C_L, Θ and σ using the complex plane impedance method.

From figure 2-2a the cell impedance is given by[37]

$$Z = R_{sol} + \frac{1}{j\omega C_L + \frac{1}{\Theta + \sigma\omega^{\frac{1}{2}} - j\sigma\omega^{\frac{1}{2}}}} \qquad (2.47)$$

After separation of the real and imaginary parts of Z we obtain

$$Z = Z' - jZ'' \qquad (2.48)$$

where Z' and Z'' are given by

$$Z' = R_{sol} + \frac{\Theta + \sigma\omega^{-\frac{1}{2}}}{(\sigma\omega^{\frac{1}{2}}C_L+1)^2 + \omega^2 C_L^2(\Theta + \omega^{-\frac{1}{2}})^2} \qquad (2.49)$$

and

$$Z'' = \frac{\omega C_L(\Theta+\sigma\omega^{-\frac{1}{2}})^2 + \sigma\omega^{-\frac{1}{2}}(\sigma\omega^{\frac{1}{2}}C_L+1)}{(\sigma\omega^{\frac{1}{2}}C_L+1)^2 + \omega^2 C_L(\Theta+\sigma\omega^{-\frac{1}{2}})^2} \qquad (2.50)$$

Although equation (2.48) is very complex, its two limiting cases, at low and high frequencies, give important results.

(a) at low frequencies (2.48) reduces to

$$Z = R_{sol} + \Theta + \sigma\omega^{-\frac{1}{2}} - j(\sigma\omega^{-\frac{1}{2}} + 2\sigma^2 C_L) \qquad (2.51)$$

This equation predicts that a plot of Z' vs. Z'' gives a straight line of 45^o slope (figure 2-2b).

(b) At high frequencies for a fairly irreversible reaction, concentration polarisation (W) can be neglected and (2.48) reduces to

$$Z = R_{sol} + \frac{\Theta}{1 + \omega^2 C_L^2 \Theta^2} - j\frac{\omega C_L \Theta^2}{1 + \omega^2 C_L^2 \Theta^2} \qquad (2.52)$$

In this case, if the real and imaginary parts of the impedance are plotted against each other, a semicircle is obtained. Values of R_{sol}, Θ and C_L can be computed from such plots as is shown in figure 2-3a. At lower frequencies diffusion polarisation will give rise to a distortion of the semicircle, as illustrated in figure 2-3b, culminating in the attainment of a line of 45^o slope. The extent of this distortion is dependent upon the relative values of Θ, σ and C_L.

Fig. 2-3a Z' - Z'' plot for irreversible reaction in the absence of concentration polarisation

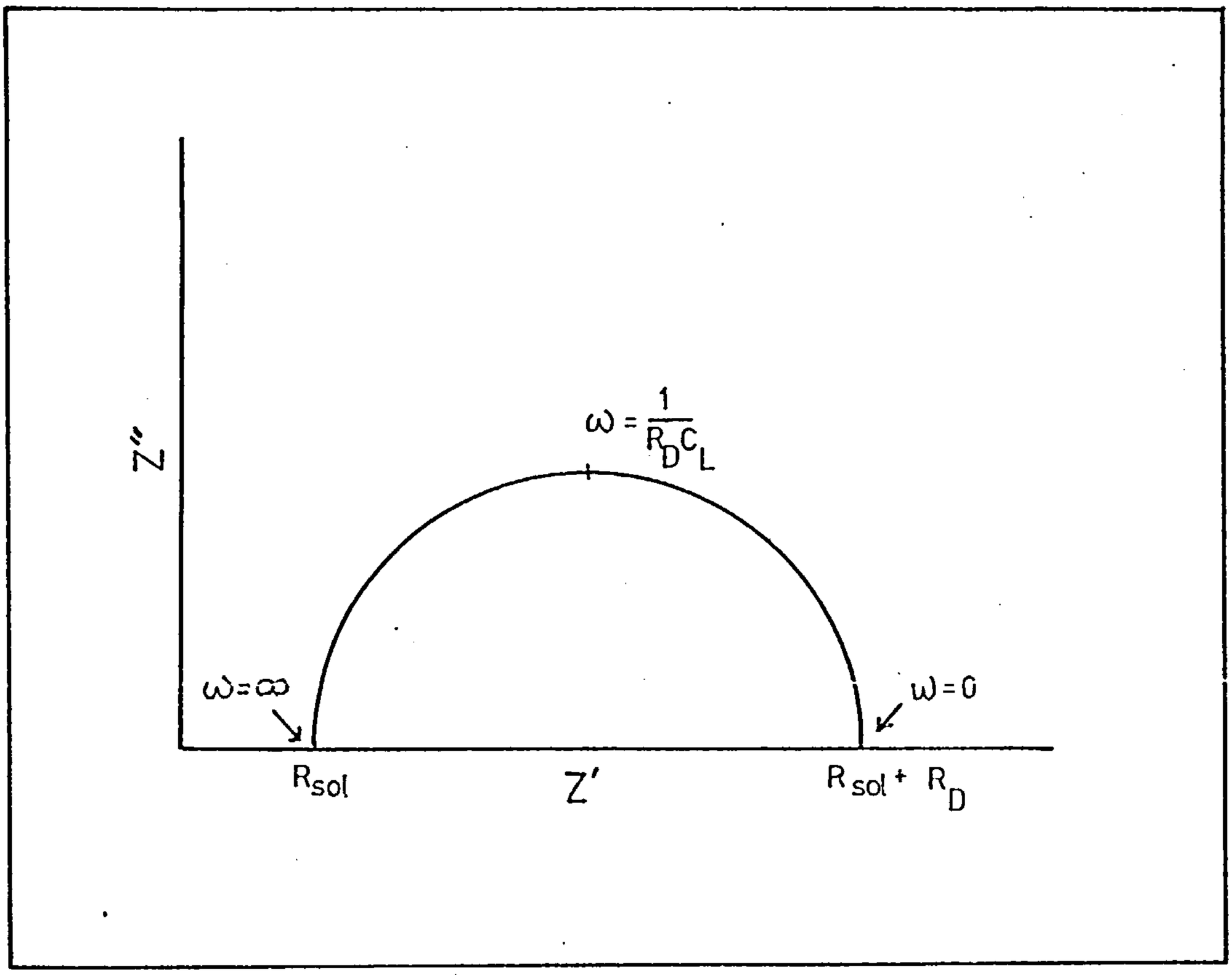

Fig. 2-3b Z'-Z'' plot over whole frequency range

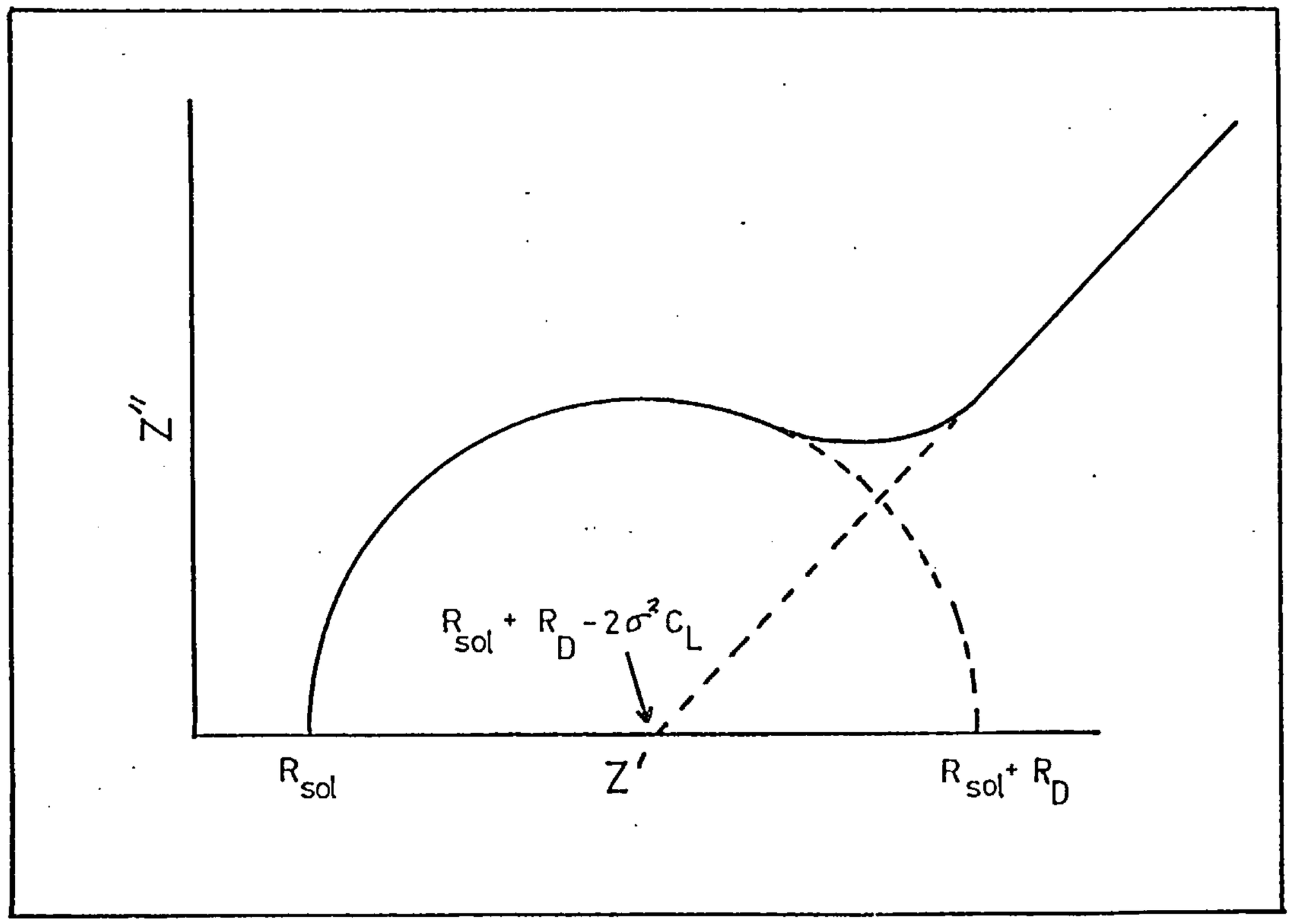

CHAPTER 3

EXPERIMENTAL TECHNIQUES

3.1. Electrolytic Systems

3.1.1. Electrolyte solutions

Electrolytes were prepared from AnalaR grade chemicals and water bidistilled from deionised stock. Stock solutions of $InCl_3$ and $In(ClO_4)_3$ were prepared by dissolving indium metal (99.999%, Johnson Matthey Ltd.) in the appropriate AnalaR grade acid. It was found necessary to reflux the reaction mixture to hasten dissolution of the indium. Analyses of electrolytes are described in appendix 1.

The electrolytes used for differential capacitance measurements were purified by constantly pumping over specially prepared activated charcoal. (The preparation of the charcoal is described in appendix 1). The activated charcoal was contained in a purification limb attached to the cell (figure 3-1). White spot nitrogen, deoxygenated by passing over copper at 400°C and prehumidified, was used to effect circulation of the electrolyte through the charcoal bed. Generally electrolytes were circulated for at least 14 days before measurements were made. Where necessary pH's were adjusted by adding the appropriate AnalaR grade acid and allowing 7 days for circulation prior to making measurements.

3.1.2. Electrolytic cells

All cells were made from borosilicate glass and cell fittings were lubrication free ground glass joints. The cells used for equilibrium potential measurements were H-types, one cavity housing the indium electrode the other the reference electrode.

The cell used for differential capacitance measurements is illustrated in figure 3-1. Figure 3-2a shows the cell used for both rotating disc and linear sweep voltammetric measurements. For faradaic impedance studies the cell is shown in figure 3-2b. Figure 3-3 shows the cells used for galvanostatic polarisation studies.

Electrolytic cells and all glassware were cleaned by steeping for a week in a 50:50 mixture of nitric and sulphuric acids. The acid was removed by thoroughly washing with bidistilled water and finally by soaking in bidistilled water for 24 hours. The cleaned cells were finally dried in an oven at $\sim 120^{\circ}C$.

3.1.3. Electrodes and test electrode pretreatment techniques

3.1.3a differential capacitance measurements

Two types of indium test microelectrode were used for these measurements. Figure 3-4a shows an electrode (superficial area 3.3×10^{-2} cm^2) made by extruding the soft indium into Teflon by use of a mild steel die which also served as the electrical contact. Figure 3-4b shows an electrode (superficial area 7.0×10^{-2} cm^2) fabricated by encapsulating the indium in polythene. This latter method involved building a polythene sheath around indium rod by carefully melting on layers of polythene and then cutting at right-angles to the long axis to expose the reacting electrode area.

The indium test electrode pretreatment technique was established by performing differential capacitance measurements and observing the form and reproducibility of the results obtained for the various pretreatment methods employed. The most satisfactory indium microelectrode pretreatment procedure consisted of mechanically polishing on roughened glass, using bidistilled water as lubricant,

Fig·3-1 Cell used for double layer studies

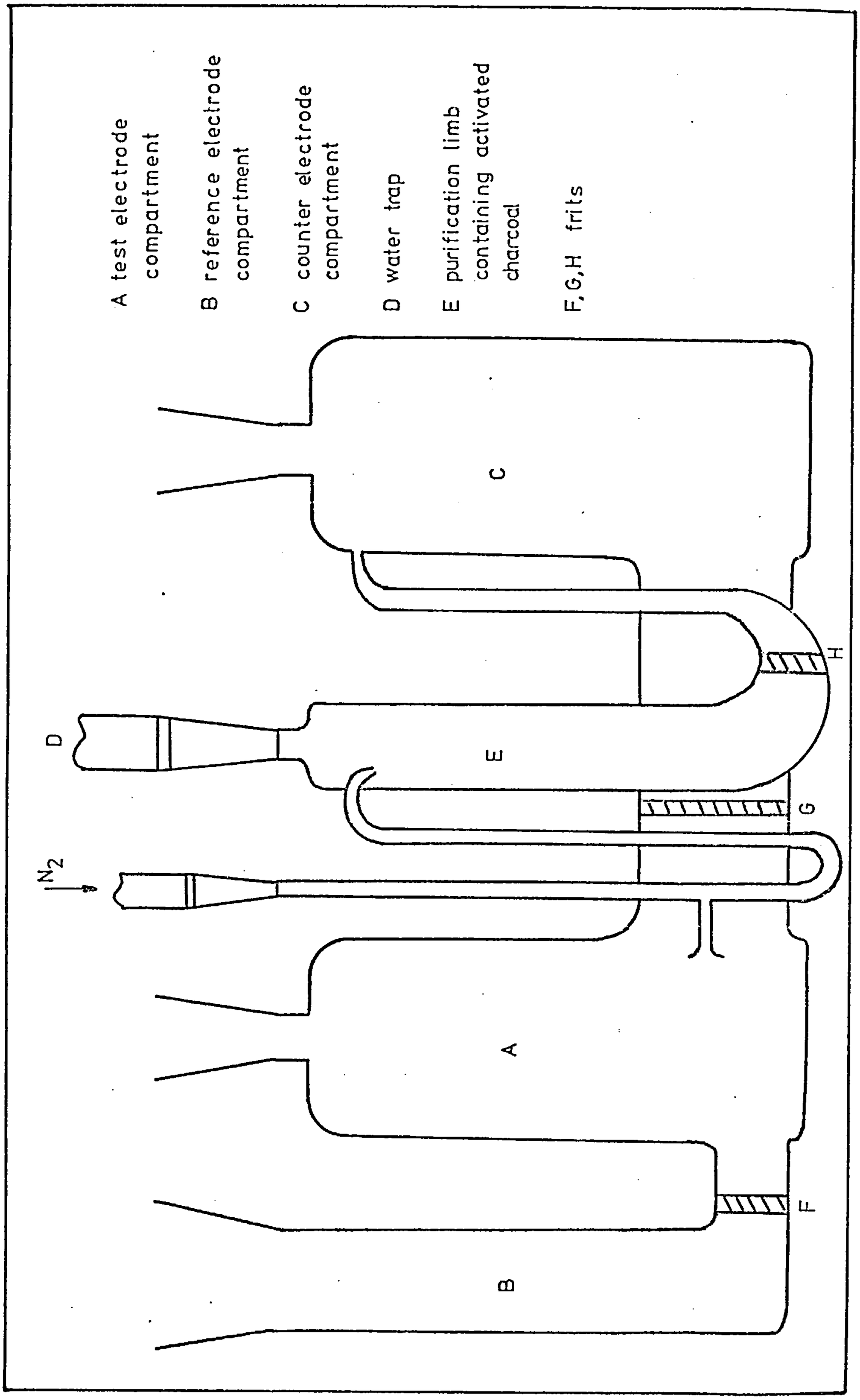

Fig.3-2a Rotating disc electrode and L.S.V cell

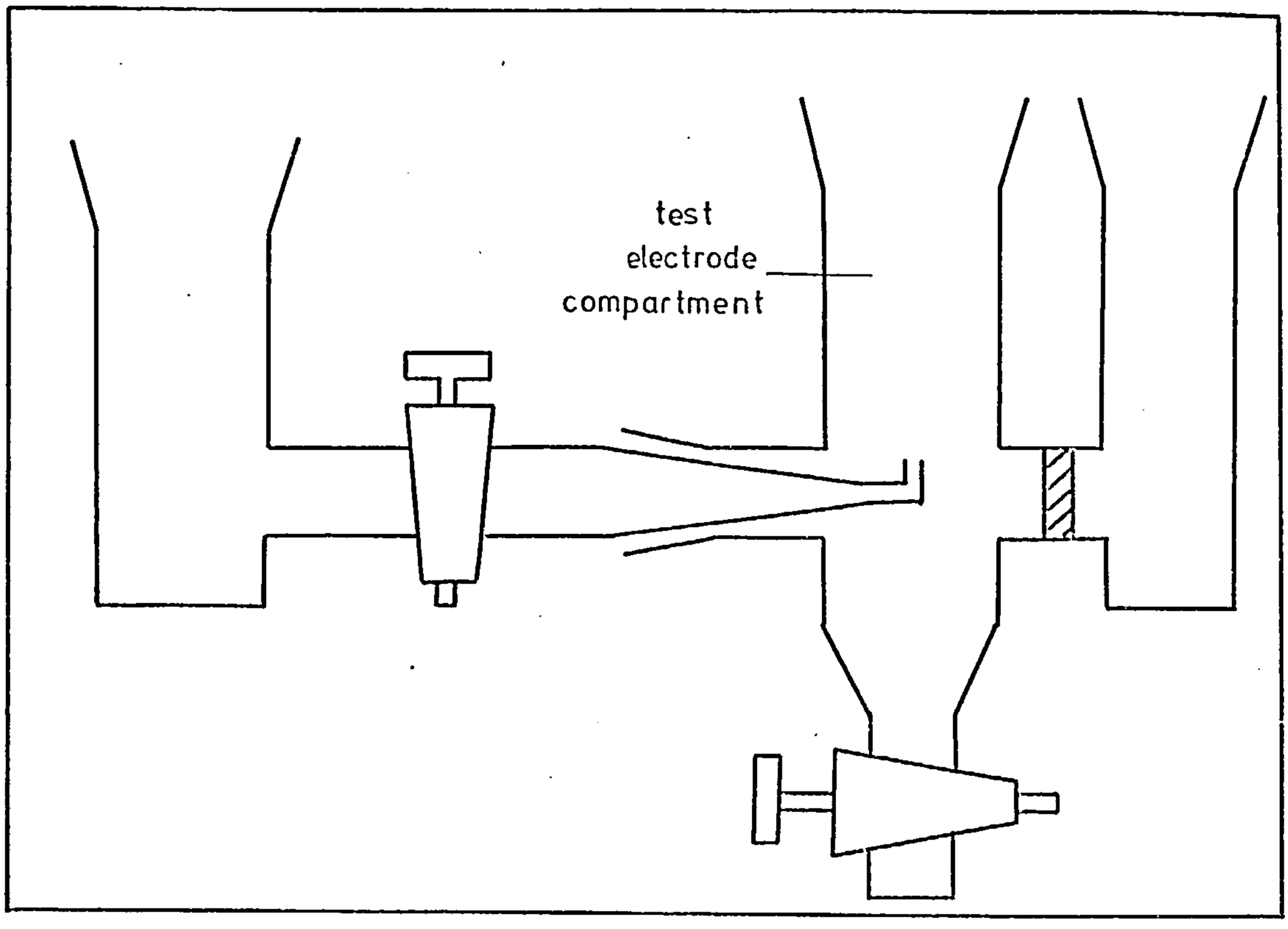

Fig.3-2b Impedance cell

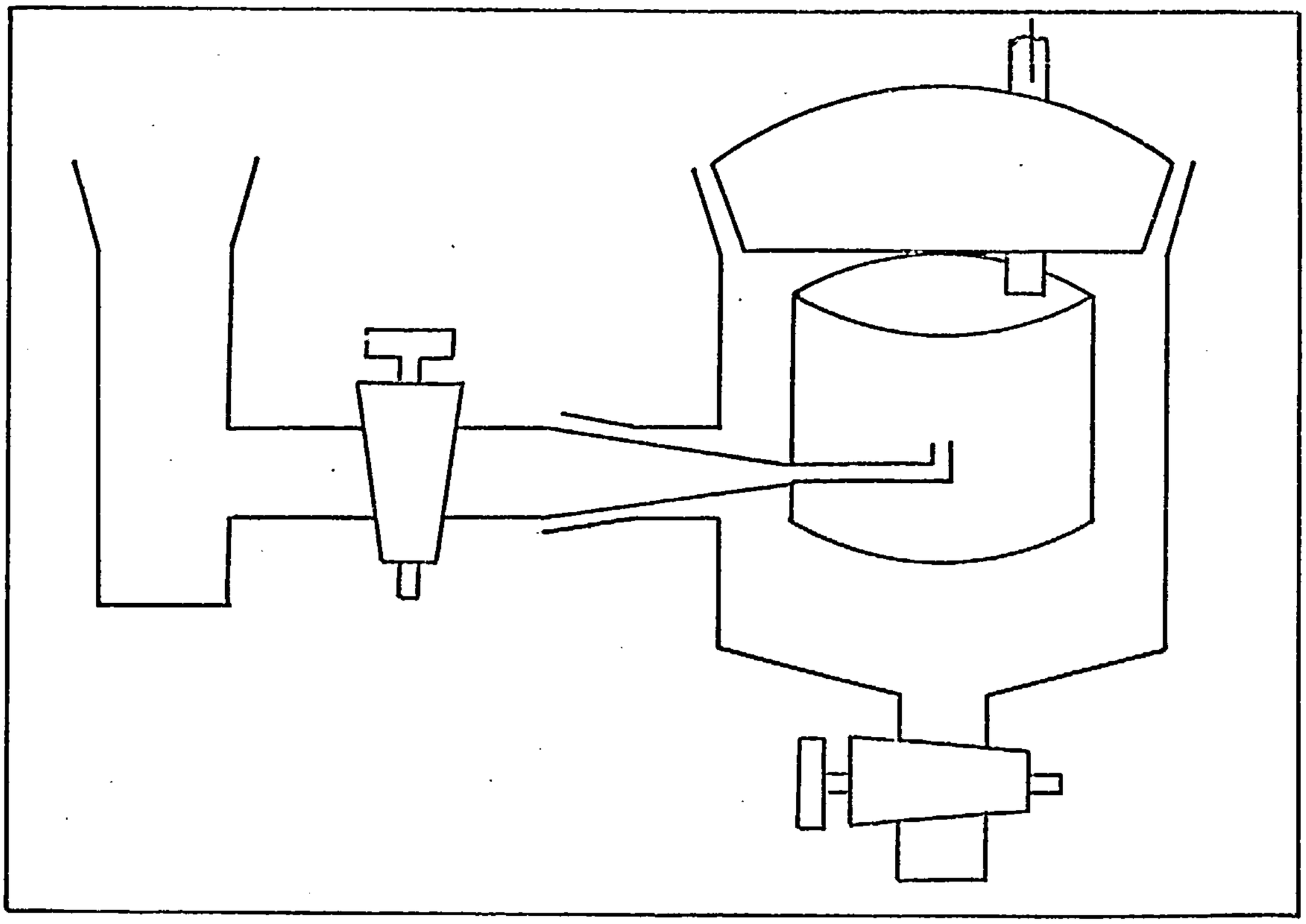

Fig·3-4b Indium microelectrode

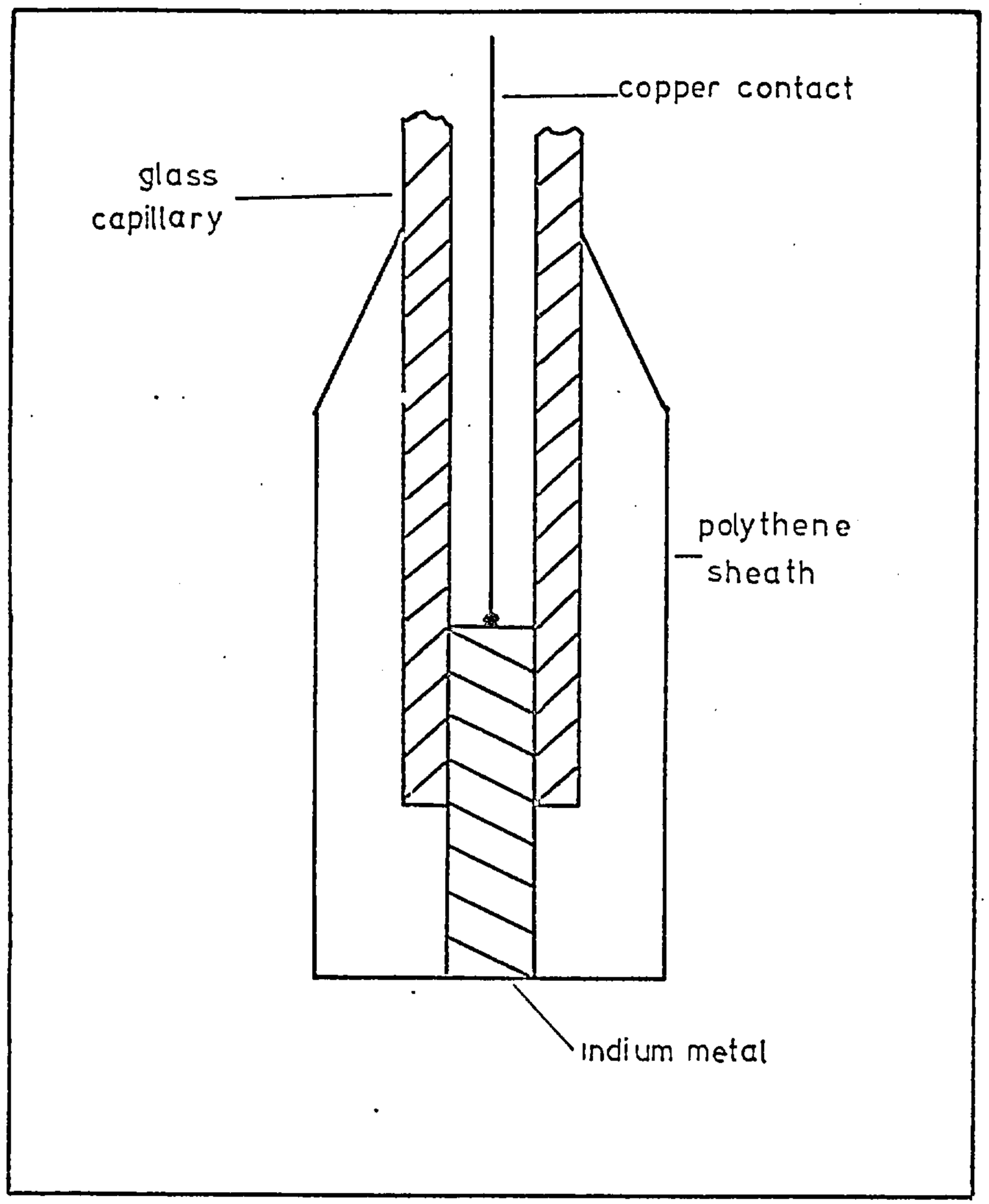

Fig·3-4a Extruding indium test electrode

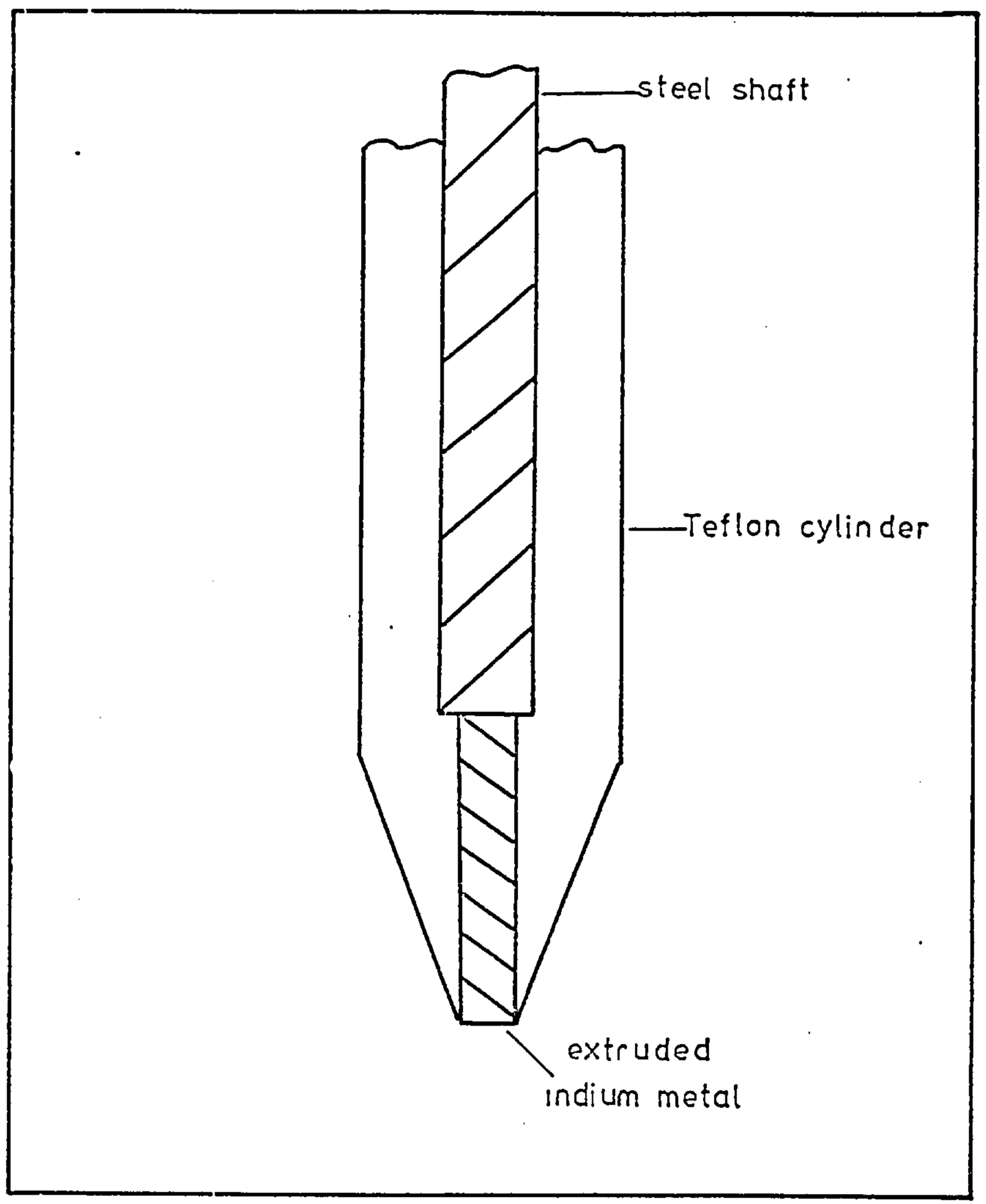

followed by a light chemical etch (e.g. 5 sec. 20% $HClO_4$ v/v). The electrode was finally washed thoroughly with bidistilled water before introducing (wet) into the electrochemical cell. This procedure was found to give results reproducible to $\leq \pm$ 10% which is very acceptable for a solid metal electrode. This pretreatment technique was employed for all measurements using the electrodes shown in figures 3-4a and 3-4b and for rotating disc electrode studies. It should be noted that the results obtained were independent (within experimental error) of which of the two electrodes, described above, was used.

Electropolishing of indium microelectrodes was best done according to the instructions of Goss and Vernon[38]. However, the technique was found to be unsatisfactory since the resulting microelectrode became severely pitted. This latter observation was confirmed by Buck[39] who also found that electropolishing of an indium microelectrode could only be satisfactorily performed if the indium electrode was placed surface upwards in the cell. Buck[39] also reported that satisfactorily electropolished electrodes showed no better reproducibility of experimental results than electrodes pretreated using a simple polish and chemical etch procedure.

Mechanical polishing of indium microelectrodes using silicon carbide abrasive papers proved highly unsatisfactory. Microscopic examination of electrodes treated in this way revealed that the soft metal surface was almost completely covered with embedded silicon carbide particles, thus drastically reducing the reacting area. A similar phenomenon was observed by Dasarathy[40], who noted that indium specimensbecame almost completely embedded with alumina when using a suspension of fine alumina in water as an abrasive medium.

For differential capacitance measurements the counter electrode was a large surface area platinum gauze ($\sim$20 cm^2). The reference electrode was a wick type calomel; saturated KCl (saturated NaCl for perchlorate electrolytes).

3.1.3b equilibrium potential measurements

The test electrode (figure 3-5a) consisted of indium metal rod (3.2 mm diameter) mounted in glass and attached to a stout copper lead by a silver based epoxy resin (Thermosetting silver preparation, types FSP 49H and FSA 49R in a 50:50 mixture, Johnson Matthey Metals Ltd.). The indium was sealed into the glass with Araldite. Before use the test electrodes were electropolished in alcoholic.nitric acid[39] and washed thoroughly with bidistilled water.

Silver/silver chloride reference electrodes were prepared from massive silver (99.9999%, Johnson Matthey Metals Ltd.) sheathed in polythene and cut perpendicular to the long axis so that an area of $\sim$ 0.2 cm^2 was exposed. A thin layer of silver chloride was deposited on the exposed silver (AnalaR HCl). These electrodes were found to be extremely reproducible (replicates did not differ in potential by more than 0.005 mV) and gave the correct potential against the hydrogen electrode in 0.01 mol kg^{-1} HCl.

3.1.3c rotating disc studies

The rotating disc electrode is shown in figure 3-5b. The shape and dimensions of the electrode were in accord with hydrodynamic requirements[41]. Electrical contact between the indium metal and the shaft of the drive system was effected using a stout spring. A mercury pool provided the electrical contact between the rotating electrode and the external circuit. The electrode pretreatment

Fig·3-5b Rotating disc electrode

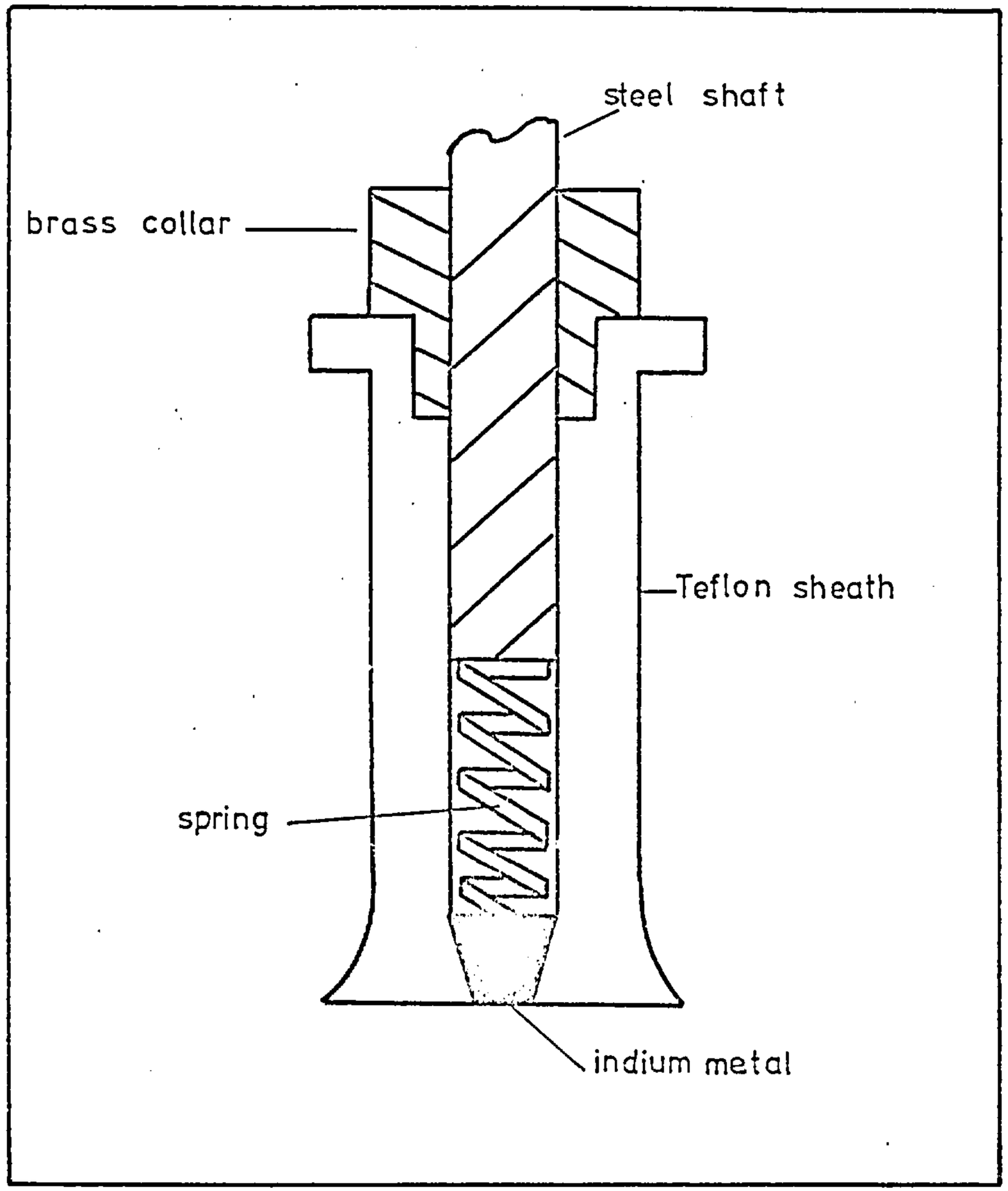

Fig·3-5a Equilibrium potential electrode

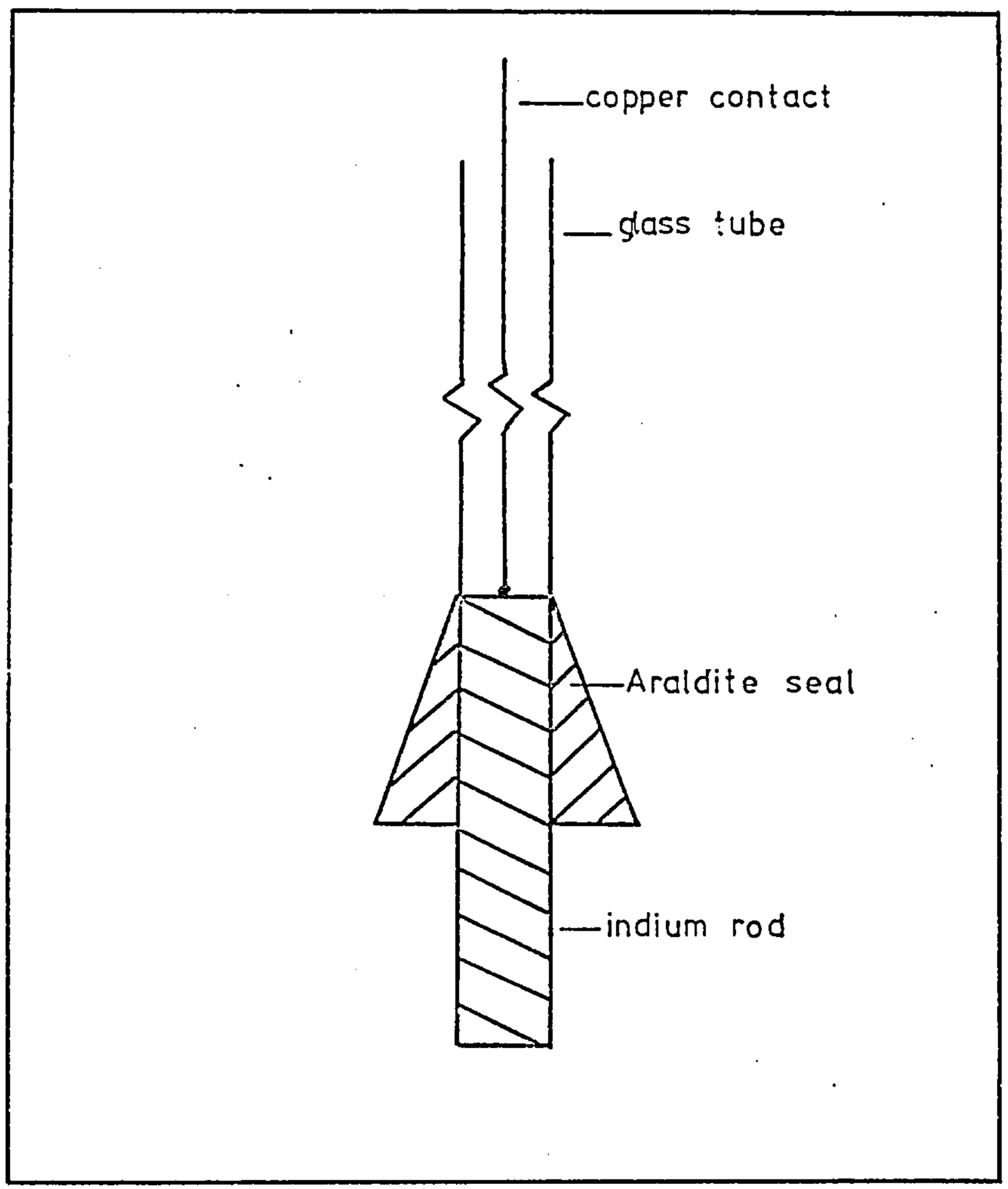

technique employed was the simple polish and chemical etch procedure described for the indium microelectrodes in 3.1.3a.

The counter and reference electrodes were as used for differential capacitance studies and are described in 3.1.3a. The reference electrode compartment of the cell was joined to the test electrode compartment by a luggin capillary and closed liquid seal tap. For alkaline electrolyte solutions a wick type HgO/Hg reference electrode was used.

3.1.3d faradaic impedance measurements

The test electrode is shown in figure 3-4b, and the pretreatment technique described in 3.1.3a.

The counter electrode was a high surface area cylindrical platinum gauze which surrounded the working electrode. The reference electrode used is as described in 3.1.3a and was joined to the working electrode compartment of the cell via a luggin capillary system and closed liquid seal tap.

3.1.3e linear sweep voltammetry (L.S.V.)

The test (figure 3-4b) and counter electrodes used are as described in 3.1.3a. A wick type HgO/Hg reference electrode was joined to the working electrode compartment of the cell by a closed liquid seal tap and luggin capillary arrangement.

3.1.3f galvanostatic polarisation studies

Details of the electrode system and test electrode pretreatment technique are described in the relevant chapter (9.1.1).

3.2. Electrical Circuits.

3.2.1. Equilibrium potential measurements

Potential measurements were made using a Tinsley

potentiometer (type 4363E-Auto) in series with a buffer amplifier (Ancom, type 15A-37). The balance was detected with a Scalamp galvanometer (Pye, catalogue number 7892/S). The sensitivity of this arrangement made measurements to 10μV readily available.

Temperature was controlled using a large volume water bath, contact thermometer (Jackson Thermoregulator, type TD) and relay.

3.2.2. Double layer and faradaic impedance measurements

A Schering bridge[42] (figure 3-6) was used to match the interphase as a series combination of resistance and capacitance (R_{xs} - C_{xs}).

Two types of a.c. generator and detector were used in the circuit.

(1) The a.c. was obtained from an audio-frequency generator (Solartron, type CO 546.2). The out of balance signal was passed via a filter (Muirhead, type D. 925. B), set to reject 50 Hz., to a tuned amplifier (General Radio, type 1232-A). The amplifier was continuously tunable in the frequency range 20Hz - 20 kHz.

(2) The tuned amplifier and a.c. generator described in (1) were replaced by a phase sensitive lock in amplifier (Brookdeal, model 401A) in conjunction with a signal source and reference unit (Brookdeal, model 472). This latter arrangement was used for all faradaic impedance measurements and differential capacitance studies at frequencies below 1kHz.

In both cases the output from the a.c. signal source was applied to the bridge via an isolated 65:1 step down transformer. The amplitude of the a.c. was adjusted to 7mV peak to peak.

The bridge components were as follows: C_4 was a 1.0μF mica condenser (Muirhead, type B-517-C), R_1 a resistance ratio box

Fig. 3-6 Electrical circuit for double layer and faradaic impedance studies

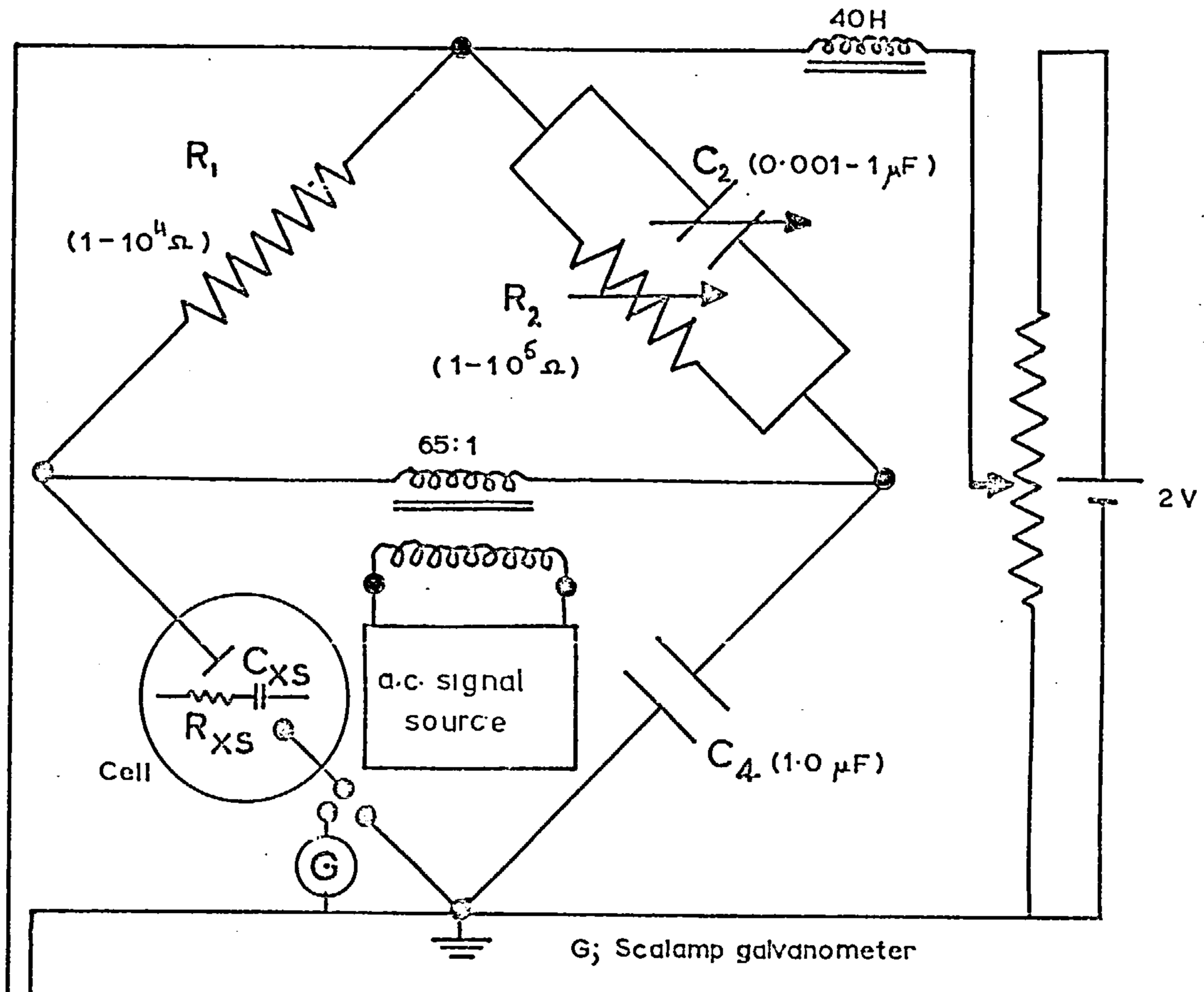

$$C_{XS} = \frac{C_4 R_2}{R_1} \quad : \quad R_{XS} = \frac{R_1 C_2}{C_4}$$

(Muirhead, type D-94-C), C_2 a decade condenser box (Muirhead, type B-21-F) and R_2 a decade resistance box (Sullivan, serial number 8472/1961).

The polarising circuit consisted of a simple battery/resistance combination. The a.c. and d.c. circuits were separated by a 40H choke. Potentials were measured using a Hewlett Packard multimeter (type 3490A), the imput impedance of which was effectively infinite ($>10^{10}\Omega$).

3.2.3. Rotating disc studies

A block diagram of the apparatus is shown in figure 3-7. Currents were measured at fixed potentials using a Scalamp galvanometer (Pye, catalogue number 7892/S) in conjunction with a potentiostat (Chemical Electronics, type TR70-2A). The indium electrode was rotated at a strictly controlled speed using a servo drive unit (Chemical Electronics, type RD1). The speed of rotation was measured using a stroboscope (Dawe, Stroboflash, type 1200E). Potentials were measured using a Hewlett Packard multimeter (type 3409A).

3.2.4 Linear sweep voltammetry (L.S.V)

The electrical circuit consisted of a scanning potentiostat (Kemitron, 0.5A) in conjunction with an X-Y recorder (Bryans, type 26000 A4). Potentials were measured with a Hewlett Packard multimeter (type 3409A). The experimental set up is shown in figure 3-8.

3.2.5. Galvanostatic polarisation measurements

The electrical circuit is shown in figure 3-9. Potentials were monitored throughout the experiments using a Hewlett Packard multimeter (Type 3409A). Currents were measured using shunted galvanometers (Cambridge Unipivot, accuracy 0.2%).

Fig.3-7 Circuit for rotating disc electrode experiments

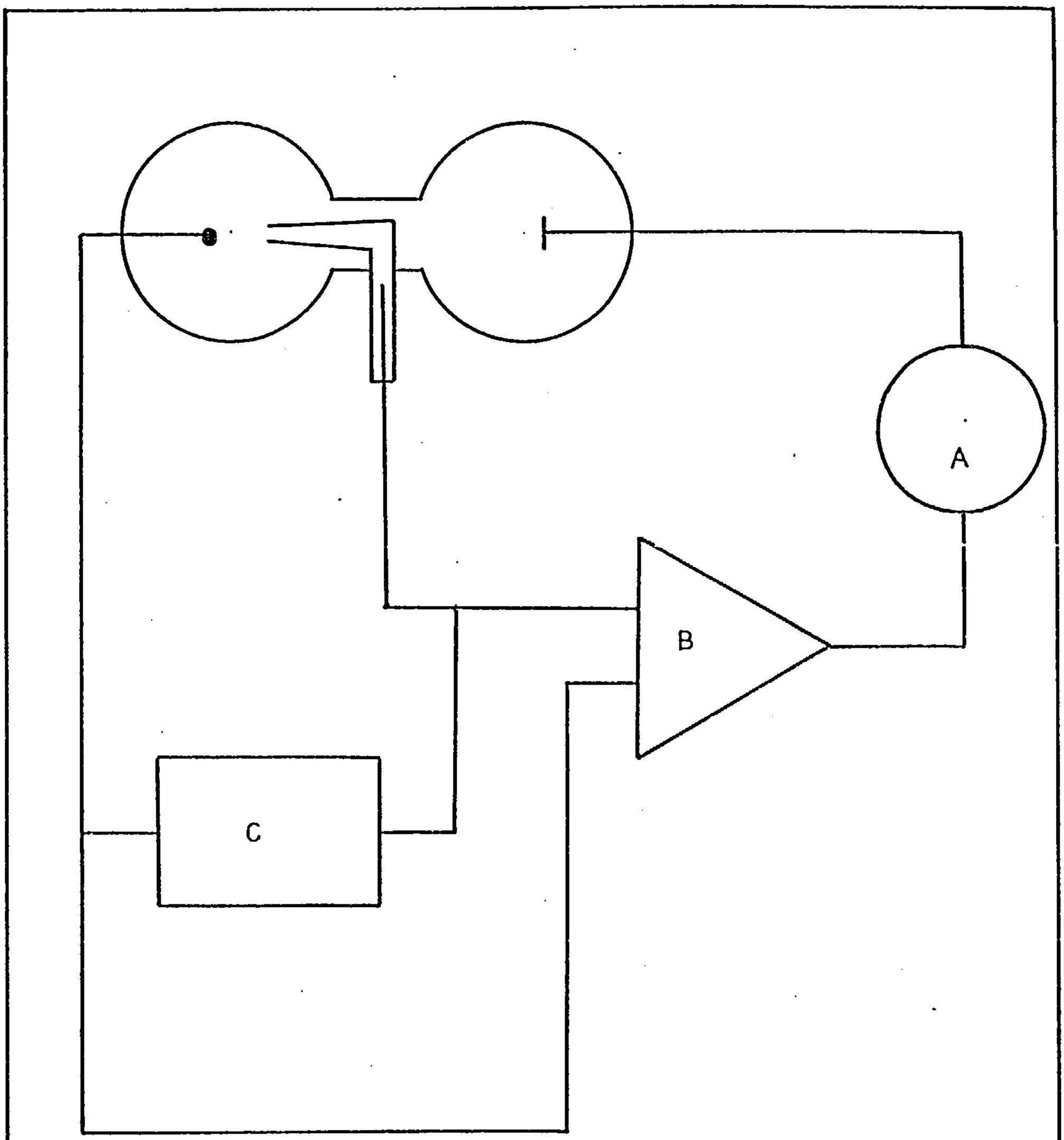

A ammeter
B potentiostat
C digital voltmeter

Fig. 3-8 Linear potential sweep circuit

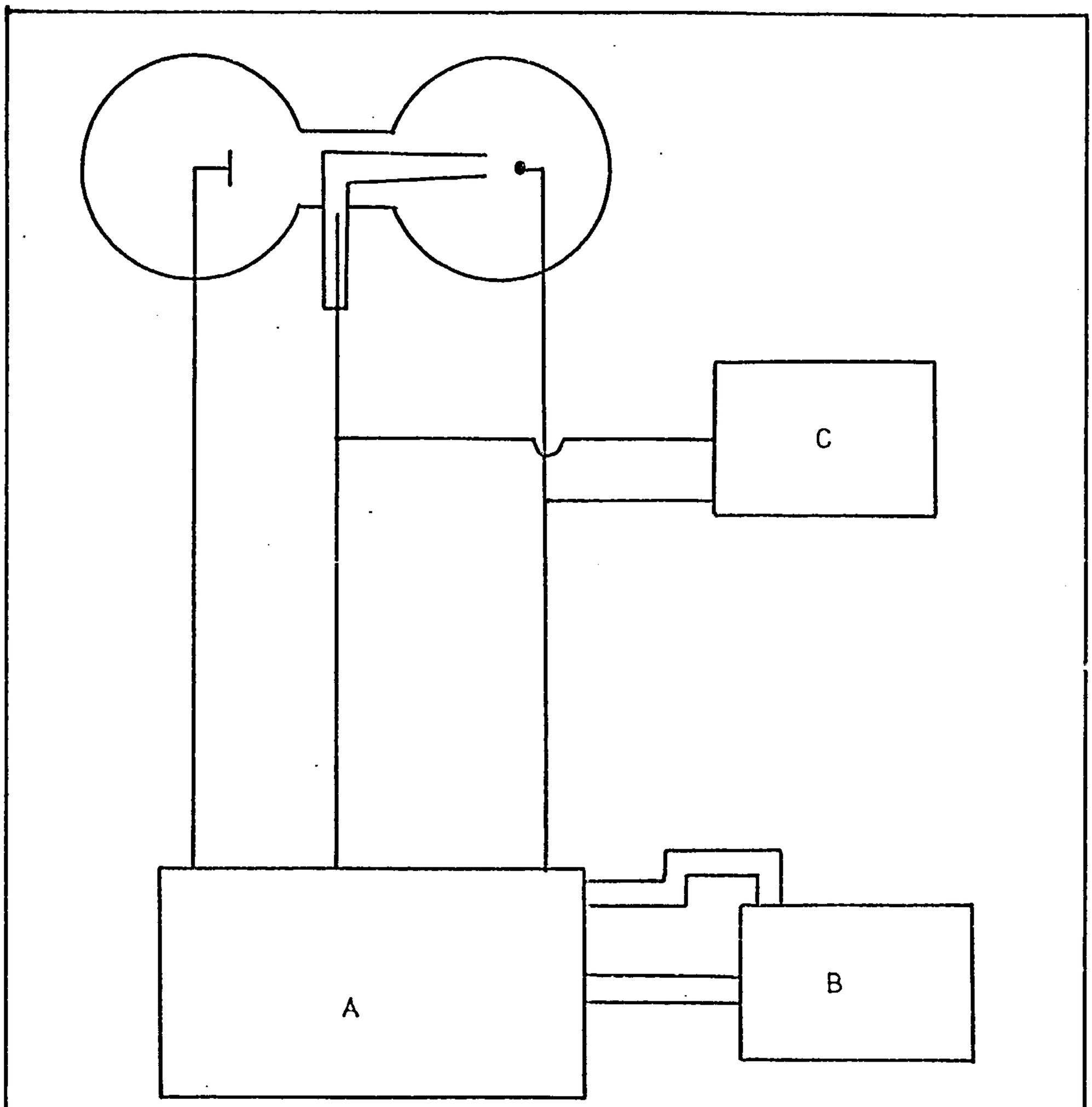

A scanning potentiostat
B X-Y recorder
C digital voltmeter

Fig.3-9 Galvanostatic polarisation circuit

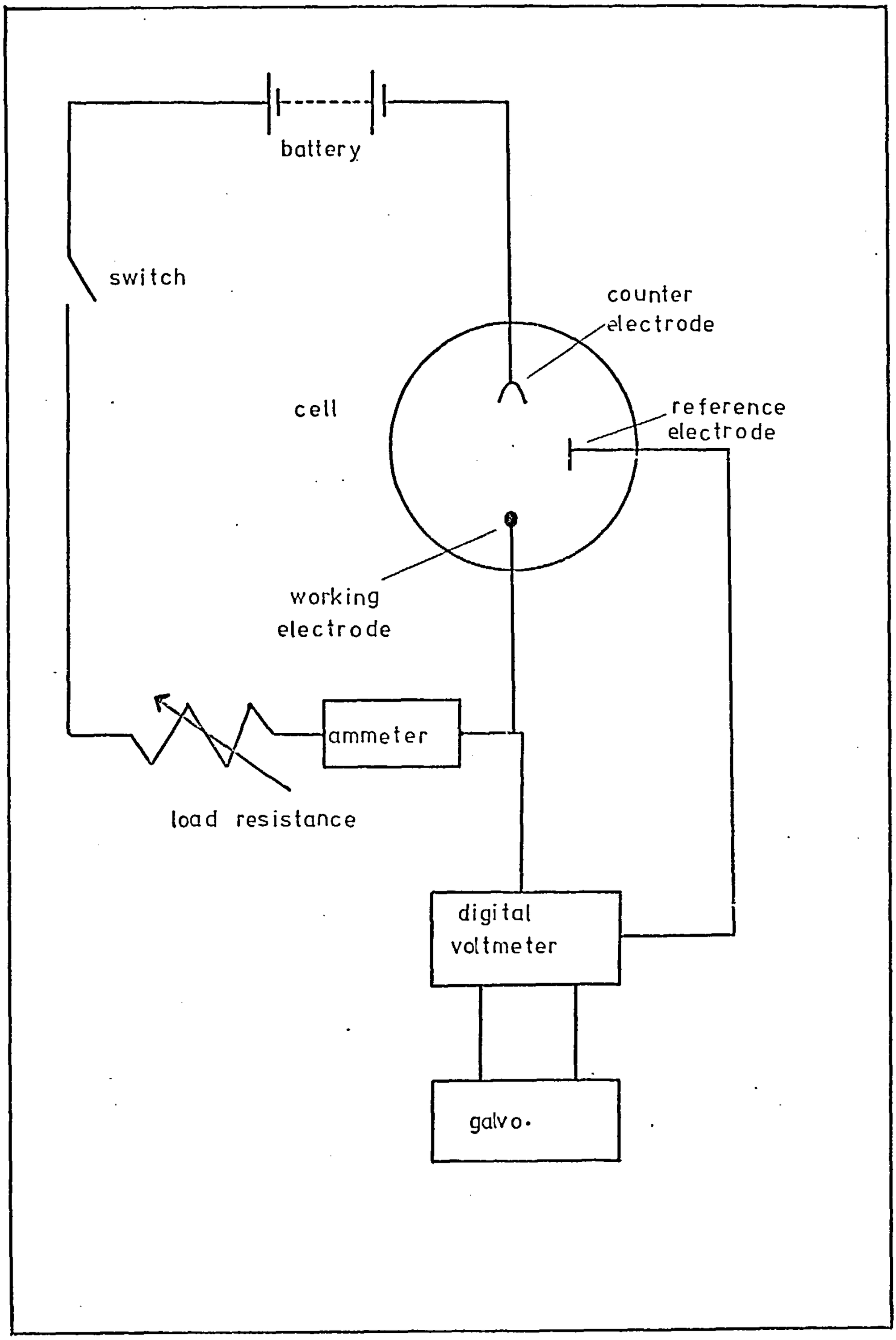

the $In^{3+}(aq)$ ion. To account for these observations, Latimer[49] has taken the approximate potentials for the various indium couples to be

$$In^{+} + e \longrightarrow In \qquad E^{\ominus} = -0.25\ V$$

$$In^{2+} + e \longrightarrow In^{+} \qquad E^{\ominus} = -0.35\ V$$

$$In^{3+} + e \longrightarrow In^{2+} \qquad E^{\ominus} = -0.45V$$

The equilibria between $In^{3+}(aq)$ and In(m) have been investigated by Hepler et. al.[4] Equilibrium constants for the reactions: $2In(m) + In^{3+}(aq) = 3In^{+}(aq)$ and $In(m) + 2In^{3+}(aq) = 3In^{2+}(aq)$ were found to be 2.4×10^{-11} and 1.9×10^{-8} respectively. From these results the potentials were calculated:

$$In^{+}(aq) + e = In(m) \qquad E^{\ominus} = -0.14\ V$$

$$In^{2+}(aq) + e = In^{+}(aq) \qquad E^{\ominus} = -0.40\ V$$

$$In^{3+}(aq) + e = In^{2+}(aq) \qquad E^{\ominus} = -0.49\ V$$

Losev and co-workers[50,51] have examined the participation of low valence ions into the equilibrium between indium and amalgam electrodes and aqueous indium salt solutions. Thus Losev and Pchel'nikov[51] have studied the dependence of the potential of the indium electrode on the concentration of $In(ClO_4)_3$ and of $HClO_4$ It was shown that for low acidities (3×10^{-3} - 1×10^{-2} M $HClO_4$) the equilibrium potential followed the Nernst equation, whilst for more acid solutions, this relation was destroyed. A theoretical analysis of the origin of the potential was given for systems

involving a number of successive electrochemical stages, considering unstable products capable of oxidation by the components of the solution. The results of this analysis were compared with experimental data for the indium electrode and it was shown that unstable univalent ions apparently participate in setting up the equilibrium. For the amalgam electrode[50] a potentiostatic method was described for studying the applicability of the Nernst equation to electrodes in solution containing In^{3+} at very low concentrations. Here again, experimental data for the indium amalgam at low ion concentrations did not agree with the Nernst equation, possibly due to the participation of In^{+}.

4.2. The Double Layer at the Indium/Aqueous Solution Interphase

The double-layer capacity of indium amalgams was measured by Butler et. al.[52] at 25°C in 0.1M $HClO_4$ using a dropping electrode. Fourteen amalgams ranging from 0.001 - 64.4% In were studied. Below 0.001% the capacity was identical to pure mercury; at higher concentrations a pseudo-capacity due to the dissolution of indium was observed at potentials more positive than the $In-In^{3+}$ equilibrium potential. As the concentration of indium in the amalgam was varied from 1-70%, the p.z.c. shifted 0.4 V more negative, the capacity-potential curve showing a corresponding shift. The capacity-surface charge curve for concentrated indium amalgams showed the same "hump" near the e.c.m. as pure mercury. At a surface charge of $-10\mu Ccm^{-2}$, the capacity varied from $15\mu Fcm^{-2}$ for mercury to $20\mu Fcm^{-2}$ for 64% indium amalgam, at a surface charge of $+10\mu Ccm^{-2}$ the capacity of a 64% amalgam was approximately twice that of mercury at the same surface charge. The potential drop across the diffuse double layer was calculated. The influence of

the diffuse double layer was found to be greater for concentrated amalgams than for mercury.

Russian workers[53] have reported on the electrocapillary behaviour of indium amalgams containing from 0.1 to 57.7% by weight In and the adsorption of inorganic anions and surface-active organic substances on the surface of the amalgams investigated. Introduction of indium into mercury displaced the maximum of the electrocapillary curves in the direction of negative potentials, the dependence of the maximum interfacial tension on the indium concentration passed through a minimum. With increasing negative potentials a transition occurred from positive adsorption of indium to negative adsorption.

Indium amalgam electrodes have been used to show that the rate of anion electroreduction is determined by the structure of the electrical double layer. Thus Yakovleva et. al.[54] examined the differential capacitance of the electrical double layer on electrodes of 2% and 51% indium amalgam and calculated the surface charge densities and the potentials at the outer Helmoltz plane. It was shown that the Tafel plots corrected for the reduction of $S_2O_8^{2-}$ and $Fe(CN)_6^{3-}$ agree well between different base electrolyte concentrations and different amalgams. It was concluded that the rate of anion electroreduction, as a function of electrode material and in the absence of specific adsorption, was determined by change in the structure of the electrical double layer at electrodes having different p.z.c's.

For the case of solid indium relatively few data have been reported. Levin and Rotinyan[55] reported a value for the p.z.c. of -0.67 $\pm$ 0.01 V (n.h.e.) obtained from capacitance minima in

dilute, acidified Na_2SO_4 solution. Grigor'ev et.al[56] confirm that the p.z.c. lies in this region on the basis of similar measurements in NaF, $HClO_4$ and NaCl solutions.

4.3. The Exchange Reaction at the Indium Electrode

The In/In^{3+} electrode reaction involves a 3-electron charge-transfer and this is not likely to occur in one step. This is clear from the work of many groups. For example[57-59], for the electrochemical dissociation of In(Hg) Kozin et al[57] have claimed that the limiting step of the process is the loss of the first electron and the In^{3+} ions are formed as a result of a secondary disproportionation reaction involving the In^{+} ions. For the metal, Kiss et al[58,59], found that the oxidation of indium at a rotating disc occurred in stages, the rate of the first process being larger than the succeeding process. Later work with a ring disc assembly indicated that the reduction of In^{3+} occurred in one-electron steps, the rate determining reaction depending on the release of the second electron. These examples typify the complicated nature of the reaction. For convenience the reported work is reviewed by anion type.

In only relatively few electrolytes has the In^{3+}/In exchange been studied. Of these, perchlorate supported electrolytes have formed the majority of the systems investigated for both solid and amalgam electrodes. To some extent the results of experiments with amalgam and solid electrodes are similar, however, in the interests of scholarship and completeness the two types of electrode will be considered separately.

4.3.1. Perchlorate electrolytes

4.3.1a amalgam electrodes

Straumanis and Martin[60] reported that for the anodic dissolution of indium amalgams In(I) could not be found in the solution phase, however, Budov and Losev[61] concluded, from a study of the electrode processes on an indium amalgam using a radioactive technique, that the anodic and cathodic processes were of a stepwise nature.

$$In \longrightarrow In^{+} + e \qquad (4.1)$$

$$In^{+} \longrightarrow In^{2+} + e \qquad (4.2)$$

$$In^{2+} \longrightarrow In^{3+} + e \qquad (4.3)$$

The most probable mechanism appeared to be that the stages involving the first and second electrons (4.1) and (4.2) were equilibrium stages and the overall rate was determined by the rate of the last stage. This mechanism was based on a cathodic transfer coefficient $\alpha = 0.91 \pm 0.02$ and an anodic transfer coefficient $\beta = 2.2 \pm 0.07$. It was further shown[62] that with the exception of F^{-}, the halide and sulphate ions take a direct part in the anodic dissolution of indium. Recently[63] it has been shown, apparently unequivocally, that In^{+} ions are participants in the anodic dissolution of indium. The effect of pH on the anodic dissolution of indium has also been examined by Losev and Molodov[64]. It was also found[64] for the cathodic reduction of the hydrated indium ion, the rate was first order with respect to hydroxyl ion concentration. This was interpreted as indicating the involvement of cations $[In(H_2O)_5OH]^{2+}$ in the charge transfer step rather than the hexaquo cation. The

slowness of the cathodic reduction of indium is therefore to be ascribed to the difficulty of removal of a hydrogen ion from the bound hydration shell of the In^{3+} ion. Molodov and Losev[65] in a further investigation used a combined polarisation and radiochemical method to study the formation of indium by cathodic reduction at a stationary electrode of indium amalgam in perchlorate solutions. Two parallel reduction processes were found: indium was formed either by direct discharge of the $In(H_2O)_6^{3+}$ ion, or by discharge of partially hydrolysed indium ions. The rate constant of the former process was about 10^5 times less than that of the latter. This latter process was found to be preceded by two consecutive chemical reactions - first the hydrolysis of $In(H_2O)_6^{3+}$ ions in the solution, which limited the cathode process at high pH and was independent of potential, and then the partial dehydration of $[In(H_2O)_5OH]^{2+}$ ions on the surface (this limited the rate of the second process at low pH and depended weakly on potential). The difficulty of dehydration of indium ions was emphasised by Chernom'orskii[66] and what amounts to the same suggestion is contained in other references by Russian workers[67,68].

The transition between control of the electrochemical reaction by one rate process and another has been further studied in the case of indium by Molodov and Losev[69]. The dependence of the rate of the anodic processes and of the intensity of the exchange current on the concentration of the indium amalgam was measured in a solution of perchloric acid. It was found that at high concentrations of the amalgam the exchange current determined by the radiochemical method was lower than the exchange current determined by extrapolating the Tafel section of the curve to the equilibrium potential. A linear section with a slope (2.3RT/3F) of 0.019 V appeared on the anodic

current-voltage curve close to the equilibrium potential which corresponded to the limitation of the indium oxidation process by a subsequent chemical reaction[67]. At low concentrations of the amalgam this phenomenon was not observed - it was shown that by increasing the ratio of the concentration of indium in the solution to that in the amalgam a transition occurred from the region where the kinetics were determined by the limiting chemical reaction to the region where the kinetics were electrochemically controlled.

A very detailed review[26] by Losev summarises some of the salient features of the indium exchange in perchlorate electrolyte from the mechanistic viewpoint. Losev concludes that in the reaction only one of the electron transfers is rate determining ($\alpha_a + \alpha_k = 3.11$, see appendix 2) and that In^+ ions are in equilibrium with indium atoms in the amalgam.

4.1.3b solid electrodes

A number of investigations of the exchange at a solid indium electrode have been reported[2,3,70-81]. Pchel'nikov and Losev[2] established that the anodic dissolution reaction occurred with the formation of In(I) species which then reacted to form In(III) either chemically by reaction with H^+ in solution or by direct oxidation at the electrode. This caused the apparent valence from faradaic charge calculations to differ from 3. Subsequently[72] the effect of NaI and NaCl on the reactions occurring at the indium electrode in perchlorate solutions was studied. It was shown that these additives promoted the electrode reactions. A brownish-red deposit formed on the anode in the presence of NaI, the valence of the indium in this deposit being close to one. It was concluded that this deposit was InI, as confirmed by comparing the chemical properties of the deposit and those of InI synthesised from the

elements at high temperature. A deposit of InI also formed reversibly on the electrode at NaI concentrations greater than 1×10^{-2}M, the indium metal functioning as a reversible electrode of the second kind under these conditions. Additions of Cl^- ions to perchlorate solutions increased the value of the apparent valency of dissolving indium in comparison with that for the perchlorate solutions, the reversible indium potential being determined by the concentration of the $[InCl_2]^+$ complex of trivalent indium. It is noteworthy that F^- has no effect on the In^{3+}/In exchange[73].

Similar conclusions about the participation of univalent indium species have been obtained by Visco and co-workers[3,70,74,79]. In Visco's experiments[3,70,79] the In(I) ion formed during anodization could be swept away from the electrode surface and detected polarographically in the bulk of the solution. The current efficiency in stirred solutions for In(I) production was about 2% in the case of dilute amalgams but for indium metal anodes, the current efficiency for In(I) production under the same conditions was at least 75% and was dependent on the anodic current density. The effects of mass transport conditions during electrochemical oxidation and of added complexing agents on the quantity of In(I) formed were also investigated. Based on overpotential decay curves, the polarographic behaviour of In(I) and In(III) and coulometric experiments, an electrochemical mechanism was proposed which postulates that the In(I)/In(O) couple is at equilibrium and that the interfacial concentration of In(I) is not vanishingly small. An irreversible electrochemical step is associated with the further oxidation of In(I) to In(III). The rate constant of the formation of In^+ in the system has been reported[68] as 3.2×10^{-6} lm^2 s^{-1}.

In a later paper with Miller[74], Visco used the rotating ring-disc electrode to verify that the mechanism of the anodic dissolution of indium at a disc in 0.7M $HClO_4$ was a rapid one-electron reaction to an In(I) species, sufficiently stable to be detected in theoretical amount at the ring. The Tafel behaviour of the disc reaction and the anodic and cathodic ring collection efficiencies were in accord with the above; the ring current-potential curves further showed that the slowness of the In(I)-In(III) reaction permits the thermodynamically less favoured state to be formed in quantity.

Losev and Pchel'nikov[75] using a combination of radiochemical and electrochemical methods have measured the exchange rate at a solid electrode. There was satisfactory agreement between exchange currents determined by the radiochemical method and by extrapolation of the anodic polarisation curve to the equilibrium potential. The authors concluded that the exchange current increased with increasing In^{3+} ion concentration in the presence of added Cl^- ions and rose with increasing pH of the solution. The kinetic parameters for the electrode reaction were determined from the relation between the exchange current and the $In(ClO_4)_3$ concentration, the values obtained being, for the anodic transfer coefficient $\beta = 1.85$ and $i_o = 2.88 \times 10^{-3}$ A cm^{-2}.

The cathodic process of discharge of indium ions on an indium electrode in perchlorate solutions in relation to potential and acidity of the medium was also investigated by Losev and Pchel'nikov[71]. With increase in acidity, on a solid indium electrode, similar to the amalgam, a retardation of the cathodic process occurred, during which the rate of discharge of indium was almost

independent of potential. In the presence of iodide ions the cathodic process was sharply accelerated and its rate began to be limited by diffusion. It was shown that the discharge of indium ions in perchlorate solutions was accompanied by preceding chemical reactions, during which the ions taking part are not the $In(H_2O)_6^{3+}$ ions predominating in the solution but are evidently the partially dehydrated hydrolysed ions of indium. This conclusion was verified in a more recent publication by the same authors[80] who investigated the influence of acidity and stirring on the cathodic reaction. It was found that the rate of indium discharge was inversely proportional to the acid concentration in the range studied (3×10^{-3} - 1M) and that the limiting current of the discharging indium ions was kinetic and not diffusional in nature. This is in general agreement with work using indicator electrodes[81] in which detection of hydrolysed $[In(OH)_2]^+$ ions confirmed the above suggested mechanism.

In dealing with the corrosion of indium in perchlorate media, Losev et al[77] have formulated a stepwise corrosion mechanism for the metal in which the final corrosion product is formed by a complex electrochemical-chemical mechanism comprising the following steps: $M \longrightarrow M^+ + e$; $M^+ \longrightarrow M^{n+} + (n-1)e$; $M^+ + (n-1)O_x \rightarrow M^{n+} + (n-1)O^-_x$ and $O_x + e \longrightarrow O^-_x$. A criterion of such a corrosion mechanism is the deviation of the experimental corrosion rate (i_c) from the reduction rate of oxidant O_x at the corrosion potential (i_c^{extr}) found by extrapolation. Cathodic polarisation curves on indium were measured and its corrosion rate was determined by a radiotracer method in aqueous $NaClO_4 + HClO_4$ solutions of varying acidity. i_c was considerably higher than i_c^{extr}, the ratio i_c/i_c^{extr} approaching 3 with increasing acidity. In the same

solutions containing 0.2 M NaCl $i_c = i_c^{extr}$ independent of acidity.

4.3.2. Chloride electrolytes

Markovac and Lovrecek[82] have investigated the kinetics of the reaction at a 0.3% In amalgam in chloride electrolyte. It was reported that the exchange reaction was fairly reversible up to a limit of 0.1 Acm^{-2}, however, when the current density was increased over this, the first step ($In^{3+} \longrightarrow In^{2+}$) in the cathodic reaction was rate determining. During anodic polarisation, disproportionation reactions were thought likely to occur. The quasireversibility of the reduction of indium at the D.M.E. was confirmed by the work of Jain and Gaur[83] who found k_s, the first order standard rate constant, to be $\sim 10^{-4}$ cm s^{-1}. It was emphasised by these authors[83] that the reduction is diffusion controlled at the D.M.E. The reduction of In^{3+} was reported to be a three electron reversible reaction from an a.c. polarographic study by Kopanskaya[84]. Losev[26] has pointed out in connection with the reduction of indium in chloride solutions that breaks in Tafel curves invoked by Lovrecek[82] to indicate mechanistic changes may, in the case of indium, indicate a reaction hindered by a preceding chemical reaction. In this case the hydrolysis of the hexaquo complex prior to the rate-determining charge transfer step.

For the solid electrode in chloride solution the dissolution reaction is accelerated. This was studied by Pchel'nikov et al[85] who found that the reaction and the effect of chloride were consistent with a stepwise dissolution

$$In \rightleftharpoons In^{+} + e \qquad (4.4)$$

$$In^{+} \longrightarrow In^{3+} + 2e \qquad (4.5)$$

which was complicated by the reaction of the intermediate In^+ with hydrogen ions ($In^+ + 2H^+ \longrightarrow In^{3+} + H_2$). The effect of chloride was specifically traced to the acceleration of reaction (4.5).

4.3.5. Alkaline electrolytes

Armstrong et al[86] have studied the electrochemical behaviour of indium amalgams in alkaline solutions using potentiostatic and impedance techniques. It was found that the anodic dissolution followed a three-stage oxidation process, similar to the process in acidic solutions. This does not, however agree with the later work of Leontovich[87] who suggested the limiting step $In(OH)^{2+} + e = In(OH)^{+}$ and this was claimed as similar to the mechanism in acid solution.

The anodic films produced on indium amalgams[86] were amorphous indium hydroxide. They were similar to anodic mercuric oxide and thallous chloride films in that those grown at very positive potentials were very thin whereas those grown at less positive potentials were much thicker. Anodic films formed on 1% amalgam in 0.1 M NaOH were found to be neither appreciable ionic nor electronic conductors.

The solid indium electrode[1,87-96] has attracted more attention than the amalgam mainly because of the metal's possible use in energy conversion devices. Boswell[1] has evaluated the potentialities of In, Bi-In and Pb-In alloys as energy producing electrodes in small sealed cells. Bismuth is claimed to have value in promoting electrode reactivity at high current densities. The results indicated that indium could be stored in alkaline solutions without deterioration and function usefully after storage. It was concluded that these characteristics made indium a metal of potential interest in the energy conversion field.

Popova and Simonova[89] have shown that in alkaline solution passivation is due to an adsorbed monolayer. The behaviour is similar to that observed with all non-activating anions. With activating anions (Cl^-, ClO_4^-) the activating action is related to the displacement of adsorbed oxygen from the surface of the electrode, activation increasing with increased activator concentration. A more detailed investigation by Faizullin et al[90] demonstrated that in the anodic polarisation of indium in solutions of potassium hydroxide under galvanostatic conditions, three anodic processes took place on an indium electrode, including the process of evolution of oxygen. The first anodic process was the transition of indium into the solution of alkali in the form of univalent ions, which, as a result of the disproportionation reaction, were oxidised to trivalent ions, forming indate ions (InO_2^-). In the second stage, indium undergoes anodic dissolution with direct formation of trivalent indium ions (InO_2^-). Both in the first and in the second stages of anodic polarisation, the phase oxide $In(OH)_3$ was formed on the indium surface. The anodic evolution of oxygen occurred on a passivated indium surface. In a further investigation[91] it was shown that the phase oxide film formed at the first two stages of the anodic polarisation of indium was not the basic cause of its passivation in alkaline solutions. Anodic passivation of indium occurred as a result of the formation of a second surface oxide film, situated directly on the metal under the phase oxide film. The structure of the passivating oxide film was identified as In_2O_3. The electrochemical parameters of the passivating film were determined. By determining the type of conductivity, it was hypothesised that the passivating

oxide film possessed a nonstiochiometric composition and contained an excess of In^{3+} cations. Work by Fillippova and Kuzmin[92], Lewis and Partridge[94] and Armstrong et al[95] throws doubt on the work of Faizullin and Amirkhanova[90]. The main dissolution product at low current densities according to these authors[92,94,95] is In(III). Evidence for this was the relative dissolution current magnitudes at the In(I) and In(III) potentials[92,94] and the results obtained from a rotating ring-disc study[95].

Salem and Ismail[93] considered that the anodic polarisation occurred in two stages: (i) the formation of indate ions and (ii) the formation of indium hydroxide. The initial discharge of hydroxide ions governed the overall reaction rate, whilst the formation of InO_2^- on the electrode, it was suggested, was the rate determining step. The number of electrons transferred from the electrode was 3.

In a more recent publication Armstrong et al[95] have shown that in KOH and NaOH solutions indium undergoes anodic dissolution at potentials more positive than -1.16 V (HgO/Hg). The Tafel slope for this process was found to be about 26 mV/decade and the order of reaction with respect to hydroxide ion 3. It was reported[95] that three types of passivating layer are produced; in the sequence $In(OH)_3$, InOOH and In_2O_3 at progressively more anodic potentials. The first layer is porous and not very protective but In_2O_3 is highly protective and difficult to reduce. The presence of bismuth was reported to reduce the passivating properties of these layers, especially those of In_2O_3.

Semiconductor effects of n-type indium oxides have been investigated by Salem and Ismail[96] who demonstrated that the current/potential curves for the systems showed that the current multiplication factor was in the range 1.88-2.73, consistent with the material being a semiconductor.

CHAPTER 5

A STUDY OF THE DIFFERENTIAL CAPACITANCE OF INDIUM IN SOME AQUEOUS ELECTROLYTES

5.1. Introduction

The electrochemistry of solid indium in aqueous solutions is poorly documented. Reasons for the lack of data include experimental difficulties associated with the manipulation of a metal as soft as indium, but more importantly, the need to avoid the intrusion of oxide films into the indium/aqueous solution interphase. Thus Butler and Dienst[97] suggest that an indium electrode electropolished in a 2:1 mixture of methanol and acetic acid becomes covered with a thin oxide layer and consequently prepolarisation at -1.25V (SCE) is necessary to achieve reproducible current-potential data at low current densities. Furthermore, Pourbaix[98] reports that in non-complexing solutions of pH in the range approximately 5-11 indium tends to cover itself with a film of oxide, In_2O_3.

The isolation of conditions in which the interphase is uncomplicated by adsorption or films can be conveniently investigated by studying the double layer characteristics as a function of bias potential in a range of electrolyte solutions. Previous work pertaining to the double layer at the indium/aqueous electrolyte interphase is reviewed in section 4.5. In the present work measurements of the impedance of indium in aqueous solutions of KF, Na_2SO_4, $NaClO_4$, KCl and KNO_3 are presented. Particular attention was paid to the pH of the electrolytes and to the history of the indium electrode prior to impedance measurements.

5.2. Experimental

The electrical circuit is described in 3.2.2. The cell is shown in figure 3-1. Electrolyte solutions were purified by pumping over activated charcoal as outlined in 3.1.1. Electrodes and the test electrode pretreatment technique are described in 3.1.3a. The potential of the working electrode was never allowed to remain uncontrolled. Generally electrodes were maintained at the negative extreme of the potential range before measurements were commenced.

5.3. Results

Figure 5-1 shows a series of steady state current-bias potential curves for an indium electrode in a range of electrolyte solutions. In each case the electrode was introduced into the cell at the most negative potential in the experimental range and the system was allowed to equilibrate ($\sim$45 mins, after which time the observed cathodic current was time-independent).

Figure 5-2 shows a family of differential capacitance-potential curves for an indium electrode in a series of Na_2SO_4 solutions. The variation of the electrode resistance, R_{xs}, with potential is also shown.

Figure 5-3 shows the effect of dilution on the differential capacitance-bias potential curves for an indium electrode in KF solutions. The effect of prepolarisation on the capacitance-potential curve obtained for an indium electrode in 0.02 mol l^{-1} KF solution is shown in figure 5-4.

Figure 5-5 shows capacitance-potential curves for an indium electrode in a series of unacidified KCl solutions. The effects of reducing the pH of the chloride and perchlorate systems are shown

Fig. 5-1 Faradaic current-potential curves

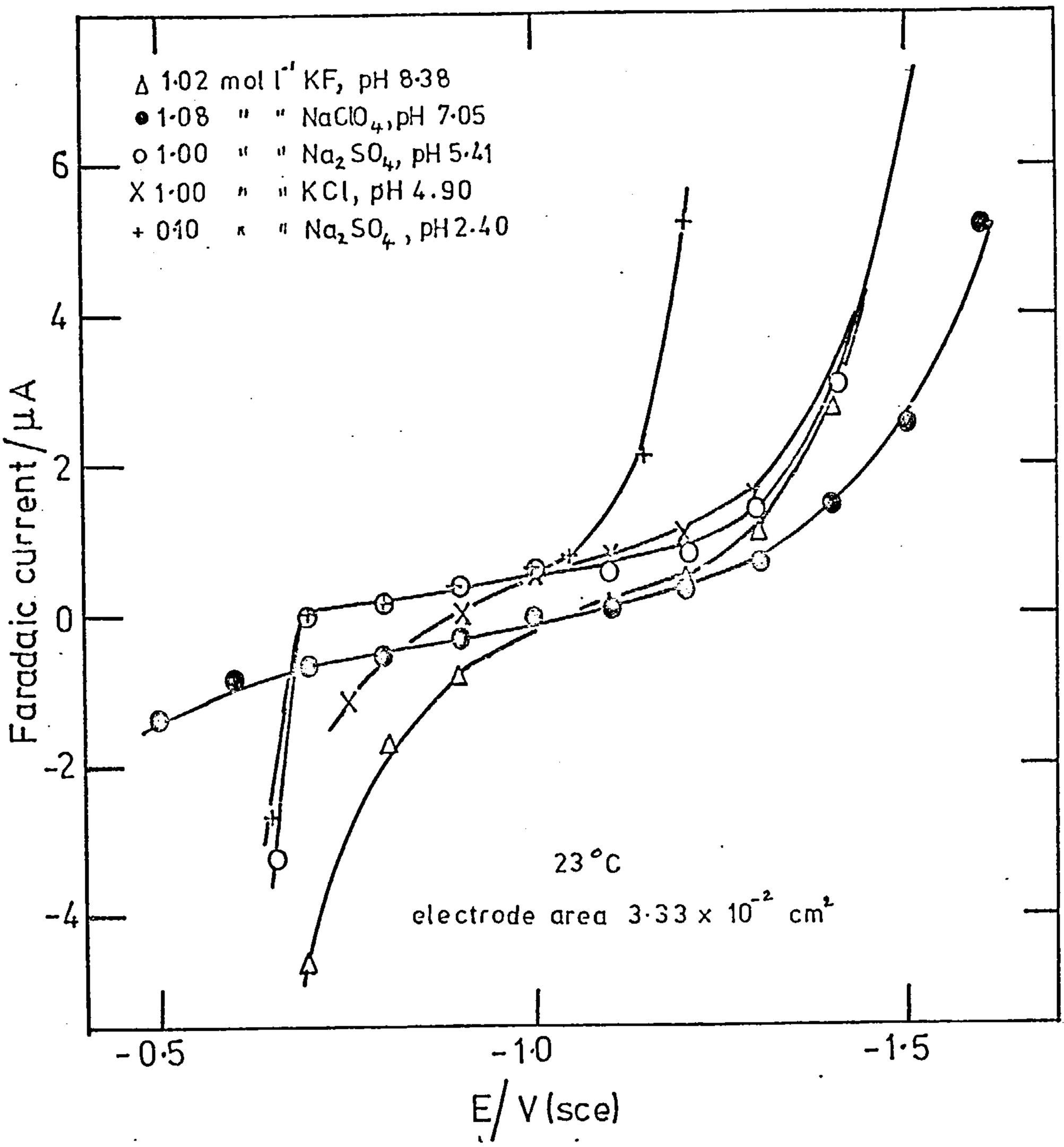

Fig·5-2 Differential capacitance-potential curves; Na_2SO_4 electrolytes

23°C, 312 Hz. Electrode area $3{\cdot}33 \times 10^{-2}$ cm²

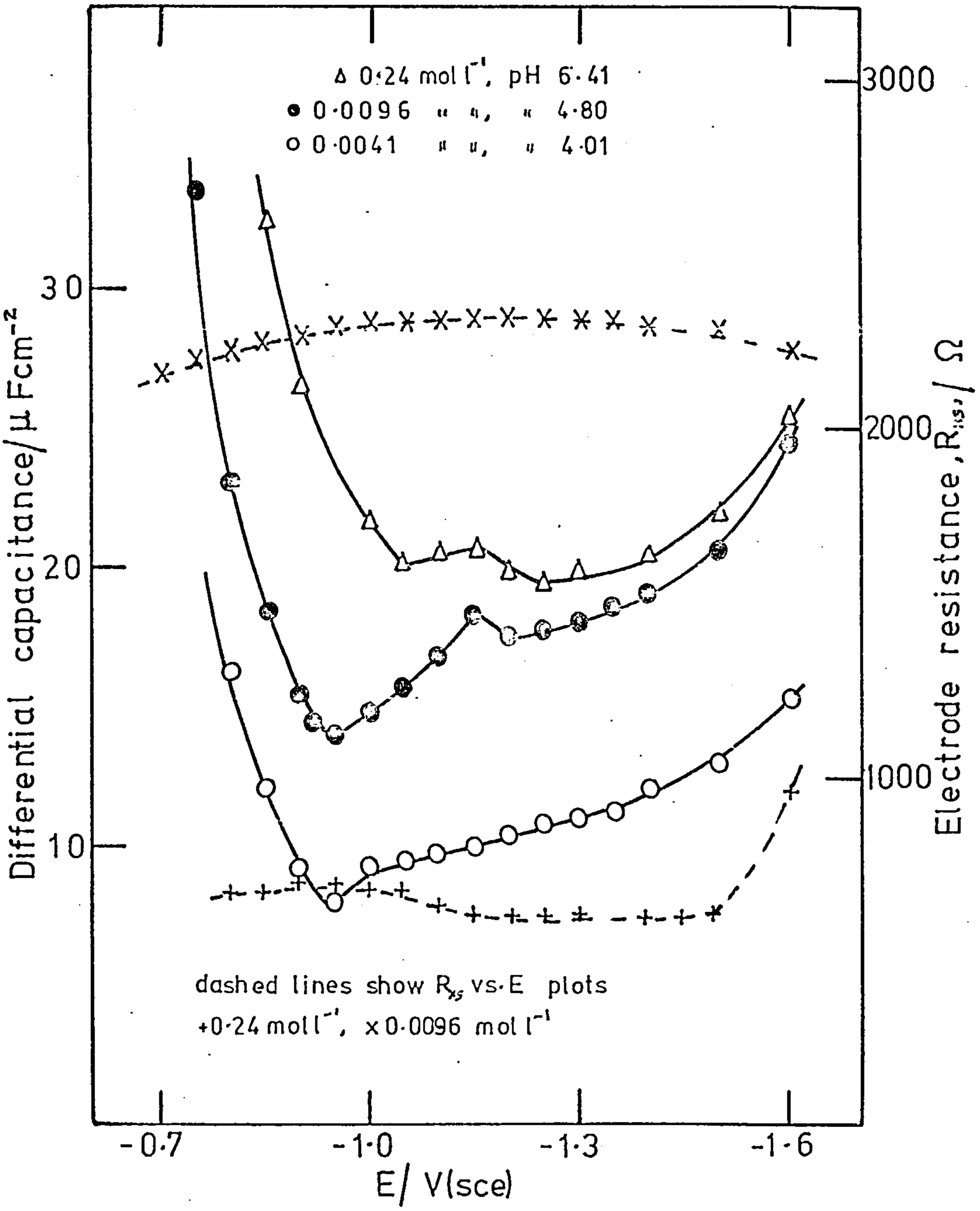

Fig. 5-3 Differential capacitance -potential curves; KF electrolytes

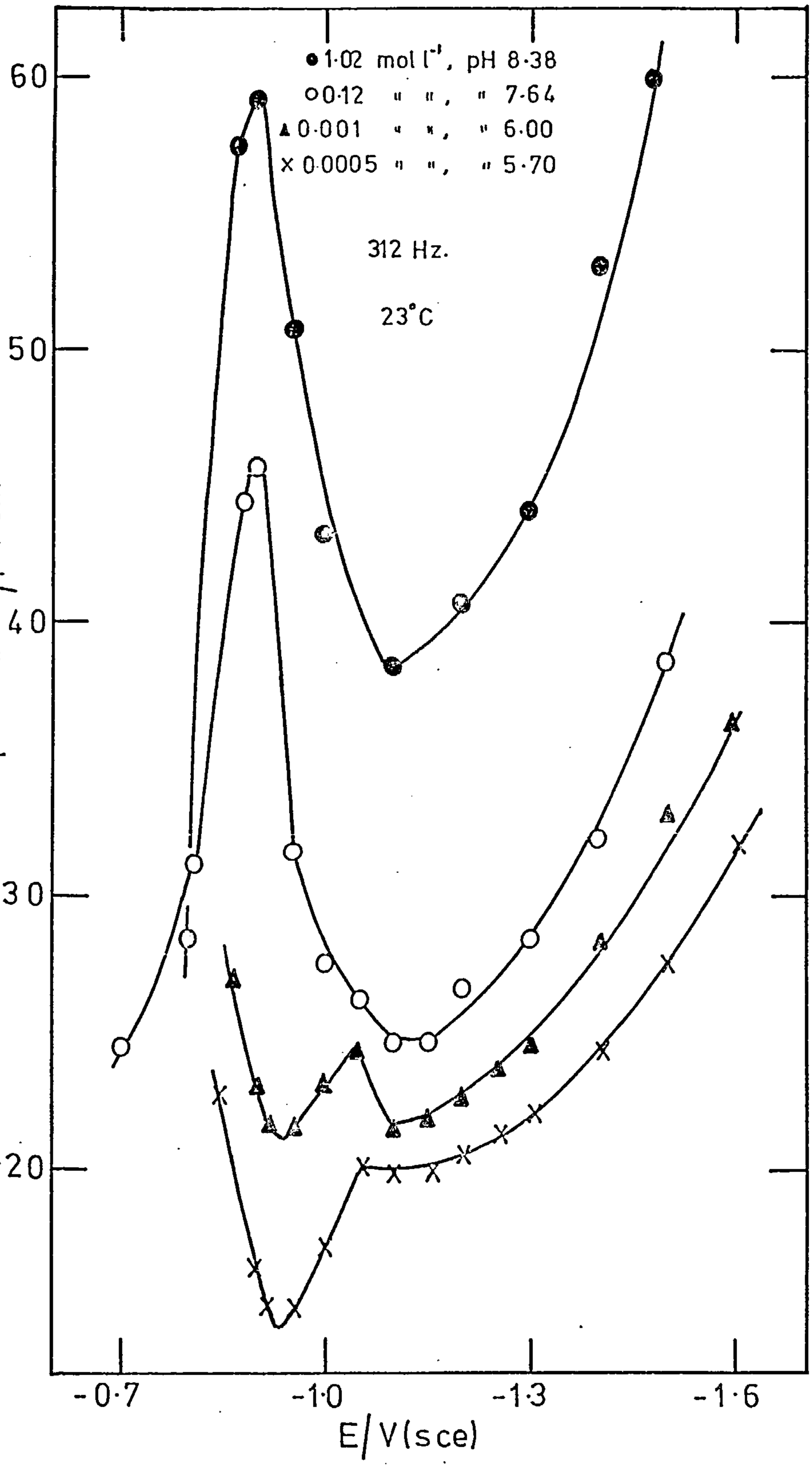

Fig. 5-4 Effect of prepolarisation on differential capacitance curves; 0·02 mol l^{-1} KF

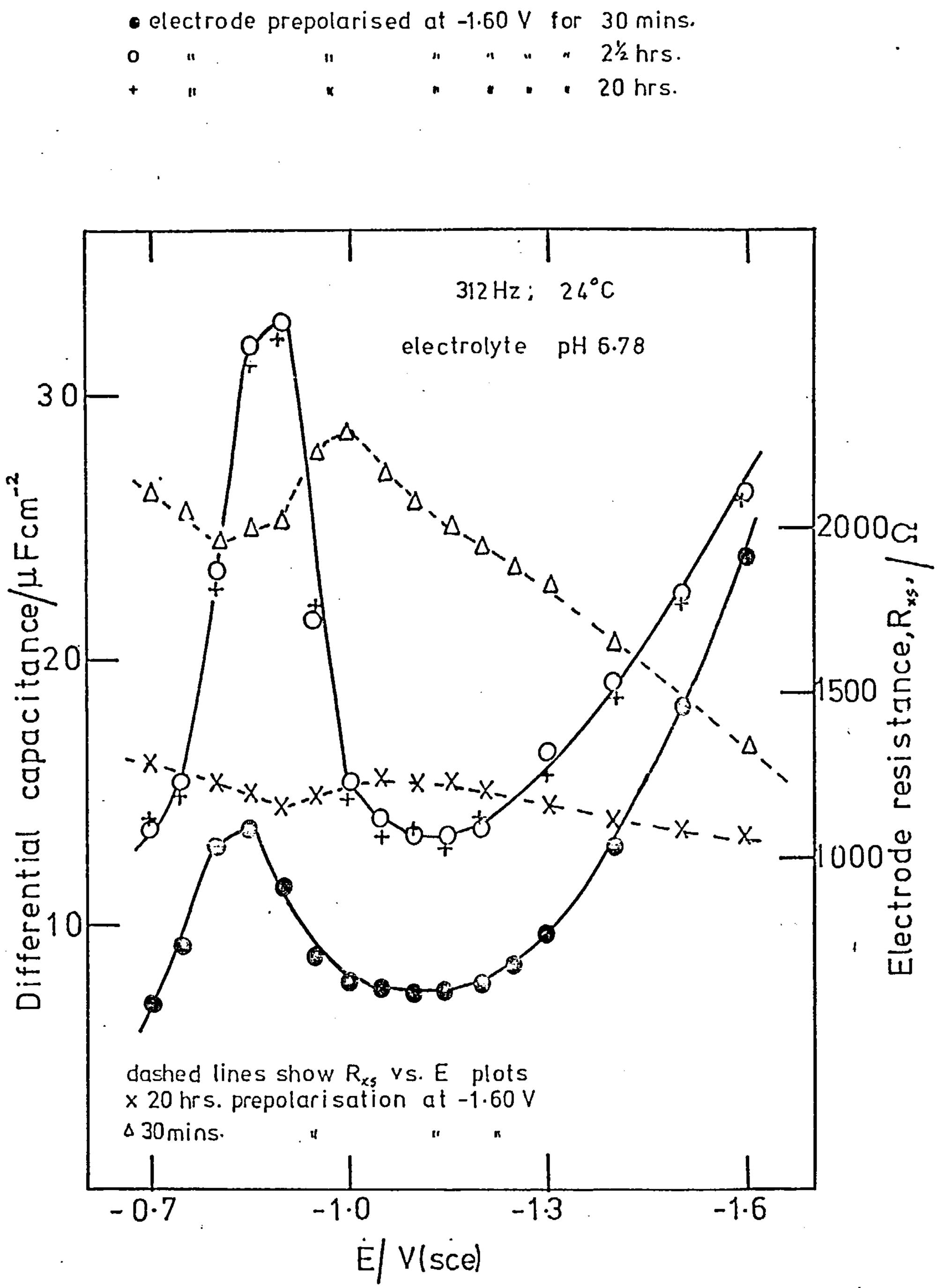

Fig5-5 Differential capacitance-potential curves;
KCl electrolytes

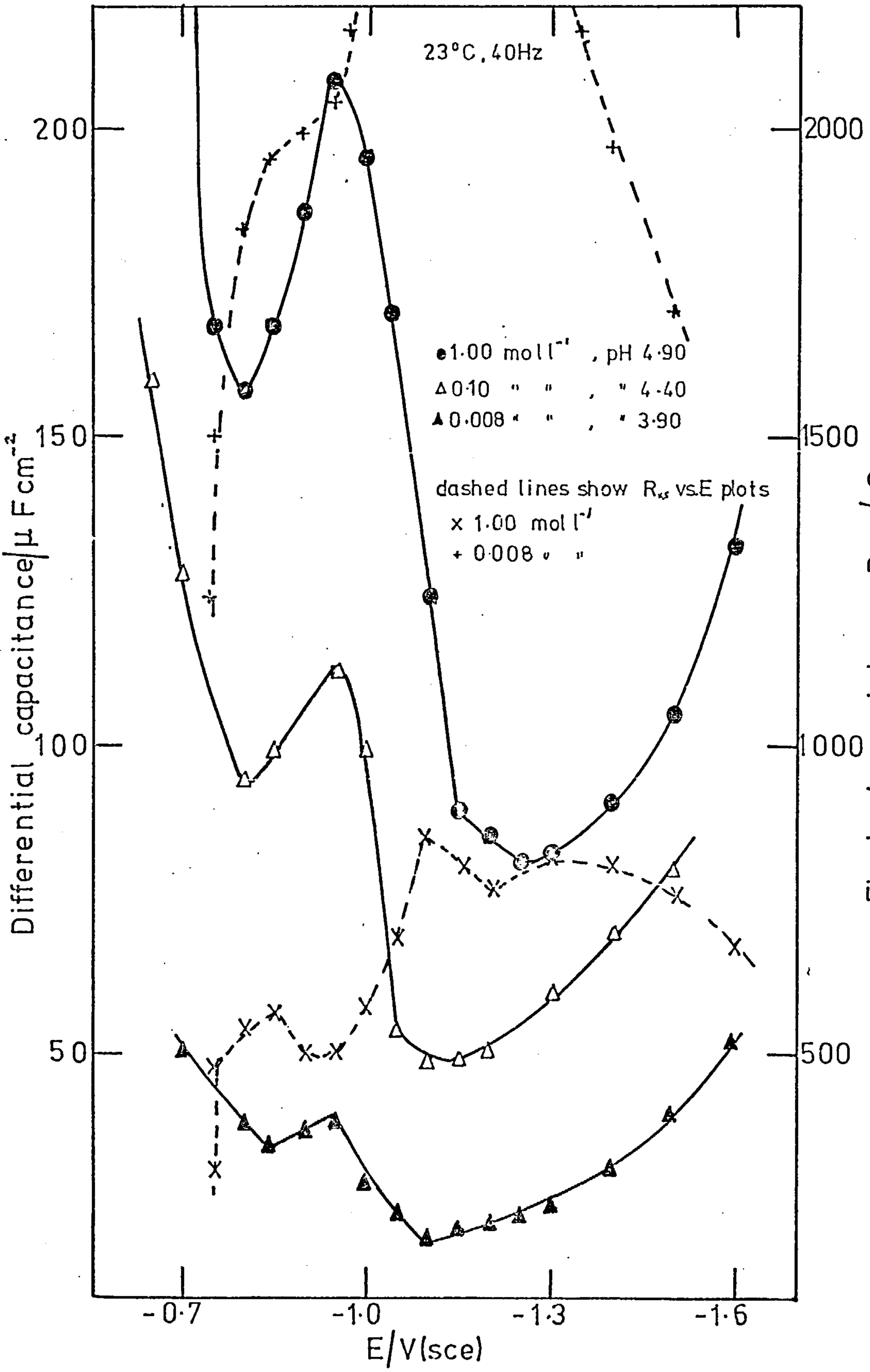

in figures 5-6 and 5-7.

Figure 5-8 shows differential capacitance-bias potential curves for an indium electrode in dilute perchlorate electrolyte (0.004 mol l^{-1}) of varying pH.

Figures 5-9 to 5-11 show frequency dispersions of the capacitance for an indium electrode in concentrated KF, $NaClO_4$ and KCl electrolyte solutions.

Figure 5-12 shows a typical steady state current-bias potential curve corresponding to an indium electrode in 1.0 mol l^{-1} KNO_3 electrolyte. At potentials more negative than $\sim$-1.15 V attempts to maintain the potential constant by galvanostatic control resulted in oscillations of potential in the range -1.2V to -1.5V. Attempts to control the system potentiostatically in the range -1.2V to -1.5V gave oscillations in the faradaic current. At potentials $<$-1.5 V the increase in the current on moving the potential to more negative values was due to the h.e.r. This behaviour is to be contrasted with the other electrolyte solutions investigated (figure 5-1) which gave the expected faradaic current-bias potential curves; viz, a region of potential in which the faradaic current was so small that the systems could be considered experimentally polarisable, bounded at $\sim$-0.7 V by the potential of lattice dissolution and at $\sim$-1.4 V by the potential of the h.e.r.

Figure 5-13 shows a typical series of differential capacitance curves corresponding to 0.1 mol l^{-1} KNO_3 (pH = 5.22) at frequencies in the range 2 kHz to 25 Hz. A pronounced capacitance peak occurs at -1.15 V. R_{xs} remains fairly constant in the region in passing from more positive values to -1.05 V but a reduction in R_{xs} corresponds to the maximum in C_{xs}. In the region -1.2 V to -1.5 V the system oscillated and neither capactiance nor resistance

Fig. 5-6 Differential capacitance-potential curves;
0·10 mol l^{-1} KCl

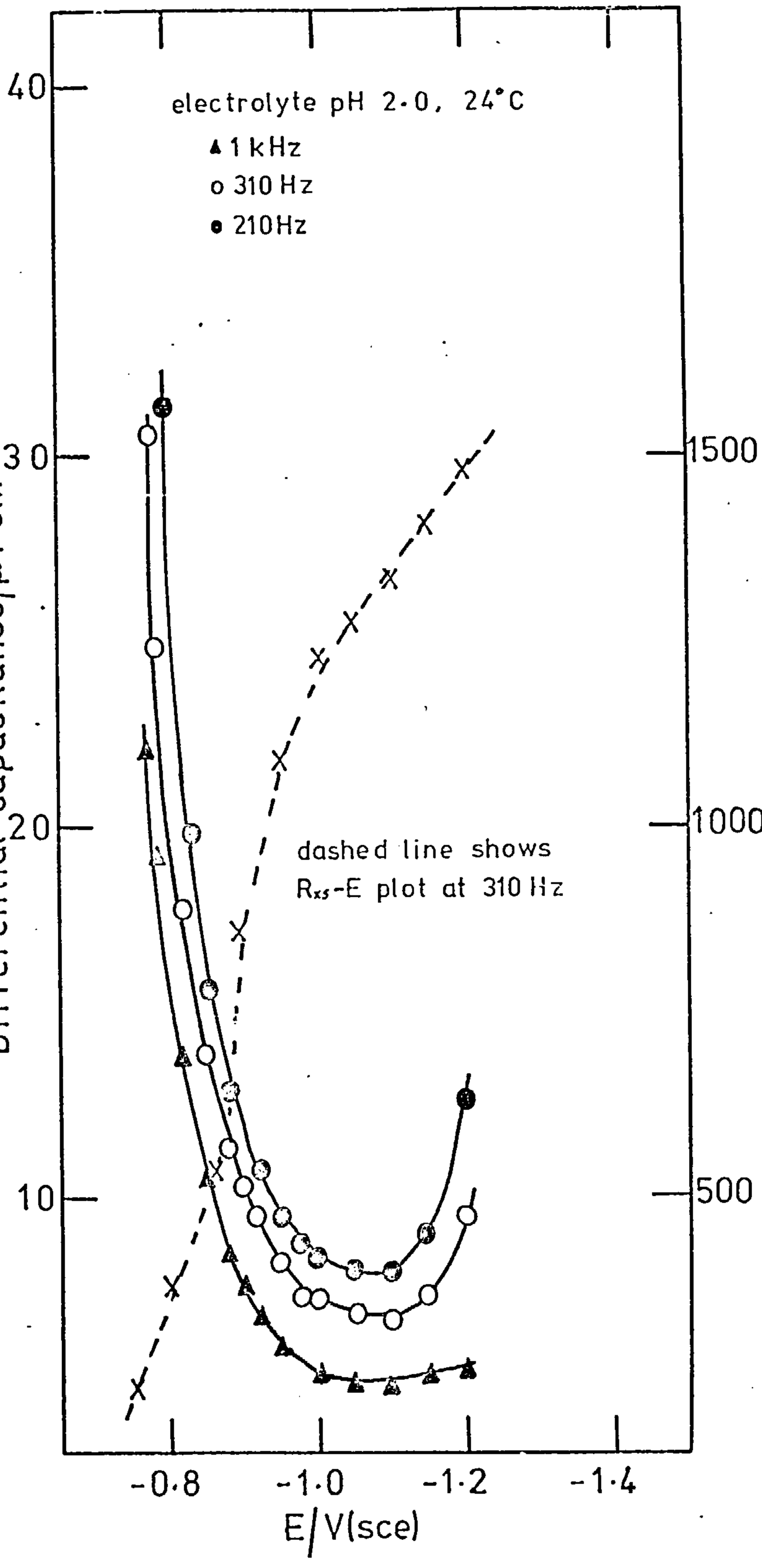

Fig. 5-7 Differential capacitance-potential curves; 0·10 mol l^{-1} $NaClO_4$

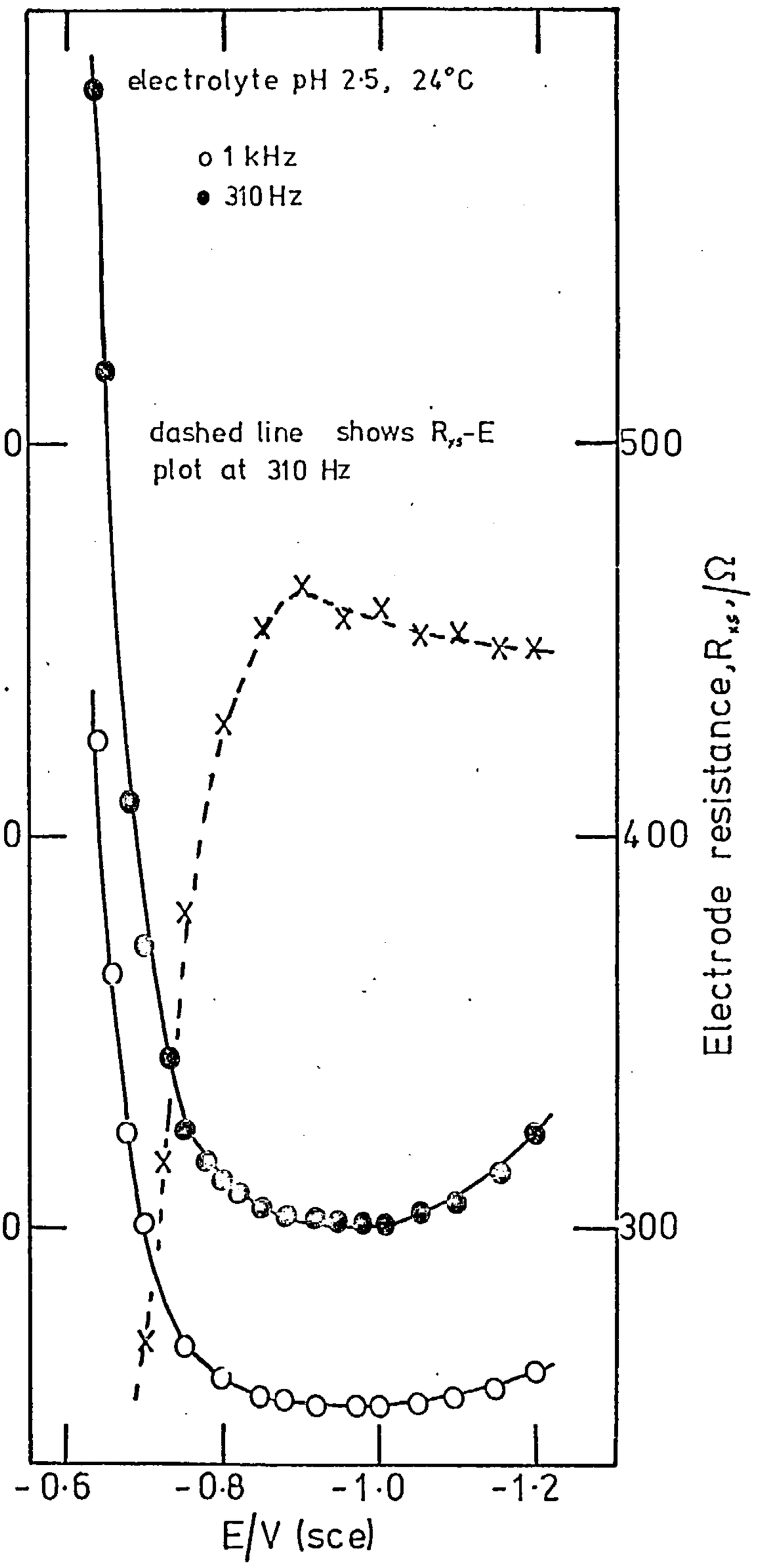

Fig.5-8 Effect of pH on differential capacitance-potential curves; 0·004 $mol\,l^{-1}$ $NaClO_4$

70 Hz, 24°C

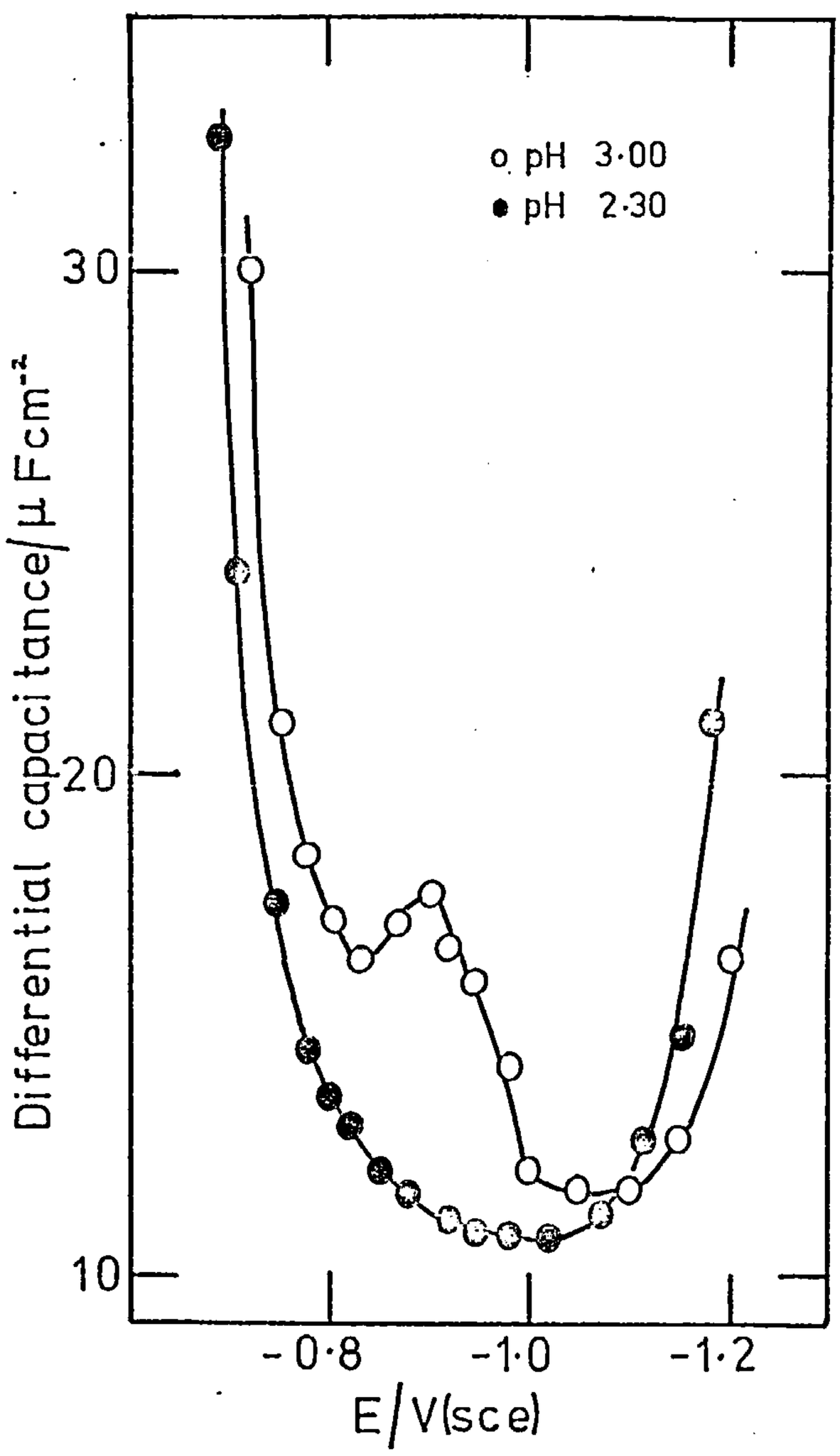

Fig.5-9 Frequency dispersion of differential capacitance-potential curves; 1·02 mol l^{-1} KF

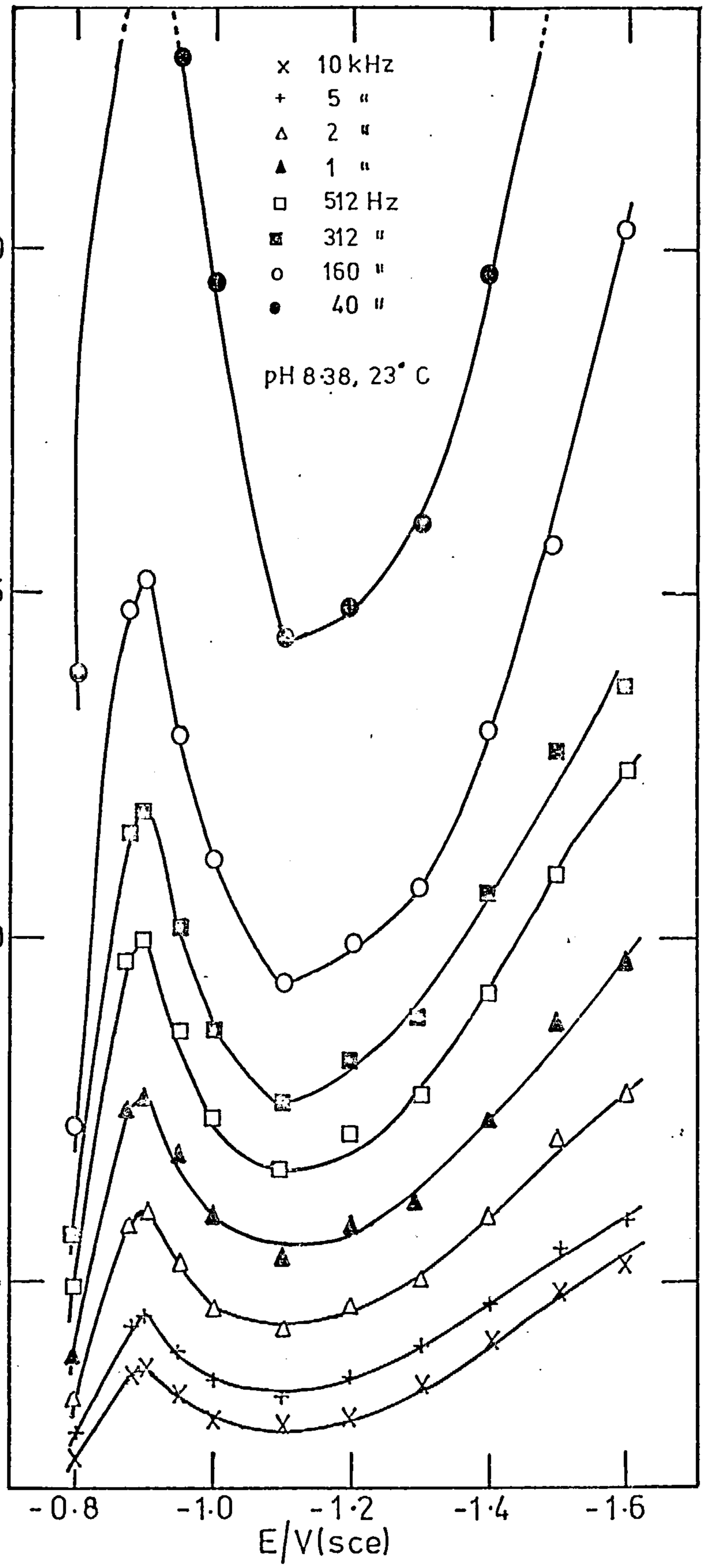

Fig·5-10 Frequency dispersion of differential capacitance-potential curves; 1·08 mol l^{-1} $NaClO_4$

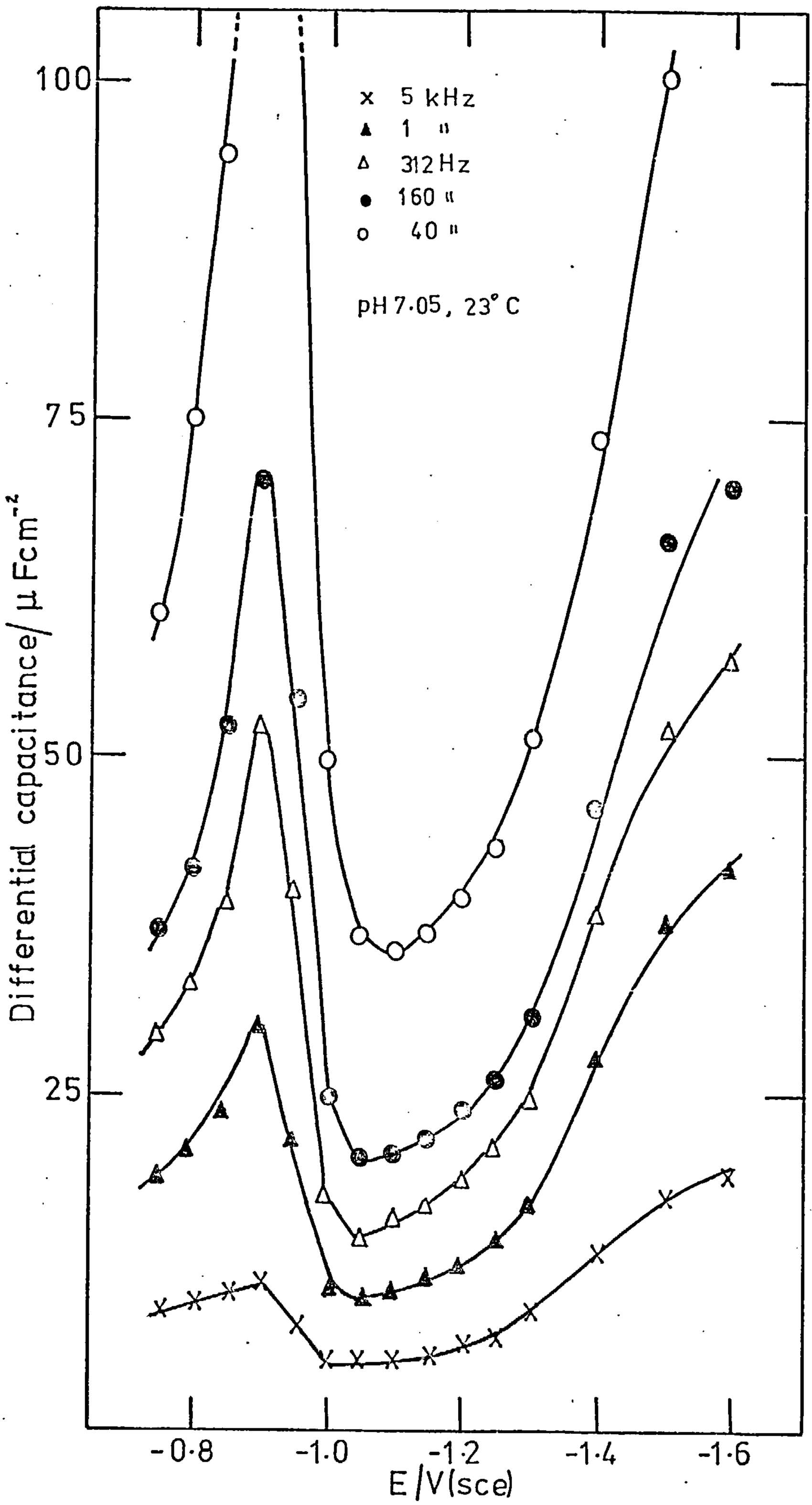

Fig.5-11 Frequency dispersion of differential capacitance-potential curves; 1·00 mol l^{-1} KCl

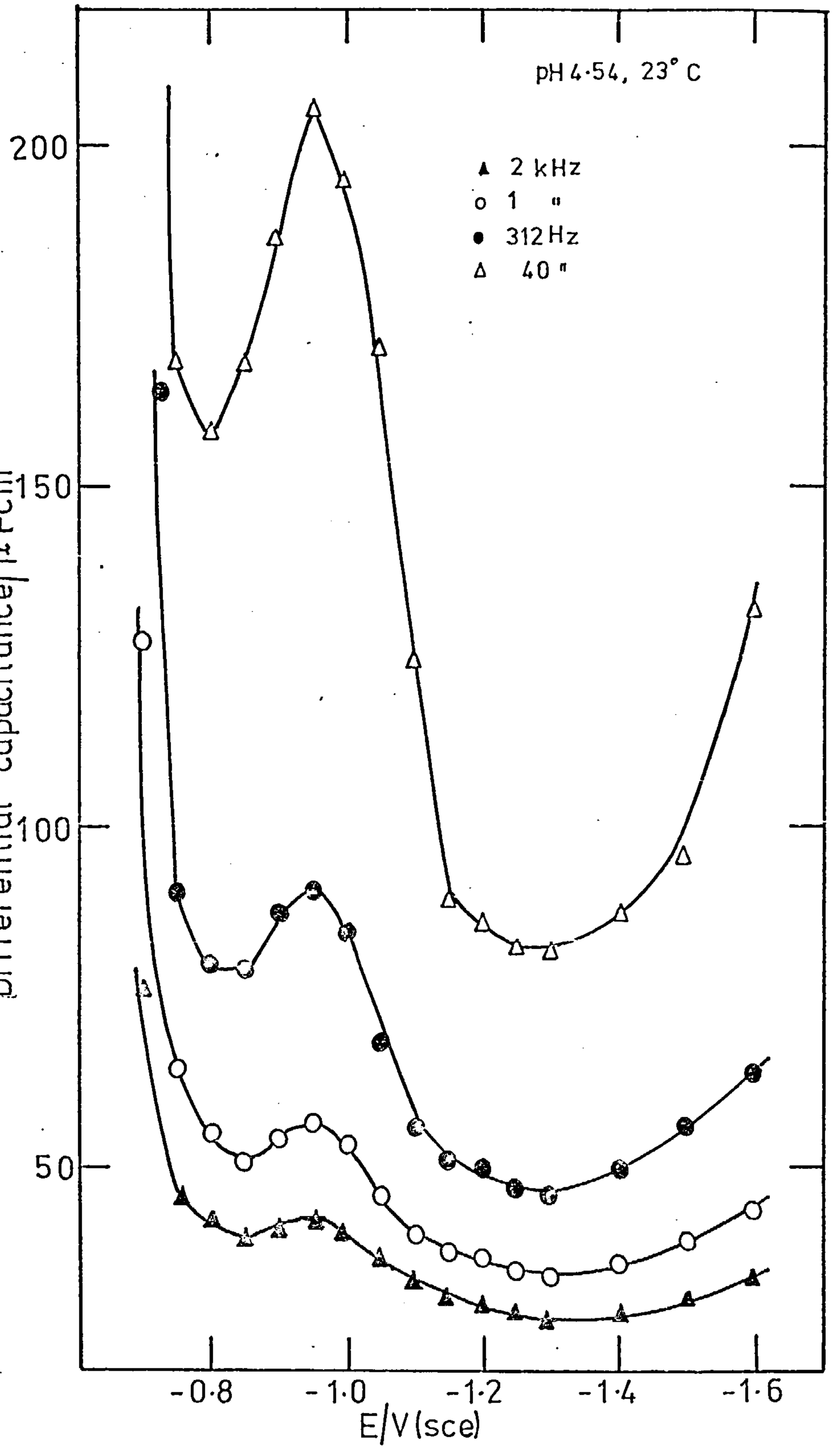

Fig. 5-12 Faradaic current - potential plot;
1·0 mol l^{-1} KNO_3

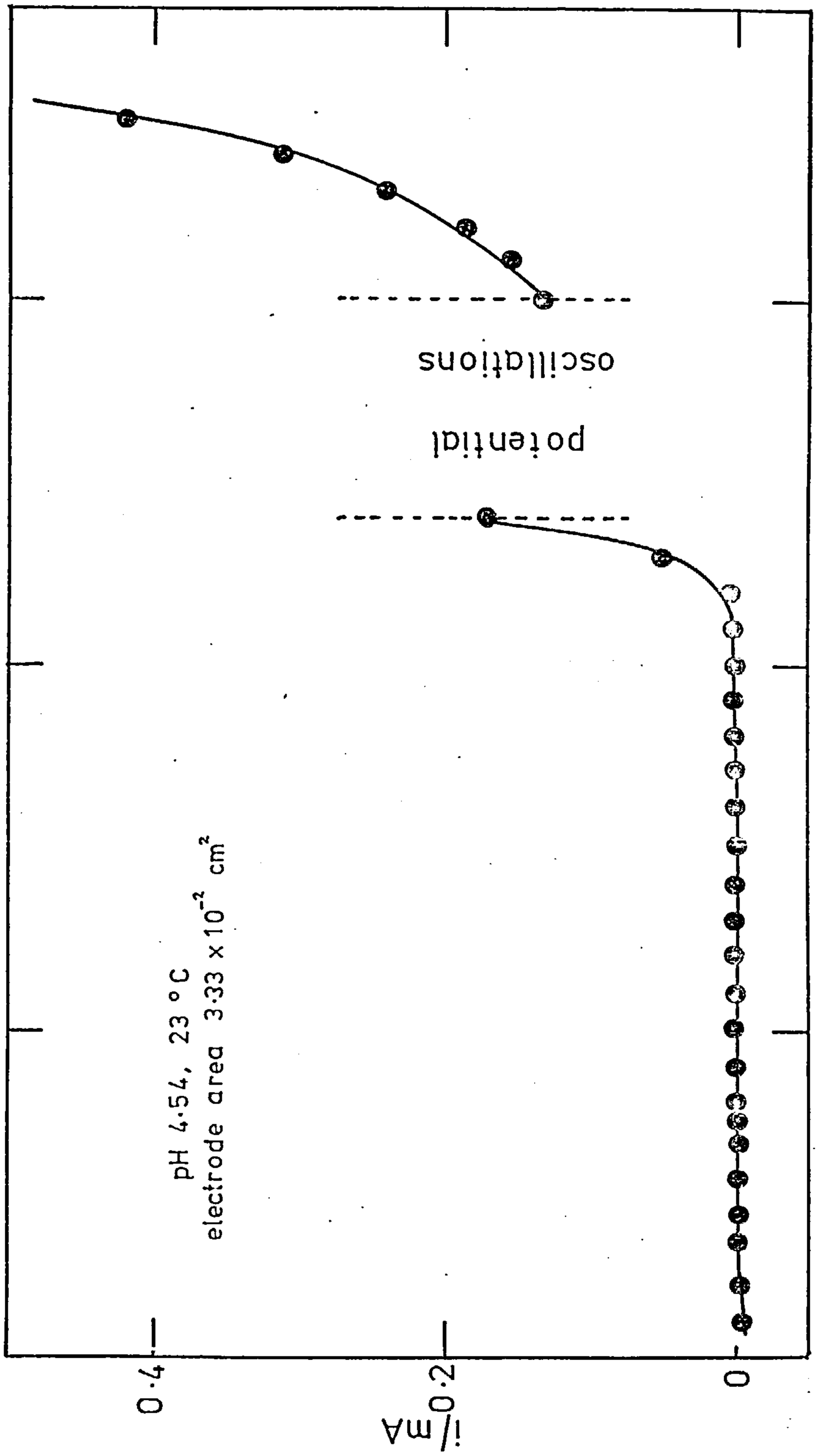

Fig. 5-13 Differential capacitance-potential curves;
0·1 mol l^{-1} KNO_3

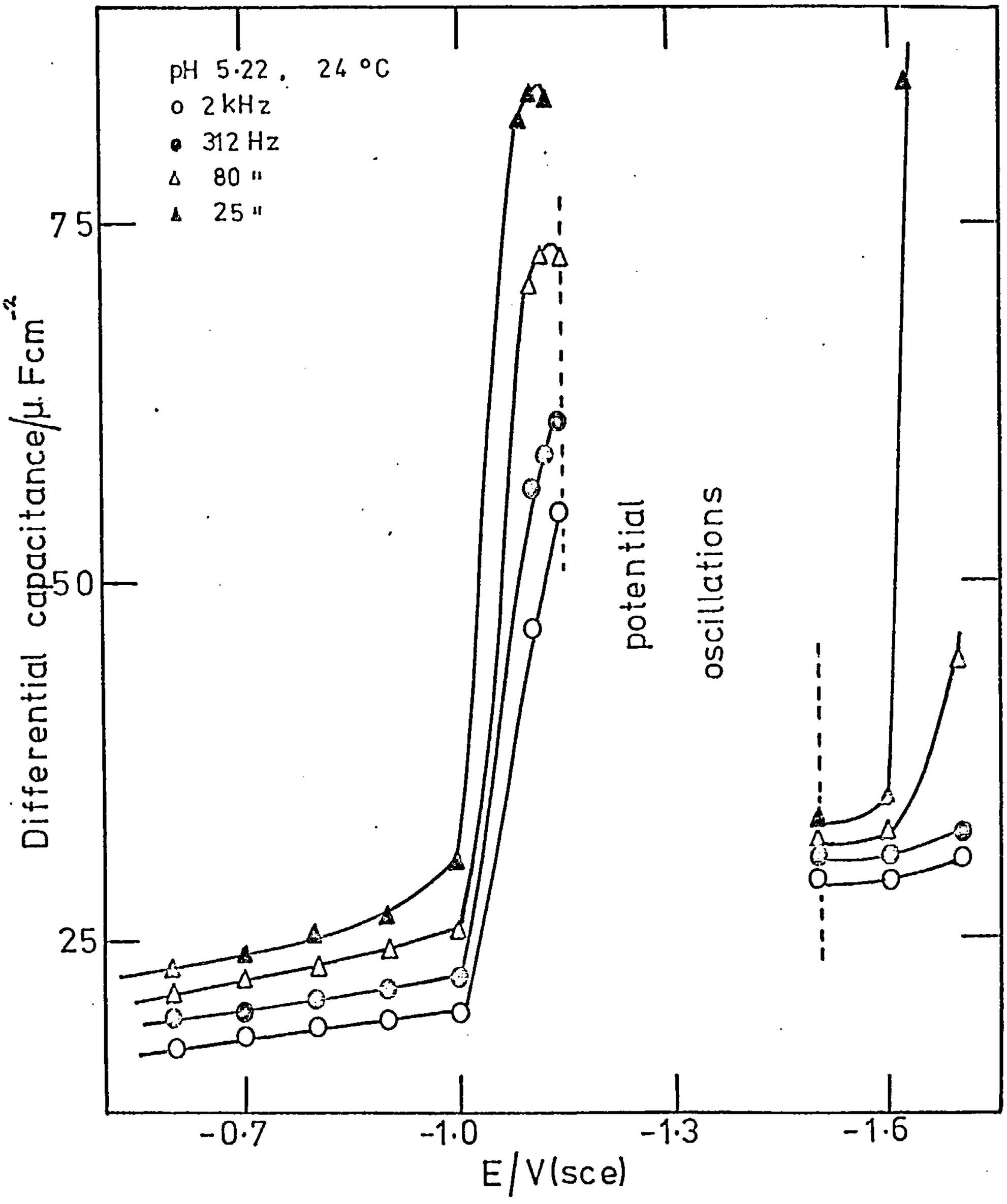

measurements were stable. Oscillations were independent of the previous polarisation history of the electrode and were unaffected by purging with N_2 or H_2.

5.4. Discussion

5.4.1. Sulphate, fluoride, perchlorate and chloride electrolytes

The faradaic current-bias potential curves illustrated in figure 5-1 exhibit a region of potential in which the faradaic current is so small that the systems can be considered experimentally polarisable. This region is bounded by the potential of lattice oxidation ($\sim$ -0.7 V to-0.8 V) and the potential of the h.e.r. ($\sim$ -1.4 V). The effect of lowering the pH is as expected, the potential of the h.e.r. being shifted to more positive potentials as typified by the data for sulphate electrolytes at pH 2.4.

The electrode capacitance and resistance data for indium in sulphate electrolytes (figure 5-2) is typical of a metal/aqueous solution interphase which is uncomplicated by specific adsorption or the intrusion of oxide (hydroxide) films. The electrode resistance curves are flat, indicating the absence of faradaic reactions in the experimentally polarisable range. As the ionic concentration is lowered the capacitance-potential curves exhibit a progressively deepening minimum. The value of this minimum (-0.95 ± 0.02 V) is considered as an estimate of the potential of zero charge (p.z.c.)* and agrees quite well with earlier Russian

---

* Footnote: Although sodium sulphate is an unsymmetrical electrolyte calculation of the magnitude of the potential shift to correct for the fact that the diffuse layer capacitance minimum does not coincide with the p.z.c. for such electrolytes[13] yields a value of 16 mV[99] and this correction is unrealistic in view of the estimated limits of the observed capacitance minimum ($\pm$ 0.02 V).

work[55]. The steep rise in capacitance at more positive potentials is attributed to the onset of lattice oxidation. Prepolarisation at the negative extreme of the potential range had no effect on the measured impedance values, which is in contrast to the other systems investigated (see for example figure 5-4).

Differential capacitance-bias potential measurements for indium in a series of KF electrolytes are shown in figure 5-3. The interesting feature is the pseudo-capacitance peak at -0.90 V observed at the higher concentrations. This is markedly different to the sulphate system where no such capacitance maximum was observed (figure 5-2). For the fluoride electrolytes it was found necessary to prepolarise the indium electrode for at least 2 hrs. at the negative extreme of the potential range in order to obtain reproducible results. Figure 5-4 clearly illustrates this requirement. As is evident, further prepolarisation does not effect the results obtained. The magnitude of the capacitance values observed when the electrode is not prepolarised leads one to suspect that the electrode is covered with an adsorbed layer which is removed during prepolarisation at potentials near to the h.e.r. The occurrence of the pseudo-capacitance peak is associated with the interaction of OH^- ions with the electrode surface.This is thought to be the case since similar capacitance maxima observed with perchlorate and chloride electrolytes (figs. 5-10 and 5-11) could be completely suppressed if the pH was lowered sufficiently (figs. 5-6 and 5-7), a phenomenon observed by other workers[100,101], whilst studying the differential capacitance of zinc in aqueous solutions. It is also interesting to note that at the higher fluoride concentrations there is no capacitance rise at the positive end of the potential axis marking the beginning of

lattice oxidation. It is concluded that at the more positive potentials an insoluble product is formed irreversibly at the electrode which inhibits lattice dissolution. This insoluble product is likely to be highly insoluble indium trifluoride (0.04 g/100 cc H_2O at 25°C)[102]. As the fluoride concentration is lowered a well defined capacitance minimum is observed at -0.93 ± 0.02 V. Thus the capacitance peak attributed to OH^- ion interaction is suppressed on dilution, a possible cause of which could be the lowering of the pH of the solutions on dilution. This behaviour, however, was not observed with chloride and perchlorate electrolytes (see for example figure 5-5) where dilution failed to suppress the pseudo-capacitance maxima. Furthermore in chloride and perchlorate electrolytes the pH had to be below 3 before the pseudo-capacitance peak was suppressed. Earlier workers[56] reported diffuse layer capacitance minima for indium in 0.01 mol l^{-1} solutions of NaF, NaCl and $HClO_4$ at potentials (vs. NCE) of -0.93 V, -0.97 V and -0.97 V respectively. For their measurements[56] in 0.1 mol l^{-1} NaF no pseudo-capacitance maximum was observed, however this may be due to the fact that no control of pH was undertaken in their experiments. From the data in figure 5-3 it is not certain that the capacitance minimum at ∿ -0.93 V corresponds to the p.z.c. in view of the suspected OH^- ion interaction at higher concentrations and the fact that pH's lower than 3 are required to suppress the pseudo-capacitance maxima in other systems investigated. It should be noted, however, that the capacitance minimum occurs in the fluoride system at very nearly the same potential as the capacitance minimum observed for the sulphate system (fig. 5-2), where it was concluded that complications due to adsorption at the interphase were absent.

Figure 5-5 shows a family of differential capacitance curves for indium in a series of KCl solutions. The noticeable feature is that the pseudo-capacitance peak at -0.95V is not suppressed as the ionic concentration is reduced, as was the case with KF electrolytes (fig. 5-3). A further difference from the fluoride system is that for chloride electrolytes the capacitance rises sharply at the positive extreme of the potential range, thus suggesting that a soluble product might be formed at the electrode, the anodic dissolution reaction being relatively unhindered. If the pH is sufficiently reduced for either the chloride or perchlorate systems (figs. 5-6 and 5-7) the pseudo-capacitance peak is completely suppressed. This observation substantiates the theory that the capacitance maximum is due to a hydroxyl ion adsorption/desorption process. It should be noted that the magnitude of the capacitance values for acidified systems are somewhat lower than those for unacidified systems of corresponding ionic concentrations. This is probably due to the adsorption of hydrogen at the electrode surface in the more acid solutions. Care was taken not to allow the potential to become too negative in the acidified systems in view of the reported possibility[98] of forming an indium-hydrogen compound (InH) at cathodic potentials in solutions of low pH. Armstrong et al[103] whilst studying the differential capacitance of copper in aqueous solutions, observed a pseudo-capacitance peak at potentials just prior to the h.e.r. which they attributed to the formation of a copper-hydrogen compound. However, indications of an indium-hydrogen compound under similar conditions were never in evidence during the present studies. A further feature of the acidified perchlorate system (figure 5-7) is the sharp capacitance

rise at the more positive potentials, a phenomenon not observed in the unacidified system (figure 5.10.). This indicates that a freely soluble electrode product is formed at these potentials in acid perchlorate solutions, thus allowing lattice dissolution to occur readily.

Figure 5-8 shows differential capacitance-bias potential curves for an indium electrode in dilute (0.004 mol l^{-1}) $NaClO_4$ solutions. It can be seen that even at pH 3 the capacitance maximum at -0.90 V as observed at higher perchlorate concentrations (figure 5-10), is present. Further reduction of pH suppresses the capacitance maximum, but fails to reveal a capacitance minimum characteristic of the diffuse double layer.

The frequency dispersions of the differential capacitance for higher concentrations of unacidified KF, $NaClO_4$ and KCl electrolytes (figs. 5-9, 5-10 and 5-11) appear too great to be ascribed to surface roughness*. This was confirmed by plotting the measured capacitance C_{xs} against $\omega^{-\frac{1}{2}}$ when a rectilinear plot results from dispersion due to inhomogeneity of the electrode surface[104]. This plot was found to be curved for each of the systems and consequently other factors must be involved, although in view of the difficulty in electropolishing an indium microelectrode (section 3.1.3a) some dispersion due to surface roughness is to be expected. Other sources of the dispersion might arise due to a redox reaction in the adsorbed state at the electrode or alternatively the removal of the electrode material itself as sparingly soluble indium hydroxide. To test this

---

*Footnote: It should be noted that earlier Russian workers[56] reported the measured capacitance to be frequency independent in the range 70-2500 Hz, for indium in NaF solutions in the concentration range 0.003 to 0.1 mol l^{-1}.

the impedance behaviour in the vicinity of the pseudo-capacitance maximum has been analysed by converting the measured series capacitive component (C_{xs}) to the equivalent parallel circuit capacitances (C_p) and studying the frequency dependence of C_p. The series capacitive component is given by[105]

$$\frac{1}{\omega C_{xs}} = \left(\frac{RT}{zF}\right) \frac{1}{zF(2\omega)^{\frac{1}{2}}} \left(\frac{1}{C_O D_O^{\frac{1}{2}}} + \frac{1}{C_R D_R^{\frac{1}{2}}} \right) \qquad (5.1)$$

In (5.1) C_O and C_R are interphase concentrations of oxidised and reduced species (mol cc^{-1}). Assuming that the charge transfer resistance for indium is zero and that $C_R \gg C_O$, the parallel circuit capacitance is given by [106]

$$C_p = \frac{C_{xs}}{2} = \frac{z^2F^2C_O}{2RT} \left(\frac{2D_O}{\omega}\right)^{\frac{1}{2}} \qquad (5.2)$$

Expressing C_O in mol l^{-1}, simplifying and adding the double layer capacity[107] we obtain

$$C_p = C_{dl} + \frac{C_O}{2\sigma\omega^{\frac{1}{2}}} \qquad (5.3)$$

where $\sigma = 1000RT/z^2F^2(2D_O)^{\frac{1}{2}}$. De Levie [108] has modified the parallel equivalent circuit to incorporate the effects of surface roughness. Following De Levie's work[108] and considerable experimental evidence[109], the apparent parallel capacity due to surface roughness (C_p^a) is proportional to $\omega^{-\frac{1}{2}}$ thus (5.3) may be written as

$$C_p = C_{dl} + \frac{C_O}{2\sigma\omega^{\frac{1}{2}}} + \frac{\beta}{\omega^{\frac{1}{2}}} \qquad (5.4)$$

(5.4) predicts that a plot of C_p vs. $\omega^{-\frac{1}{2}}$ will be linear with an intercept C_{dl}. The interphasial concentration of oxidised species (C_0) can be obtained by subtracting the slope g, due to roughness, from the total slope of C_p vs. $\omega^{-\frac{1}{2}}$ plots, hence leaving the faradaic slope $C_0/2\sigma$. It should be noted that a corresponding relationship for R_p, the equivalent parallel circuit resistance, can be obtained[106], however, only the parallel circuit capacitance is considered here. The transfer from a series, R_{xs} - C_{xs}, to a parallel, C_p - R_p, arrangement was effected using the equation

$$C_p = \left(\frac{\beta^2}{1+\beta^2}\right) C_{xs} \qquad (5.5)$$

where $\beta = \left[\omega C_{xs}(R_{xs} - R_{sol})\right]^{-1}$. R_{sol}, the solution resistance, was found by plotting Z' against Z'' and extrapolating to infinite frequency[110]. Figure 5-14 shows this plot to be a straight line at -1.10 V for the fluoride system. Straight line plots of Z' vs. Z'' were also obtained for the perchlorate system at -1.05 V and the chloride system at -1.3 V.

Figure 5-15 shows plots of C_p vs. $\omega^{-\frac{1}{2}}$ corresponding to various potentials around the capacitance peak, at -0.90 V, for the fluoride system at high concentration (figure 5-9). It is clear that there is a significant faradaic component of C_p at the peak potential (-0.90 V) compared to -1.10 V where the faradaic reaction is considered negligible (figure 5-9). Furthermore figure 5-15 shows that the faradaic reaction is greatly inhibited at -0.80 V, which supports the proposed theory that an insoluble electrode product is formed at the positive extreme of the potential axis for the higher fluoride concentrations. Assuming a faradaic reaction of the

Fig. 5-14 Plot of Z' vs. Z'' ; 1·02 mol l^{-1} KF

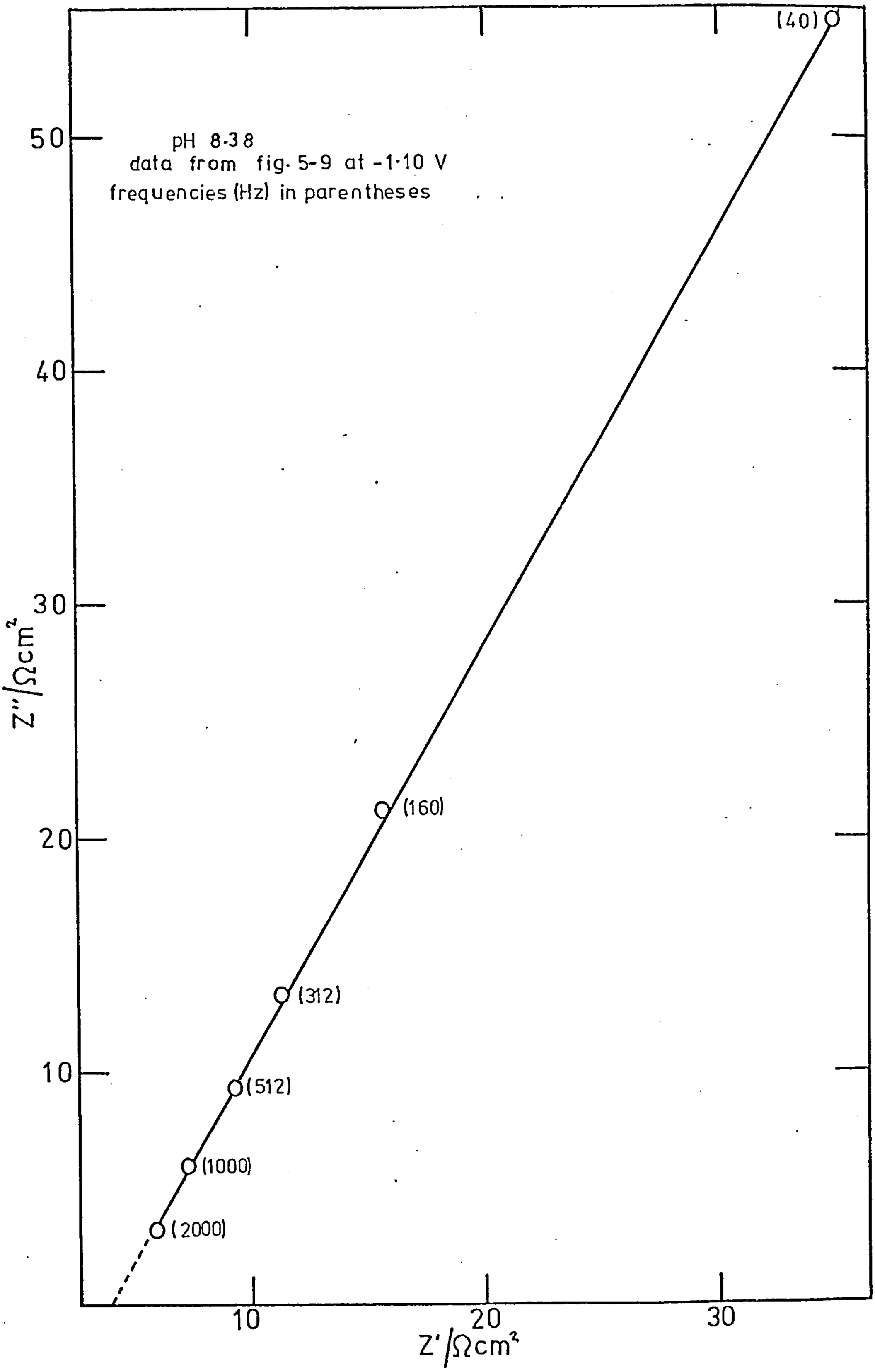

Fig.5-15 C_p vs. $\omega^{-1/2}$ plots; 1·02 mol l^{-1} KF

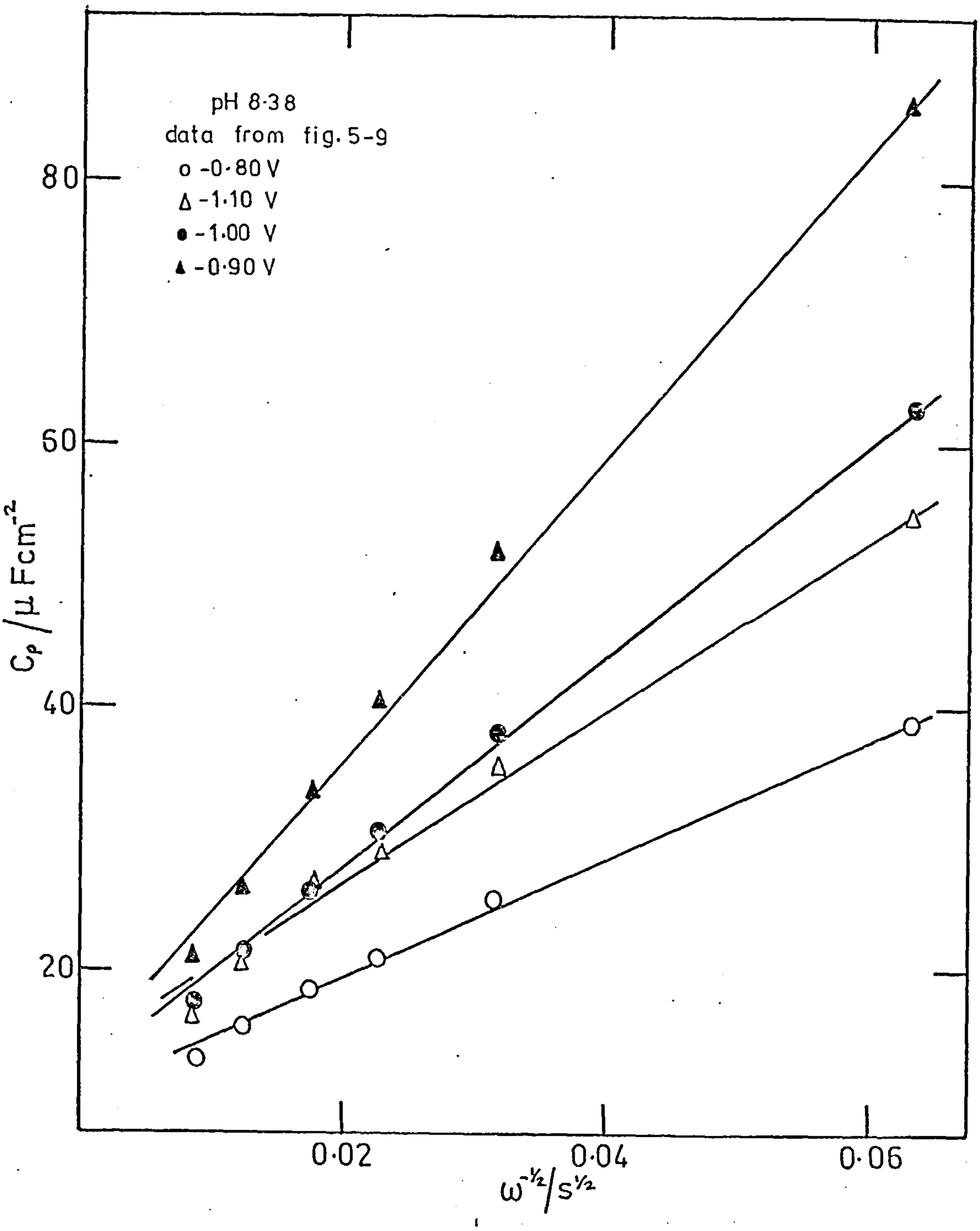

type

$$In = In(III)_{soln} + 3e \qquad (5.6)$$

C_0 at -0.90 V for the fluoride system can be estimated. Taking the slope due to roughness to be that at -1.10 V when least faradaic reaction is present, then C_0 at -0.90 V is 7.0×10^{-6} mol l^{-1} for $z = 3$ and $D_0 = 10^{-5}$ cm^2 s^{-1}.

Figure 5-16 shows C_p vs. $\omega^{-\frac{1}{2}}$ plots for various potentials around the capacitance peak for the chloride system at high ionic concentrations (fig. 5-11). As with the fluoride case (fig. 5-15) there is an appreciable faradaic reaction at the peak potential (-0.95 V) compared to the potential where the faradaic process was considered negligible (-1.30 V). Calculation of C_0 at -0.95 V by the method outlined above affords a value of 1.7×10^{-5} mol l^{-1}. Figure 5-16 also shows that at -0.70 V the lattice dissolution reaction is occurring relatively unhindered.

Extrapolation of the C_p vs. $\omega^{-\frac{1}{2}}$ plots to infinite frequency yields values of C_{dl}, the differential double layer capacitance per unit electrode area, in the region 10-20μFcm^{-2} for both fluoride and chloride systems. Exact values of C_{dl} are unrealistic in view of the difficulties in extrapolation.

5.4.2. Nitrate electrolytes

As is evident from figures 5-12 and 5-13 the indium/aqueous potassium nitrate system behaves in a rather unexpected manner, in that oscillations of potential occurred in the potential range $\sim$-1.2 V to$\sim$-1.5 V.

Fig. 5-16 C_p vs. $\omega^{-1/2}$ plots; 1·00 mol l^{-1} KCl

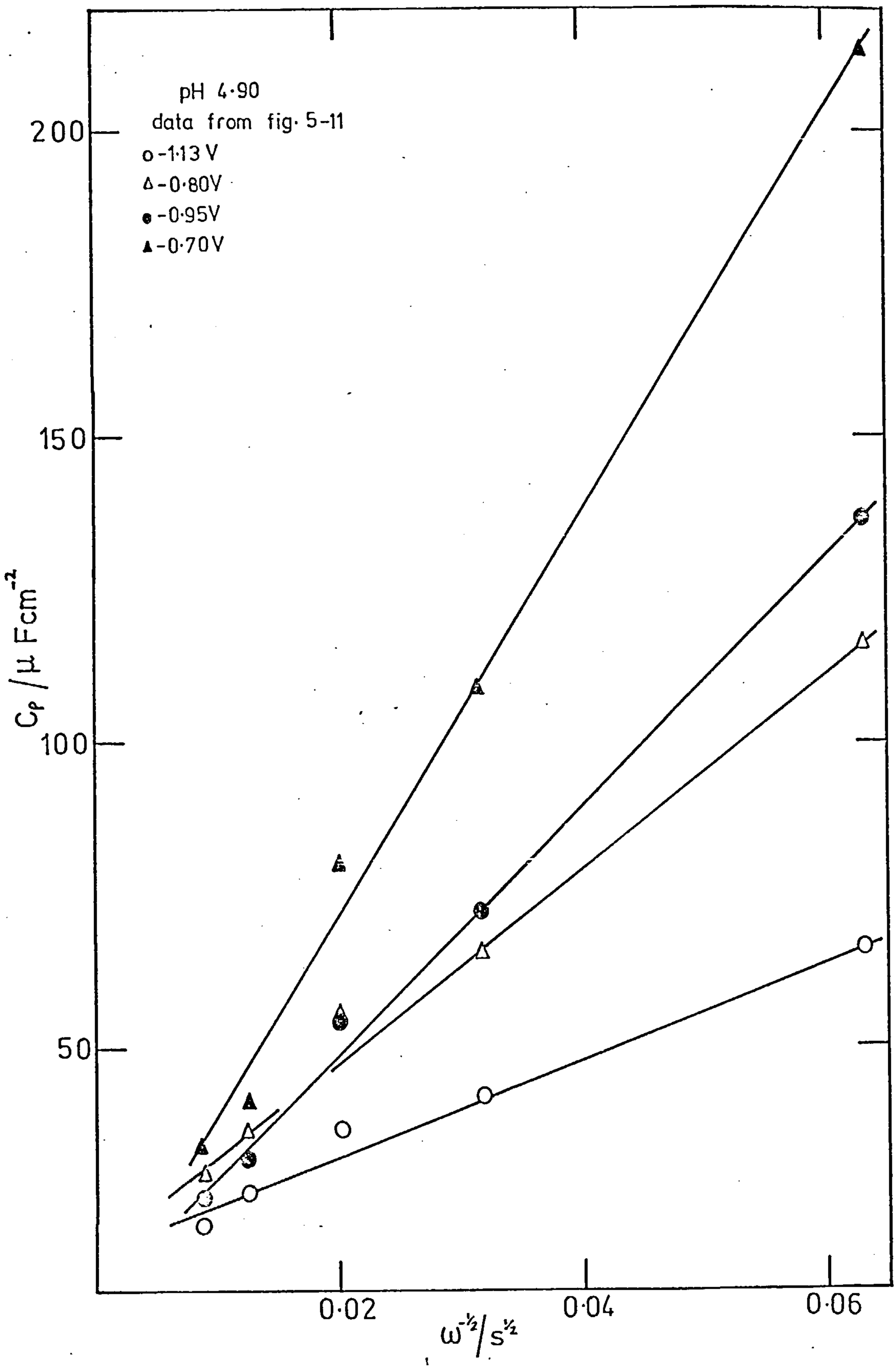

The occurrence of spontaneous oscillations of potential is of some interest, for although they have been noted in a few systems they have rarely been reported as the result of a cathodic reaction. The explanation of oscillating potential is generally formulated in terms of two reactions which occur sufficiently closely in potential for an impressed current to correspond to two possible potentials (conversely at a given potential two current values are possible) and the system oscillates between these two values provided that one of the electrode processes can be inhibited (the occurrence of a passivation region with negative resistance on the polarisation curve). Izidinov and Red'ko[111] discussed the nature of spontaneous oscillations of potential of a PbO_2 anode in aqueous chloride electrolytes in terms of parallel reactions of oxygen and chlorine evolution, the adsorption/desorption of oxygen providing the passivation process. The continual reduction of a chemisorbed layer of oxygen at the surface of the electrode might possibly have given rise to the present oscillations. This is considered unlikely since oscillations were observed in nitrate systems carefully freed from O_2 (by N_2 purging), also oscillations were not observed in unpurged systems of other electrolytes, neither were oscillations present in other aqueous electrolyte solutions which had been purged with oxygen.

Attention is therefore directed towards the nitrate ion. Data concerning the double layer structure of other solid metals in nitrate electrolytes have been recorded; Deriaz[112] has reported differential capacitance curves for the $Pb/KNO_{3.(aq)}$ system, Armstrong et al[103] have reported double layer data for the $Cu/KNO_{3.(aq)}$ system. In both of these there is neither evidence for oscillations of potential at -1.2 V nor for any reaction involving the nitrate ion.

Kabanov, Tomashova and Kiselvea[113], however, have shown that with alkali metal nitrate electrolyte, reduction to nitrite can occur at relatively low cathodic potentials if the alkali metal dissolves interstitially in a lead electrode. Marshall and Hampson[114] have also observed the reduction of the nitrate ion whilst studying the differential capacitance of zinc in aqueous potassium nitrate electrolytes. It might be expected that the reduction of nitrate to nitrite would take place readily at an indium electrode in view of the effect of such high valency (In^{3+}) ions on the reaction. Thus Takouka[115] has pointed out the need for the presence of high valency ions at the dropping mercury electrode if nitrates are to be reduced. In order to test this supposition, experiments were made in which an indium electrode of large area was potentiostatically polarised in KNO_3 solution (1.0 mol l^{-1}) at -1.2 to - 1.4 V (the mean current was 30 mA). After a few hours the solution was acidified and on testing via the specific diazo reaction with aniline and β-napthol in comparison with a blank, the presence of nitrite was confirmed, produced by the reaction

$$NO_3^- + 3H^+ + 2e = HNO_2 + H_2O \qquad (5.6)$$

Two schemes which account for the potential oscillations may be formulated using reaction (5.6) and the h.e.r.

$$2H^+ + 2e = H_2 \qquad (5.7)$$

As the electrode is forced to increasingly negative potentials reaction (5.6) is suppressed in favour of reaction (5.7) due to the

greater repulsion of the electrode and the NO_3^- ion. In the oscillation region the NO_3^-/NO_2^- electrode reaction is inhibited by hydrogen adsorption and the potential becomes more negative until discharge of hydrogen ion is possible when the electrode region again changes to become predominantly (5.6). The transition again occurs as the hydrogen ion displaces the NO_3^- from the surface of the electrode forcing current from reaction (5.6) into reaction (5.7) as the potential rises prior to the discharge of adsorbed hydrogen which unblocks the electrode (negative resistance region) and so on. The form of figure 5-12 conforms to this model; two Erdey-Gruz and Volmer type curves are evident and itis suggested that oscillations occur between these two according to the degree of coverage of the electrode with hydrogen.

An alternative explanation may be formulated in terms of the removal of the nitrate from the electrode reaction layer causing a transition from reaction (5.6) to reaction (5.7) followed by a further transition back to reaction (5.6) when the concentration polarisation has died away.

It is difficult to decide between these two mechanisms on the data available, however, the fact that on a soft metal such as indium a high concentration of adsorbed hydrogen is unlikely makes inhibition due to coverage with hydrogen unlikely. Support for this view comes from Butler and Dienst[97] who found that the kinetics of the h.e.r. on indium in 0.1 mol l^{-1} $HClO_4$ conform to a slow discharge mechanism

$$H_3O^+ + In + e = H\text{-}In \longrightarrow \tfrac{1}{2}H_2 + In \qquad (5.8)$$

the second stage is unlikely to involve a high surface coverage with

hydrogen.

The extended "low current" region observed with nitrate solutions (figure 5-12, $\sim$ -0.7 V extended to$\sim$-0.2 V) indicates the presence of a current limiting process offsetting the dissolution reaction. Figure 5-13 also demonstrates this point since no rise in capacitance due to indium oxidation is observed at the anodic extreme of the potential range. The reason for this behaviour appears to be the formation of an oxide (hydroxide) or basic salt layer which suppresses the indium dissolution reaction. The occurrence of visible films on electrodes which had been polarised at the more positive potentials supports this view.

A further interesting fact which sets nitrate solutions apart from others in its relation to indium is the pronounced aggressive attack on the metal surface. Thus Mills et al[116] report that nitric acid is many orders of magnitude more aggressive towards indium than all other common etchants. Experiments were made whereby indium electrodes were polarised at various potentials in the experimental range. It was observed that aggressive attack occurred at potentials when a reduction current was flowing. It is suggested that the corrosion process:

$$In = In^{3+} + 3e \qquad (5.9)$$

when coupled with (5.6) giving

$$2In + 3NO_3^- + 6H^+ = 2In^{3+} + 3NO_2^- + 3H_2O \qquad (5.10)$$

is the cause of the aggressive attack.

5.5. Conclusions

1. Of the systems studied, the indium/sodium sulphate system is the only one to show potential regions where the electrode/aqueous solution interphase is considered to be uncomplicated by adsorption or the intrusion of films. An estimate of the p.z.c. for this system is -0.95 ± 0.02 V.

2. It is not possible to determine unequivocally the p.z.c. for indium in fluoride electrolytes, although a well-defined capacitance minimum occurs at -0.93 ± 0.02 V in dilute fluoride solutions.

3. For unacidified chloride and perchlorate electrolytes a well-defined capacitance minimum is not observed as the ionic concentration is lowered.

4. In unacidified solutions of KF and $NaClO_4$ at high ionic concentrations, the anodic rise in electrode capacitance due to lattice oxidation is suppressed, due to the irreversible formation of highly insoluble films at the electrode surface.

5. A pseudo-capacitance peak at -0.90 V in KF solutions, -0.90 V in $NaClO_4$ solutions and -0.95 V in KCl solutions is concluded as being due to OH^- ion interaction with the indium electrode surface and subsequent dissolution of the metal lattice. The concentration of solution soluble indium species in equilibrium with the electrode at the capacitance peak has been calculated for the fluoride and chloride cases (1 mol l^{-1}, unacidified solutions) at these peak potentials.

6. The results of double layer measurements on indium in aqueous nitrate electrolytes are presented. Coupled with electrometric data these show that nitrate ion is reduced to nitrite ion

with the occurrence of oscillations of potential. Possible reasons for the oscillations are discussed.

CHAPTER 6

STUDIES OF THE EQUILIBRIUM POTENTIAL OF THE INDIUM ELECTRODE IN AQUEOUS CHLORIDE ELECTROLYTES

6.1 Introduction

It is clear from studies of the indium/aqueous solution interphase (chapter 5) that it is difficult to avoid the formation of films derived from $In(OH)_3$ on the surface of the electrode unless solutions of relatively low pH are used. Because of the position of indium in the periodic table this behaviour is not unexpected, moreover, Pourbaix[98] indicates that the upper limit of the stability region of In^{3+} in aqueous solution is $\sim$pH 2.5 and that even at pH 3-5 the metal tends to be covered with a film of the oxide In_2O_3 or the hydroxide $In(OH)_3$. Busev[117] has reviewed the reported data on the behaviour of the indium ion in solution and it is clear that the ions $\left[In(H_2O)_5OH\right]^{2+}$ and $\left[In(H_2O)_4(OH)_2\right]^{+}$ exist in solutions of indium salts. Biedermann[118,119] claims that when the concentration of indium is less than 0.001 m the ions $\left[In(OH)\right]^{2+}$ and $\left[In(OH)_2\right]^{+}$ predominate among the hydrolysis products. The hydrolysis of indium trichloride solutions can be readily demonstrated; the pH of an aqueous solution of $InCl_3$ has been reported by Moeller[120] to be 2.65 (0.4141 M) and 3.75 (0.0005 M) corresponding respectively to degrees of hydrolysis of 0.0054 and 0.356. It has further been shown[121,122] that indium (indium hydroxide) is precipitated from solutions of indium trichloride at pH$\sim$3.6 and that the pH of precipitation decreases markedly as the temperature is increased[121], thus, at 10°C the pH required to initiate precipitation is 3.56, at 40°C the pH was 3.15. Accordingly, Hakomori[44] found it necessary to ensure that $InCl_3$ solutions used for In^{3+}/In equilibrium potential measurements were of sufficiently low pH by the addition

of a definite concentration of hydrochloric acid.

A more recent investigation by Covington et al[48] reported that cells of the type

$$In \;\Big|\; InCl_{3(m_1)} \;\Big|\; AgCl \;\Big|\; Ag$$

behaved satisfactorily over a temperature range 0-60°C. Although Covington's study avoided difficulties in the data treatment inherent in investigations of cells with mixed electrolyte types, no attention was paid to the hydrolysis of the indium ion and the consequent complications of precipitation of hydrous hydroxide from solution in the more dilute solutions, particularly at the higher temperatures used.

Because of the need to isolate conditions under which the In(III)/In reaction may be satisfactorily investigated in aqueous solutions, without complications at the interphase, the previously reported experiments[44,48] have been repeated and extended. This present work yields new values for $E^{\ominus}$ and $\frac{\partial E^{\ominus}}{T}$ which resolves some of the conflict which exists in the literature.

6.2. Experimental

The cells used for these studies are described in section 3.1.2. The electrodes and indium electrode pretreatment technique are described in section 3.1.3b. Details of the electrical circuit are given in section 3.4.1.

Solutions of indium trichloride were prepared from $InCl_3.3H_2O$

(B.D.H. Chemicals Limited)* and water triple distilled from deionised stock. AnalaR HCl was added when required to adjust the pH and, suitably diluted, as an addition to the total ionic concentration. After potentiometric measurements had been made, all solutions were check analysed for indium using E.D.T.A. and Eriochrome Black T indicator (see appendix 1) and for chloride by Volhard's method[124].

6.3. Results

A large number of attempts were made to obtain consistent potential measurements corresponding to cells of the type

$$In_{(s)} \mid InCl_{3(aq)(m_1)} \mid AgCl_{(s)} \mid Ag_{(s)} \qquad (6.1)$$

At temperatures $\sim 25^{o}C$ potential measurements were erratic and in all cases significantly lower than those in corresponding solutions of controlled, constant, pH $\lesssim$ 2.7. At higher temperatures, measurements made were equally erratic, however, the level of the emfs approached those obtained using cells with controlled pH electrolyte solution. The emfs of cells of type (6.1) were found to be quite time dependent, however, no limiting value of emf was observed, the measurements changing in an unpredictable way.

The acidified cells took several hours to reach constant emf values, although cells measured at higher temperatures were found

---

*Footnote: This procedure removed the difficulty of elimination of an excess of free hydrochloric acid from the solution which arises when the dissolution of indium metal in mineral acid, as described in 3.1.1. is used. The salt was recrystallised from its solution in triple distilled water (following concentration[123]) before final solutions were made. The pH of solutions of indium trichloride without added acid agreed extremely well with those values reported by Moeller[120] for solutions prepared from anhydrous $InCl_3$. It thus appears that the crystallisation of indium trichloride produces relatively little basic salt.

to equilibrate more rapidly. In view of this, cells were always left overnight in the thermostatically controlled water bath before noting their emf values. Once at a steady value the potential remained constant.

Whereas unacidified systems invariably developed turbidity after some hours, the indium electrode in these cells becoming covered with a visible surface film, the acidified solutions exhibited no turbidity at any temperatures in the experimental range and no visible films were formed on the indium electrode in these systems.

Figure 6-1 shows the variation of emf with pH for an $\sim$ 0.002 m solution of $InCl_3$ in a cell of the type

$$In_{(s)} \mid InCl_{3(aq)(0.002m)}, \; HCl_{(m_1)} \mid AgCl_{(s)} \mid Ag_{(s)} \quad (6.2)$$

The presence of a small quantity of excess HCl is necessary for the cells to function consistently. Experiments were therefore made along the lines suggested by Hakomori[44], a small quantity of HCl added to the $InCl_3$ solutions in order to suppress hydrolysis*. Although inherent errors are introduced by the lack of a satisfactory theory of mixed electrolyte types, these errors would be less (fig 6-1) than those due to hydrolysis of the $InCl_3$.

Experiments with added HCl

Table 1 shows the variation of emf with concentration of $InCl_3$, at 25°C for cells of the type

$$In_{(s)} \mid InCl_{3(aq)(m_1)}, \; HCl_{(0.02m)} \mid AgCl_{(s)} \mid Ag_{(s)} \quad (6.3)$$

*Footnote: It is difficult to decide the appropriate amount of HCl required. Figure 6-1 shows that at 25°C the addition must exceed 5×10^{-3} m; in view of the temperature range of the experiments and the existance of Hakomori's data, 2×10^{-2} m was added, which proved satisfactory.

Fig.6-1 Variation of cell EMF with pH for a cell of the type: $In_{(s)} | InCl_{3(aq)(0\cdot002m)}, HCl_{(m_1)} | AgCl_{(s)} | Ag_{(s)}$

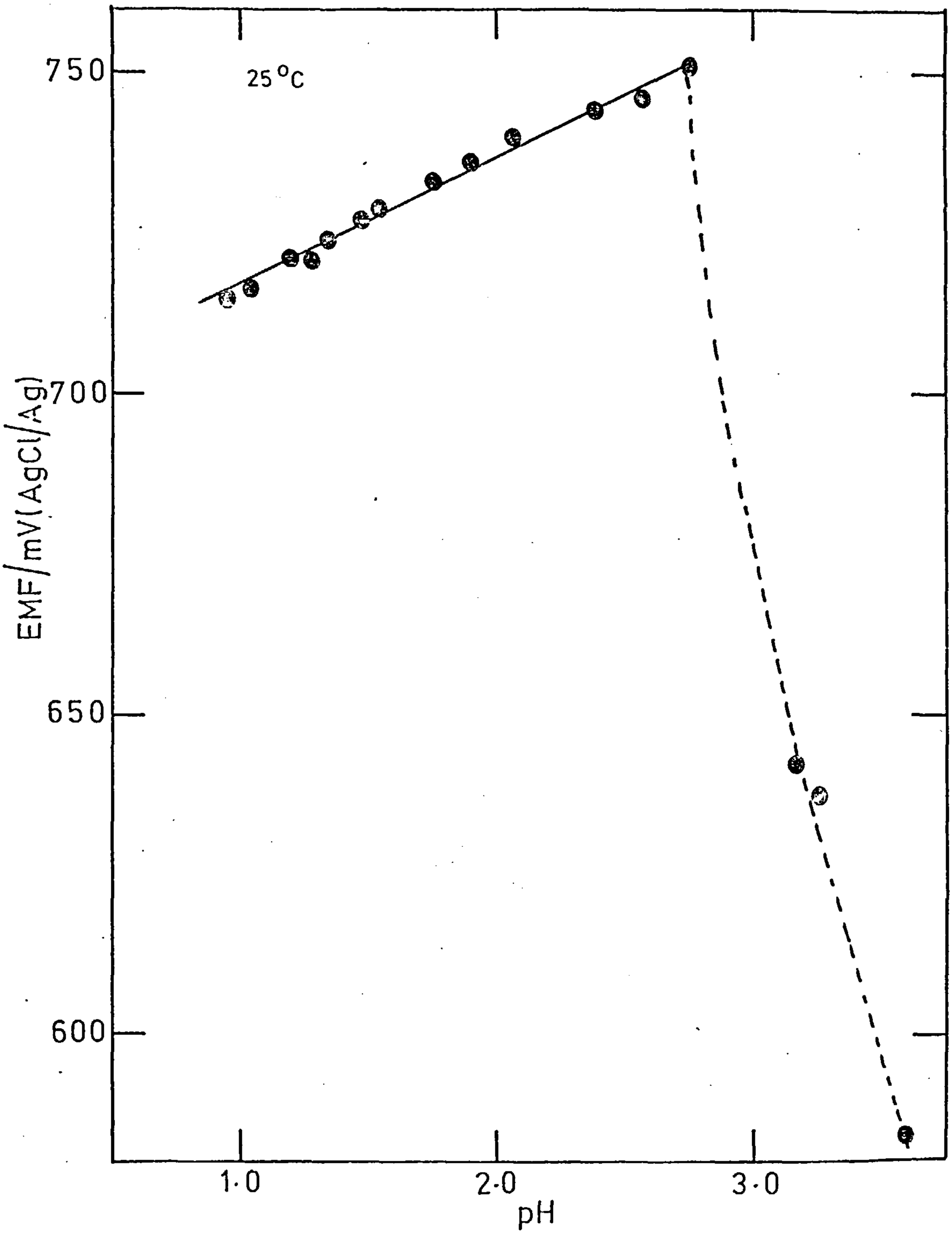

with m_1 in the range 0.0015 m to 0.0527m.

Table 6.1

m_{InCl_3}/m	m_{HCl}/m	pH	emf (mV)
0.00150	0.02	1.921	736.59
0.00697	0.02	2.006	725.23
0.01150	0.02	1.905	719.96
0.02000	0.02	2.004	712.19
0.03190	0.02	1.956	704.96
0.05270	0.02	1.922	696.82

The reported data were the time-stable, mean values for four nominally identical cells. Reproducibility was better than 0.3 mV between extremes.

Figure 6-2 shows variations in emf with temperature for cells of the type (6.3). A mean value of the slopes of these plots $(\partial E/\partial T)_p$, was obtained by the method of least squares and table 6.2 shows the values obtained with four solutions.

Table 6.2

m_{HCl} = 0.02m.				
m_{InCl_3}/m	0.00378	0.0070	0.0108	0.0219
$(\partial E/\partial T)_p/\mu VK^{-1}$	346	346	332	356

6.4. Discussion

Figure 6-1 shows that in solutions of pH in the region $\lesssim$2.7 the indium electrode behaves in a satisfactory manner. Thus with added HCl the slope of the emf-pH curve is as predicted by the equation

$$\frac{dE}{dpH} = \frac{(\log_e 10)RT}{3F} \qquad (6.4)$$

Fig. 6-2 Variation of cell EMF with temperature for cells of the type: $In_{(s)}|InCl_{3(aq)}(m_1), HCl_{(0.02m)}|AgCl_{(s)}|Ag_{(s)}$

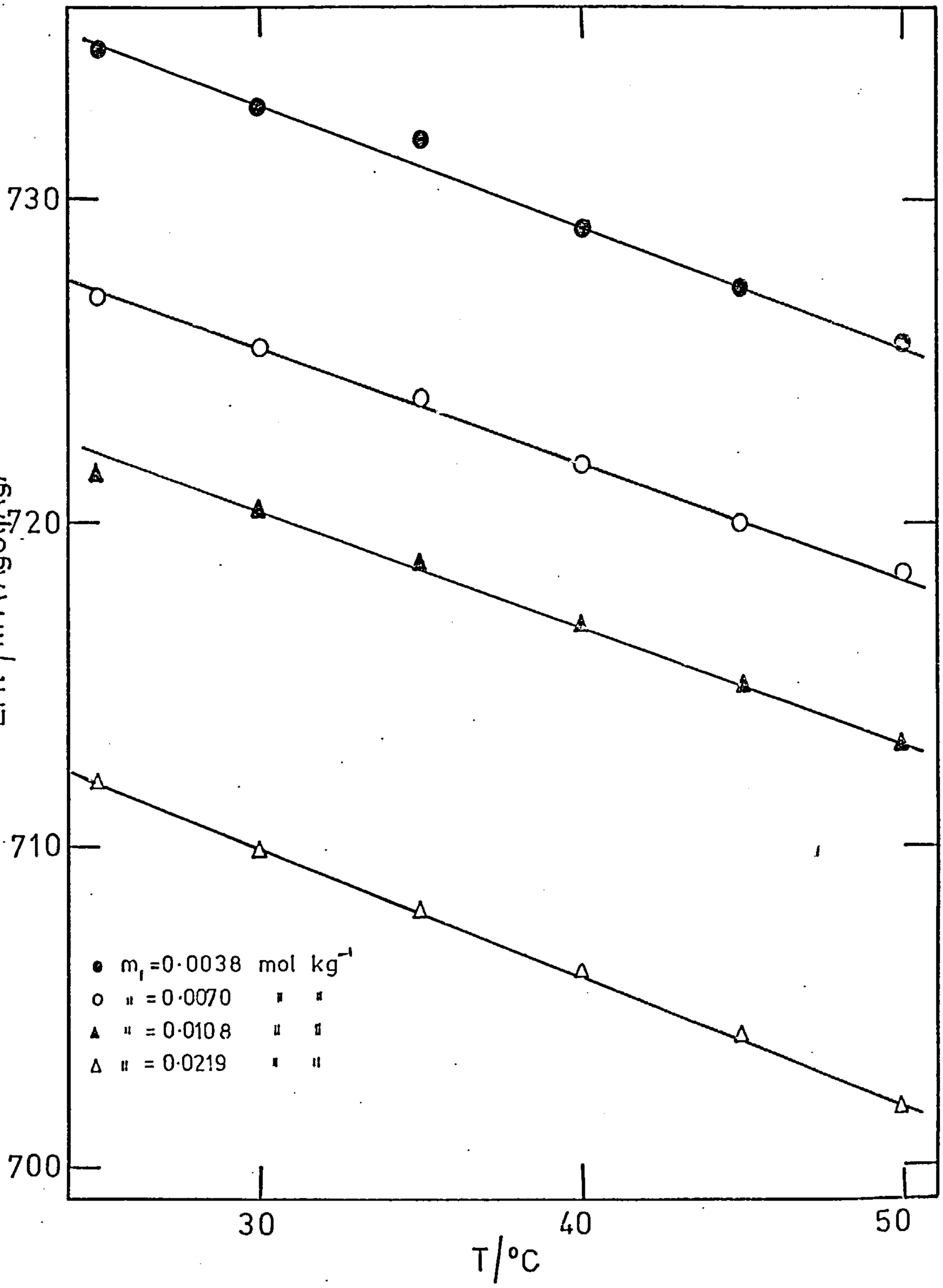

At pH's $\gtrsim$ 2.7 the emf changes markedly for small changes of pH and it must be concluded that the electrode reaction

$$In^{3+} + 3e = In \qquad (6.5)$$

is being complicated by the presence of phase hydroxide (or oxide) at the electrode, according to an equation of the type

$$In(OH)_{3(s)} + 3e = In + 3OH^- \qquad (6.6)$$

For (6.5) we may write

$$E = E^{\ominus} + \frac{RT}{3F} \log_e \frac{a_{In^{3+}}}{a_{In}} \qquad (6.7)$$

and for (6.6)

$$E_s = E_s^{\ominus} + \frac{RT}{3F} \log_e \frac{a_{In(OH)_{3(s)}}}{a_{In} a^3_{OH^-}} \qquad (6.8)$$

In (6.7) and (6.8) $a_{In^{3+}}$ and a_{OH^-} are the mean ionic activities (a ±) in the appropriate electrolyte solution. $a_{In(OH)_{3(s)}}$ and a_{In} are the corresponding activities.

At equilibrium $E = E_s$, therefore we may write

$$E_s^{\ominus} + \frac{RT}{3F} \log_e \frac{a_{In(OH)_{3(s)}}}{a_{In} a^3_{OH^-}} = E^{\ominus} + \frac{RT}{3F} \log_e \frac{a_{In^{3+}}}{a_{In}} \qquad (6.9)$$

Rearranging (6.9) we obtain

$$E_s^{\ominus} = E^{\ominus} + \frac{RT}{3F} \log_e \frac{a_{In^{3+}} a^3_{OH^-}}{a_{In(OH)_{3(s)}}} \qquad (6.10)$$

Latimer[49] gives K for the reaction

$$In(OH)_3 = In^{3+} + 3OH^- \qquad (6.11)$$

as $\sim 10^{-33}$, therefore we may write (6.10) as

$$E_s^{\ominus} = E^{\ominus} + \frac{RT}{3F} \log_e 10^{-33} \qquad (6.12)$$

which gives

$$E_s^{\ominus} = E^{\ominus} - 0.66\ V \qquad (6.13)$$

consequently we might expect a shift of standard electrode potential of $\sim$ -0.66V would result from the change in electrode class due to the development of phase oxide at the electrode. Solutions made up containing equivalent concentrations of In^{3+} and $3Cl^-$ were found to have pH values in the region 3.3 - 3.6, that is in the region where reaction (6.5) is complicated by reaction (6.6). These observations confirm the findings of Hakomori[44].

6.4.1. Treatment of results

In the present studies, analysis of the experimental results is difficult since no theory of mixed electrolyte solutions, of different valency types, exists. Hakomori[44] used the Debye-Hückel limiting law ($\log_{10} \gamma_{\pm} = -A\ z_+ |z_-| I^{\frac{1}{2}}$) to correct for non-ideality in order to extrapolate his four measurements to zero indium molality, as the ionic concentration of In(III) was reduced to zero at low hydrochloric acid concentrations (0.02 m HCl). This procedure enabled the extraction of $E_{\ominus}'$ from the experimental data. The emfs (E) of cells of type (6.3) can be expressed as follows

$$E = -E'_{\ominus} - 0.01972 \log_{10} m_{In^{3+}} \; m^3_{Cl^-} \cdot \gamma_{In^{3+}} \; \gamma^3_{Cl^-} \qquad (6.14)$$

where $m_{In^{3+}}$ and m_{Cl^-} represent molalities and $\gamma_{In^{3+}}$ and γ_{Cl^-} are mean ionic activity coefficients. Introducing a new symbol E', we may rewrite (6.14) as

$$E' = E + 0.01972 \log_{10} m_{In^{3+}} \; m^3_{Cl^-}$$

$$= -E'_{\ominus} - 0.01972 \log_{10} \gamma_{In^{3+}} \; \gamma^3_{Cl^-} \qquad (6.15)$$

A plot of the left hand side of (6.15) against some simple function of the concentration of $InCl_3$ and extrapolation to zero indium ion concentration, will yield a value of $E'_{0.02}$. Hakomori[44] defined $E'_{0.02}$ as the emf of a hypothetical cell with electrodes of indium and silver chloride, containing the ions In^{3+} and Cl^- each at 1 molal, but having $\gamma_{In^{3+}}$ and γ_{Cl^-} values such as these ions would have in a solution of 0.02 m H^+ and 0.02 m Cl^-, containing no other ions. Figures 6-3 and 6-4 show the left hand side of equation (6.15) plotted against $(m_{InCl_3})^{\frac{1}{2}}$ and (total ionic strength)$^{\frac{1}{2}}$ respectively. It is evident that these plots are difficult to extrapolate with any degree of accuracy, however figure 6-3 on extrapolation to zero indium ion concentration gives an estimate of 0.572 V for $E'_{0.02}$ and figure 6-4 a value of 0.577 V for the same parameter on extrapolating to an ionic strength of 0.02 m. Adopting 0.575 V as the best value of $E'_{0.02}$, $E'_{\ominus}$ can be found from the right hand side of equation (6.15). Taking γ_{Cl^-} [125] as 0.848 and $\gamma_{In^{3+}}$ [126] as 0.228 and expressing the final answer on the hydrogen scale a value of -0.336 V, at 25°C, is obtained for $E'_{\ominus}$. This value agrees exactly with Hakomori's[44] determination of this parameter. It is

Fig. 6-3 Variation of E' with $(m_{InCl_3})^{1/2}$ according to equation (6·15)

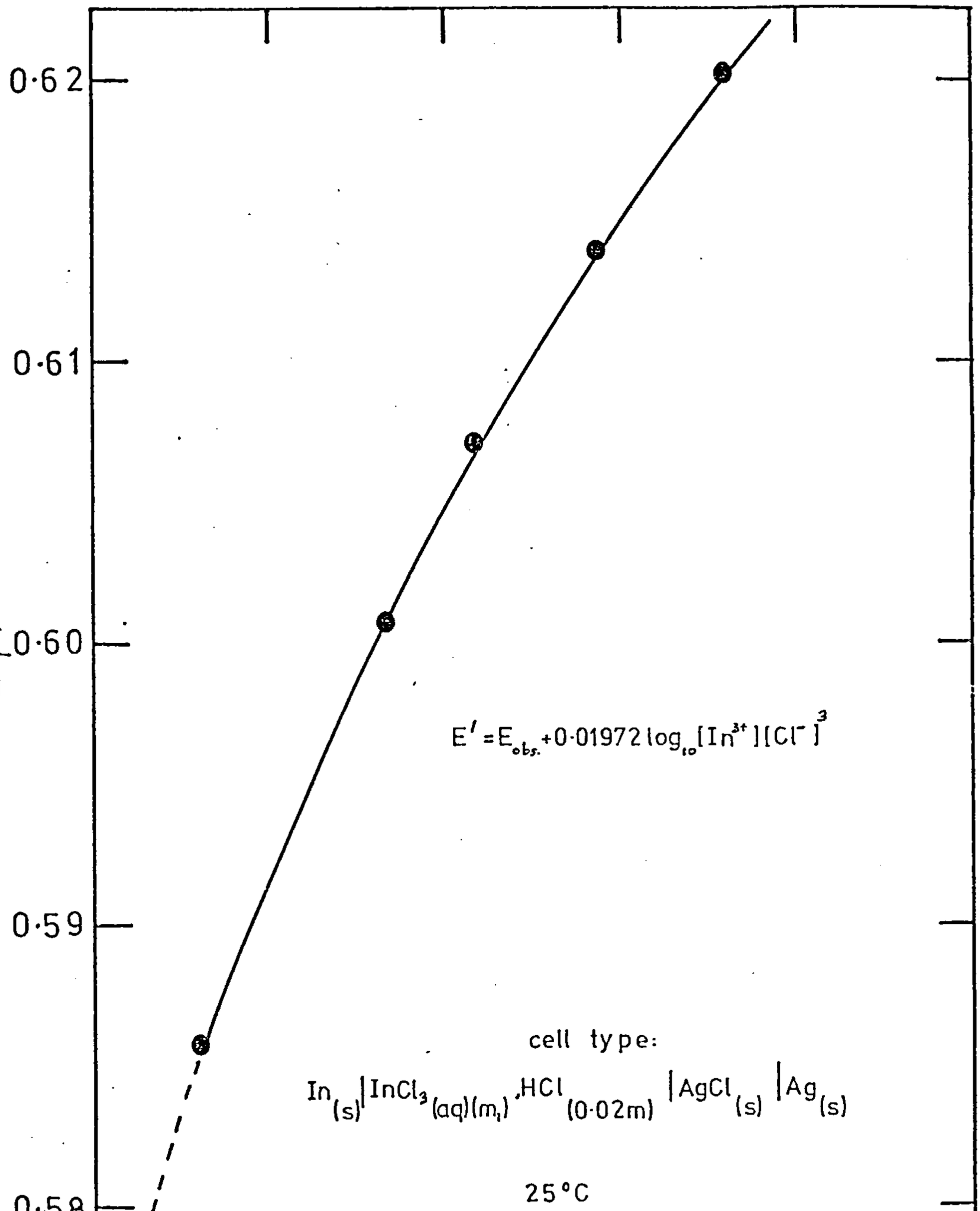

Fig. 6-4 Variation of E' with $I^{1/2}$ according to equation (6.15)

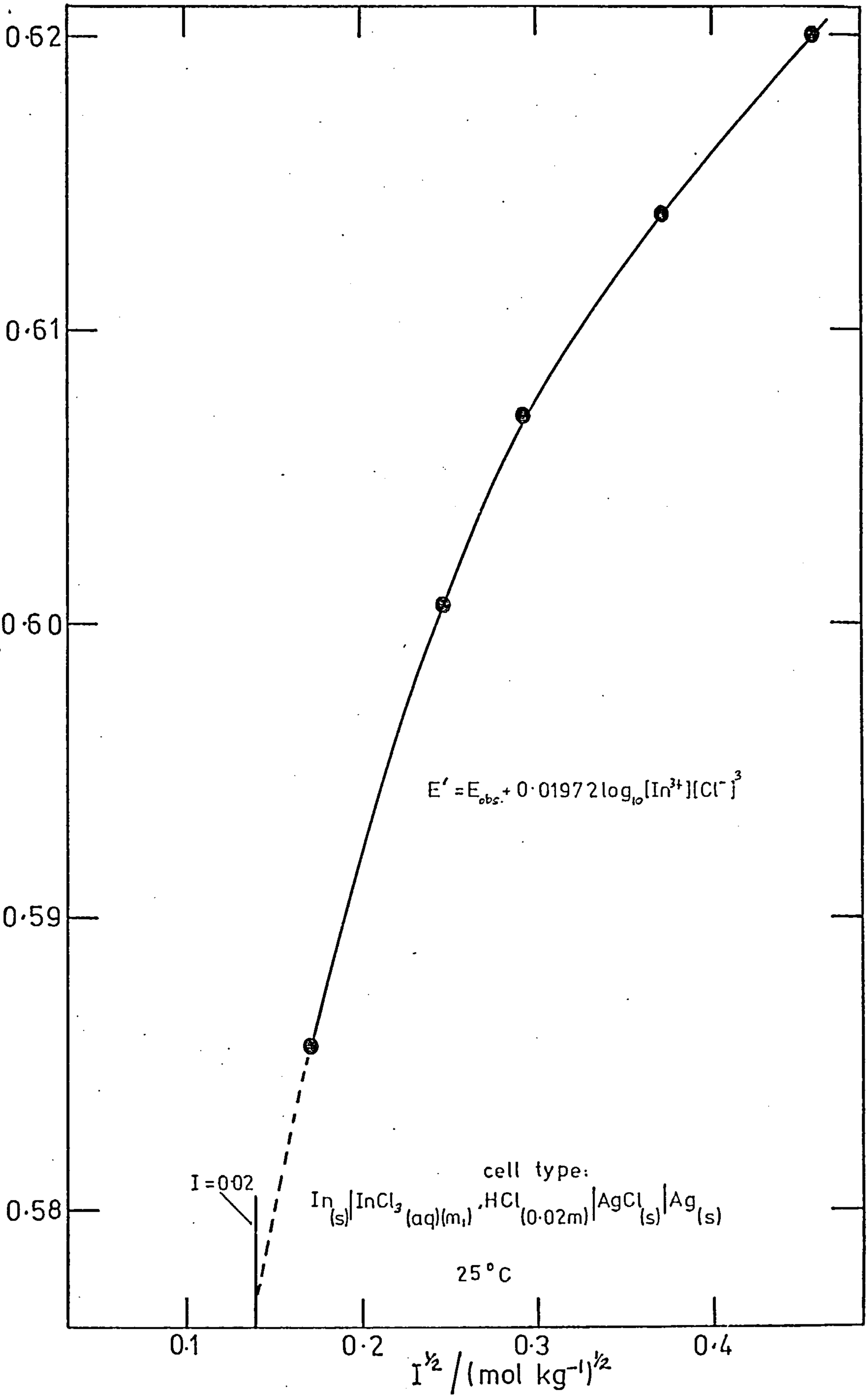

noteworthy that $E^{'}_{\ominus}$ may have been obtained directly by extrapolation of figure 6-4 to zero ionic strength, but the long extrapolation involved is much too uncertain to give a meaningful value for $E^{'}_{\ominus}$.

The Debye-Hückel limiting law, according to which $\log_{10}\gamma_{\pm}$ is a linear function of the square root of concentration at low concentrations, is not accurately obeyed under usual experimental conditions[127]. A more complete relationship between $\gamma_{\pm}$ and ionic strength is the so called "two parameter" form of the Debye-Hückel equation[127]:

$$\log_{10}\gamma_{\pm} = -\frac{A\, z_+ |z_-| I^{\frac{1}{2}}}{1 + B\overset{o}{a}\, I^{\frac{1}{2}}} + bI \qquad (6.16)$$

In (6.16) A and B are constants dependent on the absolute temperature and dielectric constant of the solvent, $\overset{o}{a}$ is the ion size parameter (the distance of closest approach of two ions) and bI is a term included to allow for short range ion-solvent and short range ion-ion interactions, which cannot be adequately represented by the rigid-spheres model used as the basis for the derivation of the Debye-Hückel equation ($\log_{10}\gamma_{\pm} = -\frac{A\, z_+ |z_-| I^{\frac{1}{2}}}{1 + B\overset{o}{a}\, I^{\frac{1}{2}}}$).

Incorporation of (6.16) into equation (6.14) gives

$$E + 0.01972 \log_{10} m_1(3m_1 + m_2)^3 - \frac{4k}{3}\frac{A\, I^{\frac{1}{2}}}{1 + B\overset{o}{a} I^{\frac{1}{2}}} = -E^{'}_{\ominus} - \frac{4}{3}kbI \qquad (6.17)$$

In (6.17) m_1 is the molality of $InCl_3$, m_2 the molality of HCl and $k = \frac{(\log_e 10)RT}{F}$. The left hand side of equation (6.17) is denoted by $E^{o'}$ and if (6.17) is obeyed a plot of $E^{o'}$ vs. I should be linear with an intercept of $E^{'}_{\ominus}$. Figure 6-5 shows such plots for various values of the product $B\overset{o}{a}$. The product $B\overset{o}{a}$ is usually close to unity[128], so a range of values from 0.5 to 1.5 was chosen in

Fig·6-5 Variation of $E^{o\prime}$ with I according to equation (6·17)

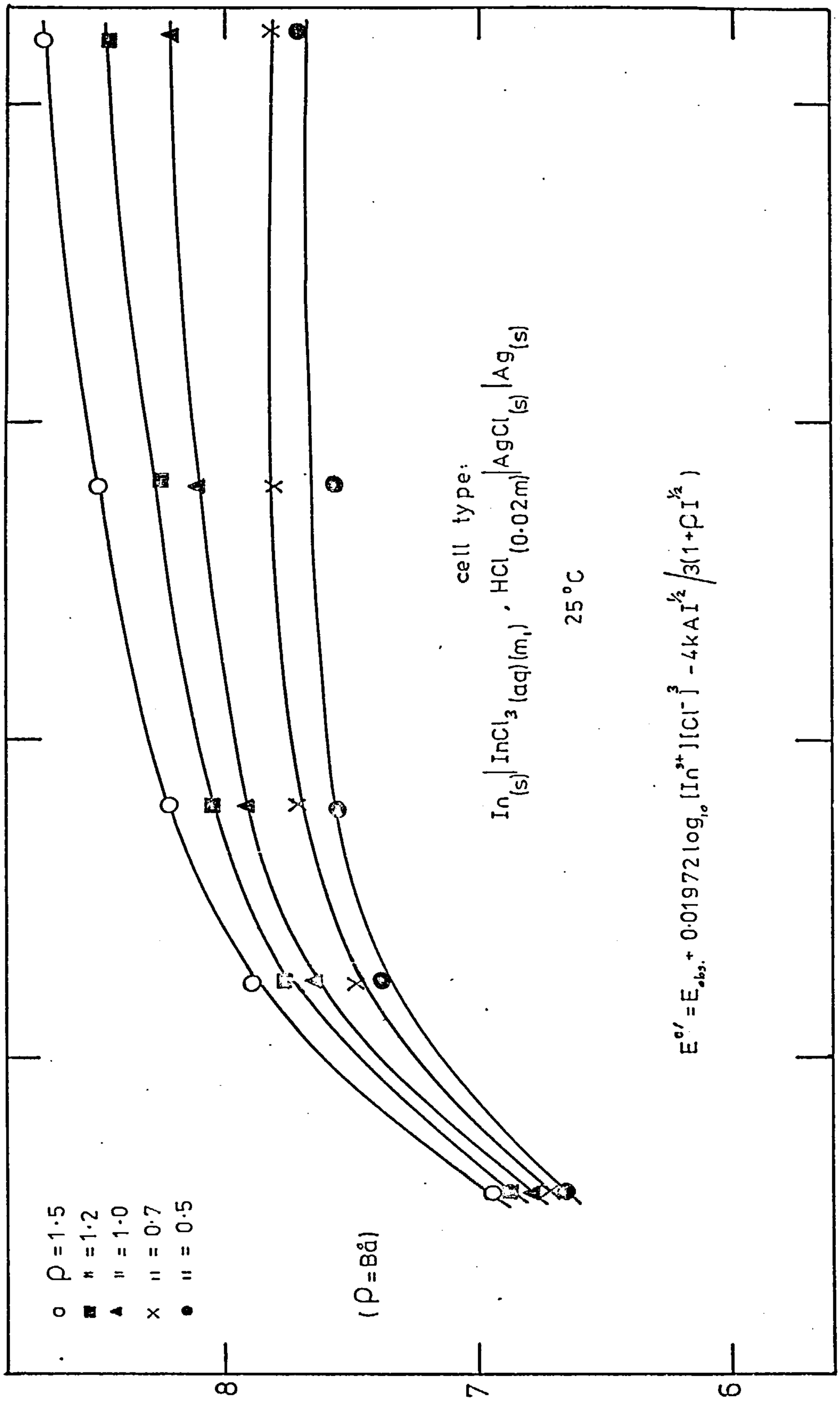

order to observe the effect of changing the magnitude of the product $\overset{o}{Ba}$ on the final form of the E^{ol} vs. I plot. Clearly as shown in figure 6-5, a linear plot of E^{ol} vs. I is not obtained with the product $\overset{o}{Ba}$ in the chosen range. This probably reflects the inherent errors due to the fact that a mixed electrolyte of differing valency types was used in the present investigation. It is interesting, however, that on extrapolation of the plots in figure 6-5 to zero ionic strength, a constant intercept of $\sim$ 557 mV is obtained, which on conversion to the hydrogen scale gives a value for $E'_\ominus$ (at 25°C) of -0.337 V, which is in very good agreement with the value of $E'_\ominus$ obtained from the previous graphical extrapolation procedures described.

Even with the attendant difficulties of the presence of ions of different charge it is to be expected that an equation of the form of (6.16) would give a reasonable fit to the experimental data. When expanded in powers of $I^{\frac{1}{2}}$ (depending upon the values of b and $\overset{o}{Ba}$) and taken to the limits of infinite dilution either a second or third order polynomial should be a satisfactory approximation.

The first approach adopted in the present investigation was to carry out a polynomial fit of the E'(calculated from (6.15) vs. $I^{\frac{1}{2}}$ data. A cubic equation was found to give the most satisfactory fit, from which values of $E'_{0.02}$ were found by calculating the potential corresponding to the acid addition. $E'_\ominus$ at 25°C was then found to be -339.8 mV on the hydrogen scale.

A second(alternative) approach of obtaining the emf at infinite dilution of In^{3+} was to carry out a polynomial fit of the E' vs, $(m_{InCl_3})^{\frac{1}{2}}$ data. This treatment was found to require only

a second order equation, from which $E'_{0.02}$ was easily calculated as the concentration independent term. The value of E'_o, at 25°C, from this method followed as -332.9 mV. The E'_o values isolated using the polynomial fit technique agreed well with the values of -342.0 mV (using $I^{\frac{1}{2}}$) and -333.0 mV (using $(m_{InCl_3})^{\frac{1}{2}}$), obtained by applying polynomial fits to Hakomori's data.

Considering the polynomial fits described above, it is difficult to decide which of the two extrapolation procedures is the better. Since the equation of the curve connecting the potential with molality of $InCl_3$ was of a lower degree than that connecting the potential with the ionic strength, the value from the former procedure is preferred as giving rise to the best value of E'_o. A further argument in favour of this value is that the concentration of indium is taken to zero and the extrapolation is not so long as that using $I^{\frac{1}{2}}$.

For the case of systems such as the present one in which a certain quantity of acid has to be added in order to suppress the formation of electrodes of the second type due to precipitation of hydroxide (oxide), there is necessarily some uncertainty due to the presence of ions of different charge type. This results in some uncertainty in extrapolation procedures. In the present work the E'_o value obtained by various methods show that an uncertainty of several mV may be present according to which of the extrapolation procedures is used. Table 6.3 summarises the E'_o values obtained in the present investigation and table 6.4 lists E^o values obtained by other workers.

Table 6.3

$E'^{\ominus}$ (V/SHE)	Extrapolation procedure
-0.336	Graphical extrapolation according to equation (6.15)
-0.337	Graphical extrapolation according to equation (6.17)
-0.340	Polynomial fit to E' vs. $I^{\frac{1}{2}}$ data
-0.333	Polynomial fit to E' vs. $(m_{InCl_3})^{\frac{1}{2}}$ data

Table 6.4

$E^{\ominus}$ (V/SHE)	Workers	Reference
-0.336	Hakomori	44
-0.338 and -0.341	Covington, Hakeem and Wynne-Jones	48
-0.340	Hattox and De Vries	45
-0.335	Kangro and Weingärtner	46

Figure 6.2 and table 6.2 show that the temperature coefficient of the cell potential is of the order of $345 \mu V K^{-1}$ and the temperature coefficient of $E'_{\ominus}$ is found from the data in figure 6-2 to be 1.13 mV K^{-1}. This value for the temperature coefficient of $E'_{\ominus}$ agrees well

with the value of $(\partial E^{\ominus}/\partial T)_p$ of 1.1 mV K^{-1} reported by Kangro and Weingärtner[46], but is considerably larger in magnitude than that reported by Covington and co-workers (40μV K^{-1}).

6.5. Conclusions

The potential of cells of the type

$In_{(s)} \mid InCl_{3(aq)(m_1)}, \quad HCl_{(0.02m)} \mid AgCl_{(s)} \mid Ag_{(s)}$ have been measured and compared with those of the nominal type

$In_{(s)} \mid InCl_{3(aq)(m_1)} \mid AgCl_{(s)} \mid Ag_{(s)}$ at a series of pH's.

Results show that the hydrolysis of $InCl_3$ is important at certain pH's and that a satisfactory estimate of $E'_{\ominus}$ and $(\partial E'_{\ominus}/\partial T)_p$ for the In^{3+}/In couple can only be made if this hydrolysis does not interfere with the electrode reaction $In^{3+} + 3e \longrightarrow In$. Values of $E'_{\ominus}$ are estimated and compared with earlier determinations.

CHAPTER 7

THE INDIUM ELECTRODE IN PERCHLORATE ELECTROLYTES - A KINETIC STUDY

7.1. Introduction

The In/In(III) reaction in perchlorate media has been fairly well investigated[2,3,26,60-81], particularly by the Russian school of Losev. Data pertaining to both amalgam[26,60-69] and solid[2,3,70-81] electrodes have been reported. The reason why perchlorate media are chosen lies in the tendency for halogen ions to have a catalytic effect on the exchange reaction (see chapter 4) and also the non-complexing nature of the perchlorate ion[129]. Interest in the indium metal exchange per se arises from it being a three electron transfer reaction which can be investigated by the normal methods. The majority of data obtained by electrochemical measurements on indium in perchlorate media refer to the anodic reaction investigated by steady state polarisation techniques. Isolated examples of other techniques exist. For example, Miller and Visco[74] used a rotating ring-disc method to study the dissolution of indium in perchlorate electrolytes.

Measurements on the cathodic side are complicated by the h.e.r and the existance of aquo-indium complexes which lose molecules of hydration only very slowly[64,65,71]. Indium can be deposited from aqueous solutions[43], however, it does not seem feasible to study the cathodic reduction of In(III) from perchlorate solutions by purely electrochemical means. Radiochemical methods of studying the cathodic reaction have been used[64,71], making it possible to record the partial cathodic polarisation curves corresponding only to deposition of indium.

Previous investigations (see chapter 4) afford a great deal of evidence that indium dissolves electrochemically in stages, first to give In(I) which is a reactive ion. Although stable as the insoluble iodide (InI)[72], in solution In(I) reacts with any reducible material to form the In(III) ion. There is little evidence so far for the existance of the In(II) species, although it has been postulated by some authors to explain their results[82, 95,130-132]. The In(I) ion is able to reduce the hydrogen ion to molecular hydrogen at a realtively fast rate; under certain conditions the anodic oxidation of indium apparently conforms to a fairly reversible one electron transfer, the rest of the reaction to In(III) occurring in solution. There has been discussion about the exact mechanism involved in the In/(In(III) exchange reaction and there is a definite need to examine the electrode behaviour of indium by methods other than steady state polarisation in which diffusion in solution is often the controlling mechanism. The present work describes results of a rotating disc study of the In/In(III) reaction in perchlorate electrolytes, here the kinetic reaction can be studied in isolation. Some impedance measurements are also described.

7.2. Experimental

7.2.1. Rotating disc studies

The electrical circuit is described in 3.2.3 and the electrolytic cell shown in figure 3-2a. The rotating disc electrode is described in 3.1.3c. The reference electrode was a wick type saturated sodium calomel electrode.

7.2.2. Impedance studies

The electrical circuit is described in 3.2.2. and the electrolytic cell shown in figure 3-2b. The electrode system is described in 3.1.3d. A wick type saturated sodium calomel reference electrode was employed for these measurements.

7.3. Results

The theory of the rotating disc electrode is described in section 2.4. Applications to that of a metal undergoing dissolution have been considered by Armstrong and Bulman[133].

If equation (2.37) is obeyed, plots of i^{-1} vs. $\omega^{-\frac{1}{2}}$ should yield straight lines, extrapolation of which to infinite rotation speed giving the true kinetic currents corrected for diffusion effects. Furthermore, as predicted by equation (2.43), the slopes of these lines should show an exponential dependence on potential and be proportional to z.

The inset in figure 7-1 shows typical i^{-1} vs. $\omega^{-\frac{1}{2}}$ plots for indium in perchlorate electrolyte with an acid concentration of 10^{-2} M. As is evident, no rotation speed dependence of the observed anodic currents is observed. Figure 7-1 shows also an anodic polarisation curve for the same electrolyte.

Figure 7-2 shows typical results corresponding to the currents of indium dissolution in 1 M perchloric acid solution presented as i^{-1} vs. $\omega^{-\frac{1}{2}}$ plots. Good straight lines in accord with equation (2.37) were obtained in the potential region -580 mV to -480 mV. Furthermore, the slopes of these lines are potential dependent and a test of equation (2.43) is shown in figure 7-3 where data are presented in the form of a $\log_{10}$(slope) versus potential plot.

Fig.7-1 Anodic polarisation curve: 10^{-2}M $In(ClO_4)_3$ + 10^{-2}M $HClO_4$, total perchlorate ion concentration 2M (added $NaClO_4$). Inset shows typical i^{-1} vs. $\omega^{-\frac{1}{2}}$ plots for the same electrolyte

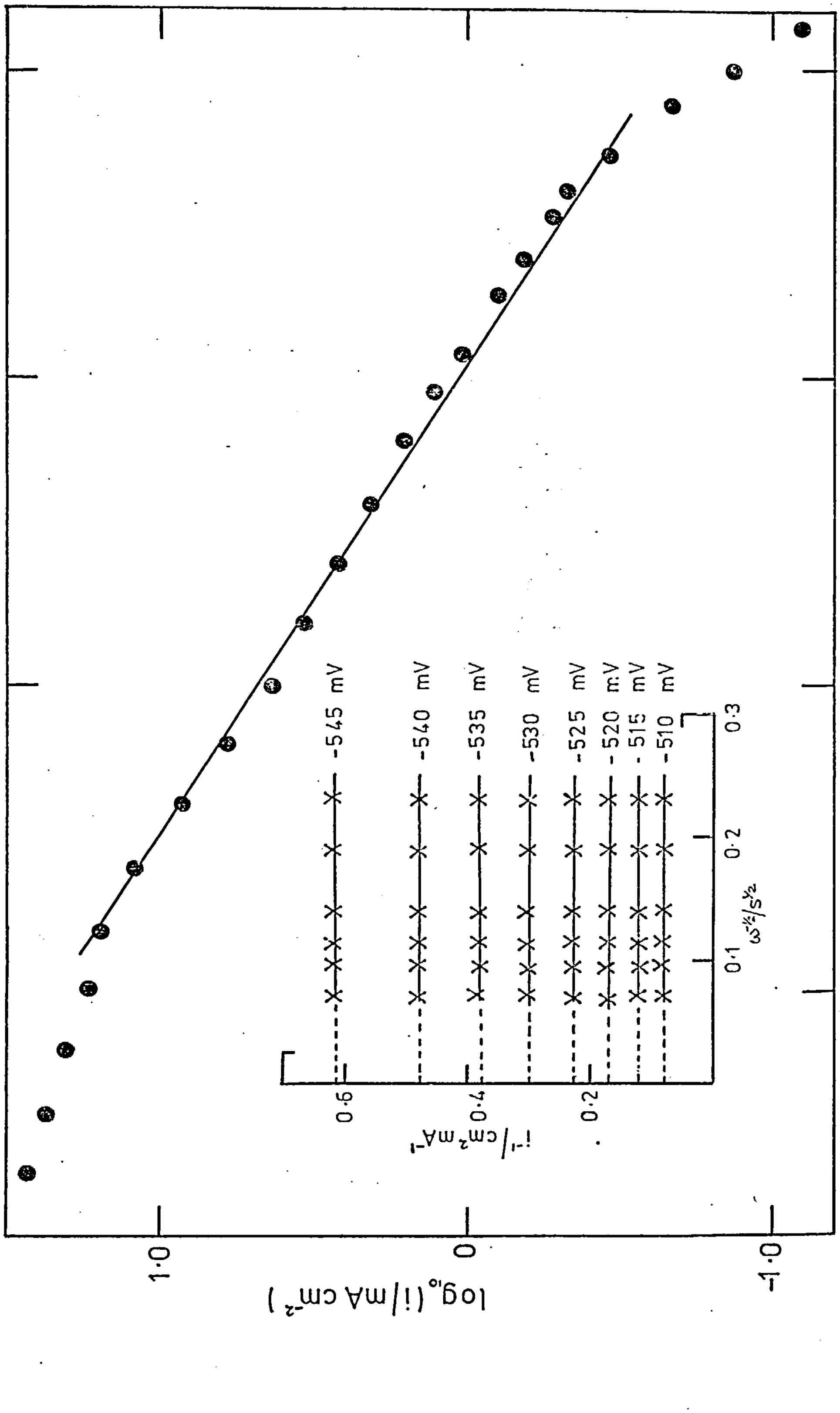

Fig. 7-2 Typical i^{-1} vs. $\omega^{-1/2}$ plots at a series of anodic potentials; 1·0M $HClO_4$

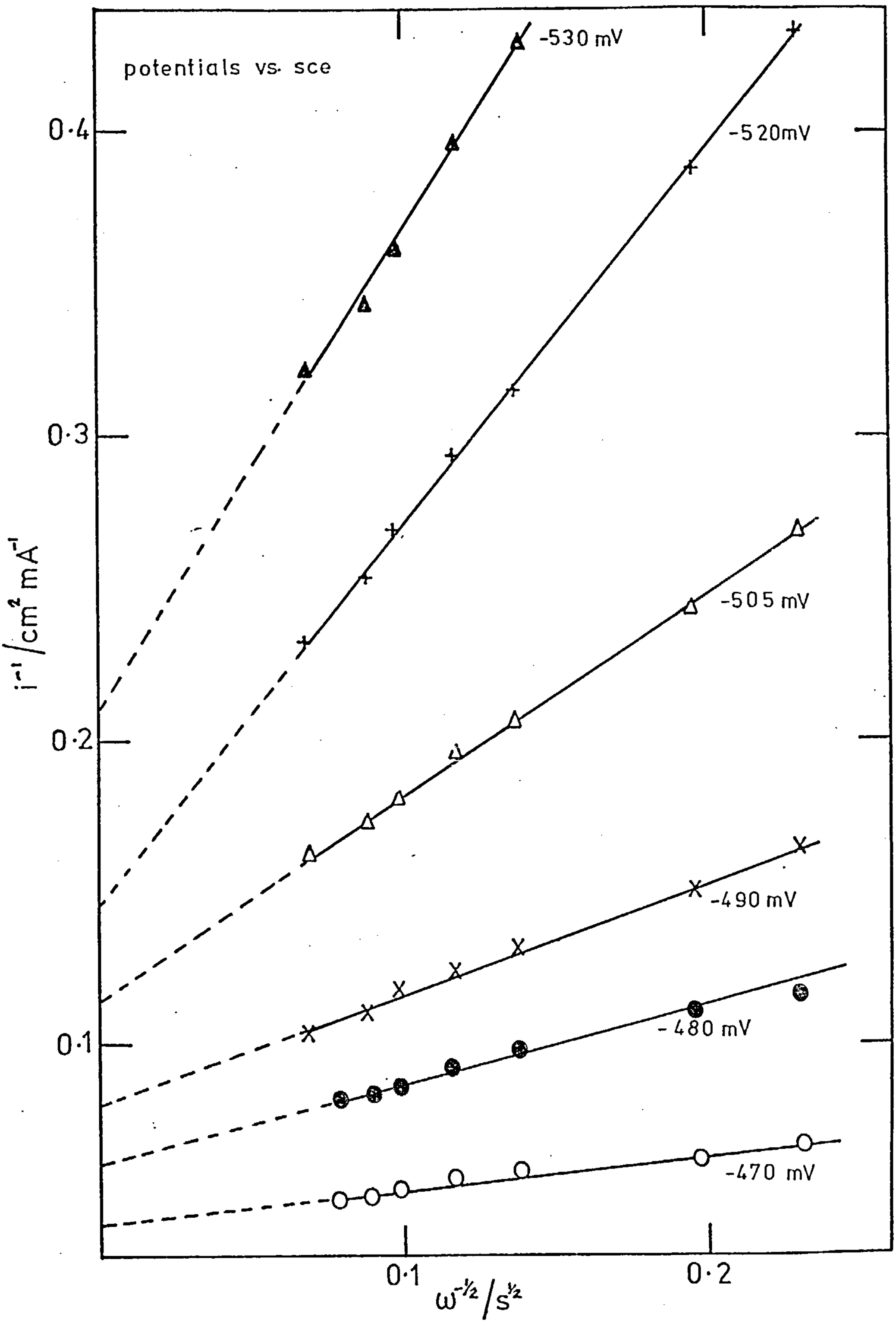

Fig.7-3 Plot of $\log_{10}(\partial i^{-1} / \partial \omega^{-1/2})$ vs. anodic potential; 1M $HClO_4$

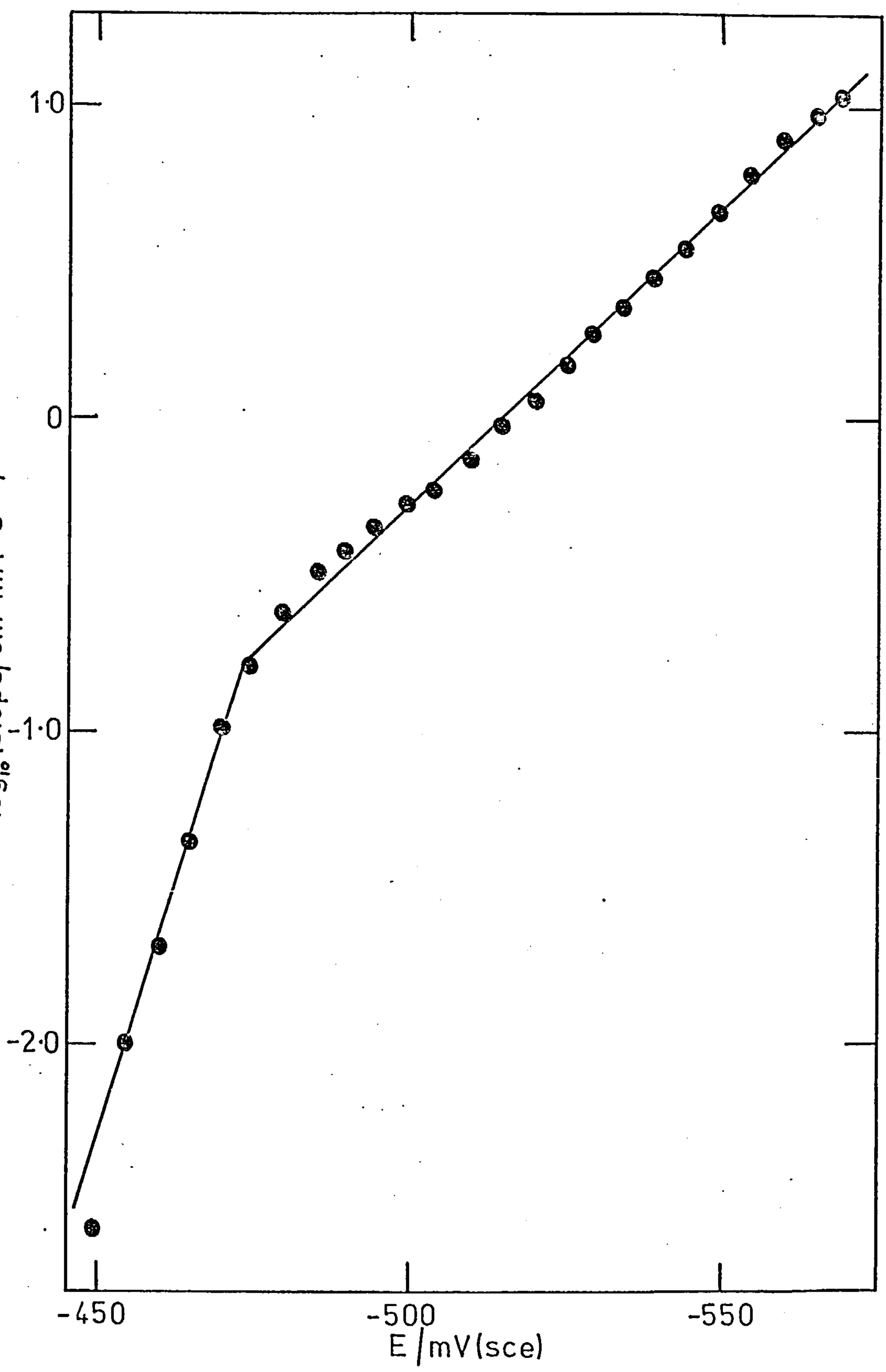

From -580 mV to ∿ -480 mV an ∿ 55 mV/decade slope is observed, whilst at potentials>∿ -480 mV the slope changes to ∿ 20 mV/decade. Data similar to figures 7-2 and 7-3 were obtained for other electrolyte solutions containing a significant acid concentration (> 0.1 M).

Figure 7-4 shows typical Tafel data obtained for the anodic dissolution of indium in perchlorate electrolytes of acid concentration 1 M and 0.7 M. The currents plotted in figure 7-4 were obtained by extrapolation of i^{-1} vs. $\omega^{-\frac{1}{2}}$ plots to infinite rotation speed. It should be noted that the solution containing 0.7M perchloric acid also contained 20 mM $In(ClO_4)_3$. The results obtained showed that over the entire range of acid concentrations used (10^{-2} to 1 M) indium (III) in solution had no effect (within experimental limits) on the measured anodic currents. This agrees with earlier work reported by Losev[26], who found that the anodic dissolution currents for indium in perchlorate solutions were independent of the In(III) concentration.

The results obtained in the present investigation also showed that presence of oxygen in the electrolyte affected the currents flowing, particularly at the more negative potentials where an increase in the electrode rotation speed caused the observed anodic currents to flow in a cathodic direction. This behaviour was interpreted as an enhancement of the oxygen reduction reaction by hydrogen ions in solution:

$$H^+ + \tfrac{1}{2}O_2 + 2e \longrightarrow OH^- \qquad (7.1)$$

This effect was completely suppressed by thoroughly deoxygenating the electrolyte.

Fig.7-4 Typical anodic Tafel plots; perchlorate electrolytes

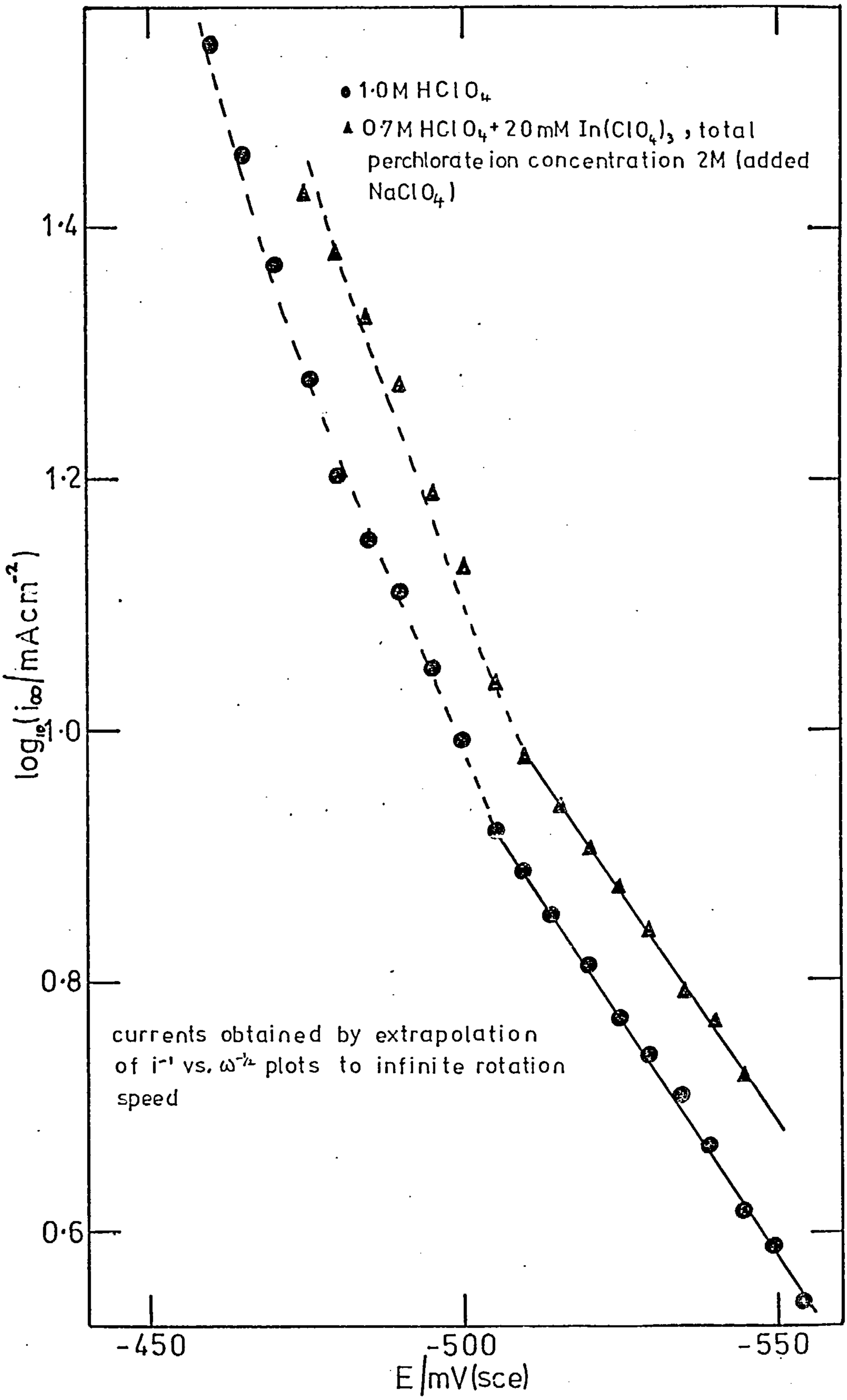

Figure 7-5 shows a complex plane impedance plot corresponding to an indium electrode in a perchlorate electrolyte, containing 0.1 M $In(ClO_4)_3$ + 1 M $HClO_4$ + 0.7 M $NaClO_4$, at the equilibrium potential. A straight line at 45^o is obtained.

Figure 7-6 shows a complex plane plot for an indium electrode in an electrolyte containing 0.0001 M $In(ClO_4)_3$ + 10^{-2} M $HClO_4$ + $\sim$2 M $NaClO_4$, at an anodic overpotential of 10 mV.

7.4. Discussion

7.4.1. Rotating disc studies

It is clear from equation (2.43) that the slope of the i^{-1} vs. $\omega^{-\frac{1}{2}}$ plots is dependent exponentially on potential. In all the solutions studied the concentration of the solution species is very much greater than that of the reduced species at the electrode, consequently, within the limits of the present experiments, the slope of the plots should be dependent on potential only. Figure 7-3 shows a plot of $\log_{10}$(slope) against potential for a perchlorate system having an acid concentration of 1 M. At low acid concentration equation (2.43) does not hold, as evinced by the inset in figure 7-1. That kinetic control of the electrode reaction cannot be the reason for this behaviour follows from the above discussion since the convectional contribution to current control should be the same at high acid concentration as at low. The reason must be sought for elsewhere. The most likely explanation is that the products of the electrode reaction stay on the electrode and their concentration is therefore not changed by changes in the speed of rotation of the electrode. This behaviour is confirmed by Losev[76] who reports that for the dissolution of indium in perchlorate solutions having an acid

Fig.7-5 Typical complex plane impedance plot ;
$0{\cdot}1M\ In(ClO_4)_3 + 1M\ HClO_4 + 0{\cdot}7M\ NaClO_4$

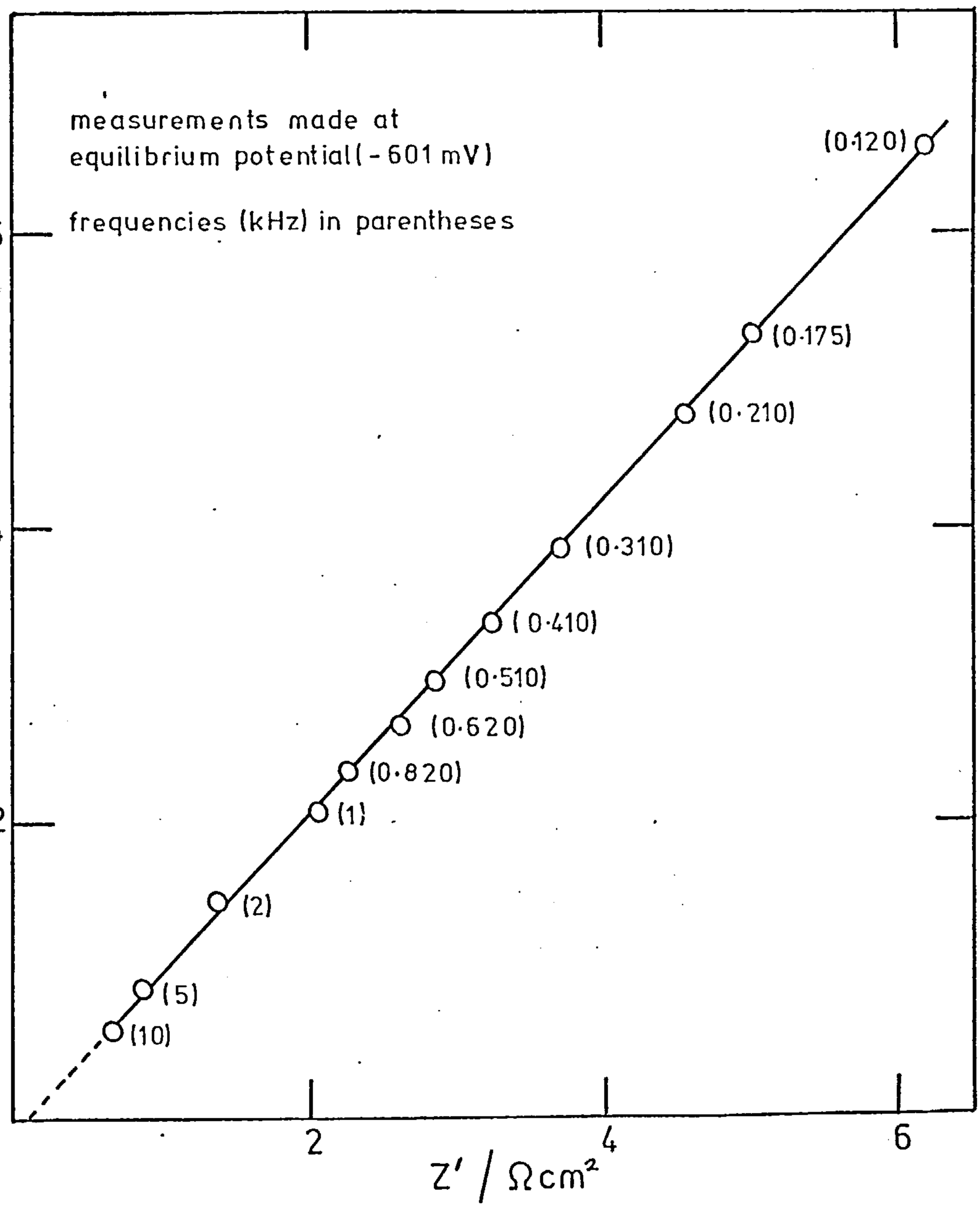

Fig. 7-6 Typical complex plane impedance plot; 0·1 mM $In(ClO_4)_3$ + 10^{-2} M $HClO_4$, total perchlorate ion concentration 2 M (added $NaClO_4$)

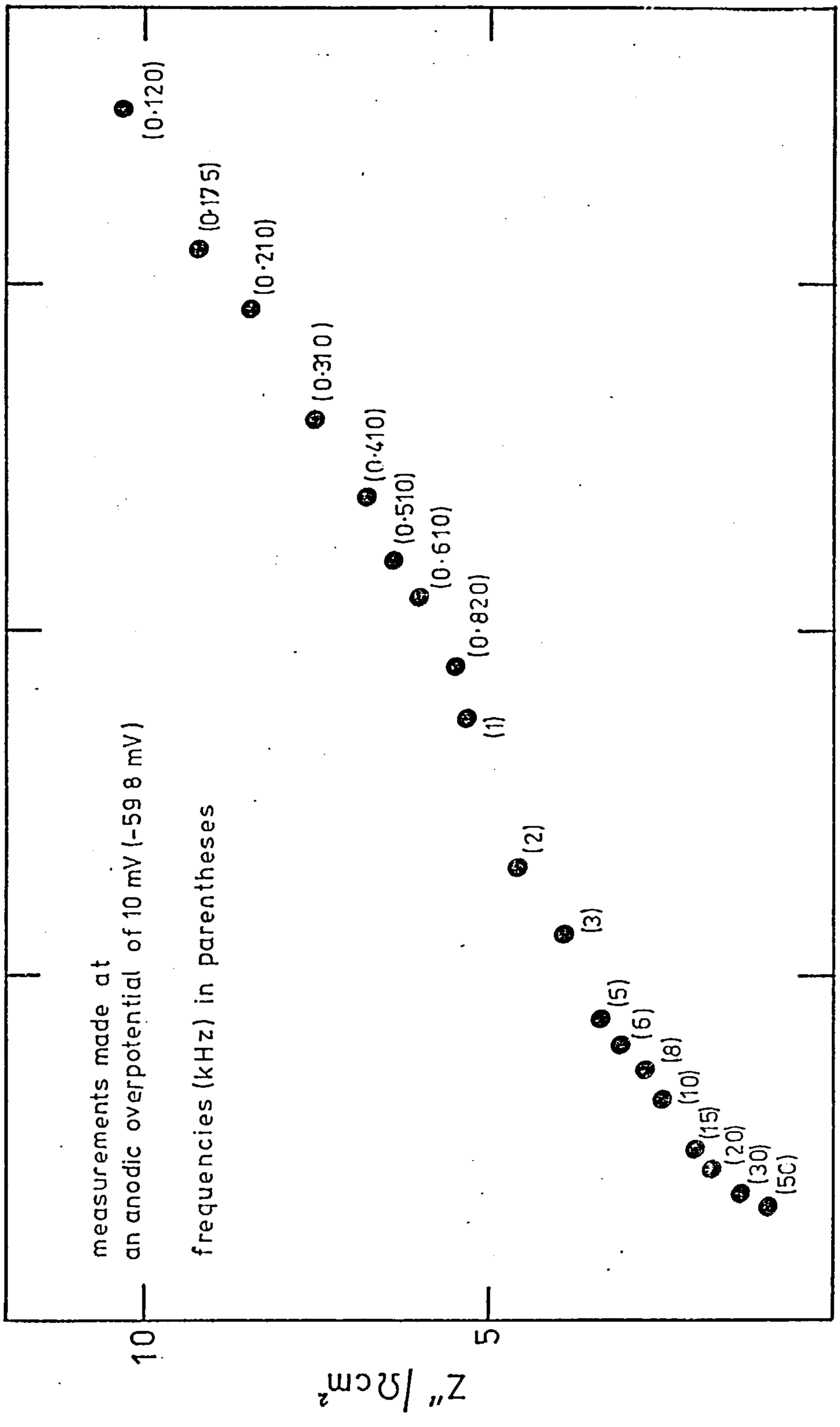

strength of 10^{-2} M, the measured anodic currents were independent of the rate of stirring. Losev proceeds in his analysis of the results to construct polarisation curves corresponding to such systems. He obtained a linear region of slope 29 mV/decade. A plot of $\log_{10} i$ versus potential for a perchlorate system having an acid concentration of 10^{-2} M is shown in figure 7-1, a slope of $\sim$ 30 mV/decade being obtained in the potential region $\sim$ -500 mV to $\sim$ -560 mV. This slope appears to increase to $\sim$90 mV/decade at very anodic potentials. There may be a variety of reasons for this curvature of the Tafel plot, although this may not necessarily be connected with any mechanistic changes in the electrode process. An explanation of the 30 mV/decade Tafel slope can be formulated in terms of a stepwise reaction in which indium is oxidised to In(I) followed by a two electron change to give In(III). In this case the In(I) would be in quasi-equilibrium with the indium metal and the rate determining step would be the succeeding two electron transfer. Theoretically with a transfer coefficient of 0.5 this mechanism would give a 30 mV/decade Tafel slope (see later), which is close to the value obtained in the present investigation. The reason for the lack of rotation speed dependence can only be due to the formation of insoluble products at the electrode. This theory is supported by the differential capacitance measurements made with perchlorate electrolytes (chapter 5), where it was shown (figure 5-10) that for systems of relatively high pH no capacitance rise due to lattice dissolution occurred. Only when the pH was reduced (figure 5-7) was a capacitance rise indicative of indium dissolution observed. The capacitance measurements and equilibrium potential studies (chapter 6) also

showed that it is important to avoid films in connection with electrochemical measurements at an indium electrode at pH's $>$ 3, although it has been known for a considerable number of years that hydrolysis of indium ions takes place relatively readily[44,120,121,134].

The abstraction of reliable Tafel data from electrochemical measurements on a filmed electrode is not completely sound, however there is evidence to show that in the present case this may not lead to completely erroneous conclusions. Thus the oxide has semi-conductor properties[96] and in addition it has been shown[95] that the film is non-passivating under many conditions. It may be concluded, therefore, that at the electrode under the present conditions of low acidity a three electron transfer occurs because there is insufficient hydrogen ion to materially effect the amount of current going into the In(I) oxidation reaction, viz $In(I) \rightarrow In(III) + 2e$.

The i^{-1} vs. $\omega^{-\frac{1}{2}}$ plots for perchlorate electrolyte of acid concentration 1 M, shown in figure 7-2, were analysed using the treatment previously noted. Slopes of the lines $(\partial i^{-1}/\partial \omega^{-\frac{1}{2}})$ are shown in figure 7-3 plotted against the potential. Over the experimental range $<\sim$ -490 mV a straight line is obtained with a slope of $\sim$ 55 mV/decade. This indicates that the species in equilibrium with the electrode is the In(I) ion. At potentials more positive than $\sim$-490 mV this line is seen to curve-off, the slope approximating to 20 mV/decade which suggests that equilibrium with the electrode now involves the In(III) ion. These results are in general agreement with the data presented by Miller and Visco[74], although it should be noted that their presentation did not correct the measured currents for mass transport effects in solution. This may be why their data do not show the change in slope at the more positive potentials.

Extrapolation of the i^{-1} vs. $\omega^{-\frac{1}{2}}$ plots to infinite rotation speed enables the true kinetic currents to be evaluated. Typical data for systems of low pH are presented as Tafel plots in figure 7-4. The Tafel slope in the region up to $\sim$-500 mV is $\sim$120 mV/decade, corresponding to a one electron charge transfer. These data agree with those of figure 7-3 if a transfer coefficient of 0.5 applies to the rate determining electron transfer reaction. At higher potentials there is some evidence that the Tafel slope changes. Similar suggestions of slope changes in this potential region were observed in all other systems where a rotation speed dependence of the measured current was observed.

The process can be explained in terms of the electrochemical oxidation of In to In(I) followed by the oxidation to In(III) by either a chemical reaction involving hydrogen ions or an electrochemical reaction, viz.

$$In \longrightarrow In^{+} + e \qquad (7.2)$$

then either

$$In^{+} + 2H^{+} \longrightarrow In^{3+} + H_2 \qquad (7.3)$$

or

$$In^{+} \longrightarrow In^{3+} + 2e \qquad (7.4)$$

If reaction (7.3) is absent, then for reaction (7.4) being slow and (7.2) being fast we have for (7.2)

$$(E-E_r) = \frac{RT}{F} \log_e \frac{[In^{+}]}{[In]} \qquad (7.5)$$

and for (7.4)

$$\underset{\rightarrow}{i} = 2F\underset{\rightarrow}{k}^{o} \left[In^{+}\right] \exp \frac{2(1-\alpha)F}{RT}(E-E_r) \qquad (7.6)$$

leading to

$$\underset{\rightarrow}{i} = 2F\underset{\rightarrow}{k}^{o} \left[In\right] \exp \frac{(3-2\alpha)F}{RT} (E-E_r) \qquad (7.7)$$

Putting $\alpha = 0.5$, (7.7) gives a Tafel slope of 30 mV/decade. We would expect as the potential is driven more positive that the Tafel slope would change from 120 to 30 mV/decade as reaction (7.4) becomes more predominant. No solution was found in the present investigation where it was possible to obtain such a Tafel slope change. An experimental reason for not observing this behaviour may lie in the fact that at very positive potentials the observed currents were time dependent, thus making it impossible to obtain data at these potentials. However, the concentration of hydrogen ion effects the kinetics of reaction (equations (7.2) to (7.4)), so that at low hydrogen ion concentration the intruding In(I) chemical oxidation (7.3) would not be expected to occur to any very large extent. The data of figure (7.1) shows that the Tafel slope is $\sim$ 30 mV/decade (10^{-2} M $HClO_4$) in agreement with this theory. Reaction with hydrogen ion could, theoretically, be suppressed even further by using solutions of higher pH, but as previously mentioned the presence of films at high pH may interfere with the interfacial reaction. Losev's[76] anodic Tafel plots in solutions of low pH, produced by steady state polarisation measurements, gave a constant Tafel slope of 54 mV/decade. This should be compared with the log(slope) vs. potential plots (fig. 7-3) of the present

investigation, since under Losev's experimental conditions the major factor hindering current flow is the concentration polarisation, the kinetic contribution being only a minor factor. This can be seen from the i^{-1} vs. $\omega^{-\frac{1}{2}}$ data presented in fig 7-2, in which the slope of those lines corresponding to the potential region of the majority of Losev's experiments is very large indeed.

It would be desirable to show the transition from a 120 mV/decade Tafel slope to a 30 mV/decade Tafel slope as the result of a change in potential as well as by a change in hydrogen ion concentration. The rate of the chemical reaction between In(I) and hydrogen ions (equation (7.3)) is given by

$$V = k \left[In^{+}\right]\left[H^{+}\right]^{2} \qquad (7.8)$$

If we assume that In(I) species are in equilibrium with the electrode, then

$$\left[In^{+}\right] = \left[In\right] \exp \frac{F(E-E_r)}{RT} \qquad (7.9)$$

This is tantamount to considering the In/In(I) reaction to be infinitely fast, which is manifestly not the case. However since it is clearly fast in relationship to the In(I)/In(III) reaction, no great error is introduced by this assumption. Putting (7.9) into (7.8) and expressing the reaction velocity as an equivalent current, i_{chem}, we obtain

$$i_{chem} = 2Fk \left[In\right]\left[H^{+}\right]^{2} \exp \frac{F(E-E_r)}{RT} \qquad (7.10)$$

this can be compared with equation (7.7) to give

$$\frac{i_{electrochem}}{i_{chem}} = \frac{\vec{k}^{o} \exp 2(1-\alpha)F(E-E_r)/RT}{k[H^+]^2} \qquad (7.11)$$

This equation predicts that (if $\alpha = 0.5$) a decade change in concentration of hydrogen ion has the same effect on the ratio $i_{electrochem}/i_{chem}$ as a 120 mV/decade change in potential. The results obtained show that in order to see the change from one controlling process to the other, a change in hydrogen ion concentration from 1 M to 10^{-2} M is required. Equation (7.11) predicts that an equivalent effect could be obtained by changing the potential through 240 mV, which could not be obtained experimentally as previously described.

7.4.2. Impedance studies

The impedance data at high acid concentration confirm that the indium exchange is fast since there is no sign of a semicircle in the complex plane plot (figure 7-5). The possibility that a small semicircle, at very high frequencies, is present could not be investigated further because of the limitations imposed by the apparatus. Lines at 45^{o}, indicating diffusion control[37], were obtained at the high acid concentrations with In(III) in the concentration range 0.1 M to 10^{-3} M. Figure 7-5 shows typical data for a solution containing 0.1 M In(III), measurements being made at the equilibrium potential. Transformation of the measured values from a series connection (C_{xs} - R_{xs}) to a parallel connection (C_p - R_p) as described in chapter 5, enables C_p vs. $\omega^{-\frac{1}{2}}$ data to be obtained. The frequency dependence of the parallel circuit resistance, R_p, may also be investigated. For zero charge transfer

resistance and $C_R \gg C_O$, R_p is given by[106]

$$R_p = 2\sigma/\omega^{\frac{1}{2}}C_O \qquad (7.12)$$

where $\sigma = 1000RT/z^2F^2(2D_O)^{\frac{1}{2}}$. Figure 7-7 shows plots of C_p vs. $\omega^{-\frac{1}{2}}$ and R_p vs. $\omega^{-\frac{1}{2}}$ obtained by transformation of the data in figure 7-5. C_p values were calculated using (5.5) and R_p values were computed using

$$R_p = (1 + \beta^2)\ (R_{xs} - R_{sol}) \qquad (7.13)$$

where β is as defined in chapter 5.

The form of the plots in figure 7-7 show that equations (5.4) and (7.12) are obeyed, thus indicating that at high acid concentrations i_o is large and the reaction is diffusion controlled. From the slopes of C_p vs. $\omega^{-\frac{1}{2}}$ and R_p vs. $\omega^{-\frac{1}{2}}$ plots the concentration of oxidised species in equilibrium with the electrode (C_O) was estimated using equations (5.4) and (7.12) and in all cases was far below the concentration of In(III) in solution. A typical value for C_O was 4×10^{-4} M calculated from figure 7-7, where the concentration of In(III) in solution was 0.1 M. In the calculation of C_O, z was taken as 1 and D_O as 8×10^{-6} cm^2 s^{-1} [85], measurements having been made at the equilibrium potential. It should be noted that the exact value of C_O will be somewhat lower than the value given above since electrode roughness effects have been ignored (see chapter 5). Values of C_O calculated from C_p (equation (5.4)) and R_p (equation (7.12)) data were identical. It can be concluded that because C_O is far below the bulk concentration of In(III),

Fig.7-7 C_p vs. $\omega^{-1/2}$ plot; 0·1M $In(ClO_4)_3$ + 1M $HClO_4$ + 0·7M $NaClO_4$. Dashed line represents corresponding R_p vs. $\omega^{-1/2}$ plot

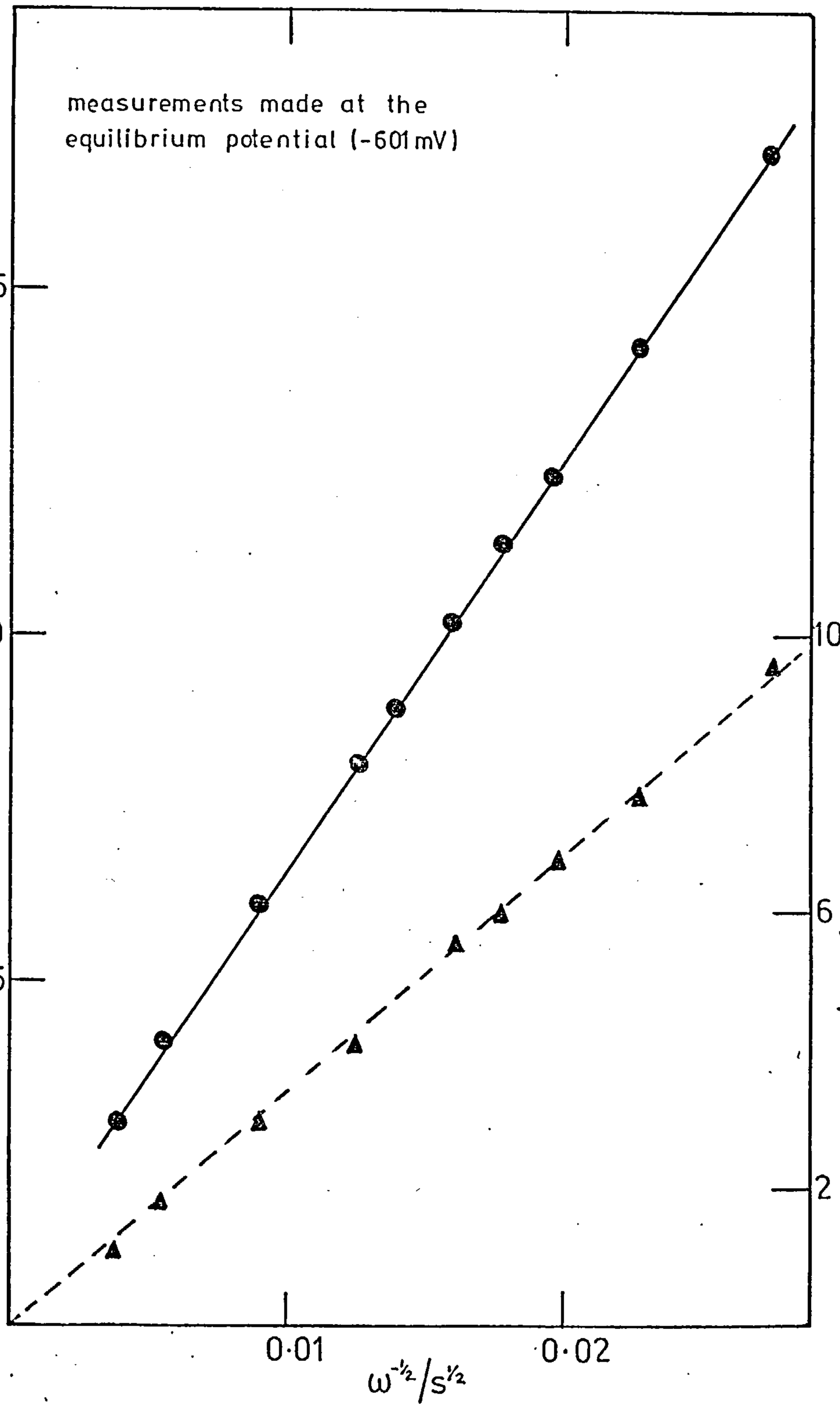

the species in equilibrium with the electrode must involve some oxidation state of indium other than three, since at the equilibrium potential $C_0^b = C_0^s$ (in the absence of specific adsorption). In view of the rotating disc measurements at low overpotentials the most likely species in equilibrium with the electrode under the present conditions is In(I) (figure 7-3). It is noteworthy that in the calculation of C_0 the choice of $z = 1$ was completely arbitrary, however if a value of 2 or 3 is selected for z the values of C_0 are lower than those obtained using $z = 1$.

At low acid concentrations there was evidence of small semicircles in the impedance plots (figure 7-6), although it was not feasible to accurately determine their radii. C_p vs. $\omega^{-\frac{1}{2}}$ plots for systems of low acidity were observed to tail off at high frequencies, as illustrated by the data in figure 7-8. This behaviour is indicative of a process exhibiting some extent of irreversibility, the value of i_o for such systems being smaller than for an entirely diffusion controlled system[28].

The impedance data therefore agrees quite well with the rotating disc data in that at high acidity the reaction corresponds to a very fast one electron transfer between the metal and In(I) species in solution. At low acid concentration it is possible to identify a charge transfer reaction in the frequency range up to $\sim$ 2 kHz. The appearance of a semicircle in the complex plane plot is usually indicative of a charge transfer controlled reaction[37]. However, in the present system of low acidity caution is necessary in the interpretation of the impedance data since complications due to the formation of electrode films are in evidence as previously discussed.

Fig. 7-8 C_p vs. $\omega^{-1/2}$ plot; 0·1mM $In(ClO_4)_3$ + 10^{-2} M $HClO_4$, total perchlorate ion concentration 2M (added $NaClO_4$)

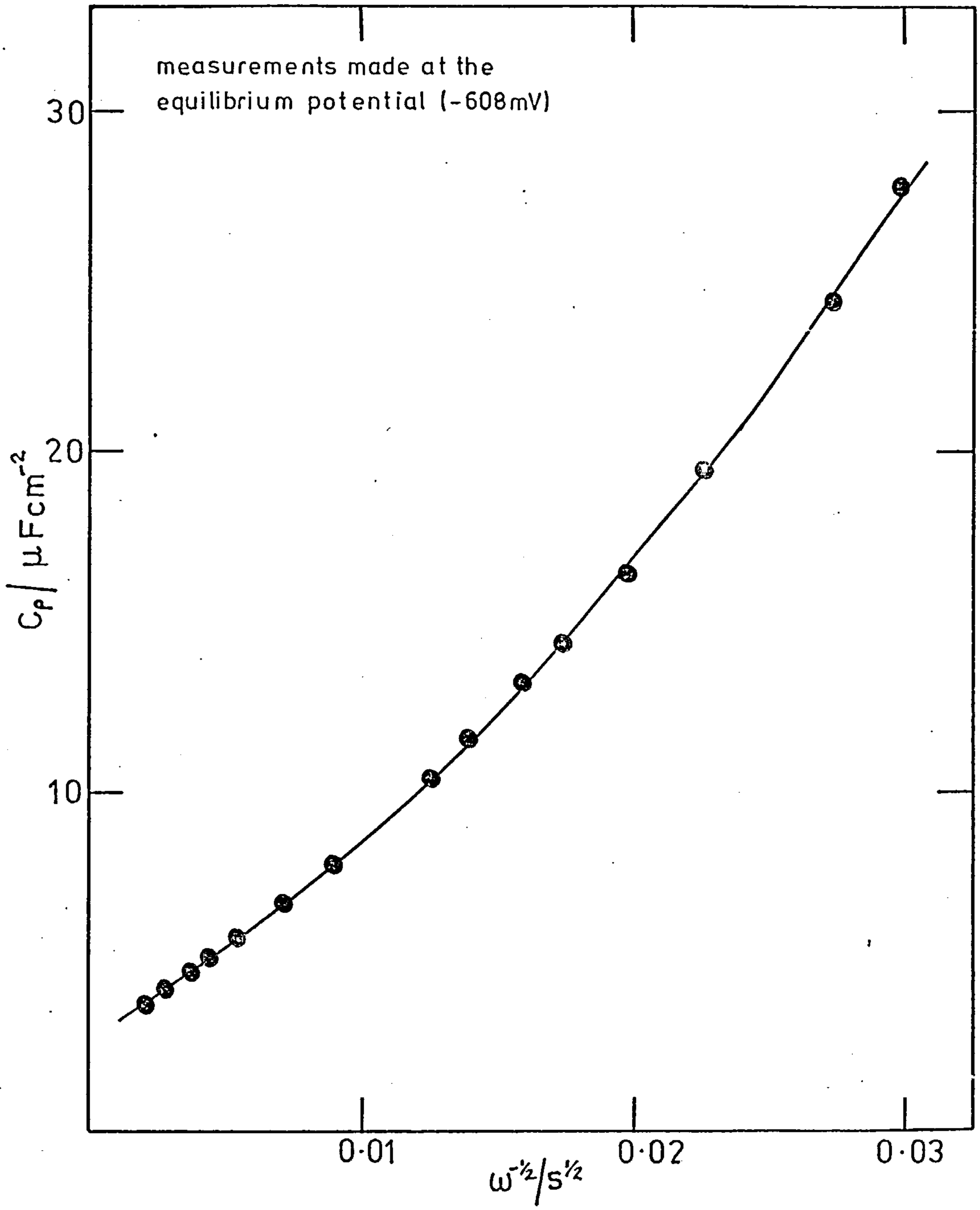

7.4.3. The equilibrium potential of the indium/aqueous perchlorate system

An interesting fact is that at high acid concentration the equilibrium potential appears to be practically unaffected, within fairly wide limits, by the concentration of In(III) in solution. Thus in the present work approximately the same equilibrium potential was observed in solutions of 1 M acid concentration with In(III) in the concentration range 0.1 to 10^{-3} M. This can be interpreted as potential control by the In/In(I) equilibrium, the concentration of In(I) being controlled by the hydrogen ion concentration in solution in accord with equation (7.3). This agrees with the investigation of Losev and Pchel'nikov[51] who studied the dependence of the potential of the indium electrode on the concentration of $In(ClO_4)_3$ and $HClO_4$. These authors reported that only at acid concentrations $\lesssim 10^{-2}$ M was the reversibility of the In/In(III) system observed.

7.5. Conclusions

The rotating disc measurements showed that at high pH the anodic current was independent of the electrode rotation speed. Lowering the pH resulted in a rotation speed dependence of the observed currents. This dependence indicated that at the electrode equilibrium existed between In(O) and In(I) at the more negative potentials and between In(O) and In(III) at the more positive potentials. There was indication that at the more negative potentials the kinetic current was controlled by a one electron change (In/In(I)) and at more positive potentials the Tafel slope indicated a change in mechanism.

Impedance measurements in solutions of varying pH are in satisfactory agreement with the rotating disc data.

CHAPTER 8

THE INDIUM ELECTRODE IN CHLORIDE ELECTROLYTES - A KINETIC STUDY

8.1. Introduction

In chapter 7 the anodic behaviour of indium in perchlorate electrolytes was discussed. Results obtained agreed with those of previous workers in the cases where comparisons could be made. It could only be concluded that in perchlorate media the behaviour is very complex due to the stability of the In(I) ion, which under certain conditions can react with available hydrogen ions at a faster rate than that appropriate to the heterogeneous, potential dependent, rate constant for the In(I)/In(III) oxidation.

It is not only in kinetic measurements that the stability of the In(I) ion complicates the picture; in making equilibrium potential measurements in perchlorate electrolytes it has been reported[51], that only at pH's $\geqslant$ 2 is the reversibility of the In/In(III) system observed. In chloride solutions (chapter 6) the electrode behaves almost reversibly over a much more extensive pH range provided that the pH does not rise above $\sim$2.7, in which case the In(III)/In reaction is complicated by the presence of a phase hydroxide (or oxide) at the electrode giving rise to an electrode of the second kind. This agrees with some preliminary Russian observations[72,85] that chloride ions accelerate the In/In(III) reaction. It is claimed[72] that chloride ions give rise to an In(III) complex, $\left[InCl_2\right]^+$. It would therefore be expected that the electrochemical behaviour of indium in chloride electrolytes would differ from that in perchlorate electrolytes.

This work records the results of an impedance study of the electrochemical behaviour of indium in aqueous chloride electrolytes. Some rotating disc measurements are also presented. Differences between the behaviour in chloride and perchlorate electrolytes are highlighted where possible.

8.2. Experimental

Experimental details of the impedance and rotating disc techniques are outlined in section 7.2.

All electrolytes were deoxygenated by thoroughly purging with oxygen-free nitrogen prior to making measurements.

All potentials were measured using a wick type saturated sodium calomel electrode.

8.3. Results

Figure 8.1. shows typical complex plane impedance plots for an indium electrode in 0.1 M $InCl_3$ solution of varying acidity. Measurements were made at the equilibrium potentials.

Figure 8-2 shows the variation of i_o (obtained from impedance measurements[37] at the equilibrium potentials) with pH for a series of $InCl_3$ solutions.

Figure 8-3 shows the dependence of i_o on $InCl_3$ concentration at constant pH.

Figure 8-4 shows typical complex plane impedance plots obtained as a function of anodic bias potential for an electrolyte consisting of 0.02 M $InCl_3$ + 1.28 M NaCl at pH 1.75.

Figure 8-5 shows the variation of the apparent charge transfer resistance, θ' , (obtained from impedance measurements) with anodic bias potential for solutions with $InCl_3$ concentrations of 0.1 M and 0.02 M.

Fig. 8-1 Typical complex plane impedance plots;
0·1M $InCl_3$ + 1M KCl

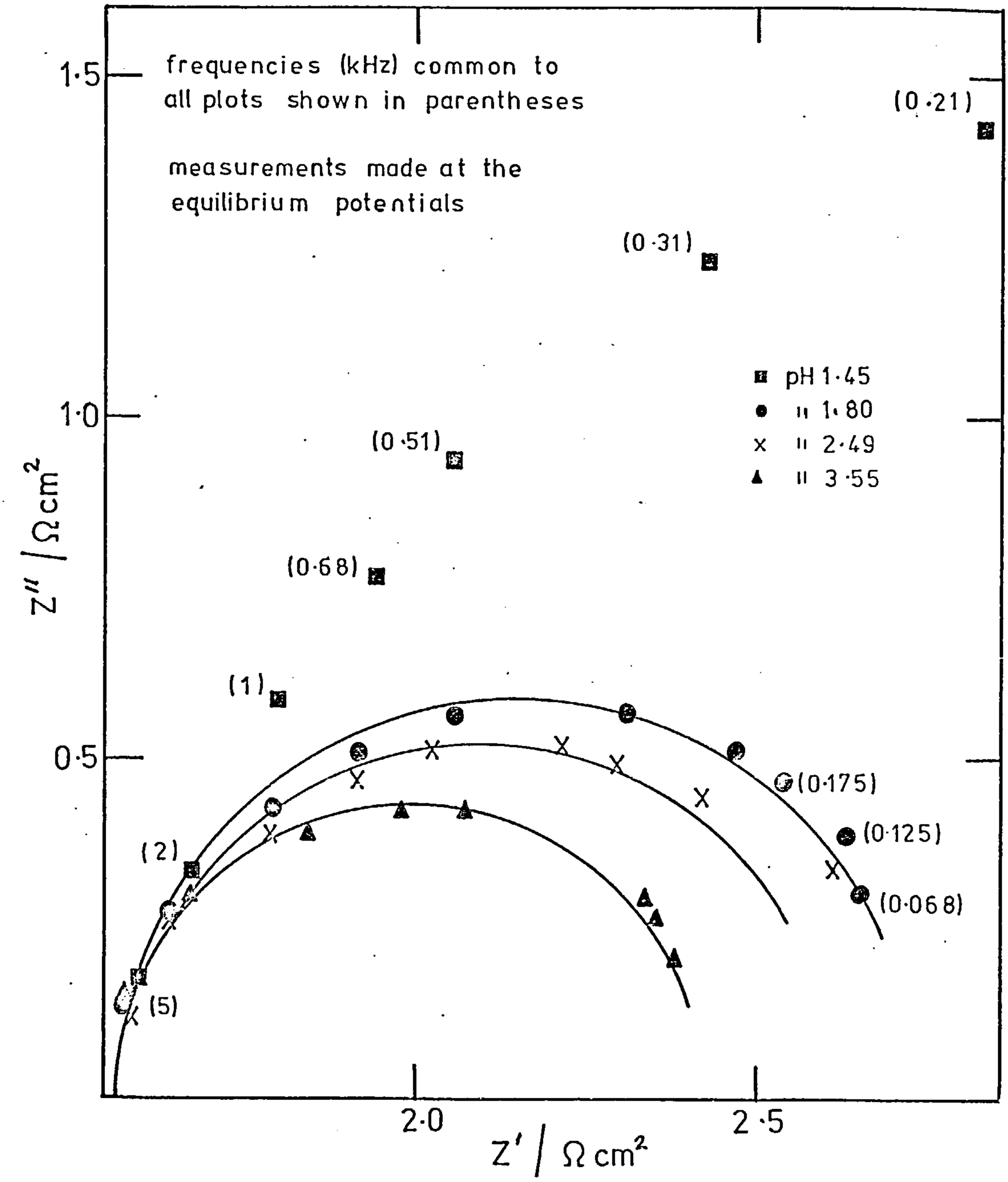

Fig·8-2 Plot of $\log_{10} i_o$ vs. pH for a series of electrolytes of varying In(III) concentration

▲ [In(III)] 0·005 M
o " 0·01 M
Δ " 0·05 M
● " 0·1 M

Total chloride ion concentration adjusted to 1·3 M in all cases by the addition of KCl

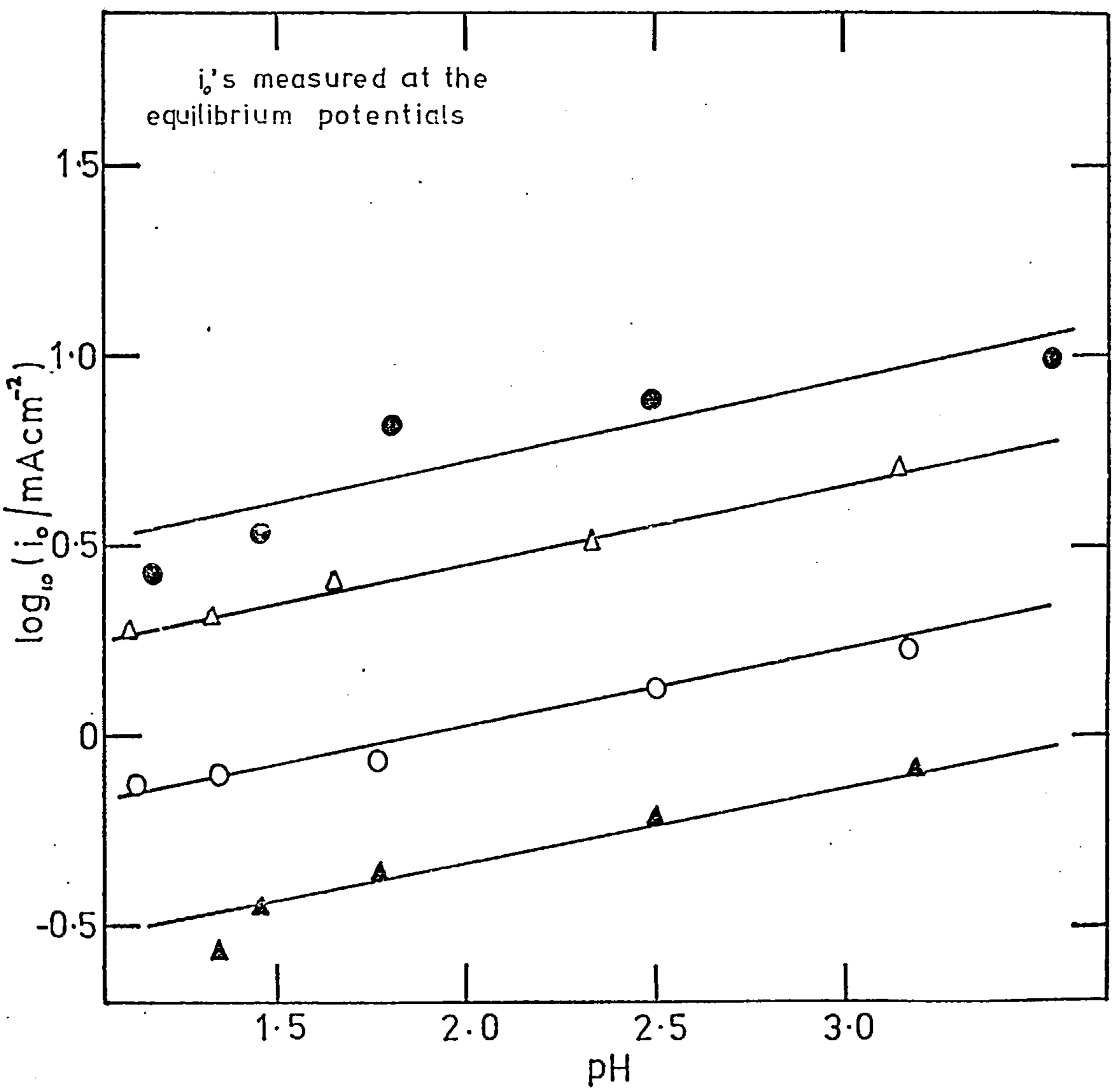

Fig.8-3 i_o dependence of In(III) concentration at constant pH. Data abstracted from Fig.8-2 at pH 2·30

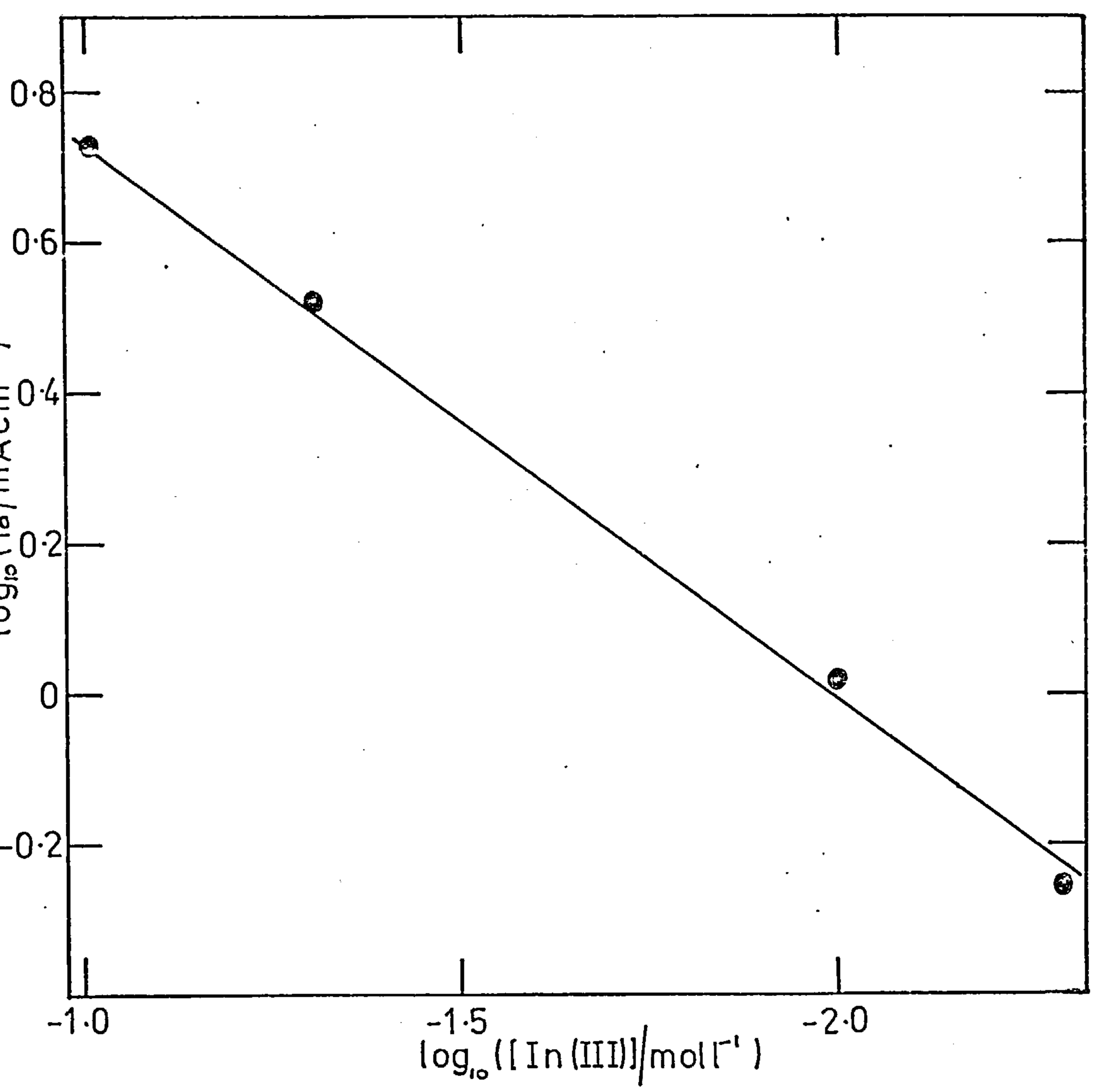

Fig.8-4 Typical impedance plots; 0·02M $InCl_3$ +1·24M NaCl, pH 1·75, at a series of anodic potentials

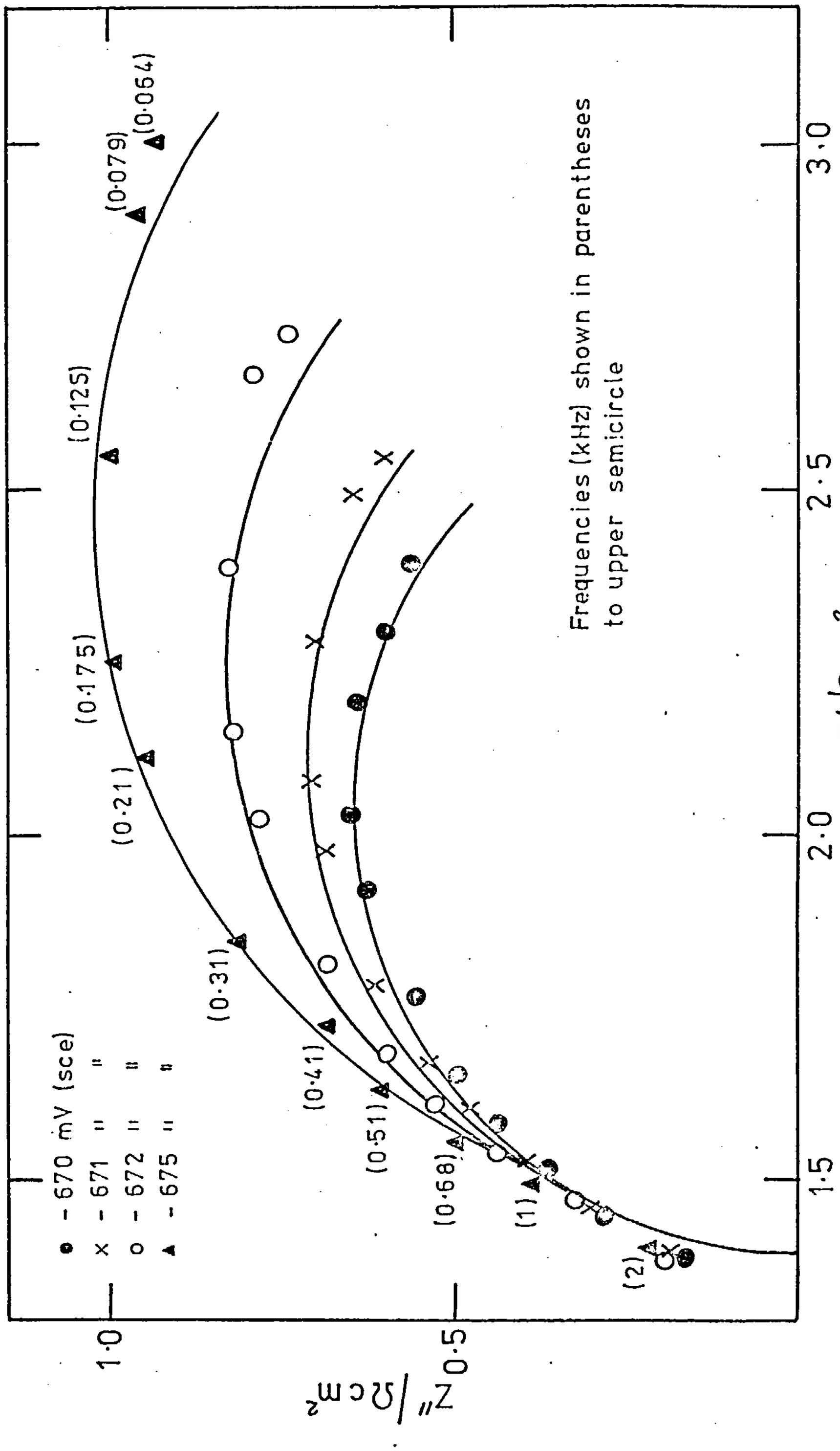

Fig·8-5 $Log_{10}\Theta'$ vs. potential plots; chloride electrolytes

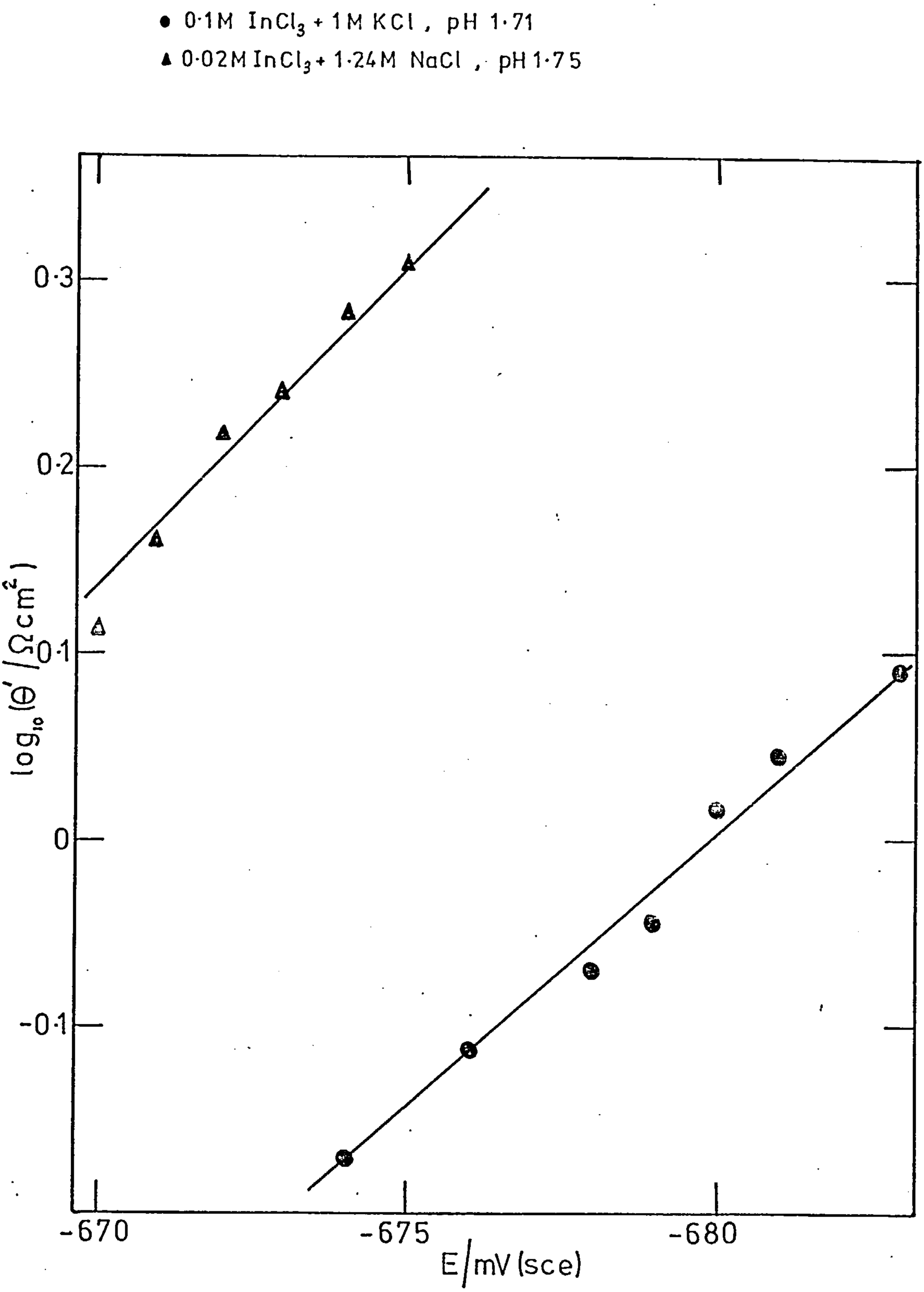

Figure 8-6 shows typical 1^{-1} vs $\omega^{-\frac{1}{2}}$ plots for the anodic dissolution of indium in 0.05 M HCl + 0.95 M NaCl. The logarithms of the slopes of these lines are plotted as a function of potential in figure 8-7.

Figure 8-8 shows a family of Tafel plots for the anodic dissolution of indium in a series of chloride electrolytes of varying acid concentrations. The currents were obtained by extrapolation of i^{-1} vs. $\omega^{-\frac{1}{2}}$ plots to infinite rotation speed. It should be noted that time stable currents could not be obtained at low anodic overpotentials. It was therefore found necessary to commence experiments at least 10 mV anodic of the rest potential in all chloride systems investigated by this technique.

Figure 8-9 shows the effect of perchlorate ions on typical impedance loci obtained for indium in chloride media.

8.4. Discussion

Figure 8-1 shows that the complex plane impedance plots, obtained at the equilibrium potentials, for an indium electrode in an electrolyte 0.1 M in In(III) are dependent on pH. This behaviour was observed for other In(III) concentrations investigated (0.005 - 0.1 M $InCl_3$). It can be seen that over the frequency range investigated, semicircles are obtained, which are indicative of a charge transfer controlled process[37]. The diameters of the semicircles, Θ , are related to the exchange current density, i_o, by equation (2.14). Figure 8-1 clearly illustrates that for a given In(III) concentration, as the pH is lowered the magnitude of the exchange current density is reduced. The variation of i_o with pH for $InCl_3$ containing solutions is rather unexpected. It may indicate catalysis by H^+ or alternatively by undissociated HCl, however it

Fig. 8-6 Typical i^{-1} vs. $\omega^{-1/2}$ plots at a series of anodic potentials; 0·05 M HCl + 0·95 M NaCl

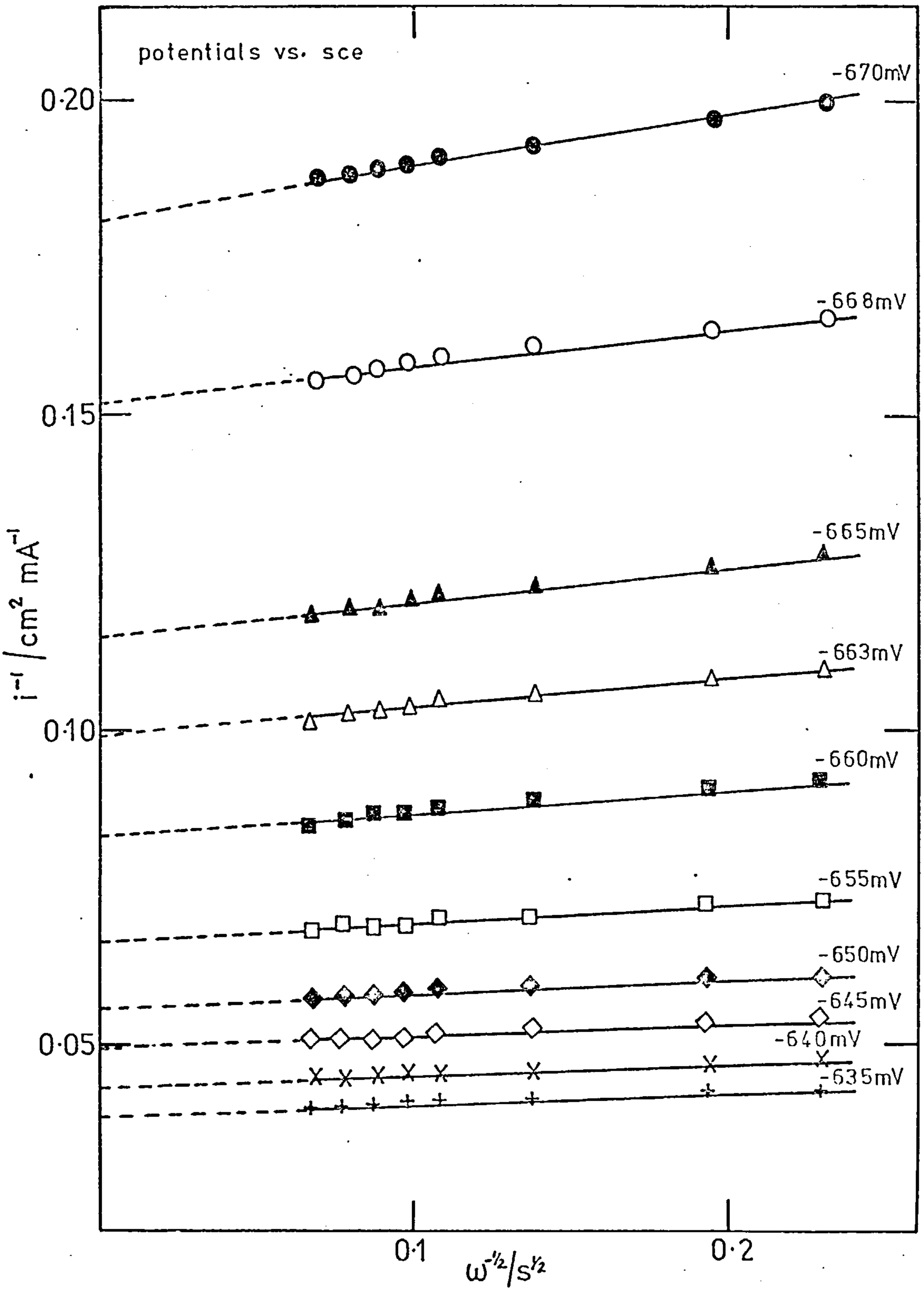

Fig. 8-7 Plot of $\log_{10}(\partial i^{-1}/\partial \omega^{-1/2})$ vs. anodic potential; 0·05 M HCl + 0·95 M NaCl

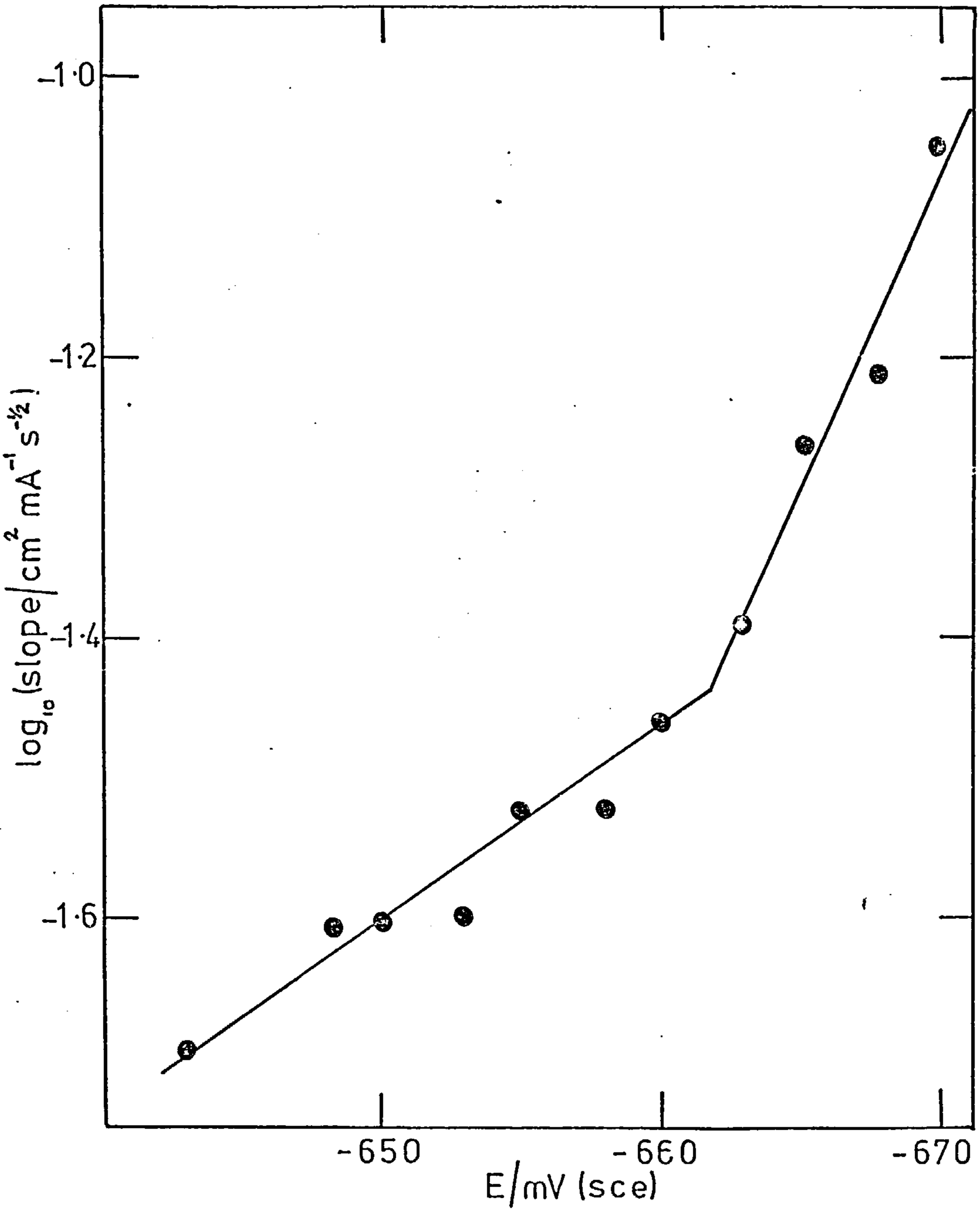

Fig.8-8 Anodic Tafel plots; chloride electrolytes of different acid concentrations

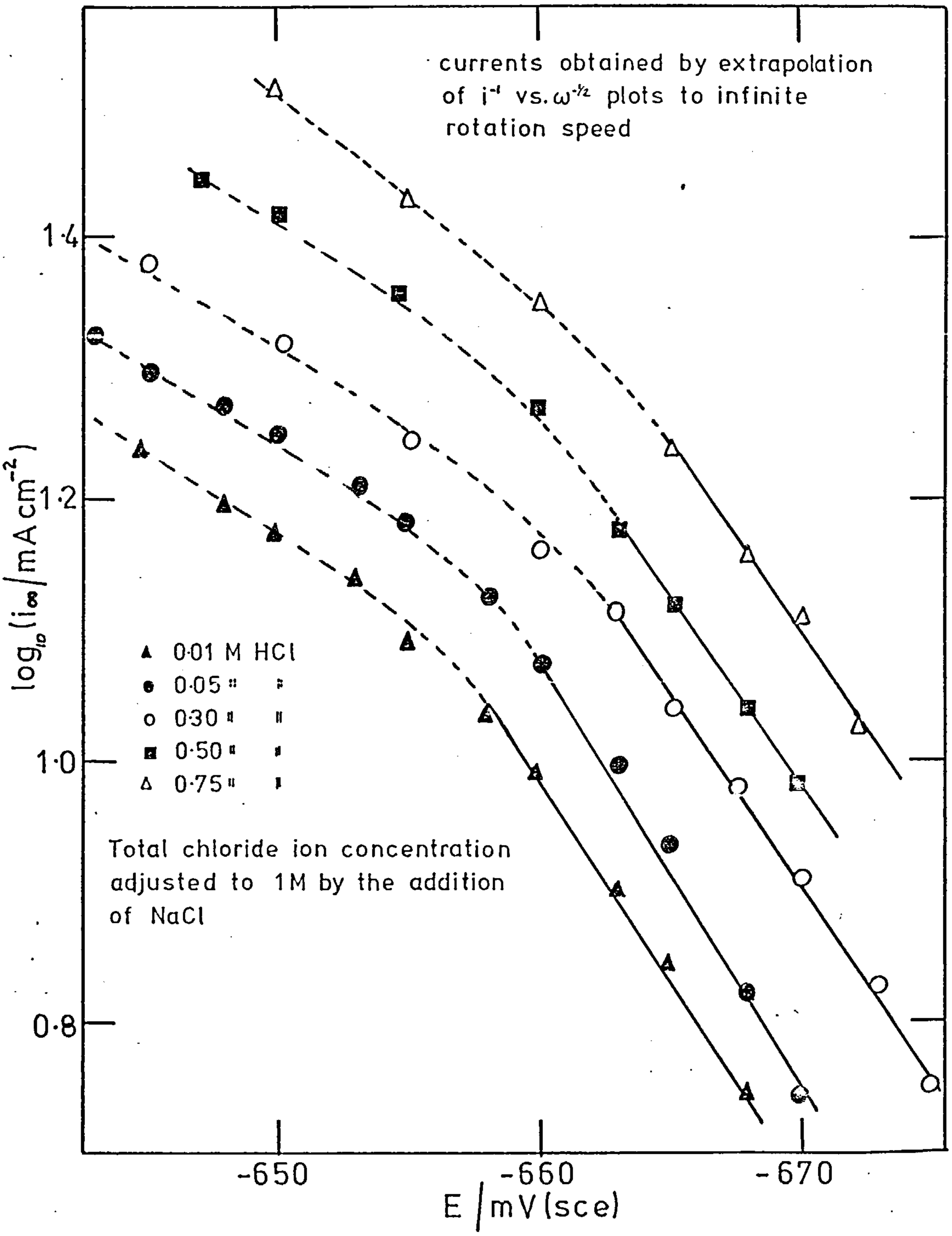

Fig. 8-9 Complex plane plots showing the effect of perchlorate ions on typical impedance data obtained in pure chloride electrolytes

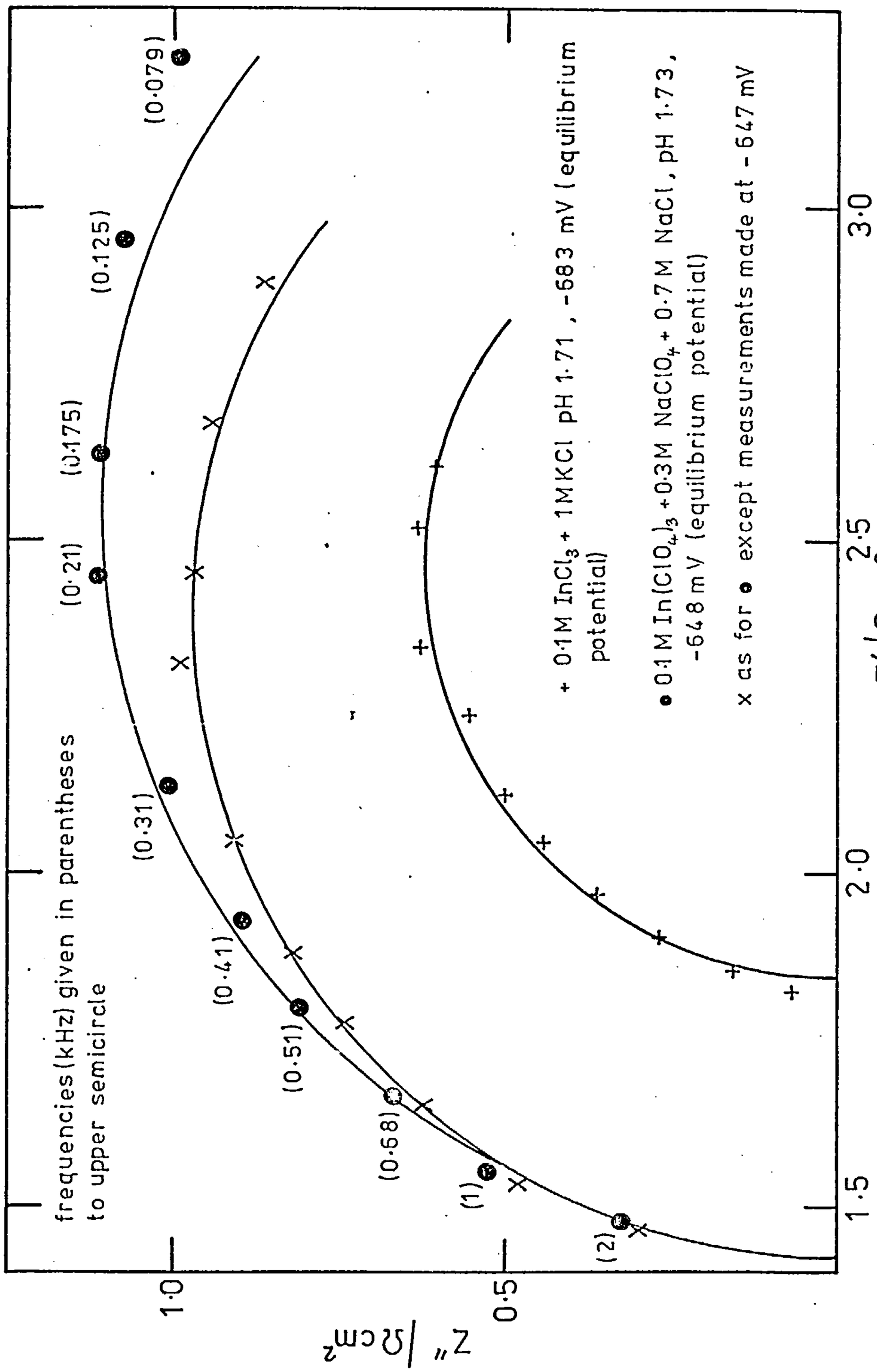

is not clear why the effect should be so pronounced. Figure 8-2 shows the variation of i_o (calculated from (2.14) assuming z = 3) with pH for a series of $InCl_3$ solutions. Measurements were made at the equilibrium potentials. The data are presented in the form of $\log_{10} i_o$ vs. pH plots and a set of parallel straight lines are obtained. $\text{Log}_{10}\, i_o$ vs. $\log_{10}\left[\text{In(III)}\right]$ correlation data at constant pH are straight line plots (figure 8-3). The slope of this plot $(\partial \log_{10} i_o / \partial \log_{10}\left[\text{In(III)}\right])_{\text{In, pH}}$ can be used to analyse the mechanism of the anodic reaction. Processes in which a number of electrons are transferred successively or simultaneously have been comprehensively reviewed[26] (see appendix 2). It is shown that for a multistep process with a single limiting step, the exchange current-concentration relationship is

$$i_o = i_o^o \left[M\right]^{\alpha_{k/n}} \left[M^{n+}\right]^{\alpha_{a/n}} \qquad (8.1)$$

where i_o^o is the standard exchange current. In (8.1) α_a and α_k refer to the transfer coefficients governing the overall potential dependence of the rate of the reaction. α_a and α_k are related to the symmetry coefficients, β_a and β_k, as follows

$$\alpha_a = m-1 + \beta_{a,m} \qquad (8.2)$$

$$\alpha_k = n-m + \beta_{k,m} \qquad (8.3)$$

where n(or z) is the total number of electrons involved in the overall charge transfer process and m is the ordinal number of the rate determining step. β_a and β_k refer only to the limiting step and obey the usual condition

$$\beta_{a,m} + \beta_{k,m} = 1 \qquad (8.4)$$

It follows from (8.2) (8.3) and (8.4) that

$$\alpha_a + \alpha_k = n \qquad (8.5)$$

From (8.2) and (8.3) we obtain

$$\frac{\alpha_a}{\alpha_k} = \frac{(m-1+\beta_{a,m})}{(n-m+\beta_{k,m})} \qquad (8.6)$$

therefore the ratio α_a/α_k depends on the ordinal number of the rate determining step (m). Losev[26] has listed values of α_a/α_k for possible combinations of n and m (assuming $\beta_{a,m} = \beta_{k,m} = 0.5$) Table 8.1 gives α_a/α_k values for the various mechanistic possibilities of a stepwise process with a single limiting step with n = 3.

Table 8.1

Rate determining step	α_a/α_k (for $\beta_{a,m} = \beta_{k,m} = 0.5$)
$M = M^+ + e$	0.2
$M^+ = M^{2+} + e$	1.0
$M^{2+} = M^{3+} + e$	5.0
$M = M^{2+} + 2e$	0.5
$M^+ = M^{3+} + 2e$	2.0

From figure 8-3 $(\partial \log_{10} i_c / \partial \log_{10}[In(III)])_{In,pH} = 0.73$. It follows from (8.1) that

$$\left[\frac{\partial \log_{10} i_o}{\partial \log_{10}[M^{n+}]}\right]_M = \frac{\alpha_a}{n} \qquad (8.7)$$

therefore using (8.5) and (8.7) and assuming n = 3 a value for α_a / α_k of 2.7 is obtained, which suggests that the limiting step in the dissolution reaction under the present conditions (using the single limiting step model[26]) is:

$$In^{+} \longrightarrow In^{3+} + 2e \qquad (8.8)$$

It should be noted that in perchlorate electrolyte the same limiting step was apparent only at relatively high pH's ($\geqslant 2$) where insufficient hydrogen ion was available to materially effect (8.8) via the competing chemical reaction $In^{+} + 2H^{+} \longrightarrow In^{3+} + H_2$. In the present investigation impedance results were difficult to analyse with any degree of accuracy at pH's $\lesssim 1$ in view of the large diameter semicircles that were obtained (see for example figure 8-1).

To substantiate the proposed mechanism, the potential dependance of i_o was investigated for indium in chloride electrolytes. The apparent charge transfer resistance can be related to potential as follows: for a stepwise reaction with a single limiting step the exchange current is related to the concentrations of O and R by

$$i_o = nFk^o\, c_O^{\alpha_{a/n}}\, c_R^{\alpha_{k/n}} \qquad (8.9)$$

which may also be written as

$$i_o = nFk_{sh}\, c_O^{\alpha_{a/n}}\, c_R^{\alpha_{k/n}} \qquad (8.10)$$

where k_{sh} is defined as the standard heterogeneous rate constant. The charge transfer resistance, Θ , is related to the exchange current density by equation (2.14). Incorporation of (2.14) into (8.10) gives

$$\Theta = \frac{RT}{n^2F^2k_{sh}\, C_O^{\alpha_{a/n}}\, C_R^{\alpha_{k/n}}} \qquad (8.11)$$

For a metal in which C_R is not varied and may be assumed constant, (8.11) may be written as

$$\log_e \Theta = \text{constant} - \frac{\alpha_a}{n} \log_e C_O \qquad (8.12)$$

From the Nernst equation we obtain

$$(E-E^{\Theta}) = \frac{RT}{nF} \log_e \frac{C_O}{C_R} \qquad (8.13)$$

which on differentation gives

$$\frac{dE}{d \log_e C_O} = \frac{RT}{nF} \qquad (8.14)$$

We may write

$$\frac{d \log_e \Theta}{dE} = \frac{d \log_e \Theta}{d \log_e C_O} \cdot \frac{d \log_e C_O}{dE} \qquad (8.15)$$

which from (8.12) and (8.14) gives

$$\frac{d \log_e \Theta}{dE} = -\left(\frac{\alpha_a}{n}\right)\left(\frac{nF}{RT}\right) \qquad (8.16)$$

Integrating (8.16) we obtain

$$\log_e \Theta = -\left(\frac{\alpha_a}{n}\right)\left(\frac{nFE}{RT}\right) + C \qquad (8.17)$$

when $E = E^{\Theta}$, $\log_e \Theta = \log_e \left[\frac{RT}{n^2F^2k_{sh}\ c_O^{\alpha_{a/n}}\ c_R^{\alpha_{k/n}}} \right]$

therefore

$$\log_e \Theta' = \log_e \left[\frac{RT}{n^2F^2k_{sh}\ c_O^{\alpha_{a/n}}\ c_R^{\alpha_{k/n}}} \right] - \frac{\alpha_a F}{RT}(E-E^{\Theta}) \qquad (8.18)$$

At potentials different from E^{Θ}, Θ becomes Θ' the apparent charge transfer resistance, and i_o becomes i_o', the interfacial current alone[28]. Thus a plot of log i_o vs. potential gives a Tafel slope.

Figure 8-4 shows a typical series of impedance loci obtained as a function of anodic bias potential for an electrolyte containing 0.02 M In(III). It is clear that as the potential is driven more anodic the apparent exchange current increases. A test of equation (8.18) is shown in figure 8-5 for two solutions of different In(III) content at approximately the same pH. In each case a straight line plot is obtained with a slope of $\sim$30 mV/decade. From(8.18) the slope of these plots is $\alpha_a F/RT$, which leads to a value of α_a of 2.0 and hence an α_a/α_k value of 2.0. This is in reasonable agreement with the α_a/α_k value calculated from figure 8-3. Abstraction of Θ' vs $\log_{10}$ [In(III)] data from figure 8-5 leads to a value of 0.64 for $(\partial \log_{10}(1/\Theta')/\partial \log_{10}[\text{In(III)}])_{E,pH}$ which is equivalent to $\partial \log_{10} i_o'/\partial \log_{10}[(\text{In(III)}])_{E,pH}$ and hence using (8.5) and (8.7) a value of $\sim$ 1.8 is obtained for α_a/α_k, which agrees well

with the two previous determinations of this parameter.

The use of the rotating disc electrode as a means of investigating a metal undergoing anodic dissolution has been discussed in section 2.4. Figure 8-6 shows a test of equation (2.37) data being presented as i^{-1} vs. $\omega^{-\frac{1}{2}}$ plots. Data conforming to (2.37) were obtained for all solutions studied by this method ($[H^+]$ in the range 0.01 - 0.75 M). It is interesting to note that in perchlorate electrolytes at an acid concentration of 0.01 M the observed anodic currents were independent of rotation speed. This behaviour is confirmed by differential capacitance measurements (chapter 5). For chloride electrolytes a capacitance rise indicative of lattice dissolution was observed for unacidified solutions (figure 5-5), whereas for perchlorate electrolytes the solution pH had to be lowered before a capacitance rise attributable to indium dissolution was observed (see figures 5-10 and 5-7).

The logarithms of the slopes of the i^{-1} vs $\omega^{-\frac{1}{2}}$ plots of figure 8-6 are shown in figure 8-7 as functions of potential (equation 2.43). Plots showing features similar to figure 8-7 were obtained for all other chloride solutions investigated. At the more negative potentials ($<\sim$-660 mV) the slope of figure 8-7 is $\sim$ 20 mV/decade which indicates that In(III) species are in equilibrium with the electrode at these potentials. For perchlorate electrolytes the corresponding data (figure 7-3) showed that the species in equilibrium with the electrode at the more negative potentials ($<\sim$ -490 mV) was the In(I) ion. At potentials more positive than $\sim$ -660 mV figure 8-7 curves off, the slope tending to $\sim$ 60 mV/decade which suggests that the In(I) species is in equilibrium with the electrode at these potentials. This again

contrasts with perchlorate systems where at the more positive potentials investigated ($>\sim$-490 mV) it was concluded that In(III) species were in equilibrium with the electrode. The reason for the change of slope of figure 8-7 is obscure. This behaviour may be connected with the non-establishment of the In(III)/In equilibrium as the potential is driven more positive, whereby the rate of the dissolution reaction is increased which possibly causes mechanistic changes.

Figure 8-8 shows a series of Tafel plots for the anodic dissolution of indium in chloride electrolytes of varying pH. It can be seen that at the more negative potentials a linear region of $\sim$ 30 mV/decade is obtained. This $\sim$ 30 mV/decade Tafel slope occurs over the same potential region in which the In(III) ion is in equilibrium with the electrode (figure 8-7). For a stepwise process with a single limiting step the anodic Tafel slope is given by

$$\frac{\partial E}{\partial \log_e i} = \frac{RT}{\alpha_a F} \qquad (8.19)$$

Thus using (8.19) and (8.5) a Tafel slope of 30 mV/decade gives an α_a/α_k value of 2.0 which is in excellent agreement with the three determinations of this parameter using the impedance techniques described. On passing to more positive potentials the Tafel slope curves off, corresponding to the change from In(III) to In(I) as the species in equilibrium with the electrode (figure 8-7). Markovac and Loverecek[82] whilst studying the electrochemical kinetics of indium (as 0.3% indium amalgam), by the galvanostatic single pulse method, also observed an increase in the anodic Tafel slope at higher

current densities; a phenomenon they attributed to a change in mechanism. These authors[82] postulated that at low anodic potentials the $In^{2+} \longrightarrow In^{3+} + 2e$ reaction was rate determining, whilst at higher anodic potentials the $In \longrightarrow In^{+} + e$ reaction became rate determining. Pchel'nikov et al[85] investigated the electrochemical behaviour of solid indium in chloride electrolytes using steady state polarisation methods. A constant anodic Tafel slope of ∿ 20 mV/decade was reported. This value should be compared with figure 8-7, since under these authors'[85] conditions diffusion in solution was the rate controlling process, whereas the currents in the Tafel plots of figure 8-8 are the true kinetic currents, having been corrected for diffusion effects.

In the present investigation the exact cause of the change of Tafel slope cannot be extracted from the available data, although it is possible that a change in the electrochemical mechanism at the higher rates of reaction is involved. It is noteworthy that in perchlorate electrolytes a change in Tafel slope from ∿120 mV/decade to smaller values, on passing to more anodic potentials (figure 7-4) was attributed to a balance of rates of the electrochemical In(I)/In(III) oxidation and the competing reaction of hydrogen ions with the In(I) ions. It was not possible, however, due to experimental limitations to obtain potentials sufficiently anodic to completely suppress the competing chemical reaction in perchlorate media. Only when the acidity was lowered to 0.01 M was it possible to obtain an anodic Tafel slope of 30 mV/decade, which corresponds to that observed at low anodic potentials in the present investigations for all electrolyte solutions($[H^+]$ in the range 0.01 - 0.75 M). It therefore appears that in chloride

electrolytes, over a considerable pH range, the competing chemical reaction of hydrogen ions with In(I) species is suppressed. The reason for this behaviour may lie in the accelerating effect of chloride ions on the second step of the electrochemical oxidation mechanism (reaction(8.8)), although the acceleration is not great enough to make the $In \longrightarrow In^+ + e$ step rate determining at low anodic potentials. This conclusion agrees with the work of Losev et al[85,135] and Krautsov et al[136] who have previously discussed the accelerating influence of chloride ions on the $In(I) \longrightarrow In(III) + 2e$ reaction.

Figure 8-10 shows the effect of hydrogen ion concentration on the anodic reaction of indium in chloride electrolytes. This data was obtained by abstraction of $\log_{10} i$ vs. $\log_{10} [H^+]$ data, at constant potential, from the low anodic potential region of figure 8-8. It is evident from the form of figure 8-10 that some complicating factor is interfering with the effect of hydrogen ions on the anodic reaction in chloride media. Were a simple involvement of hydrogen ions the case a plot of $\log_{10} i$ vs. $\log_{10} [H^+]$ would be linear with an integral slope, the magnitude of which would represent the order of the reaction with respect to hydrogen ions. Although figure 8-10 shows that hydrogen ions accelerate the anodic reaction to some extent, their effect is hindered by some complicating factor, possibly the acceleratory nature of the chloride ions on the anodic reaction.

Figure 8-9 shows clearly that addition of perchlorate ions to chloride solutions results in a retardation of the anodic process. The impedance plot at the equilibrium potential (-683 mV) for 0.1 M $InCl_3$ + 1 M KCl solution gives rise to a much smaller diameter semicircle (and hence a larger i_o) than the impedance plot at the

Fig. 8-10 Plot of $\log_{10} i$ vs. $\log_{10}[H^+]$, at constant potential; chloride electrolytes of varying pH

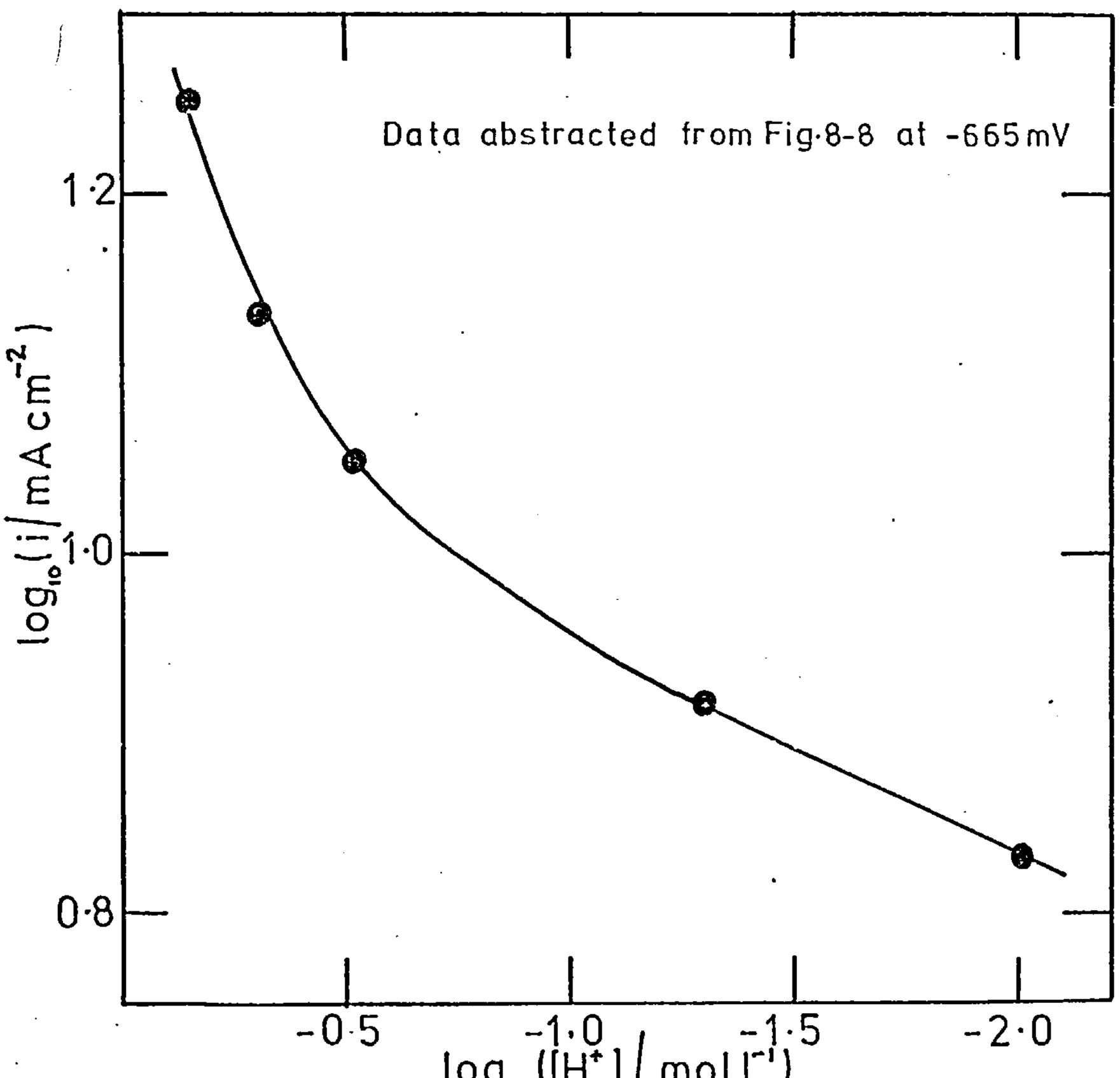

equilibrium potential (-648 mV) for an electrolyte of the same pH consisting of 0.1 M $In(ClO_4)_3$ + 0.3 M $NaClO_4$ + 0.7 M NaCl. If impedance measurements were made in pure chloride electrolyte at the same potential as the equilibrium potential of the mixed Cl^-/ClO_4^- electrolyte, viz. -648 mV, the apparent exchange current would be even higher than that obtained at the equilibrium potential in the pure chloride electrolyte, since the semicircle diameter is reduced as the potential is driven more positive (cf. figure 8-4). Further evidence that the anodic reaction is much faster in chloride electrolytes is illustrated by the potential range in which significant currents flowed. For chloride electrolytes the experimentally accessible potential range studied in which anodic currents flowed was $\sim$ -680 mV to $\sim$ -630 mV, whereas in perchlorate media the potential range in which significant anodic currents flowed was $\sim$ -550 mV to $\sim$ -450 mV.

8.5. Conclusions

It is shown that at low anodic potentials the $In(I) \longrightarrow In(III) + 2e$ reaction is rate determining over a considerable pH range. The difference in the anodic behaviour of the indium electrode in chloride and perchlorate electrolytes is attributed to the accelerating effect of the chloride ion on the dissolution reaction in chloride media. At higher anodic potentials a change of mechanism apparently occurs in chloride media, a phenomenon thought to be connected with the non-establishment of the In(III)/In(O) equilibrium at the higher rates of reaction.

CHAPTER 9.

THE ANODIC BEHAVIOUR OF INDIUM IN ALKALINE ELECTROLYTES

9.1. Introduction

The current-potential curve for the anodic behaviour of a metal in alkali often exhibits a number of characteristic features. Initially an increase of anodic current may occur which corresponds to active dissolution of the metal. On passing to more positive potentials the electrode may become covered, or partially covered, with poorly soluble reaction products. If a protective film is formed on the electrode the current falls abruptly and passivation is said to have occurred. Thus passivity may be defined as a reduction of the rate of metal dissolution due to the formation of a barrier between the metal and the electrolyte. A small current usually flows when the electrode is in the passive state. This current may be due to film thickening or the replacement of chemically dissolved film material. A new soluble substance may form when the anodic potential is increased beyond the passive region. This phenomenon may arise because the film changes in composition, or because the metal (and the passivating layer) can dissolve in a higher valcency state. A secondary passivation may subsequently be observed when a new protective film is formed on the electrode. At still more positive potentials oxygen evolution or perhaps oxidation of the soluble solution products may occur on the filmed electrode surface.

The present work describes an investigation of the passivation processes occurring at an indium electrode in alkaline electrolytes, using linear sweep voltammetric and galvanostatic polarisation techniques. The mechanism of active dissolution of indium in alkali

has also been studied using a rotating disc electrode.

9.2. Experimental

9.2.1. Galvanostatic polarisation studies

The electrical circuit and cells are described in 3.4.5 and 3.1.2. respectively. The working electrode was an indium disc (0.5 cm^2, 0.075 mm thick). Electrical contact was made by attaching a copper wire to the electrode using silver based epoxy resin (Thermosetting silver preparation, types FSP 49H and FSA 49R in a 50:50 mixture, Johnson Matthey Metals Ltd.). The working electrodes were carefully polished using cotton wool, briefly etched (5:1 water/perchloric acid, 5 sec) and washed thoroughly with bi-distilled water. The counter electrode was a platinum coil and the reference electrode was an unpolarised strip of indium foil; the potential measurements were thus overpotentials. This reference electrode was preferred to others since its use avoided uncertainties due to junction potentials; the immediate formation of a film of oxide on the electrode surface provided adequate potential-determining species for the strip to function as an electrode of the second kind ($In(OH)_3 + 3e = In + 3OH^-$) in the high impedance reference electrode circuit.

9.2.2. Potentiostatically controlled studies

Linear sweep voltammetric and rotating disc studies were used to study the anodic reaction of indium in alkali. The cells, electrical circuits, electrodes and electrode pretreatment techniques are described in chapter 3. Potentials were measured against a HgO/Hg electrode. All electrolytes were deoxygenated by thoroughly

purging the systems with oxygen free nitrogen.

9.3. Results

9.3.1. Galvanostatic polarisation studies

The following electrolyte solutions were used in this investigation. 0.1M, 1 M, 4M and 7M KOH solutions and 4M NaOH solution. Each system was studied using both horizontal and vertical indium test electrodes.

Figures 9-1 to 9-3 show typical overpotential-time curves. The curves consist of two regions in which the potential is fairly constant: a short region at $\sim$ 0.05 V (versus the indium reference electrode) followed by a rapid transition to a second approximately constant overpotential. The value of the potential corresponding to this second plateau (terminated at the point of passivation, t_p) depended strongly on the current density. The form of the overpotential-time curves obtained were independent of the test electrode orientation for all alkali concentrations.

Figure 9-4 shows the correlation between current density, i, and passivation time. It is clear that the time to passivation increases markedly as the current density is reduced.

9.3.2. Potentiostatically controlled studies

Figure 9-5 shows a typical anodic potential sweep obtained for a stationary indium electrode in 1M KOH electrolyte. At the negative extreme of the potential range hydrogen evolution occurs. At $\sim$ -1050 mV active dissolution of the indium occurs which is inhibited by passivation at $\sim$ -975 mV (peak 'a'). On passing to more positive potentials a reduced anodic current flows, increasing to a second maximum at approximately 140 mV. Oxygen evolution occurs

Fig.9-1 Typical overpotential-time curve for a horizontal indium anode in 4M KOH

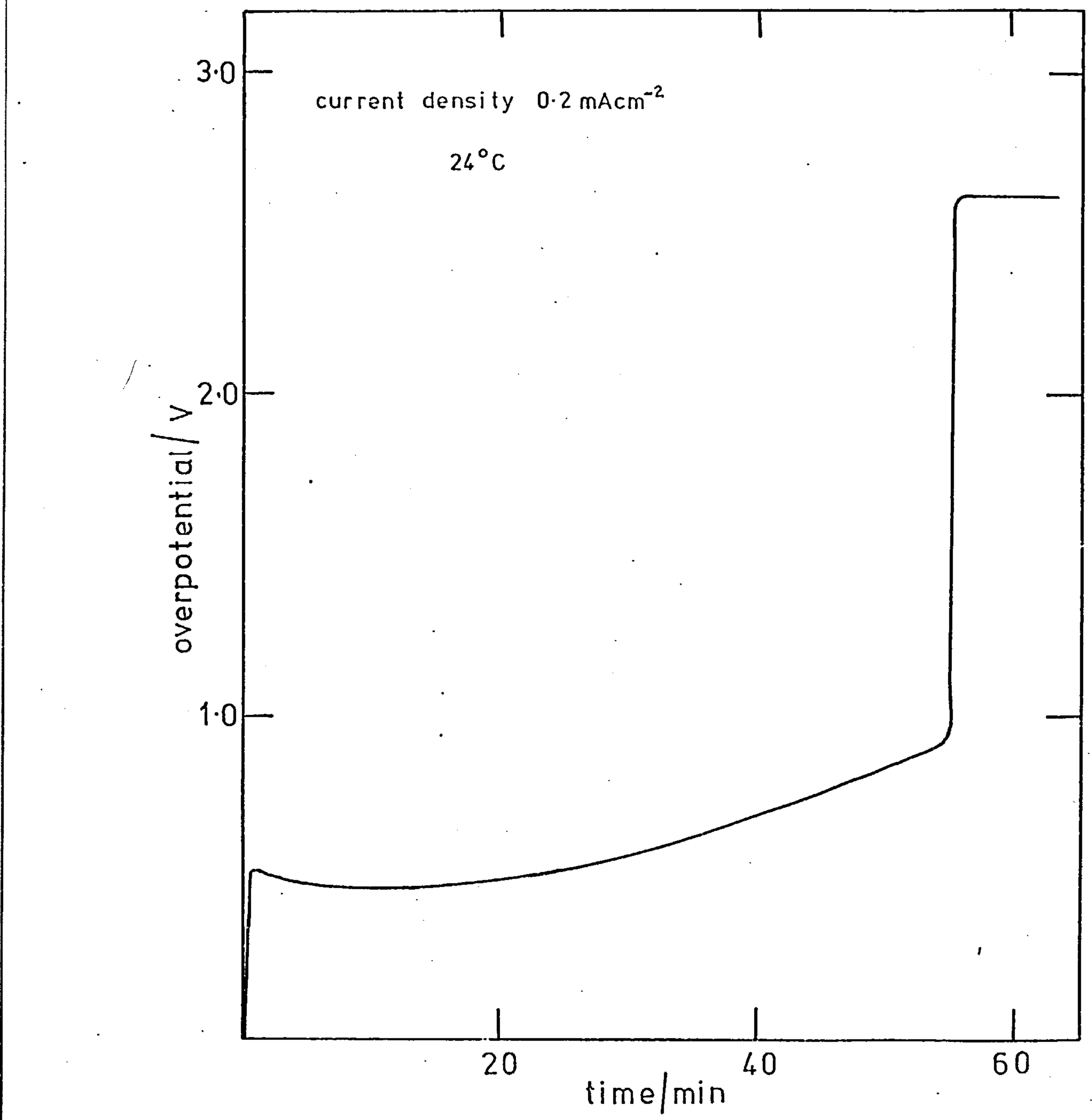

Fig·9-2 Typical overpotential-time curve for a horizontal indium anode in 4 M NaOH

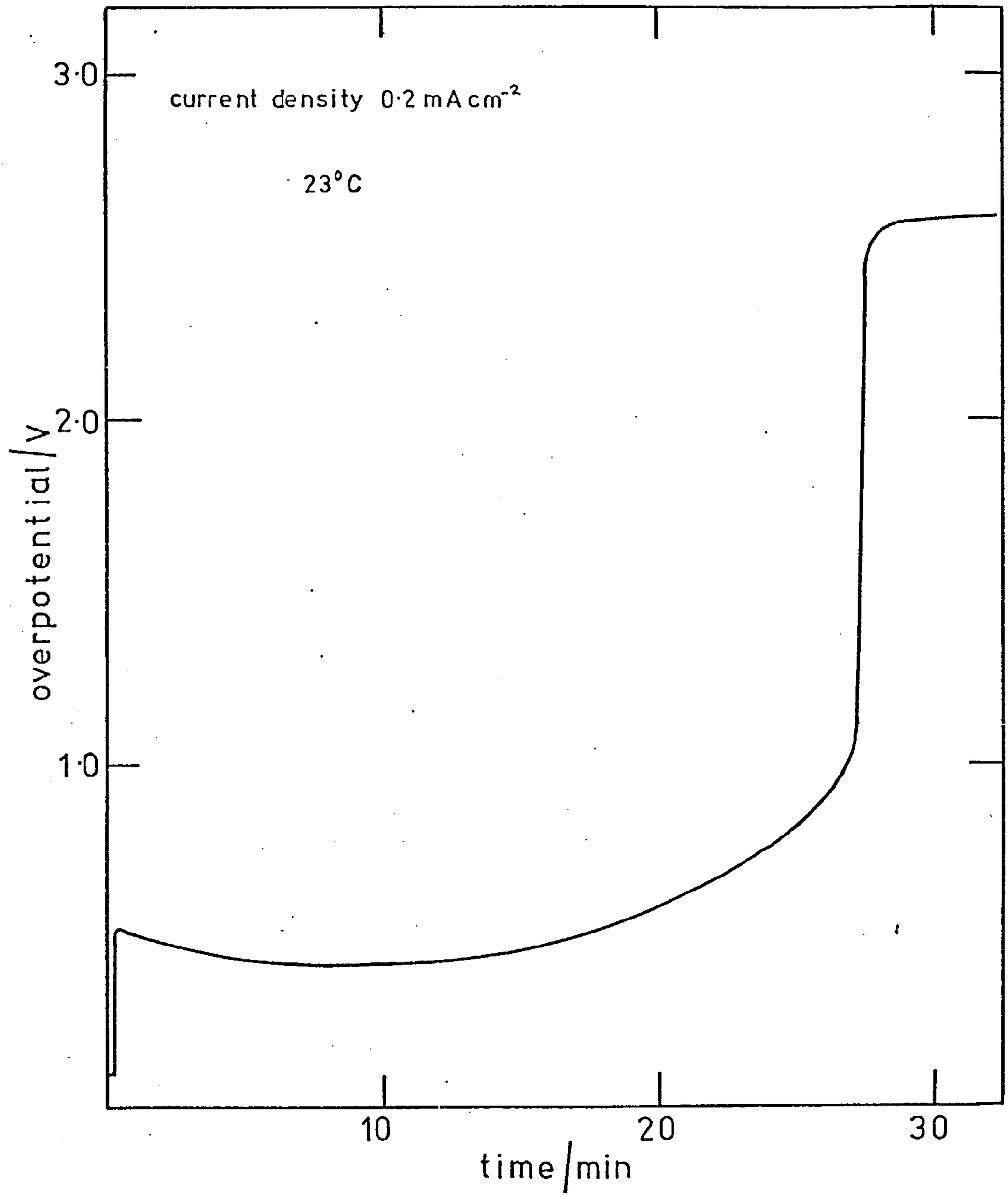

Fig.9-3 Typical overpotential-time curve for a vertical indium anode in 4 M NaOH

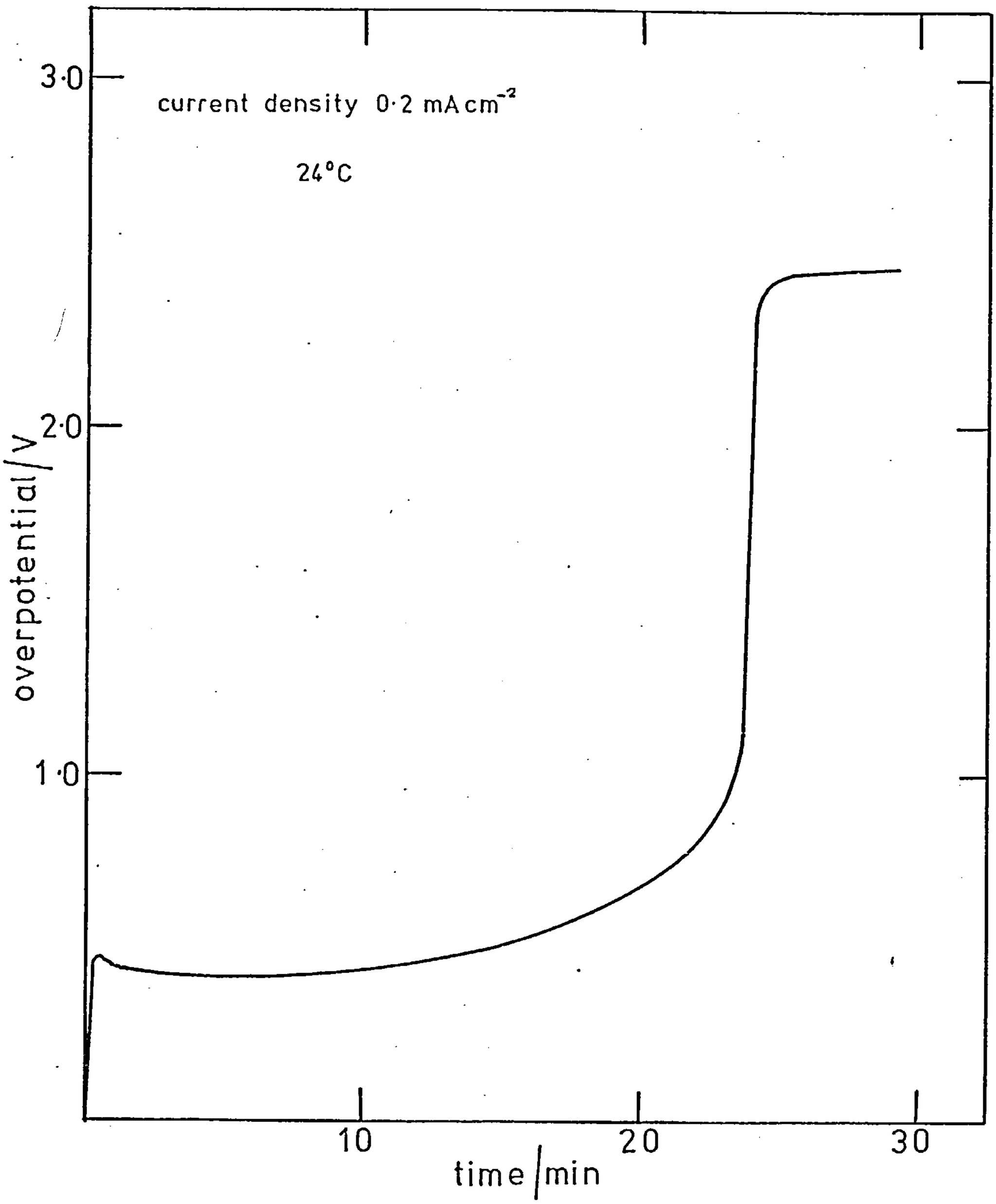

Fig.9-4 Passivation time-current density data

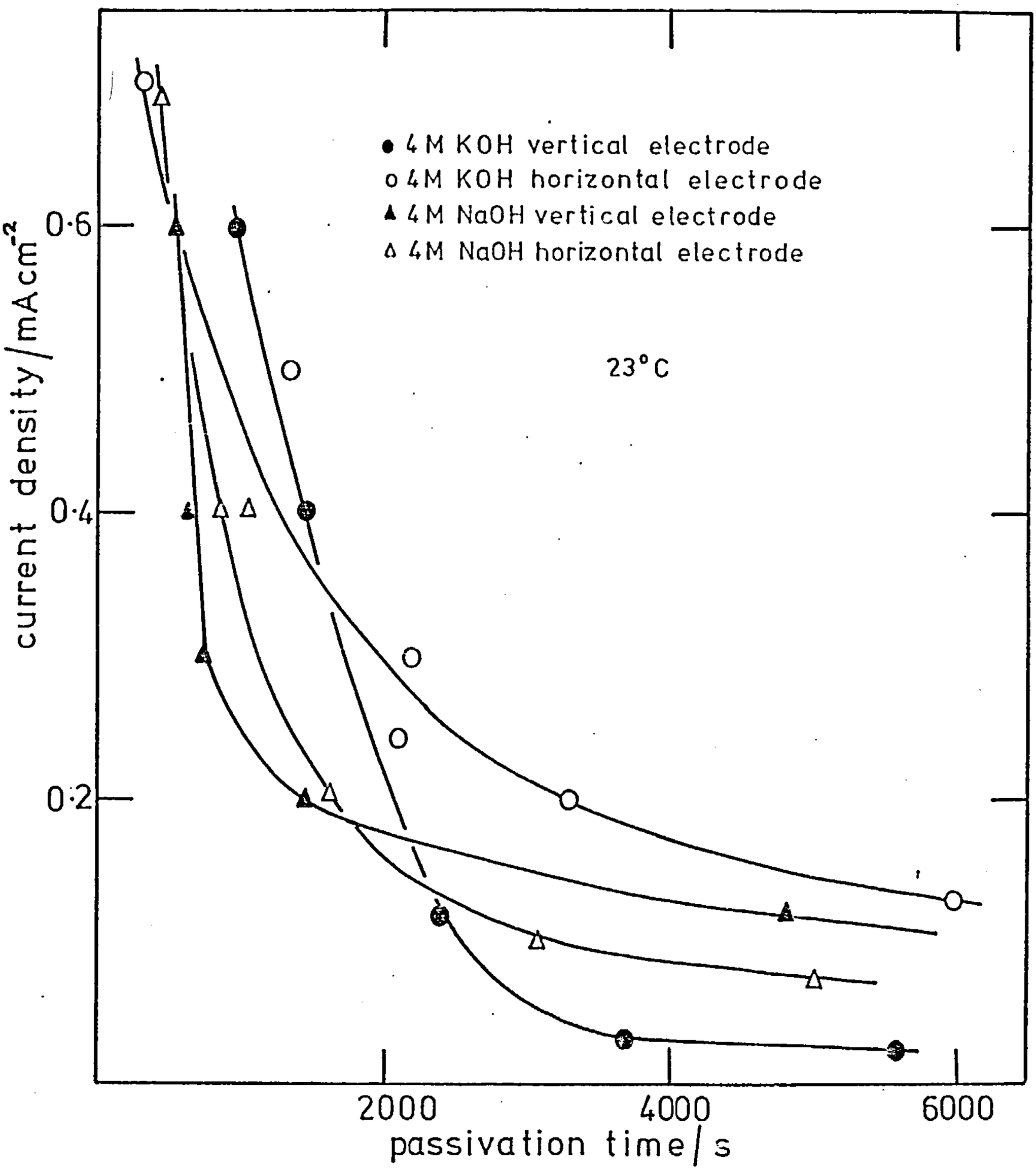

Fig.9-5 Anodic potential sweep; 1M KOH

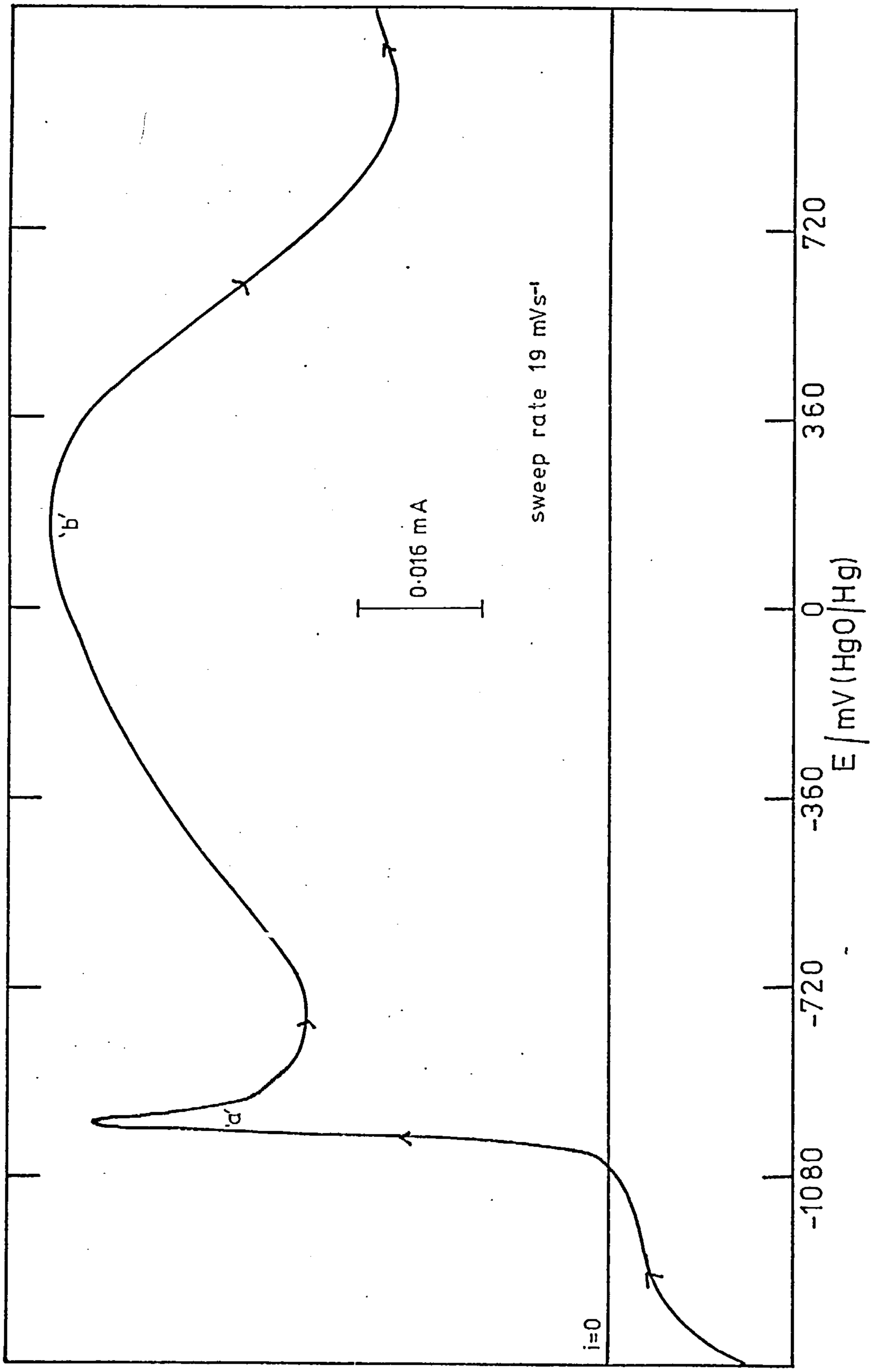

above ∿ 1200 mV. During the negative-going sweep (figure 9-6) negligible current flows between about 690 and -990 mV. On moving to more negative potentials a reduction process occurs (peak 'c'). The effect of increasing the sweep speed was to increase the magnitude of the currents flowing during both directions of the sweep. Increasing the KOH concentration in the range 1 to 8.5 M had a similar effect.

Figure 9-7 shows the effect of terminating the anodic-going sweep at a potential prior to the occurrence of the second peak ('b') for an 8.5 M KOH electrolyte solution. It is evident that an anodic process occurs during the reverse sweep. This behaviour was observed for 8.5 M KOH at all sweep rates investigated (1-300 mV s^{-1}), whereas for 5 M KOH and 3 M KOH electrolytes such a phenomenon was observed only at sweep rates less than ∿150 mV s^{-1} and ∿ 20 mV s^{-1} respectively. For 1 M KOH solution an anodic process was not observed during the reverse sweep, at any of the sweep speeds investigated (1-300 mV s^{-1}). For all cases where an anodic process was not observed during the negative-going sweep when the positive-going sweep was terminated prior to peak 'b', a reduction peak, 'd', occurred at potentials more positive than the reduction peak 'c' observed when the second anodic passivating process was allowed to occur. Such maxima were observed at ∿ -1100 mV for 1 M KOH, ∿ -1140 mV for 3 M KOH and ∿ -1160 mV for 5 M KOH. Figures 9-8a to 9-8c show the effect on peak 'd' of terminating the positive-going sweep at various potentials around peak 'a'. For all electrolyte solutions investigated (1-8.5 M KOH) when the anodic sweeps were allowed to proceed beyond the second current maximum ('b') the reverse sweeps exhibited features similar to figure 9-6 for all sweep speeds investigated.

Fig·9-6 Cyclic potential sweep; 1M KOH

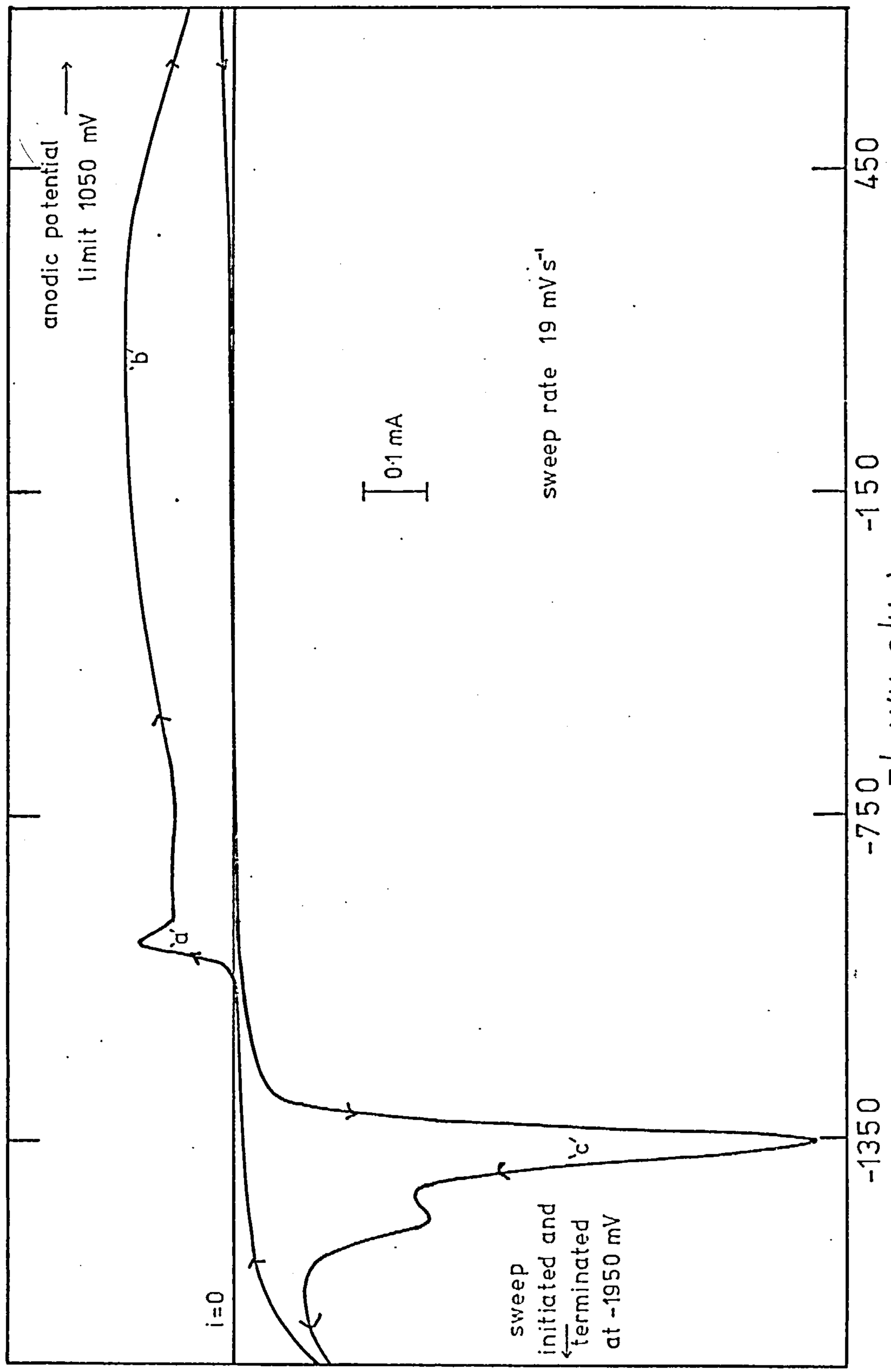

Fig·9-7 Effect of terminating the anodic-going sweep at a potential prior to peak 'b'; 8·5 M KOH

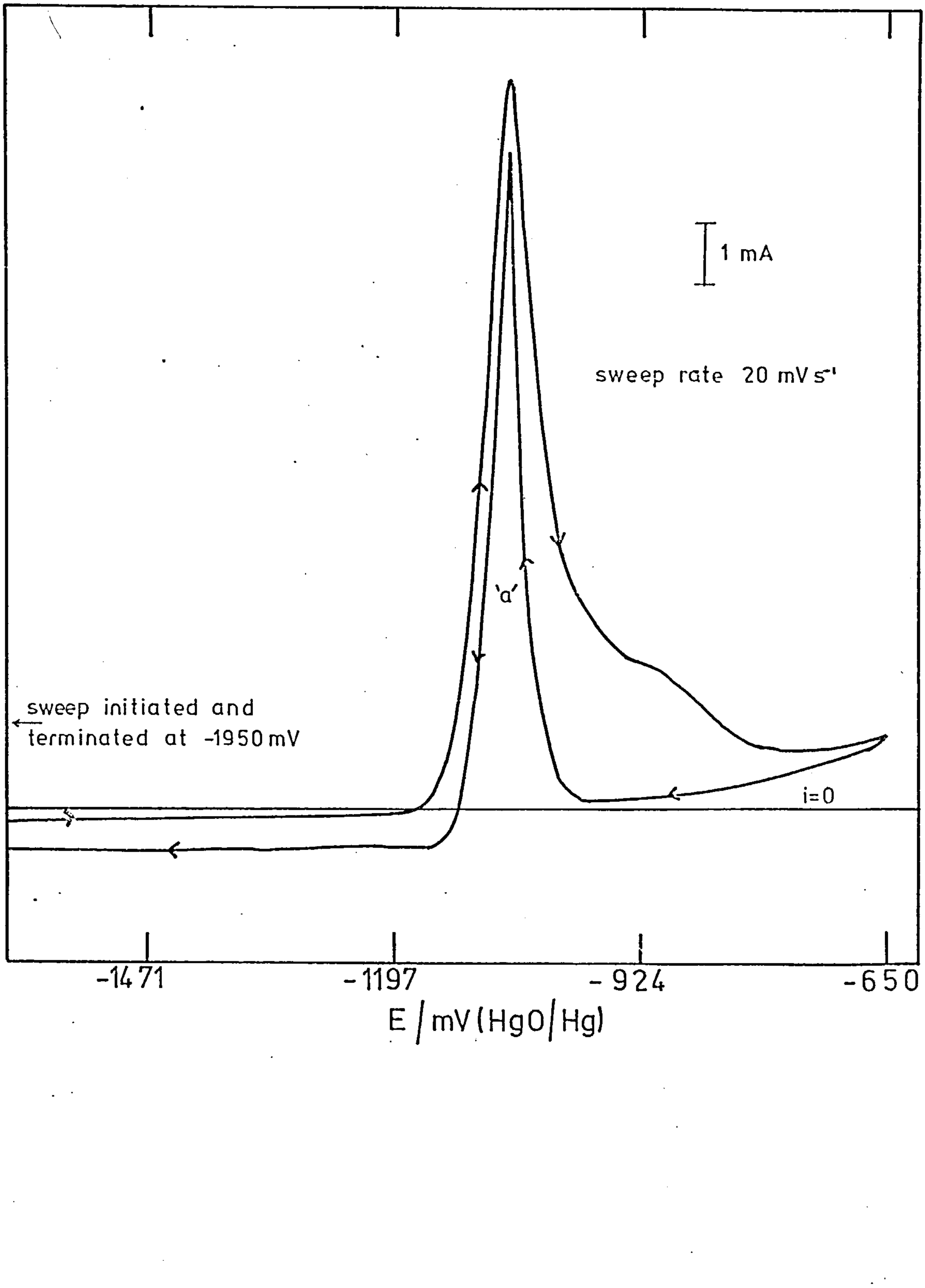

Fig.9-8 Effect on peak 'd' of terminating the anodic sweep at various potentials around peak 'a'; 1M KOH, sweep rate 31 mV s^{-1}

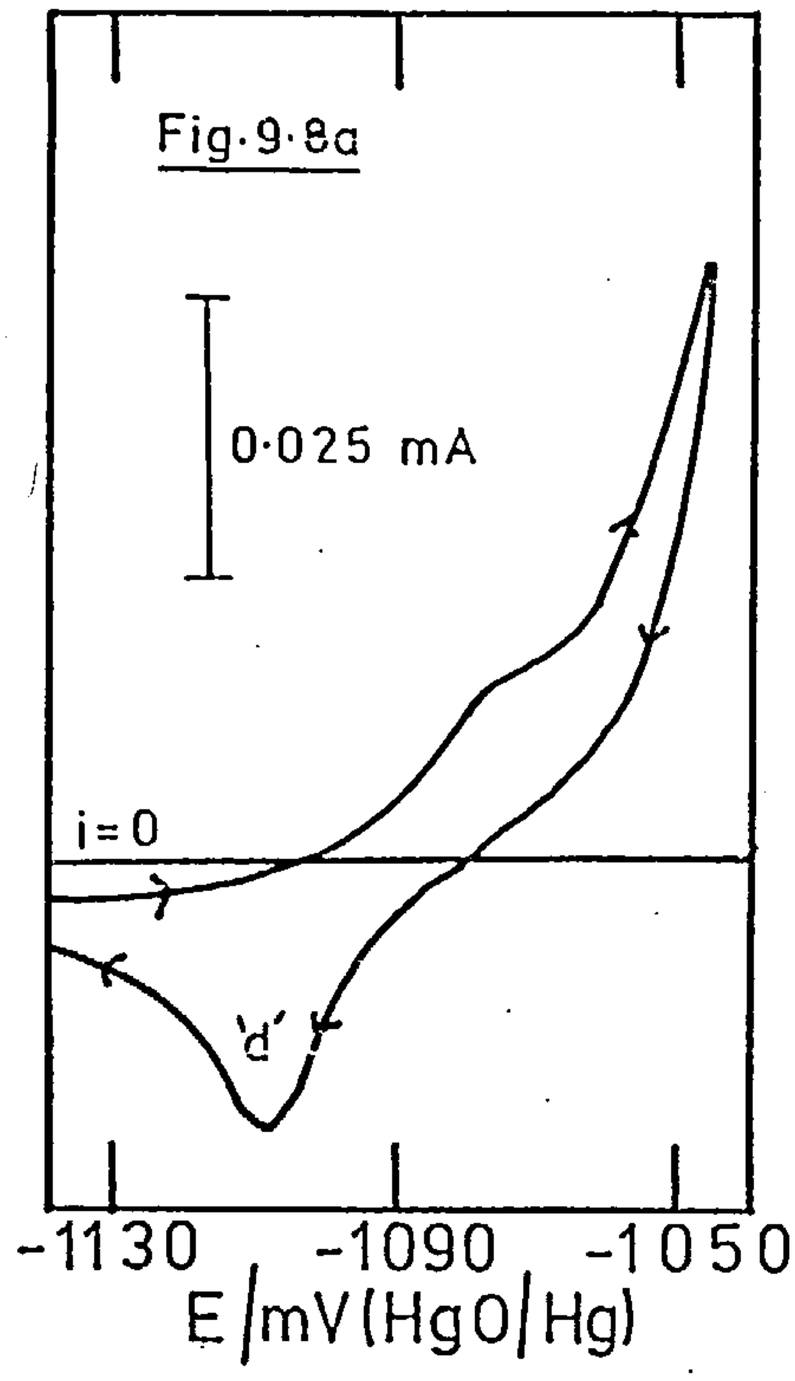

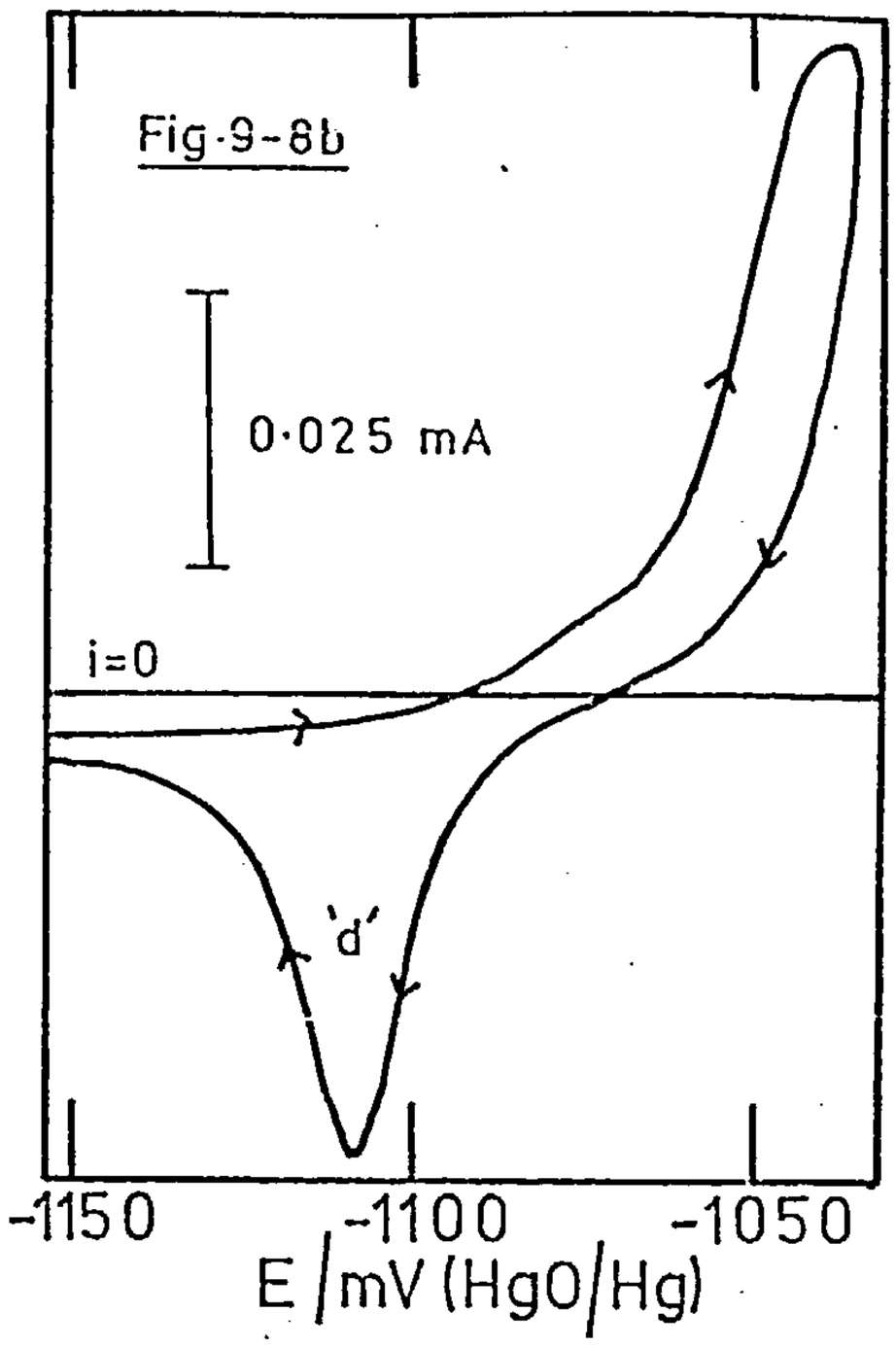

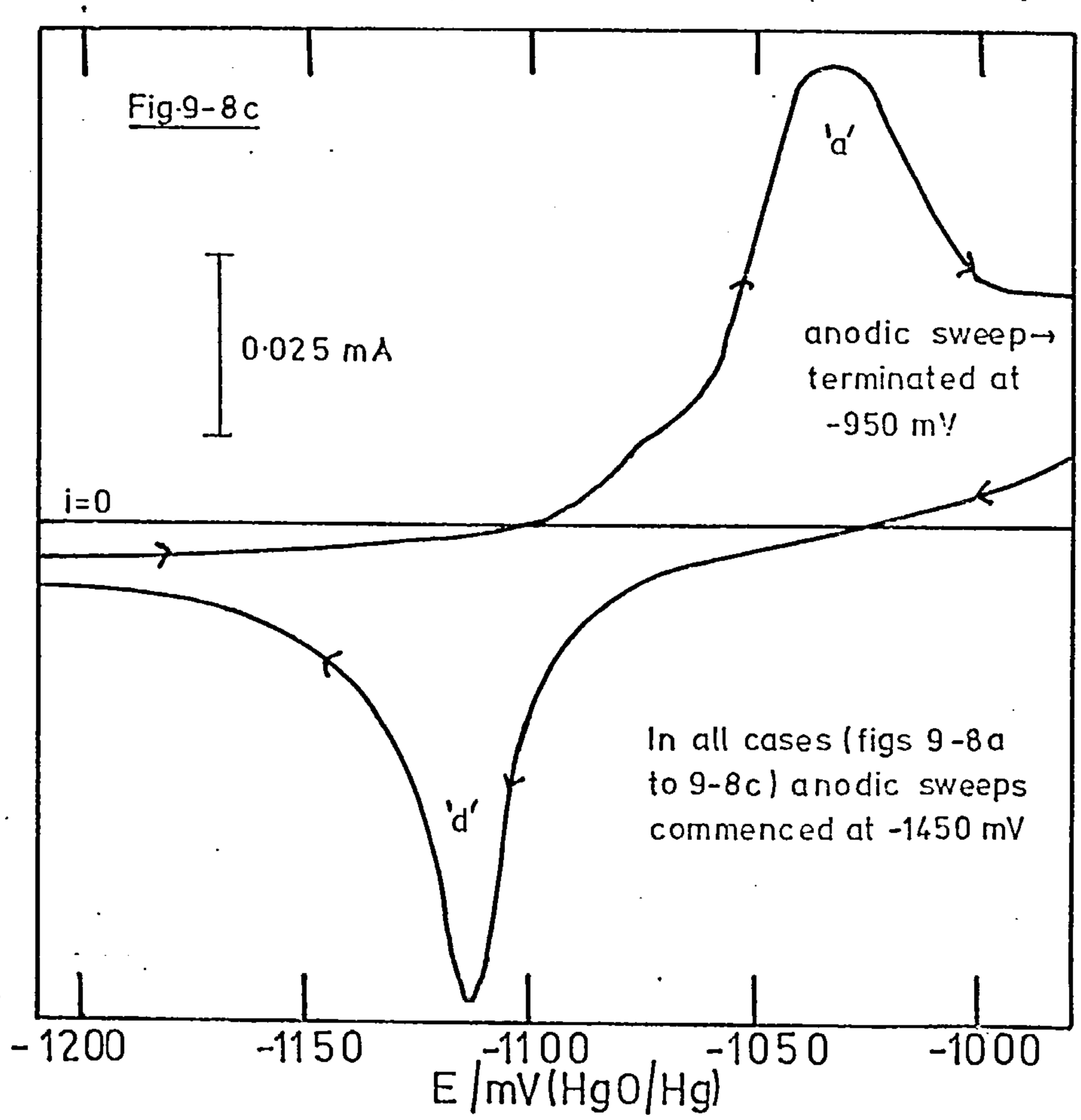

Figure 9-9 shows plots of passivating charge versus sweep rate for the first passivating process of the anodic sweep (peak 'a').

Figure 9-10 shows typical i^{-1} vs. $\omega^{-\frac{1}{2}}$ plots obtained for the anodic oxidation of indium in 8.5 M KOH solution. A rotation speed dependence of the currents was only obtained at the lower rotation speeds ($< \sim 700$ r.p.m.). For KOH concentrations less than 5 M a rotation speed dependence of the measured currents was not observed, even at the lowest rotation speeds investigated. Figure 9-11 shows the potential dependence of the slopes of the i^{-1} vs. $\omega^{-\frac{1}{2}}$ plots obtained for 8.5 M KOH; a straight line plot of slope $\sim$ 23 mV/decade being obtained. Figure 9-12 shows a family of Tafel plots obtained for the anodic dissolution of indium in a series of KOH electrolyte solutions, measurements being made at an electrode rotation speed of 2500 r.p.m. Strictly i_∞ values should be plotted (equation 2.37), but figure 9-12 shows that for 8.5 M KOH (where a rotation speed dependence of the measured anodic currents was observed) not too great an error arises by making measurements at a fixed, relatively high electrode rotation speed. (Armstrong et al[95] also used this approximate method to obtain current densities, corresponding to the charge transfer process, during their study of the anodic behaviour of indium in alkali). Figure 9-12 shows that for the systems investigated at 2500 r.p.m. Tafel slopes of 22-24 mV/decade are obtained, whereas the $\log_{10} i_\infty$ vs. potential plot for the 8.5 M KOH system has a slope of $\sim$ 26 mV/decade. Abstraction of $\log_{10} i$ vs. $\log_{10} a_{OH^-}$ data at a fixed potential gives a straight line plot with a slope $\left(\frac{\partial \log_{10} i}{\partial \log_{10} a_{OH^-}}\right)_E$ of 2.8. This slope

Fig.9-9 Plots of passivating charge vs. sweep rate for the first passivating process of the anodic sweep (peak 'a')

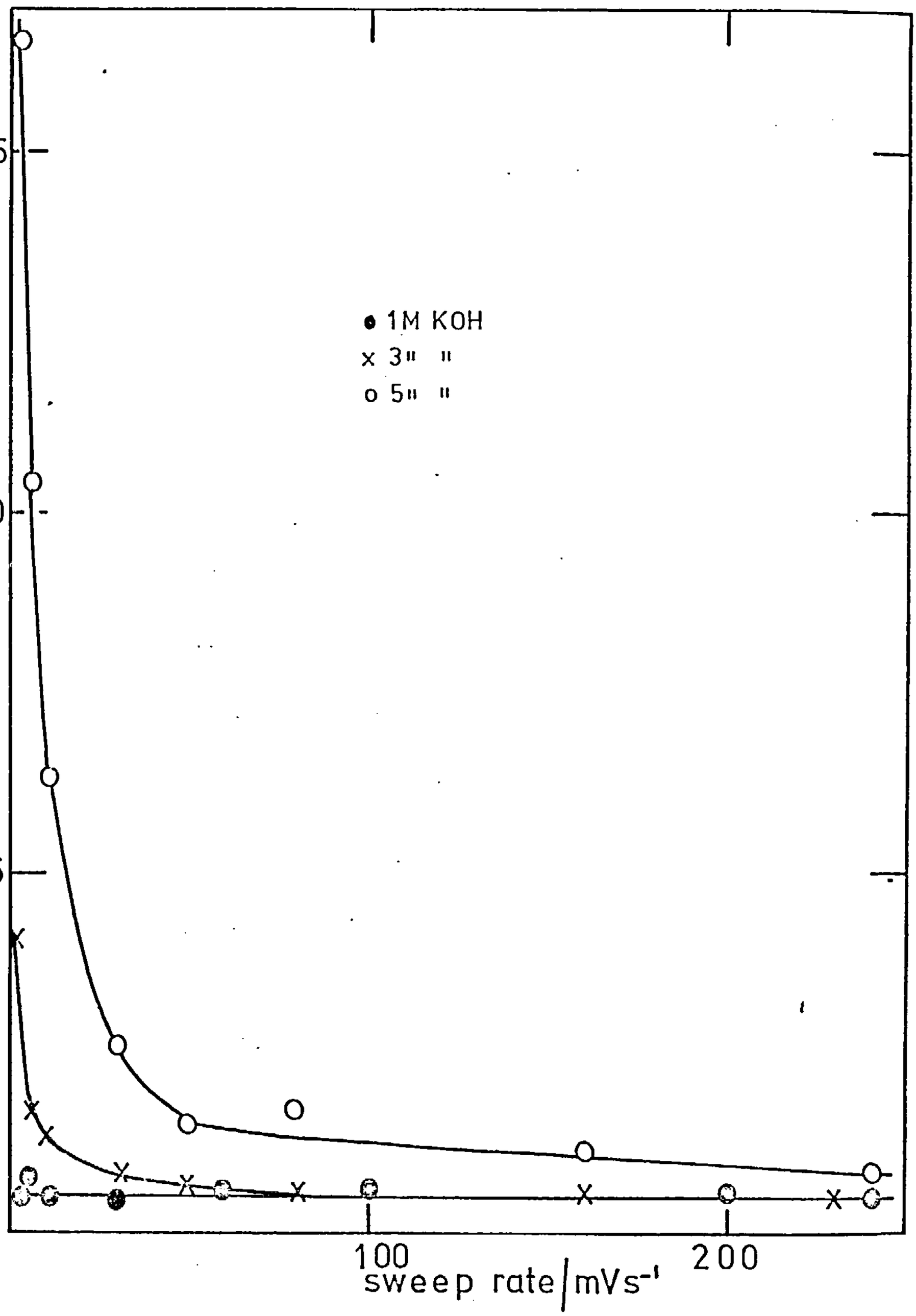

Fig.9-10 Typical i^{-1} vs. $\omega^{-\frac{1}{2}}$ plots at a series of anodic potentials; 8·5M KOH

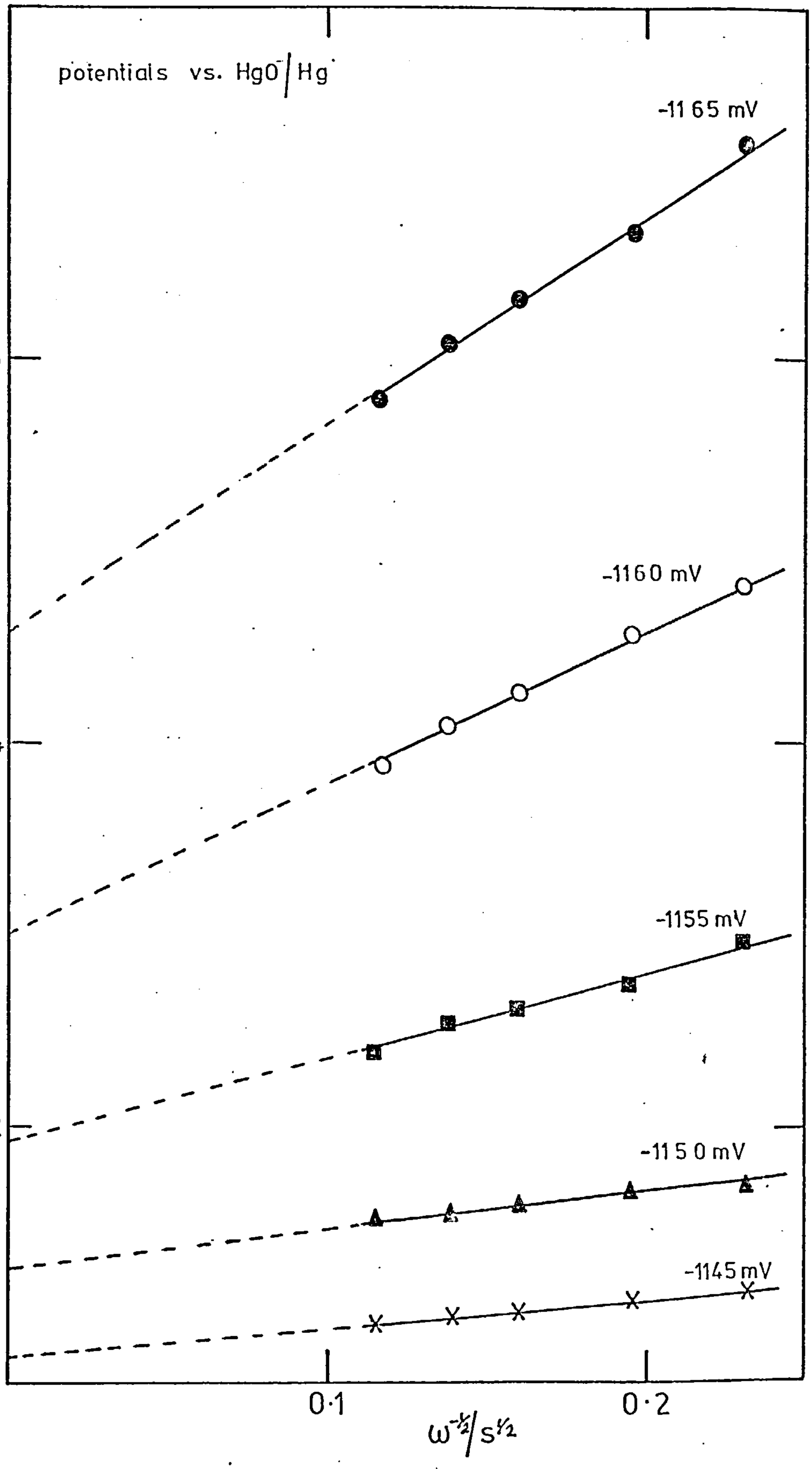

Fig. 9·11 Plot of $\log_{10}(\partial i^{-1}/\partial \omega^{-1/2})$ vs. anodic potential; 8·5 M KOH

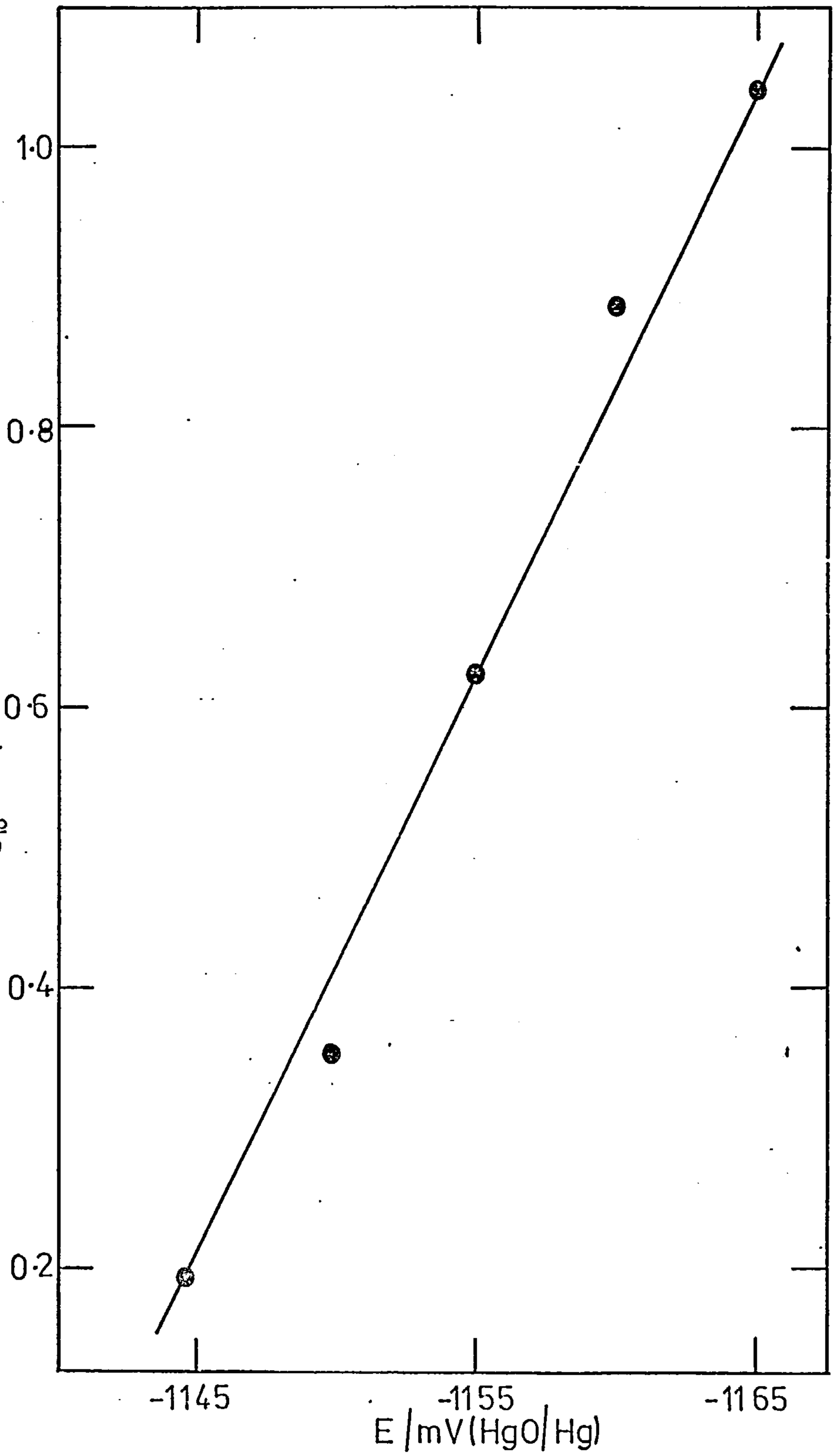

Fig. 9-12 Typical anodic Tafel plots; KOH electrolytes. Measurements made at an electrode rotation speed of 2500 r.p.m. Dashed line shows i_∞-potential data for 8·5 M KOH

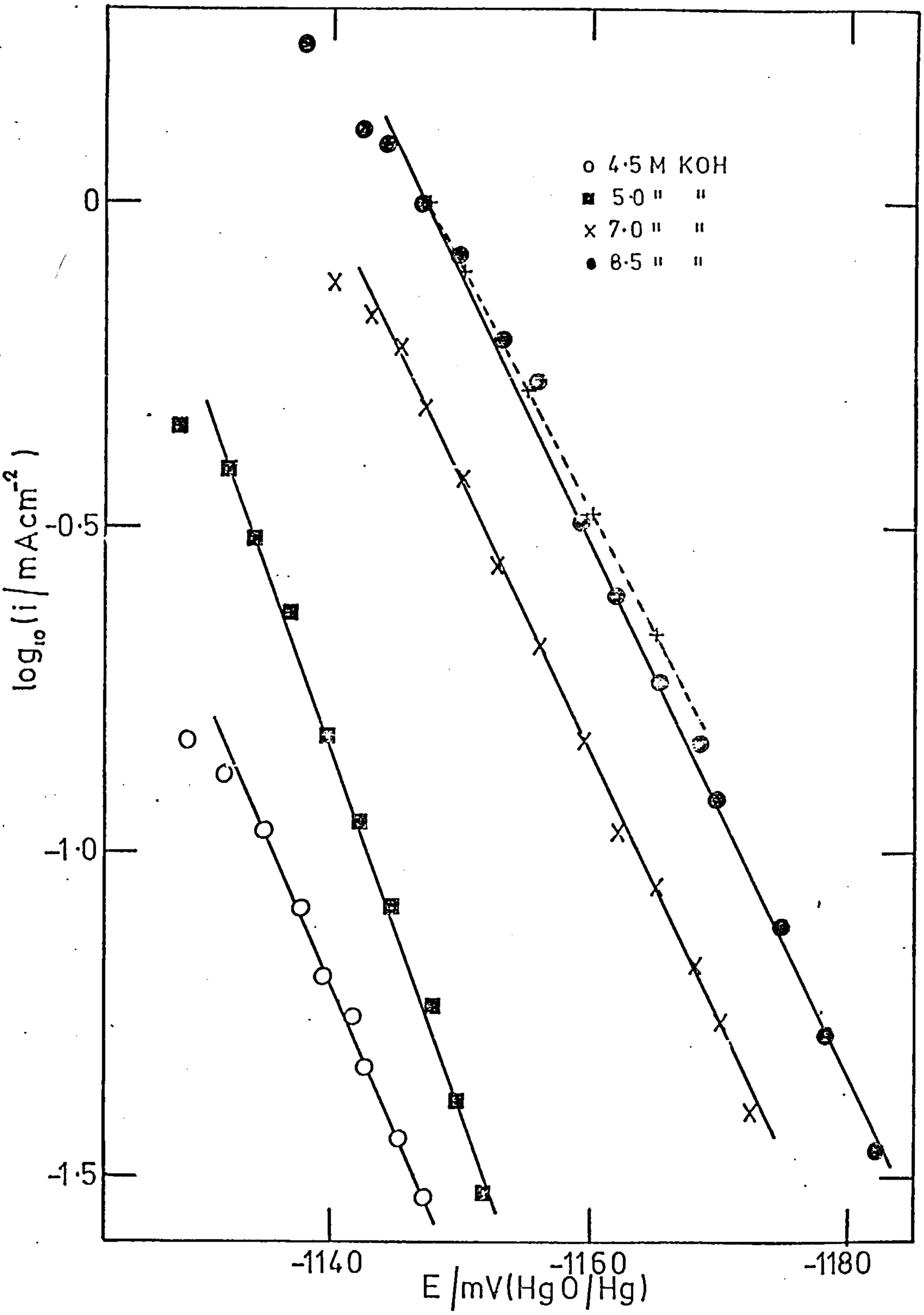

represents the anodic reaction order with respect to hydroxyl ions. The activities were calculated using the activity coefficient data of Robinson and Stokes[127].

9.4. Discussion

9.4.1. Galvanostatic polarisation studies

The general form of the polarisation curves (figures 9-1 to 9-3) agrees with those previously reported for indium in 4 M NaOH[93]. An initial arrest at ∿100 mV overpotential is followed by an abrupt rise in potential to a second plateau at ∿400 mV followed by a final transition at ∿2600 mV to the potential of oxygen evolution. In detail, however, the present investigation reveals some significant differences with previously reported curves under nominally similar conditions. The first potential arrest is much shorter in duration than anticipated from earlier work[93]. A difference between the work of Salem and Ismail[93] and the present work which may partly account for this, is that the present experiments were started immediately after electrode/electrolyte contact, whereas Salem et al commenced their experiments at the potential of hydrogen evolution. Due to the reported presence of corrosion region in the hydrogen region[98] this procedure was avoided. In a number of experiments the initial plateau could not be observed particularly at the higher rates of polarisation and with KOH electrolytes a first plateau at 100 mV could not be observed at all with the present experimental set up. The first plateau appears to be due to the formation of a solution soluble In(III) species of the type $In(OH)_x^{(3-x)+}$ according to the scheme

$$In \xrightarrow{-3e} In^{3+} \underset{}{\overset{*K_3}{\rightleftharpoons}} In(OH)^{2+} \overset{*K_2}{\rightleftharpoons} In(OH)_2^{+} \overset{*K_1}{\rightleftharpoons} In(OH)_3$$

The magnitudes[137] of each of the above *K values are all $\sim 10^{-2}$ and the solubility product for $In(OH)_3$, K_{sp}, 0.7×10^{-32}, thus it is to be expected that a first plateau, representing an anodic reaction in which a soluble product leaves the electrode, will rarely be observed in experiments on the time scale of the passivation experiments described here.

The plateau at $\sim$ 400 mV represents the formation of an insoluble layer, probably of $In(OH)_3$, at the electrode. This was confirmed in experiments in which unsuccessful attempts were made to reactivate passive electrodes by resting them in the electrolyte solution; once formed the passivating layer could not be removed by dissolution in the electrolyte solution. Cathodic polarisation of passivated electrodes enabled practically the whole of the passivating charge to be recovered before the potential fell to that corresponding to the hydrogen evolution reaction. Thus the amount of In(III) leaving the electrode is only very small, the majority remains as an insoluble film according to

$$In + 3OH^- = In(OH)_3 + 3e \qquad (9.1)$$

which occurs when the electrode system is passive for the solution reaction

$$In + 3OH^- = In(III)OH_x^{(3-x)+} + (3-x)OH^- \qquad (9.2)$$

The first transition from 100 mV to 400 mV can be regarded as a change in the electrode from one of the first kind (9.2) to an

electrode of the second kind (9.1).

The reduction in the overpotential often observed during the second plateau is interesting since few cases of such phenomenon have been recorded. Often such cases can be traced to a nucleation process, however, in the present case the time over which the reduction in overpotential is observed appears to be too long. A more likely explanation is in terms of the n-type semiconductor properties of indium oxide[138]. It is likely that during the formation of the passive hydroxide layer loss of molecules of water from the hydroxide occurs so that the semiconducting oxide In_2O_3 is produced[96] causing an increased conductivity of the solid phase forming at the electrode. During the early stages of polarisation, semiconducting oxide formation within the (mainly indium hydroxide) electrode film causes the effective conductivity of the electrode film to increase; ultimately the passivating film thickens and the electrode potential finally rises to that corresponding to oxygen evolution. Support for this theory comes from Faizullin and Amirkhanova[91], who as a result of galvanostatic and potentiostatic polarisation measurements in conjunction with electron diffraction studies, concluded that passivation of indium occurs as a result of a secondary surface oxide film situated directly on the metal under the $In(OH)_3$ film. These authors[91] determined the electrochemical parameters of the passivating film and proposed that it possessed a non-stiochometric composition, containing an excess of In^{3+} cations.

The mechanism of ultimate passivation by solid phase blocking of the electrode formed by film growth on the electrode surface is supported by the (negative) evidence that the passivation

data do not conform to diffusion control (figure 9-4), requiring that i vs. t_p data expressed in the form of i vs. $t_p^{-\frac{1}{2}}$ plots would give straight lines passing through the origin. For both lead and cadmium in alkali[139] films develop early in the anodic polarisation and consequently no simple relationship between passivation time and current density was observed for these metals. In contrast, the corresponding data for zinc[140] could be correlated in the form

$$(i - i_l)t_p^{\frac{1}{2}} = k_p$$

where i_l is the limiting current below which passivation does not occur. In this case soluble zincate is produced in the initial step when zinc undergoes anodic polarisation in alkali and passivation is due to an accumulation of zincate at the electrode causing a depletion of OH^- concentration which ultimately causes the zincate to precipitate as oxide or hydroxide. For the present case of indium no simple relationship between i and t_p was apparent for alkali concentration in the range 1 to 7 M. Usually i vs. $t_p^{-\frac{1}{2}}$ plots were straight lines only at higher current densities, at lower current densities the plots curved off towards the origin. In the cases even where a quasi-linear relationship was observed extrapolation gave meaningless intercepts on the $t_p^{-\frac{1}{2}}$ axis which could not be justified by any theory of mass transport in the solution phase.

The fact that no difference was observed in the form of the overpotential-time curves when different test electrode orientations were used (e.g. figs. 9-2 and 9-3) also indicates that relatively little solution reaction occurs. For a horizontal

upward facing anode the mass of electrolyte above the electrode eliminates convection currents, mass transport in solution being due only to diffusion. For a vertical electrode the additional mass transport mode of convection is evident. However in the present experiments the electrode orientation did not effect the polarisation data obtained.

9.4.2. Linear sweep voltammetric studies

The L.S.V. measurements show that active dissolution of indium in alkali occurs only over a relatively small potential range. Figure 9-5 shows that although an initial passivating process occurs ~-975 mV (peak 'a') this process does not completely inhibit the anodic reaction. Armstrong et al[95] have shown that as a result of X-ray diffraction studies the initial passivation is due to the formation of $In(OH)_3$ which is porous and hence a substantial current flows even at potentials positive to the peak 'a' indicating that the $In(OH)_3$ layer never becomes completely protective. It was further shown[95] that the secondary passivation (peak 'b') is due initially to the formation of InOOH, which is not completely protective and ultimately at more positive potentials to the formation of the much more protective In_2O_3. In accord with this when the positive-going sweep in 8.5 M KOH was terminated at a potential negative of peak 'b' (figure 9-7) the return curve showed the first anodic maximum (peak 'a'), clearly indicating that the initial passivating layer is not wholly coherent. Figure 9-7 also shows that at more negative potentials than peak 'a' no reduction peak is observed during the reverse sweep prior to hydrogen evolution for 8.5 M KOH electrolyte solution. The residual cathodic current observed at potentials negative to peak 'a' (figure 9-7) possibly

corresponds to the deposition of indium from dissolved indate. The fact that the occurrence of an anodic peak during the reverse sweep is dependent on the electrolyte concentration reflects the extent of solubility of $In(OH)_3$. The fact also that the magnitude of the anodic current maxima observed during the reverse sweep is inversely dependent on the sweep speed also indicates that a solution process is involved. Figures 9-8a to 9-8c show examples of a lower concentration alkali solution (1 M KOH), where an anodic peak is not observed during the reverse sweep. A reduction peak ('d') is evident at ν-1100 mV. It appears that due to the reduced solubility of $In(OH)_3$ a solution process is not in evidence during the negative-going sweep and reduction of $In(OH)_3$ occurs (peak 'd'). Figures 9-8a to 9-8c show that the magnitude of peak 'd' is dependent on the potential at which the forward sweep is terminated, clearly illustrating that the peak 'd' corresponds to the reduction of the initially passivating $In(OH)_3$. The extent of solubility of $In(OH)_3$ is shown also in figure 9-9, where the passivating charge corresponding to the peak 'a' is plotted as a function of sweep rate. At the higher sweep speeds the passivating charge tends to a constant value of 0.5 mC cm^{-2} (the charge necessary to obtain monolayer coverage of the electrode surface). For the 3 M and 5 M electrolytes as the sweep rate decreases the passivating charge increases showing that some diffusion in solution occurs at lower sweep speeds. The increased solubility of the electrode reaction product is shown by the increase in passivating charge at the lower sweep rates as the KOH concentration is increased. For 8.5 M KOH electrolyte solution the passivating charge is greatly increased with respect to the 5 M solution; for example at a sweep rate of 10 mV s^{-1} the passivating

charge in 8.5 M KOH is $\sim$90 mC cm^{-2} whereas for 5 M KOH the value is only $\sim$6 mC cm^{-2}.

In view of the potential interruption experiments it can be/concluded that the reduction peak 'c' (figure 9-6), which occurs at $\sim$-1400 mV during the reverse sweep when the secondary passivating process is allowed to occur, can be attributed to the reduction of the highly protective In_2O_3 layer formed at the more positive potentials during the positive-going sweep.

It is noteworthy that the initial passivating layer of $In(OH)_3$ is apparently formed by a dissolution-precipitation mechanism[85]; that is uninhibited dissolution of indium occurs until the solution in the vicinity of the electrode becomes saturated with the products of the electrode reaction, when precipitation occurs. Consequently Armstrong et al[95] claimed that the current peak due to initial passivation was increased by increasing the rotation speed of the electrode.

9.4.3. Mechanism of active dissolution

As previously described (section 9.3.2) a rotation speed dependence of the measured currents was not observed at KOH concentrations $\leqslant$ 5M. This agrees with the galvanostatic polarisation and L.S.V. studies in that for KOH concentrations $\leqslant$ 5M relatively little solution reaction occurs. In terms of equation 2.37 the value of K for such systems is very small. Figure 9-10 shows typical i^{-1} vs. $\omega^{-\frac{1}{2}}$ plots for indium in 8.5 M KOH. In this case equation 2.37 is obeyed. The potential dependence of the slope of the i^{-1} vs. $\omega^{-\frac{1}{2}}$ plots (figure 9-11) indicates that the indium species in equilibrium with the electrode is In(III). It has been reported that measurements using a ring-disc electrode[95] have shown

that over the potential range ~-1160 mV to about -1110 mV, the product of anodic dissolution of indium in alkaline electrolytes, during relatively short time experiments, is almost exclusively dissolved In(III).

Assuming a model with a single limiting step, the anodic Tafel slope of ~24 mV/decade (figure 9-12) gives rise to an α_a/α_k value of 5, which according to table 8.1 suggests that the rate determining step for the anodic reaction is the In(II)$\longrightarrow$In(III) + e reaction. Taking the order of reaction with respect to hydroxyl ions to be 3 (figure 9-13) the anodic reaction mechanism may be represented as:

$$In + OH^- \rightleftharpoons In(OH) + e \qquad (9.3)$$

$$In(OH) + OH^- \rightleftharpoons In(OH)_2 + e \qquad (9.4)$$

$$In(OH)_2 + OH^- \longrightarrow In(OH)_3 + e \qquad (9.5)$$

$$In(OH)_3 + OH^- \rightleftharpoons In(OH)_4^-{}_{(aq)} \qquad (9.6)$$

This scheme is in agreement with the reaction mechanism proposed by Armstrong and co-workers for both amalgam[86] and solid[95] indium electrodes in alkaline electrolytes. In the above mechanism (9.5) is the rate determining step, the stiochiometric number is one and hydroxide containing species other than $In(OH)_4^-$ and possibly $In(OH)_3$ are adsorbed intermediates on the electrode surface. The formation of $In(OH)_4^-$ (or $InO_2^- + 2H_2O$) is in accord with the thermodynamic data of Pourbiax[98].

Fig.9-13 Anodic order of reaction plot with respect to hydroxyl ions; KOH electrolytes

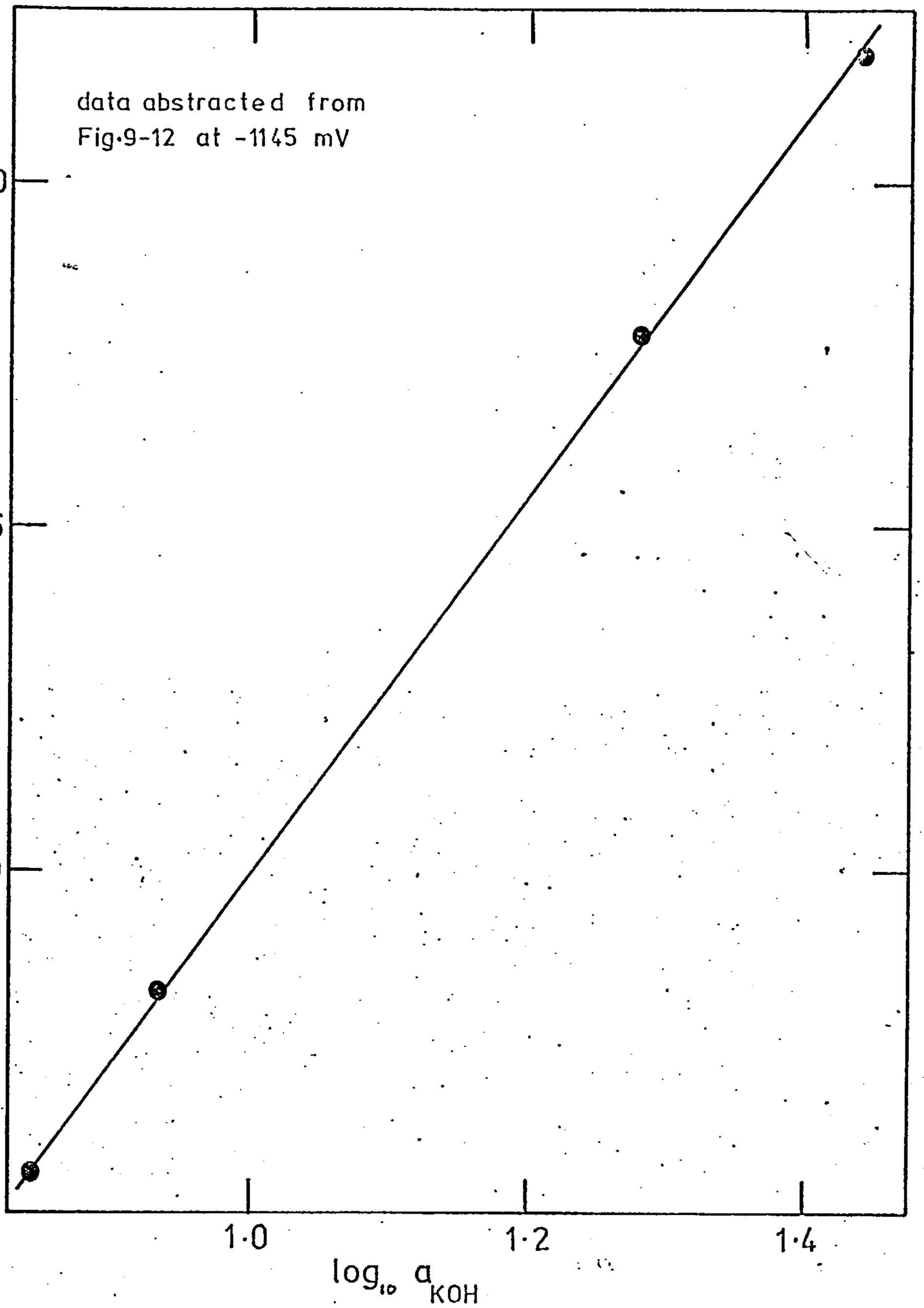

9.5. Conclusions

The anodic behaviour of solid indium in alkali is dominated by the development of a solid phase at the electrode. An interesting reduction in the potential observed during galvanostatic polarisation of indium is thought to be due to the formation of semiconducting In_2O_3 in the electrode product layer.

L.S.V. studies confirm previous work in that at least two passivating processes occur during the anodic reaction. Firstly the formation of porous $In(OH)_3$ and then at more positive potentials the formation of highly protective In_2O_3.

Active dissolution of indium in alkaline electrolyte solutions occurs only over a small potential range. It is concluded that a stepwise mechanism occurs in which the In(II)/(III) step is rate determining. The anodic reaction order with respect to hydroxyl ions is 3.

CHAPTER 10

FINAL DISCUSSION

10.1.Solution Conditions

The initial aim of this work was to isolate conditions suitable for studying the In/In(III) exchange reaction. Both differential capacitance (chapter 5) and equilibrium potential measurements (chapter 6) clearly indicate that the electrolyte solution pH must be kept relatively low in order to prevent the formation of electrode films and the hydrolysis of indium species in solution. Assuming a model whereby an ion in solution is surrounded by a hydration sheath, it is possible that a reaction can occur between the metal ion and a water molecule in the coordination sphere in which a proton is released and the solution becomes acidic, such a hydrolysis reaction is represented as

$$M(H_2O)_x^{n+} \rightleftharpoons M(H_2O)_{x-1}OH^{(n-1)+} + H^+_{(aq)} \qquad (10.1)$$

Hydrolysis is not necessarily confined to a single reaction step. It may lead to the replacement of more than one coordinated water molecule, hydrolysis continuing until the last coordinated water molecule is removed in the final step

$$M(H_2O)(OH)_{x-1}^{(n-x+1)+} \rightleftharpoons M(OH)_x^{(n-x)+} + H^+_{(aq)} \qquad (10.2)$$

Thus a series of equilibria exist in solution, each step involving the transfer of a single proton. The process sometimes involves the

production of an insoluble compound at some stage in the hydrolysis reaction. This occurs most frequently at the stage when the number of hydroxo-groups present is equal to the charge on the metal ion and the metal hydroxide is precipitated:

$$M(H_2O)_{(x+1-n)}\ (OH)^{+}_{n-1} \longrightarrow M(OH)_n + (x-n)H_2O + H^{+}_{(aq)} \quad (10.3)$$

For a number of metal ions the precipitate may be better represented as a hydrated oxide, for example the product of the precipitation of Fe^{3+} is $Fe_2O_3.H_2O$ with some FeO(OH) present also. The hydrolysis reaction should occur most readily with metal ions which strongly polarise the coordinated water molecules and facilitate the release of the proton. The polarising power of the cation increases with increasing charge and decreasing size of the cation, thus the fact that hydrolysis of the In(III) species occurred relatively readily (chapter 6) is not too surprising. The position of the equilibrium of the hydrolysis reaction will be displaced by changing the concentration of any of the species present. Thus addition of acid will drive the equilibria towards the simple aquo form, so that with acid solutions of metal ions hydrolysed species are avoided, a premise followed during the study of the equilibrium potential of the indium electrode in aqueous chloride media (chapter 6).

The fact that electrode films and solution hydrolysis are so pronounced with indium is not, as previously stated, entirely unexpected since indium hydroxide is highly insoluble (2.2×10^{-9} mol/litre H_2O[117]). Metal hydroxides of low solubility have a solubility product $K_{sp} = a_{M^{n+}} \cdot a^{n}_{OH^-}$ * and the maximum pH of the

---

* Footnote: the activities mentioned here are strictly mean ionic activities.

solution before precipitation occurs will depend on the concentration of the metal ion and the solubility product. The a_{OH^-} may be replaced by K_w/a_{H^+}, where K_w is the ionic product for water, thus giving for K_{sp}

$$K_{sp} = a_{M^{n+}} \cdot \left(\frac{K_w}{a_{H^+}}\right)^n \qquad (10.4)$$

taking logs and rearranging (10.4) leads to

$$\frac{1}{n} \log_{10} K_{sp} = \frac{1}{n} \log_{10} a_{M^{n+}} + \log_{10} K_w - \log_{10} a_{H^+} \qquad (10.5)$$

thus

$$pH = \frac{1}{n} \log_{10} K_{sp} - \frac{1}{n} \log_{10} a_{M^{n+}} - \log_{10} K_w \qquad (10.6)$$

The solubility product decreases with increasing charge on the cation, so that, for a given metal-ion concentration, (10.6) predicts that precipitation occurs at lower pH the higher the charge on the cation. Table 10.1 illustrates this and clearly shows that the difficulties of solution hydrolysis and film formation encountered with indium in the present work are due to the relatively low pH of precipitation of $In(OH)_3$ from aqueous solutions.

Table 10.1 (continued overpage)
Solubility product and pH of precipitation of selected metal ions (0.01 mol dm^{-3}) as hydroxides

	$K_{sp}/(mol^3 dm^{-3})$	$K_{sp}/(mol^4 dm^{-12})$	$K_{sp}/(mol^5 dm^{-15})$	pH of precipitation
Mg^{2+}	1.3×10^{-10}			10.0
Ca^{2+}	1.0×10^{-17}			6.5
Fe^{2+}	1.0×10^{-14}			8.0
Cu^{2+}	5.0×10^{-19}			5.5
Al^{3+}		3.7×10^{-15}		9.8

	$K_{sp}/(mol^3dm^{-3})$	$K_{sp}/(mol^4dm^{-12})$	$K_{sp}/(mol^5dm^{-15})$	pH of precipitation
Cr^{3+}		6.7×10^{-31}		4.8
In^{3+}		$\sim 10^{-33}$		$\sim$ 3.4
Fe^{3+}		1.0×10^{-38}		2.1
Ti^{4+}			7.9×10^{-54}	1.2

In order to suppress hydrolysis and the formation of films on indium electrodes it was usually found necessary to lower the electrolyte pH by the addition of acid. However, the added acid in some instances caused inherent complications. For equilibrium potential measurements with indium trichloride solutions the added acid caused difficulties in the data treatment, since no satisfactory theory of activity coefficients exists for mixed electrolytes of differing valency types. It was therefore found necessary to adopt a number of approximate extrapolation procedures in order to abstract values of $E^{\ominus}$. The results obtained (chapter 6) show clearly that the $E^{\ominus}$ value depends on the extrapolation procedure used. Hydrogen ions were also found to have a pronounced effect on the kinetics of the dissolution reaction (chapters 7 and 8), in that the In(I) ion, concluded to be a participant in the anodic reaction, can be oxidised by available hydrogen ions in solution. Consequently in perchlorate media the anodic reaction mechanism was found to be dependent upon the balance of the rates of oxidation of In(I) by either an electrochemical reaction or chemically by reaction with hydrogen ions. In chloride media a similar phenomenon was observed, however an extra complication arose due to the accelerating effect of chloride ions on the electrochemical In(I)/ In(III) oxidation step.

10.1.1 Complex-ion formation

Complex formation in solution is important as it may have an influential effect on the course of the electrode reaction. In addition to hydrolysis reactions, complex formation arises as a result of the replacement of water molecules in the coordination-sphere of aquated ions. The replacement reactions can be represented by a series of equilibria in which one water molecule is replaced by an ionic species in each step:

$$M(H_2O)_x^{n+} + X^- \rightleftharpoons M(H_2O)_{x-1}X^{(n-1)+} + H_2O \qquad k_1$$

$$M(H_2O)_{x-1}X^{(n-1)+} + X^- \rightleftharpoons M(H_2O)_{x-2}X^{(n-2)+} + H_2O \qquad k_2$$

$$M(H_2O)X_{x-1}^{(n-x+1)+} + X^- \rightleftharpoons MX_x^{(n-x)+} + H_2O \qquad k_x$$

Each step is an equilibrium process with an equilibrium constant k_n (stepwise formation constant). The formation constant k_1 will be of the form

$$k_1 = \frac{a_{MX^{(n-1)+}}}{a_{M^{n+}} \cdot a_{X^-}} \qquad (10.7)$$

In (10.7) the number of water molecules in the hydration sphere is omitted. The size of the stepwise formation constant is a measure of the amount of a given complex species in solution. This is obviously dependent upon the properties of the metal ion and the ligand (X^-). In general the size of the formation constant

increases with increasing charge and decreasing size of the cation. In addition, for a given cation the smaller F^- ion usually produces a more stable complex than the larger Cl^- ion. It is noteworthy that the large ClO_4^- ion has very little tendency to form complex ions. It would be expected that due to its high charge and small size the In^{3+} ion would have a tendency to form relatively stable complexes in some aqueous solutions.

It has been reported[129] that in perchlorate media indium does not form complexes by coordination with perchlorate ions. However, there is considerable evidence that partially hydrolysed aquo-indium complexes exist in perchlorate electrolytes[64,65,71,80]. These complexes are particularly in evidence during the cathodic reaction at an indium electrode in perchlorate electrolytes where under conditions of low pH partial dehydration of $[In(H_2O)_5OH]^{2+}$ on the electrode surface is apparently the rate determining step.

There is ample data to suggest that indium forms halide complexes[117]. During the anodic dissolution of indium in chloride electrolytes it is claimed that the In(III) complex $[InCl_2]^+$ is formed. It has been further shown that addition of Cl^- ions to perchlorate solutions increases the apparent valence of dissolving indium in comparison with that for perchlorate solutions, the reversible indium electrode potential being determined by the concentration of $[InCl_2]^+$. These observations are of considerable inportance as they suggest that In(III) is stabilised in chloride electrolytes due to the formation of chloro-complexes, alternatively In(I) species are destabalised in chloride electrolytes due to the preferential formation of In(III) chloro-complexes. This conclusion is supported by the differences in behaviour of the indium electrode in chloride

and perchlorate electrolytes. Equilibrium potential measurements in chloride electrolytes (chapter 6) show that reversibility of the In/In(III) system is observed over a wide pH range, whereas in perchlorate electrolytes at pH's < 2 the indium electrode potential is apparently determined by the In/In(I) couple. Also in making kinetic measurements at low anodic overpotentials in chloride electrolytes (chapter 8) In(III) species were shown to be in equilibrium with the electrode, whereas for perchlorate electrolytes (chapter 7) at low anodic overpotentials In(I) species were in equilibrium with the electrode.

It is important that perchloric acid is frequently used to prevent hydrolysis of metal ions since its use avoids the added problem of the formation of complexes between the metal ion and the anion of the acid. However, during the present work perchloric acid was used to suppress hydrolysis only when the electrolyte was of a perchlorate base. The main reason for this choice was that, as described above, perchlorate ions apparently effect the In/In(III) equilibrium, a factor found to be of particular importance when studying the equilibrium potential of the In/In(III) system.

10.2 Nature of the Electrode Surface

For the case of electrode reactions at solid metal electrodes, in addition to solution processes and the charge transfer step(s), the additional problems of the exchange of metal atoms with the crystal lattice exist. Incorporation of a metal atom into a metal lattice is thought to occur by one of two mechanisms:

(i) diffusion of the metal ion in solution to a point opposite a growth site (kink site) in the lattice, followed by charge transfer

and incorporation into the lattice.

(ii) charge transfer and incorporation of adspecies at a point of low coordination on the metal surface followed by diffusion across the surface to a kink site (point of higher coordination). Mechanism (i) necessitates a major loss of the hydration sheath in one stage, whereas in mechanism (ii) the hydration sheath is discarded in stages. Conway[141] considers that the mechanism involving diffusion in solution, followed by direct incorporation at a growth site, is unlikely for both statistical and energetic reasons. Oriani and Frankenthal[142] have shown that whether or not surface diffusion of adspecies can control the rate of the overall electrode process depends on the ratio of the mean free path for diffusion to the mean distance between kink sites.

For the case of mercury or a liquid amalgam the electrode surface is smooth and homogeneous and consequently metal atoms can be incorporated at any point on the electrode surface since all points are equivalent. For a soft, low melting point metal such as indium (melting point $\sim 156^{\circ}C$) the metallurgical properties are expected to be similar to those of mercury in that a large percentage of the atoms in the metal lattice are labile. It would therefore be expected that electrocrystallisation effects for indium are negligible. This is in accord with the present work where no such complications were observed under any experimental conditions.

10.3 The Charge Transfer Process

For a metal M in contact with a solution containing simple ions M^{n+} of the metal M, the overall electrode process, involving multiple electron transfer, may be written as

$$M = M^{n+} + ne \qquad (10.8)$$

Many workers have tended to consider (10.8) as a simple one-step process which does not involve the formation of low valence intermediates of M.

One of the earliest studies in which the stepwise nature of reactions of type (10.8) was proposed is due to Kabanov and co workers[143,144], who studied the anodic dissolution of iron in alkaline solutions

$$Fe + 2OH^- = Fe(OH)_2 + 2e \qquad (10.9)$$

In explaining the experimental results[144] it was assumed that an initial one-electron step proceeds under quasi-equilibrium conditions, leading to the formation of an intermediate surface compound $Fe(OH)_{ads}$:

$$Fe + OH^- = Fe(OH)_{ads} + e \qquad (10.10)$$

followed by a second, rate controlling step

$$Fe(OH)_{ads} + OH^- = FeO_{ads} + H_2O + e \qquad (10.11)$$

and then a fast chemical reaction involving FeO_{ads} resulting in the eventual formation of a $Fe(OH)_2$ precipitate. Conway and Bockris[145,146], for the reaction $Cu = Cu^{2+} + 2e$, calculated the approximate realtive free energies of the transition states for the various steps of the overall reaction. It was found that for the one-step

discharge of Cu^{2+} ions, the activation energy is much greater than for a stepwise process involving the formation of Cu^{+} ions. In the case of $Ni = Ni^{2+} + 2e$ such calculations were found to be more difficult since stable Ni^{+} ions do not exist in solution. Losev[26] has recently, comprehensively, reviewed the theoretical principles and experimental criteria for stepwise mechanisms and the salient theoretical features of Losev's work are given in appendix 2.

10.3.1. Choice of model for the charge transfer process

For the case of indium, in which the most stable solution species is In(III), the possibility that low valence intermediates participate in the electrode reactions should be considered. The work in this thesis, pertaining to the kinetics of the anodic dissolution of indium in various electrolyte solutions, has been interpreted in terms of a model involving a stepwise charge transfer process with a single rate-limiting step. For such a model it follows that $\alpha_a + \alpha_k = n$, a very useful premise, since for the case of indium it is difficult to obtain data on the cathodic side by purely electrochemical means and hence abstract a value for α_k. (A value of α_k could in principle be obtained by studying the dependence of the exchange current density on the concentration of an indium amalgam electrode at constant In(III) concentration). It is possible that the reaction could occur via a mechanism involving comparable rate constants for successive steps, in which case the premise that $\alpha_a + \alpha_k = n$ no longer holds. For such a reaction scheme, for the situation where $n = 3$, the apparent transfer coefficient sum is given by $\alpha_a + \alpha_k < 2$, clearly indicating that if such a model is in evidence an experimental determination of α_k must be made.

The experimental data obtained in the present investigations could be adequately explained in terms of a single limiting step model. Justification for this choice of model comes from the work of Molodov and Losev[69]. These authors[69], on the basis of radiochemical measurements on indium amalgams in perchlorate electrolytes, obtained a value for α_k of 0.91, which on coupling with an α_a value of 2.20 (obtained from anodic polarisation measurements on identical systems) gives a transfer coefficient sum close to $n(\alpha_a + \alpha_k = 3.11)$, thus confirming that the single limiting step model is applicable.

10.3.2 Causes of relative slowness of the last charge-transfer step

During the present studies the last step of the charge transfer process was invariably found to be rate determining, viz; for the anodic reaction in perchlorate electrolytes the $In^{+} \longrightarrow In^{3+} + 2e$ step was rate determining at the higher potentials or higher pH's when reaction of hydrogen ions with the In(I) species was suppressed. In chloride electrolytes the $In^{+} \longrightarrow In^{3+} + 2e$ was also rate determining. Foractive dissolution of indium in alkaline electrolytes the results indicated that the $In^{2+} \longrightarrow In^{3+} + e$ step was rate limiting.

It is interesting to consider the causes of the small rate of the final charge transfer step. An analysis[26] of available kinetic data for reactions of type (10.8) has clearly shown that the exchange current density tends to decrease with increasing valence of the cations, this decrease being accompanied by a considerable increase in the activation energy of the electrode process and in the free energy of hydration of the corresponding cations.

The hydration energy, ΔH_s, of ions of a given element in different oxidation states increases as the charge of the cation increases. Since ΔH_s is approximately proportional to the square of the ionic charge, the change in ΔH_s for a given ion upon an increase of charge by one, is greater, the greater the charge of the initial cation[147]. Although the activation energy is only a small part of ΔH_s, for the corresponding cation, it is known that the activation energy is largely due to the change in the structure of the hydration sheath following the change in the charge of the reacting particle.[145,146].

It appears therefore, that for a stepwise process the fact that the limiting stage is the final step is due to the very large differences in ΔH_s for cations taking part in the last step of the reaction sequence. For earlier steps, the difference should be very much smaller. Since univalent ions are more weakly hydrated, the step $M = M^+ + e$ usually requires only a relatively low activation energy, thus in comparison with subsequent charge-transfer steps this initial step is often a quasi-equilibrium process.

An important implication of the fact that the last step in the reaction scheme was found to be rate determining is that the electrode serves only as a source or sink of electrons for this step. Consequently metallurgical effects involving the electrode surface, as outlined in section 10.2, are of little importance. Support for this deduction comes from the fact that kinetic parameters determined for solid indium and indium amalgam electrodes are very similar in magnitude[26]. With respect to the $M = M^+ + e$ step, the kinetic parameters can be quite different for solid and amalgam surfaces[26]. However, owing to its relatively high rate,

the $M = M^+ + e$ step is often practically reversible and hence should not effect the kinetics of the overall process.

10.4. The Indium Electrode in Alkali-Possible Applications to the Energy Conversion Field

Although indium has some advantages over metals such as zinc or cadmium as a potential anode material for primary alkali batteries, it has serious disadvantages which preclude its use for such applications. In view of its higher hydrogen overvoltage, indium should have a lower open circuit corrosion rate than zinc, a definite advantage since this corrosion process seriously limits the life of zinc/alkali cells. A further advantage is that the discharge curves obtained for indium in alkali are appreciably flatter than those obtained with zinc, especially at low temperatures. Unfortunately when an indium/alkali cell is short circuited (passivation of the indium electrode occurs) the indium electrode does not reactivate on open circuit, a phenomenon illustrated in the present work during galvanostatic polarisation measurements (chapter 9). It was found that passive electrodes could not be reactivated by resting in the electrolyte solution; only when the passivated electrodes were cathodically polarised could the majority of the passivating charge be recovered. Further disadvantages are that indium is reported[95] to severely polarise at current densities greater than about 2.5 mA cm^{-2} and in addition, whilst active, a solid anodic product is formed during discharge and this product is extremely bulky. Other, more obvious, disadvantages of indium as a potential electrode material for commercial applications are its cost and the fact that the metal is very soft and therefore

difficult to handle.

The reason why indium fails to recover satisfactorily when the cell is short circuited appears to be due to the very negative potential ($\sim$ -1.40 V (HgO/Hg)) required for the reduction of the protective In_2O_3 film (chapter 9). If indium is alloyed with bismuth the protective properties of all the passivating layers formed on indium are reduced[95]. $Bi(OH)_3$ is formed at $\sim$ -0.30 V (HgO/Hg) and is reduced at $\sim$ -0.59 V (HgO/Hg) and it is thought that these processes could account for the partial disruption of the In_2O_3 layer in the presence of bismuth. The formation of less protective layers allows the Bi/In alloy to sustain high currents to much more negative potentials than does pure indium; it also accounts for the greater speed of recovery of the alloy electrodes after the cell has been short circuited.

Even though alloying bismuth with indium improves the discharge performance of the cells, the use of such alloys does not significantly effect the amount of solid product formed during discharge and in addition In/Bi alloys appear to corrode more rapidly than pure indium[95].

10.5 Further Work

Relatively little work has been reported concerning the electrochemistry of solid indium, consequently many interesting areas of electrochemical research remain uninvestigated. The following are topics highlighted by the present work as being potentially interesting:

1. The kinetics of the electrode reaction in various electrolytes should be investigated using indium amalgam electrodes. From

a study of the dependence of i_o on the amalgam concentration it should be possible to confirm, unequivocally, that the single limiting step model of charge-transfer, adopted in the present work, is the correct choice.

2. A more thorough investigation of the NO_3^-/NO_2^- reduction at an indium electrode should prove to be of interest. One possible approach would be to use linear sweep voltammetry in order to study the oxidation and reduction processes involved.

3. A comparison of the effect of the various halide ions on the anodic reaction of solid indium would be of interest. This investigation should include the effect of halide ions as additives to perchlorate media and also the behaviour in pure F^-, Br^- and I^- containing electrolytes.

4. A rotating ring-disc study of the anodic behaviour of indium in acidic media may yield information regarding the apparent non-participation of the In^{2+} ion under conditions of low pH.

REFERENCES

1. T.L. BOSWELL, J. Electrochem. Soc., 105 (1958) 239.
2. A.P. PCHEL'NIKOV and V.V. LOSEV, Zash. Metal., 1 (1965) 482.
3. R.E. VISCO, J. Electrochem. Soc., 112 (1965) 932.
4. L. HEPLER, Z.Z. HUGUS and W.M. LATIMER, J. Amer. Chem. Soc., 75 (1953) 5652.
5. G. BIEDERMANN and T. WALLIN, Acta. Chem. Scand., 14 (1960) 594.
6. W.M. SPICER and C.J. BANICK, J. Amer. Chem. Soc., 75 (1953) 2268.
7. H. HELMOLTZ, Wied. Ann., 7 (1879) 377.
8. A. GOUY, J. Phys., 9 (1910) 457.
9. D. L. CHAPMAN, Phil. Mag., 25 (1913) 475.
10. O. STERN, Z. Elektrochem., 30 (1924) 508.
11. D.C. GRAHAME, Chem. Revs., 41 (1947) 441
12. M.A.V. DEVANATHAN, J. O'M BOCKRIS and K. MÜLLER, Proc. Roy. Soc, London, A274 (1963) 55.
13. D.C. GRAHAME, J.Chem. Phys., 21 (1953) 1054.
14. R. PAYNE, J. Electroanal. Chem., 41 (1973) 277.
15. A. N. FRUMKIN, Svensk. Kemish, Tidskrift, 77 (1965) 300.
16. A.N. FRUMKIN, J.Res. Inst. Catalysis, Hokkaido Univ., 15 (1967) 61.
17. W.A. CASPARI, Z. Physik. Chem., 30 (1899) 89.
18. T. ERDEY-GRUZ and M. VOLMER, Z. Phisik. Chem., 105A (1930) 203
19. R.A. MARCUS, J. Phys. Chem., 67 (1963) 853.
20. K.J. VETTER, Z. Physik. Chem., 194 (1950) 284.
21. K.J. VETTER, Z. Elektrochem., 56 (1952) 931.
22. J. TAFEL, Z. Physik. Chem., 50 (1905) 641.
23. J.A.V. BUTLER, Proc. Roy. Soc., 157A (1936) 423
24. T. BERZINS and P. DELAHAY, J.Amer. Chem. Soc., 77 (1955) 6448.
25. J.E.B. RANDLES, Trans. Farad. Soc., 48 (1952) 828.

26. V.V. LOSEV, Modern Aspects of Electrochemistry, Vol. 7, Ed. B.E. Conway and J.O'M Bockris. Butterworths (1972) p.314.

27. B. LEVICH, Acta. Physicochim. URSS, 17 (1942) 257.

28. J.A. HARRISON and H.R. THIRSK, Guide to the Study of Electrode Kinetics, Academic Press, (1972).

29. W. NERNST, Z. Physik. Chem., 47 (1904) 52.

30. J.E.B. RANDLES, Disc. Farad. Soc., 1 (1947) 11.

31. J.E.B. RANDLES, Trans. Farad. Soc., 48 (1952) 951.

32. E. WARBURG, Ann. Physik., 67 (1899) 493; 6 (1901) 125.

33. M. SLUYTERS-REBACH, D.J. KOOIJMAN and J.H. SLUYTERS, Polarography, Ed. G.J. Hills, MacMillan Press, (1964), p. 143.

34. P. DELAHAY and T.J. ADAMS, J. Amer. Chem. Soc., 74 (1952) 5740.

35. H. GERISCHER, Z. Physik. Chem., 202 (1953) 302.

36. K.J. VETTER, Z. Physik. Chem., 199 (1952) 285.

37. J.H. SLUYTERS, Rec. Trav. Chim., 79 (1960) 1093.

38. A.J. GOSS and E. VERNON, Proc. Phys. Soc., 65 (1952) 905.

39. A.E. BUCK, Ph.D. Thesis, University of Texas at Austin, (1971).

40. C. DASARATHY, Pract. Metalogr., 7 (1970) 45.

41. A.C. RIDDEFORD, Advances in Electrochemistry and Electrochemical Engineering, Vol. 4, Ed. P. Delahay. John Willey and Son, New York, (1966), p. 167.

42. B. HAGUE (revised by T.R. Foord), Alternating Current Bridge Methods, Academic Press, London, 6th Edn., (1971).

43. R. PIERCY and N.A. HAMPSON, J. Applied Electrochem., 5 (1975) 19.

44. J. HAKOMORI, J. Amer. Chem. Soc., 52 (1930) 2372.

45. E.M. HATTOX and T.DE VRIES, J. Amer. Chem. Soc., 58 (1936) 2126.

46. W. KANGRO and F.R. WEINGÄRTNER, Z. Elektrochem., 58 (1954) 505.

47. M.R. LIETZKE and R.W. STOUGHTON, J. Amer. Chem. Soc., 78 (1956) 4520.

48. A.K. COVINGTON, M.A. HAKEEM and W.F.K. WYNN-JONES, J.Chem.Soc., (1963) 4394.

49. W.M. LATIMER, The Oxidation States of the Elements and Their Potentials in Aqueous Solutions. 2nd Edn., Prentice-Hall Inc., New York, (1952).

50. E.V. LEONTOVICH, V.V. LOSEV and M.A. DEMBROVSKII, Elektrokhimiya, 5 (1969) 32.

51. V.V. LOSEV and A.P. PCHEL'NIKOV, Elektrokhimiya, 4 (1968) 264.

52. J.N. BUTLER, M.L. MEEHAN and A.C. MAKRIDES, J. Electroanal. Chem., 9 (1965) 237.

53. N.S. POLYANOVSKAYA and A.N. FRUMKIN, Elektrokhimiya, 1 (1965) 538.

54. E.V. YAKOVLEVA and N.V. NIKOLAEVA-FEDOROVICH, Elektrokhimiya, 6 (1970) 35.

55. E.D. LEVIN and A.L. ROTINYAN, Elektrokhimiya, 7 (1971) 372.

56. N.B. GRIGOR'EV, I.A. GEDVILLO and N.D. BARDINIA, Elektrokhimiya, 8 (1972) 409.

57. L.F. KOZIN, E.E. KOBRAND and I, A. SHEKA, Ukr. Khim. Zh., 32 (1966) 154.

58. L. KISS, A. KOROSI and J. FARKAS, Nagy. Kém. Falyóiriat, 73 (1967) 551.

59. L. KISS, J. FARKAS and A. KOROSI, Nagy. Kém. Falyóiriat, 75 (1969) 66.

60. M.E. STRAUMANIS and R.L. MARTIN, Z. Anorg. Allegm. Chem., 334 (1965) 321.

61. G.M. BUDOV and V.V. LOSEV, Dokl. Akad. Nauk. SSSR, 129 (1959) 6.

62. V.V. LOSEV and A.I. MOLODOV, Dokl. Akad. Nauk. SSSR, 130 (1960) 111.

63. A.I. MOLODOV, G.N. MARKOS'YAN and V.V. LOSEV, Elektrokhimiya, 9 (1973) 1368.

64. V.V. LOSEV and A.I. MOLODOV, Dokl. Akad. Nauk. SSSR, 135 (1960) 1432.

65. A.I. MOLODOV and V.V. LOSEV, Elektrokhimiya, 1 (1965) 651.

66. A.I. CHERNOM'ORSKII, Elektrokhimiya, 5 (1969) 206.

67. V.V. LOSEV, A. I. MOLODOV and V.V. GORODETZKII, Electrochim. Acta, 12 (1967) 475.

68. L.F. KOZIN, E.E. KOBRAND and I.A. SHEKA, Ukr. Khim. Zh., 32 (1966) 951.

69. A.I. MOLODOV and V.V. LOSEV, Elektrokhimiya, 1 (1965) 1253.

70. R.E. VISCO, J. Phys. Chem., 69 (1965) 202.

71. A.P. PCHEL'NIKOV and V.V. LOSEV, Elektrokhimiya, 1 (1965) 1058.

72. A.P. PCHEL'NIKOV and V.V. LOSEV, Elektrokhimiya, 5 (1969) 284.

73. V.V. LOSEV and A.I. MOLODOV, Dokl. Akad. Nauk. SSSR, 148 (1963) 1114.

74. B. MILLER and R.E. VISCO, J. Electrochem. Soc., 115 (1968) 251.

75. V.V. LOSEV and A.P. PCHEL'NIKOV, Elektrokhimiya, 6 (1970) 41.

76. V.V. LOSEV, Electrochim. Acta, 15 (1970) 1095.

77. V.V. LOSEV and A.P. PCHEL'NIKOV, Electrochim. Acta, 18 (1973) 589.

78. A.P. PCHEL'NIKOV and V.V. LOSEV, Elektrokhimiya, 7 (1973) 977.

79. R.E. VISCO, J. Electrochem. Soc., 113 (1966) 636.

80. A.P. PCHEL'NIKOV and V.V. LOSEV, Elektrokhimiya, 9 (1972) 1031.

81. A.I. MOLODOV and V.V. LOSEV, Elektrokhimiya, 4 (1968) 835.

82. V. MARKOVAC and B. LOVRECEK, J. Electrochem. Soc., 113 (1966) 838; G.A. WRIGHT, J. Electrochem. Soc., 114 (1967) 1263.

83. D.S. JAIN and J.N. GAUR, Electrochim. Acta, 12 (1967) 413.

84. L.S. KOPANSKAYA, Elektrokhimiya, 3 (1967) 876.

85. A.P. PCHEL'NIKOV, L.I. KRASINSKAYA and V.V. LOSEV, Zh. Prikl. Khim., 45 (1972) 1000.

86. R.D. ARMSTRONG, A.B. SUTTIE and H.R. THIRSK, Electrochim. Acta, 13 (1968) 1.

87. E.V. LEONTOVICH, Issled. Elektroosazhdeniyu Rastroreniyu Metal, (1971) 99.

88. R. GLICKSMAN and C.K. MOOREHOUSE, J. Electrochem. Soc., 104 (1957) 589.

89. T. POPOVA and N.A. SIMONOVA, Izv. Akad. Nauk. SSSR Ser. Khim., 7 (1963) 1086.

90. F.F. FAIZULLIN and N.A. AMIRKHANOVA, Elektrokhimiya, 2 (1966) 805.

91. F.F. FAIZULLIN and N.A. AMIRKHANOVA, Elektrokhimiya, 2 (1966)1383.

92. L.I. FILIPPOVA AND L.L. KUZMIN, Izv. Vyssh. Ucheb. Zaved. Khim. Khim. Tecknol., 12 (1969) 1199.

93. T.M. SALEM and A.A. ISMAIL, J. Chem. Soc. (A) (1970) 2415.

94. R.W. LEWIS and A.H. PARTRIDGE, Proc. Second Int. Symp. on Batteries, Bournemouth, paper 2, (1960).

95. R.D. ARMSTRONG, T. DICKENSON, B. MACFARLANE and H.R. THIRSK, Proc. 9th Int. Power Sources Symp., Brighton, paper 26, (1974).

96. T.M. SALEM and A.A. ISMAIL, J. Chem. Soc., (A) (1970) 2419.

97. J.N. BUTLER and M. DIENST, J. Electrochem.Soc., 112 (1965) 226.

98. M. POURBAIX, Atlas of Electrochemical Equilibria in Aqueous Solutions, Pergamon Press, (1966), p.440.

99. M.P.J. BRENNAN and N.A. HAMPSON, J. Electroanal. Chem., 48 (1973) 465.

100. L.M. BAUGH and J.A. LEE, J. Electroanal. Chem., 48 (1973) 55.

101. P. CASWELL, N.A. HAMPSON and D. LARKIN, J. Electroanal. Chem., 20 (1969) 335.

102. Handbook of Physics and Chemistry, 45th Edn., Chemical Rubber Co. (1964).

103. D. ARMSTRONG, N.A. HAMPSON and R.J. LATHAM, J. Electroanal. Chem., 23 (1969) 361.

104. R. DE. LEVIE, J. Chem. Phys., 47 (1967) 2509.

105. P. DELAHAY, Advances in Electrochemistry and Electrochemical Engineering, Vol. 1, Ed. P. Delahay, Interscience, New York, (1961) chapter 4.

106. R.D. GILES, J.A. HARRISON and H.R. THIRSK, J. Electroanal. Chem., 22 (1969) 375.

107. R.D. ARMSTRONG, W.P. RACE and H.R. THIRSK, J. Electroanal. Chem., 19 (1968) 233.

108. R.DE LEVIE, Electrochim. Acta, 10 (1965) 113.

109. R.DE LEVIE, Advances in Electrochemistry and Electrochemical Engineering, Vol. 6, Ed. P. Delahay, Interscience, New York, (1967), chapter 4.

110. R. DE LEVIE, Electrochim. Acta, 10 (1965) 395.

111. S. O. IZIDINOV and F.F. RED'KO, Elektrokhimiya 7 (1971) 1610.

112. G.M. DERIAZ. Ph. D. Thesis, University of Birmingham (1951).

113. B.N. KABANOV, N.N. TOMASHOVA and I.G. KISELEVA, Elektrokhimiya, 6 (1970) 612.

114. A. MARSHALL and N.A. HAMPSON, J. Electroanal. Chem., 53 (1974) 133.

115. M. TAKOUKA, Coll. Czech. Chem. Comm., 4 (1932) 443.

116. J.R. MILLS, R.C. BELL and R.A. KING, Rare Metals Handbook, 2nd edn., C.A. Hampel (Ed.), Reinhold Publishing Corporation, (1961) p. 206.

117. A.I. BUSEV, The Analytical Chemistry of Indium, Pergamon Press, Frankfurt, (1962).

118. G. BIEDERMANN, Rec. Trav. Chim., 75 (1965) 716.

119. G. BIEDERMANN, Arkiv. Kemi., 9, No. 21, 277-279.

120. T. MOELLER, J. Amer. Chem. Soc., 62 (1940) 2444 ; 63 (1941) 1206.

121. T. MOELLER, J. Amer. Chem. Soc., 63 (1941) 2625.

122. A. CHERNIKHOV and V. SHTUTSER, Zav. Lab., 9 (1940) 531.

123. See for example E. DONGES, Handbook of Preparitive Chemistry, Vol. 1, Ed. G. Brauer, Academic Press, (1963).

124. A.I. VOGEL, A Textbook of Quantitive Inorganic Analysis, Longman Group Ltd., London (1971) p. 266.

125. G.N. LEWIS and M. RANDALL, Thermodynamics and Free Energy of Chemical Substances, McGraw Hill, New York, (1923), p. 383.

126. A.A. NOYES, J. Amer. Chem. Soc., 46 (1924) 1099.

127. R.A. ROBINSON and R.H. STOKES, Electrolyte Solutions, Butterworths. London (1955).

128. W.J. MOORE, Physical Chemistry, Longmans, London (1962), p. 358.

129. R.E. HESTER, R.A. PANE and G.E. WALRAFEN, J. Chem. Phys., 38 (1963) 249.

130. B. LOVRECEK and V. MARKOVAC, J. Electrochem. Soc., 109 (1962)727.

131. V. MARKOVAC and B. LOVRECEK, J. Electrochem. Soc., 112 (1965) 520.

132. H. INAI, J. Sci. Hiroshima Univ. Ser., A22 (1958) 291.

133. R.D. ARMSTRONG and G.M. BULMAN, J. Electroanal. Chem., 25 (1970) 121.

134. D. FERRI, Acta. Chem. Scand., 26 (1972) 747.

135. V.V. LOSEV, A.I. MOLODOV and V.V. GORODETSKII, Elektrokhimiya, 1 (1965) 572.

136. V.I. KRAUTSOV and S.A. LOGINOVA, Zh. Fiz. Khim., 31 (1957) 2438.

137. Stability Constants of Metal-Ion Complexes, Suppl. No. 1, Chem. Soc. Spec. Publ., (1971), p. 28, (London: Chem. Soc.).

138. G.Z. RUPPRECHT, Z. Physik., 139 (1954) 504.

139. J.P.G. FARR and N.A. HAMPSON, Electrochem. Technol., 6 (1968)10.

140. N.A. HAMPSON and M.J. TARBOX, J. Electrochem. Soc., 110 (1963) 95.

141. B.E. CONWAY, Theory and Principles of Electrode Processes, Ronald Press Co., New York, (1965), p. 205.

142. R.A. ORIANI and R.P. FRANKENTHAL, Metal Surfaces, Proc. Amer, Soc. for Metals and the Metallurgical Soc. of AIME, (1962) chapter 11.

143. B.N. KABANOV and D.I. LEIKIS, Dokl. Akad. Nauk. SSSR, 58 (1947) 1685.

144. B.N. KABANOV, R. BURSTEIN and A. N. FRUMKIN, Disc. Farad. Soc., 1 (1947) 259.

145. B.E. CONWAY and J.O'M BOCKRIS, Proc. Roy. Soc., A248 (1958) 394.

146. B.E. CONWAY and J. O'M BOCKRIS, Electrochim. Acta, 3 (1961) 340.

147. N.A. IZMAILOV, Elektrokhimiya Rastvorov, (1959).

APPENDIX 1

Analysis of Electrolyte Solutions and Preparation of Activated Charcoal

A.1. (a) Analysis of Fluoride, Chloride, Sulphate, Nitrate and Perchlorate Electrolytes

In all cases the sodium (or potassium) content was determined and the anion concentration then calculated.

A series of standards (of the appropriate electrolyte) in the range 5-50 p.p.m. was made up. Using a flame photometer (E.E.L) a calibration graph was constructed. The electrolyte to be analysed was diluted to $\sim$ 25 p.p.m. and its concentration then determined.

A.1. (b) Determination of Indium

To a neutral or faintly acidic solution containing indium an excess of tartaric acid was added and the pH adjusted to within the range 8-10 using an ammonium chloride-ammonium hydroxide buffer. 1:400 Eriochrome Black T-sodium chloride indicator was added and the resultant solution titrated at the boiling point with a standardised disodium EDTA solution. The end point was detected as a colour change from pink to blue which remained after boiling for 30 seconds.

A.1. (c) Determination of NaOH and KOH concentrations

Approximately 4g of sulphamic acid was accurately weighed into a 150 cc conical flask and dissolved in 30-50 cc of distilled water. Two-three drops of methyl red were added and the solution titrated with the potassium or sodium hydroxide solution for analysis. The end point was determined as the first yellow colour.

A.1. (d) Preparation of Charcoal

Granular gas adsorption charcoal was extracted in a soxhlet

apparatus with constant boiling hydrochloric acid. The acid was changed weekly and the extraction was continued until the acid remained colourless. This procedure usually took about 3 months. The charcoal was then washed by refluxing with bidistilled water (also replaced weekly) until the washings showed no positive test for chloride ion.

APPENDIX 2

The kinetics of multistep electron transfer processes

Processes in which a number of electrons are transferred successively or simultaneously have been recently comprehensively reviewed by Losev[26]. Three electrons is the largest number considered theoretically and factually.

1. Processes with a single limiting step.

The presence of a single rate determining one electron transfer step in the sequence

$$M = M^{+} + e \qquad (1)$$

$$M^{+} = M^{2+} + e \qquad (2)$$

$$M^{2+} = M^{3+} + e \qquad (3)$$

results in a current-potential relationship:

$$i = i_a - i_k = K_a[M] \exp\ (\alpha_a F\phi/RT) - K_K[M^{n+}]\ \exp(-\alpha_K F\phi/RT)^{*} \qquad (4)$$

The corresponding exchange current-concentration relationship is:

$$i_o = i_o^o\,[M]^{\alpha_K/n}\ [M^{n+}]^{\alpha_a/n} \qquad (5)$$

where i_o^o is the standard exchange current. In (4) and (5) α_a and α_K refer to transfer coefficients governing the overall potential dependence of the rate of the reaction. α_a and α_K are related to the symmetry coefficients, β_a and β_K, as follows:

$$\alpha_a = m - 1 + \beta_{a,m} \qquad (6)$$

$$\alpha_K = n - m + \beta_{K,m} \qquad (7)$$

here n is the total number of electrons involved in the overall charge

*Footnote: These equations assume that an excess of supporting electrolyte is present, in which case contributions due to ψ_1, the double-layer potential at the distance of closest approach of non-specifically adsorbed ions, can be ignored.

transfer process, in the case of (1) - (3) n = 3, m is the ordinal number of the rate determining step.

β_a and β_K refer only to the rate determining step, and obey the usual condition:

$$\beta_{a,m} + \beta_{K,m} = 1 \qquad (8)$$

It follows from (6), (7) and (8) that:

$$\alpha_a + \alpha_K = n \qquad (9)$$

The transfer coefficients α_a and α_K can be determined from the Tafel slopes b_a and b_K, viz:

$$\Delta\phi = -(RT/\alpha_a F) \ln i_o + (RT/\alpha_a F) \ln i_a \qquad (10)$$

$$\Delta\phi = (RT/\alpha_K F) \ln i_o - (RT/\alpha_K F) \ln i_K \qquad (11)$$

and $$\alpha_a/\alpha_K = b_K/b_a \qquad (12)$$

Using (9) it follows that:

$$\left(\frac{1}{b_a}\right) + \left(\frac{1}{b_K}\right) = nF/2.3RT \qquad (13)$$

A general conclusion with respect to the values of Tafel slopes for systems with stepwise mechanisms with a single rate determining step is that these slopes should decrease with increase in the value of m.

α_a and α_k can also be obtained by use of equation (5):

$$\left[\frac{\partial \ln i_o}{\partial \ln [M]}\right]_{[M^{n+}]} = \frac{\alpha_K}{n} \quad \text{or} \quad \left[\frac{\partial \ln i_o}{\partial \ln [M^{n+}]}\right]_{[M]} = \frac{\alpha_a}{n} \qquad (14)$$

It follows that for a stepwise mechanism, the experimental data (e.g. from the Tafel slope or from $i_o/[M]$, $[M^{n+}]$ data) leads only to the transfer coefficients α_a and α_K. However, by comparing the values of α_a and α_K (obtained from independent measurements) the existence of a stepwise mechanism can be proved. From (6) (7) and (12) it follows that:

$$\alpha_a/\alpha_K = b_K/b_a = (m-1 + \beta_{a,m})/(n-m + \beta_{K,m}) \qquad (15)$$

thus the ratio α_a/α_K depends on the ordinal number (m) of the rate determining step, which is illustrated in table 1.

Table 1, Values of α_a/α_K *

n	m			
	1	2	3	4
2	1/3	3	-	-
3	1/5	1	5	-
4	1/7	3/5	5/3	7

* $\beta_{a,m} = \beta_{K,m} = 0.5$ is assumed

Table 1 shows that in nearly all cases the transfer coefficients and thus b_a and b_K should differ considerably for bivalent and trivalent metals in a stepwise mechanism with a single rate determining step. For a simple one-step process α_a/α_K is usually close to unity. Therefore, a considerable deviation of α_a/α_K from unity

is an indication of a stepwise mechanism, and the magnitude of this ratio can indicate which step is the limiting one. It should be noted that in the case where n = 3 and m = 2 the above theory is not applicable since $\alpha_a / \alpha_K = 1$.

The possibility that the simultaneous transfer of two or more electrons takes place in the rate determining step should also be considered. For the overall process $M \rightleftharpoons M^{3+} + 3e$, the following rate determining steps are possible in addition to those considered in table 1.

$$M^{+} \longrightarrow M^{3+} + 2e \qquad (16)$$

for which, by considering the partial rate equations of the overall process:

$$\alpha_a / \alpha_K = (1 + 2\beta_{a,2}) / 2\beta_{K,2} \qquad (17)$$

$$= 2 \text{ (for } \beta_{a,2} = \beta_{K,2} = 0.5)$$

and: $M \longrightarrow M^{2+} + 2e \qquad (18)$

for which:

$$\alpha_a/\alpha_K = 2\beta_{a,1}/(1 + 2\beta_{K,1}) \qquad (19)$$

$$= 0.5 \text{ (for } \beta_{a,1} = \beta_{K,1} = 0.5)$$

As can be seen from table 1 the α_a/α_K ratio has entirely different values for various rate-limiting one electron steps. Thus by establishing whether α_a/α_K is close to 2 or 0.5 it is possible

to determine whether the rate determining step is (16) or (18)

2. Processes with comparable rate constants for successive steps

When the rate constants of successive charge-transfer steps are comparable, the rate equations for the multistep process have a more complex form since they include the kinetic parameters of all steps.

Considering the reaction sequence (1) - (3) (three successive one-electron steps), the rate equations for the various steps are:

$$i_1 = i_{a,1} - i_{K,1} = K_{a,1}[M] \exp(\beta_{a,1} F\phi/RT) - K_{K,1}[M^+]\exp(-\beta_{K,1} F\phi/RT) \quad (20)$$

$$i_2 = i_{a,2} - i_{K,2} = K_{a,2}[M^+]\exp(\beta_{a,2} F\phi/RT) - K_{K,2}[M^{2+}] \exp(-\beta_{K,2} F\phi/RT) \quad (21)$$

$$i_3 = i_{a,3} - i_{K,3} = K_{a,3}[M^{2+}]\exp(\beta_{a,3} F\phi/RT) - K_{K,3}[M^{3+}] \exp(-\beta_{K,3} F\phi/RT) \quad (22)$$

At equilibrium $i_1 = i_2 = i_3 = 0$ and from (20) - (22) the expressions for the exchange currents of the various steps ($i_{0,1}, i_{0,2}, i_{0,3}$) can be obtained. The overall current $i = i_1 + i_2 + i_3$. Since each step is a one-electron transfer and in the steady state $i_1 = i_2 = i_3$, the overall current is equal to three times the current for a given step. By use of this latter deduction and by eliminating $K_{a,1}$ $K_{a,2}$ etc from (20) - (21) by expressing these constants in terms of $i_{0,1}$ $i_{0,2}$ and $i_{0,3}$ and also by eliminating the concentrations of intermediates by use of the Nernst equation, the final steady-state polarisation relationship follows as:

$$i = 3\left\{ i_{0,1},i_{0,2},i_{0,3}\left[\exp\frac{(\beta_{a,1}+\beta_{a,2}+\beta_{a,3})F\Delta\phi}{RT} - \exp -\frac{(-\beta_{K,1}+\beta_{K,2}+\beta_{K,3})F\Delta\phi}{RT}\right]\right\}$$

$$x\left\{ i_{0,2},i_{0,3}\exp\left[\frac{(\beta_{a,2}+\beta_{a,3})F\Delta\phi}{RT}\right] + i_{0,1},i_{0,3}\exp\left[\frac{(\beta_{a,3}-\beta_{K,1})F\Delta\phi}{RT}\right] + \right.$$

$$\left. i_{0,1},i_{0,2}\exp\left[\frac{(\beta_{K,1}+\beta_{K,2})F\Delta\phi}{RT}\right]\right\}^{-1} \qquad (23)$$

From (23) the anodic and cathodic polarisation relationships can be obtained:

$$i = 3\, i_{0,1}(\exp \beta_{a,1}F\Delta\phi/RT)\left[1-\exp(-3F\Delta\phi/RT)\right] \; x\left\{1 + \frac{i_{0,1}}{i_{0,2}}\exp\left[-\frac{(\beta_{K,1}+\beta_{a,2})F\Delta\phi}{RT}\right]\right.$$

$$\left. + \frac{i_{0,1}}{i_{0,3}}\exp\left[-\frac{(1+\beta_{K,1}+\beta_{a,3})F\Delta\phi}{RT}\right]\right\}^{-1} . \qquad (24)$$

and

$$i = -3\, i_{0,3}\left[\exp -\frac{\beta_{K,3}F\Delta\phi}{RT}\right]\left[1 - \exp\frac{3F\Delta\phi}{RT}\right] x\left\{1 + \frac{i_{0,3}}{i_{0,1}}\exp\left[\frac{(1+\beta_{K,2}+\beta_{a,3})F\Delta\phi}{RT}\right]\right.$$

$$\left. + \frac{i_{0,3}}{i_{0,1}}\exp\left[\frac{(\beta_{K,2}+\beta_{a,3})F\Delta\phi}{RT}\right]\right\}^{-1} \qquad (25)$$

<u>At sufficiently high $\Delta\phi$</u> (24) and (25) give the following Tafel relations:

$$i = i_a = 3i_{0,1}\exp(\beta_{a,1}F\Delta\phi/RT) \qquad (26)$$

and

$$i = i_K = -3i_{0,3}\exp(-\beta_{K,3}F\Delta\phi/RT) \qquad (27)$$

(26) and (27) allow a stepwise process, the steps of which have comparable rate constants, to be proved. The sum of the apparent tranfer coefficients determined from b_a and b_K follows from (26) and (27) as:

$$\alpha_a + \alpha_K = \beta_{K,3} + \beta_{a,1} < 2 \qquad (28)$$

(since $\beta_{K,3} < 1$ and $\beta_{a,1} < 1$).

Thus if equation (28) is observed, a mechanism in which the consecutive steps have comparable rate constants is unequivocally proved.

Using the definitions of b_a and b_K in terms of transfer coefficients, (28) may be re-written as

$$\alpha_a + \alpha_K = (2.3RT/b_K F) + (2.3RT/b_a F) < 2 \qquad (29)$$

from which we obtain

$$(1/b_a) + (1/b_K) < 2F/2.3RT \qquad (30)$$

For the case of a single limiting step (13) gives

$$(1/b_a) + (1/b_K) = 3F/2.3RT \qquad (31)$$

Use of (30) and (31) enables the existence of a process, the steps of which have comparable rate constants, to be established directly from b_a and b_K at $|\Delta\phi| \gg 0$

An important situation arises where the exchange current of one of the steps is much lower than those of the remaining steps. Consider the case where $i_{0,3} \ll i_{0,2}$ and $i_{0,1}$. At a certain $\Delta\phi$ (24) and (25) lead to:

$$i = 3i_{0,3} \exp\left[(2 + \beta_{a,3})F\Delta\phi/RT\right] \qquad (32)$$

and

$$i = -3i_{0,3} \exp\left[-\beta_{K,3}F\Delta\phi/RT\right] \qquad (33)$$

For this case $\alpha_a = 2 + \beta_{a,3}$ and $\alpha_K = \beta_{K,3}$, thus $\alpha_a + \alpha_K = 3$ (putting $\beta_{a,3} = \beta_{K,3} = 0.5$) and hence the transfer coefficient sum does not indicate that the process has a stepwise nature. However, unlike the situation where a single slow step occurs, it follows from (24) that at a sufficiently large $\Delta\phi$, there should appear on the anodic polarisation curve a transition from a linear region with $b_a = 2.3RT/(2 + \beta_{a,3})F$ to a region with higher slope $2.3RT/\beta_{a,1}F$ which corresponds to step (1). The appearance of this break in the Tafel plots is due to the different dependences of the rates of different successive steps on ϕ .

For significantly different rates of the successive steps, the change in the limiting step as a function of ϕ becomes evident in the appearance of a break in the polarisation curve when $\Delta\phi$ is large. (At comparable rates of these steps, this effect is seen in an analogous break in ϕ versus $\log_{10} i_a$ and ϕ versus $\log_{10} i_K$ curves near ϕ_e.) This change in the rate determining step with change in ϕ is an unequivocal criterion of the stepwise nature of the electrode process and cannot be explained in terms of a simultaneous electron transfer process. This phenomena is usually referred to as the "break" criterion.

If the exchange currents of successive steps are of comparable magnitudes, the linear sections of the Tafel plots, corresponding to different limiting steps, become short. If the transition between these regions is near ϕ_e, the break and the two linear sections on the polarisation curve are obscured due to the effect of the reverse reaction. This disadvantage can be overcome to some extent by the

use of partial current curves obtained by the radiotracer method under conditions where no distortion arises due to the reverse process, making it possible to detect the break near ϕ_e.

As stated previously the appearance of a break on the polarisation curve is the most direct proof of a stepwise mechanism. In order to use this criterion it is necessary to consider other possible causes for the appearance of a break and the two Tafel regions on the polarisation curves. Possible sources of error may be listed as follows :

(a) Distortions of the shape of polarisation curves could be due to simultaneous electrochemical side reactions (e.g. h.e.r.).

(b) The presence of a slow preceding diffusion or chemical step, an ohmic potential drop across the solution, or electrode passivation could also lead to the appearance of a break on the polarisation curve. However, in these cases, the section of the polarisation curve following the break should not obey the Tafel relation.

(c) If the appearance of one of the two linear regions is due to the presence of succeeding diffusion or chemical steps, the region nearest to ϕ_e should have $b = 2.3RT/nF$. This section should shift in the direction of lower $\Delta\phi$ when the stirring rate is increased for the case of a slow diffusion step.

(d) If the break is due to transition of the limiting step to a "barrierless" condition ($\beta_{K,m} = 1$) or to "activationless" discharge ($\beta_{a,m} = 1$), the slopes of the corresponding sections of the polarisation curve should be $2.3RT/(m-1)F$. ($0 \leq m \leq n$, m = integer).

(e) A break with a transition to a higher Tafel slope may be due to the attainment of the region of limiting surface coverage by low valency intermediates formed in the preceding equilibrium step.

In this case the rate of the overall process in the region of high slope should be independent of the concentration of the initial substance.

(f) If the overall process can take place simultaneously along several parallel paths, the rate equations will become very complex. In this case there is also the possibility of the appearance of Tafel sections with different slopes on the polarisation curves. Thus, for example, the appearance of two sections can be due to parallel occurence of the electrode process through two paths: the stepwise and the simple one step path.

Another possibility for determining Tafel regions corresponding to different limiting steps arises from the difference in the dependence of the i_o of each step on $[M]$ and $[M^{n+}]$. Using (20)-(22) and expressing ϕ_e in terms of $[M]$ and $[M^{n+}]$ by use of the Nernst equation we obtain:

$$i_{o,1} = K_1[M]^{(2+\beta_{K,1})/3} [M^{3+}]^{\beta_{a,1}/3} \quad (34)$$

$$i_{o,2} = K_2[M]^{(1+\beta_{K,2})/3} [M^{3+}]^{(1+\beta_{a,2})/3} \quad (35)$$

$$i_{o,3} = K_3[M]^{\beta_{K,3}/3} [M^{3+}]^{(2+\beta_{a,3})/3} \quad (36)$$

from which the various i_o dependencies on $[M]$ and $[M^{3+}]$ can be written.

Additional mechanistic data can be obtained by comparing the i_o's of different steps with the i_o of the overall process determined by radiotracer or impedance measurements or from the slope of the initial (i.e. near to ϕ_e) section of the same polarisation curve. The true exchange current of the three electron process is related

in the usual way to R_D determined near ϕ_e,

$$R_D = \left[\partial(\Delta\phi)/\partial i\right]_{i=0} = \frac{RT}{3F} \cdot \frac{1}{i_o} \qquad (37)$$

Differentiation of (23) with respect to ϕ gives the transfer resistance as a function of the exchange currents of the steps (1) - (3), i.e.

$$R_D = \left[\partial(\Delta\phi)/\partial i\right]_{i=0} = \frac{1}{3} \cdot \frac{RT}{3F}\left[\frac{1}{i_{0,1}} + \frac{1}{i_{0,2}} + \frac{1}{i_{0,3}}\right] \qquad (38)$$

From (37) and (38) we obtain:

$$\frac{1}{i_o} = \frac{1}{3}\left[\frac{1}{i_{0,1}} + \frac{1}{i_{0,2}} + \frac{1}{i_{0,3}}\right] \qquad (39)$$

i.e. the relationship between the true exchange current and the exchange currents of separate steps.

For the case of a single slow step, and when the i_o for one of the steps is significantly lower than those of the remaining steps (e.g. $i_{0,1} \ll i_{0,2} < i_{0,3}$), (39) yields $i_o \backsim i_{o,ext} = 3i_{0,1}$. Thus the true exchange current coincides with the extrapolated exchange current of the rate limiting step. It follows that when the steps have comparable i_o's, the true i_o obtained from (39) should be smaller than the exchange current $i_{o,ext}$ obtained by extrapolation according to (26) and (27), e.g. when $i_{0,1} = i_{0,2} = i_{0,3}$ (39) gives $i_0 = i_{0,1} = i_{0,ext}/3$. The difference between the true and extrapolated exchange currents is therefore another criterion for a process having comparable rate constants for successive steps and is usually referred to as the "criterion of the true exchange current".

Losev has summarised criteria for identifying a stepwise process having comparable rates of successive steps as follows:

(a) The Vetter criterion: Use of equations (26) and (27) to show divergence of the values for $i_{o,ext}$ from data obtained at appreciable anodic and cathodic polarisation, i.e. $i^{a}_{o,ext} \neq i^{K}_{o,ext}$.

(b) Criterion of the transfer coefficient sum: Deviation of the sum of the transfer coefficients measured at appreciable $\Delta\phi$ from the overall number of electrons transferred in the electrode process ($\alpha_a + \alpha_K < 2$).

(c) The break criterion: Appearance of a break on the polarisation curve at appreciable $\Delta\phi$ or on the partial current curve for a given process near ϕ_e.

(d) The criterion of the true exchange current: Divergence between true and extrapolated exchange currents ($i_o < i_{o,ext}$).